
# Circadian rhythm in cartilage mechanobiology

**Lekau Dintwa**

**A thesis submitted to Cardiff University in accordance with the requirements for the degree of Doctor of Philosophy in the School of Biosciences**

**December 2024**

**Dedicated to my Mother**

**Motlaletshego**

who always believed in me and supported my education

**Acknowledgements**

First and foremost, I would like to thank my supervisors Prof. Clare Hughes and Dr. Emma Blain for the support, guidance and constructive feedback they offered throughout my PhD and most importantly for accepting my request to carrying out research under their supervision. For that I will forever be grateful.

I would like to express my gratitude to Clare Hughes for giving me an opportunity to supervise the lab work of four final year students namely, Alister Scott, Blessing Mwaisoloka, Hassan Rehman, and Thomas Capewell on her behalf and allowing me to use excess samples following the completion of their projects hence contributing hugely to my thesis outcomes. This opportunity also enhanced my teaching experience and for that I am so thankful.

I would also like to express my appreciation to Dr. Paul White for helping me with technical problems I encountered during my lab work as well as training on the use and maintenance of standard laboratory equipment.

I would also like to acknowledge my colleagues Jingyi Feng and Yixin Wang for their cooperation, professionalism, and for creating a friendly and conducive learning environment in the shared PGR student office and lab throughout our PhD journeys.

My sincere thanks go to my family, my wife and daughters for their understanding, support, and motivation when I undertook my PhD research overseas and during my thesis write-up period.

Finally, I would like to express my gratitude to the Government of the Republic of Botswana for the full sponsorship of this PhD research project.

**List of abbreviations**

| | |
|---|---|
| **18s** | 18S ribosomal RNA |
| **2D** | Two-dimensional |
| **3D** | Three-dimensional |
| **5-FAM** | Fluorescein amidites (5 carboxyfluorescein) |
| **ACAN** | Aggrecan |
| **ACL** | Anterior cruciate ligament |
| **ADAMTS** | A disintegrin and metalloproteinase with thrombospondin-1 like motifs |
| **AMPK** | Adenosine monophosphate (AMP) kinase |
| **AP-1** | Activator protein-1 transcription factor |
| **APMA** | Aminophenylmercuric acetate |
| **ARNTL1** | Aryl hydrocarbon receptor nuclear translocator-like protein 1 |
| **ASCs** | Adipose-derived stem cells |
| **ATP** | Adenosine triphosphate |
| **β-actin** | Beta-actin |
| **β-TrCP** | Beta-transducin repeat-containing protein |
| **BGN** | Biglycan |
| **BHLH** | Basic helix-loop-helix proteins |
| **BMAL1** | Brain and muscle ARNT-Like 1 |
| **BMP** | Bone morphogenetic protein |
| **CCGs** | Clock controlled/output genes |
| **cDNA** | Complementary DNA |
| **CILP** | Cartilage intermediate layered protein |
| **CK** | Casein kinase |
| **CLOCK** | Circadian locomotor output cycles kaput |
| **COL10A1** | Type X collagen alpha 1 chain |
| **COL1α1** | Type I collagen alpha 1 chain |
| **COL2A1** | Type II collagen, alpha 1 chain |
| **COL6A1** | Type VI collagen alpha 1 chain |
| **COMP** | Cartilage oligomeric matrix protein |
| **COX** | Cyclooxygenase |
| **CRY** | Cryptochrome circadian regulator |
| **CS** | Chondroitin sulphate |

| | |
|---|---|
| **CTS** | Cyclical tensile strain |
| **CZ** | Calcified zone |
| **D-box** | DNA cis-element box |
| **DBP** | Albumin D box-binding protein |
| **DCN** | Decorin |
| **DD** | Dark-dark cycle |
| **Dex** | Dexamethasone |
| **DMM** | Destabilisation of the medial meniscus |
| **DMMB** | Dimethylmethylene blue assay |
| **DNA** | Deoxyribonucleic acid |
| **dNTPs** | Deoxynucleotide triphosphates |
| **DS** | Dermatan sulphate |
| **DZ** | Deep zone |
| **E4BP4** | E4 Promoter-Binding Protein 4 |
| **E-box** | Enhancer box |
| **ECM** | Extracellular matrix |
| **FBS** | Foetal bovine serum |
| **FBXL3** | F-box and leucine rich repeat protein |
| **FCD** | Fixed charge density |
| **FDA** | Fluorescein diacetate |
| **FRET** | Fluorescence resonance energy transfer |
| **GAPDH** | Glyceraldehyde-3-phosphate dehydrogenase |
| **GNP** | Gross national product |
| **hESCs** | Human embryonic stem cells |
| **HKG** | Housekeeping genes |
| **HLF** | Hepatic leukemia factor |
| **hMSCs** | Human mesenchymal stem cells |
| **HPRT** | Hypoxanthine guanine phosphoribosyltransferase |
| **IL-1** | Interleukin-1 |
| **iNOS** | Inducible NO synthase |
| **IVD** | Intervertebral disc |
| **JNK** | c-Jun N-terminal kinase |
| **KS** | Keratan sulphate |
| **LD** | Light-dark cycle |
| **MAPK** | Mitogen-activated protein kinase |

| | |
|---|---|
| **MESOR** | Midline-estimating statistic of rhythm |
| **miPSCs** | Murine induced pluripotent stem cells |
| **MMP** | Matrix metalloproteinases |
| **mRNA** | Messenger RNA |
| **MZ** | Middle zone |
| **NFATC** | Nuclear factor of activated T cells, cytoplasmic, calcineurin dependent |
| **NFIL3** | Nuclear factor, interleukin 3 regulated |
| **NF-κB** | Nuclear factor-kappa B |
| **NO** | Nitric oxide |
| **NPAS2** | Neuronal PAS domain protein 2 |
| **NTC** | No template control |
| **OA** | Osteoarthritis |
| **OSM** | Oncostatin M |
| **PBS** | Phosphate buffered saline |
| **PCM** | Pericellular matrix |
| **PDL** | Periodontal ligament |
| **PER** | Period circadian regulator |
| **PI** | Propidium iodide |
| **PPIA** | Peptidylprolyl Isomerase A |
| **PTOA** | Post-traumatic osteoarthritis |
| **RA** | Rheumatoid arthritis |
| **REV-ERBs** | Reverse strand of *ERB*/*THR-A and -B* [thyroid hormone receptor] |
| **NR1D1/2** | Nuclear receptor subfamily 1 group D member 1/2 |
| **RNA** | Ribonucleic acid |
| **ROR** | Retinoic acid receptor-related orphan receptor |
| **ROS** | Reactive oxygen species |
| **RPL4** | Ribosomal Protein L4 |
| **RRE** | Rev-responsive element |
| **RT** | Reverse transcription |
| **RT-qPCR** | Real-time quantitative polymerase chain reaction |
| **RUNX2** | Runt-related transcription factor 2 |
| **SCF** | Skp1-Cullin-F-box protein |
| **SCN** | Suprachiasmatic nucleus |
| **SDHA** | Succinate dehydrogenase complex flavoprotein subunit A |
| **sGAG** | Sulphated glycosaminoglycan |

| | |
|---|---|
| **SLRPs** | Small leucine rich proteoglycans |
| **SMAD** | Suppressor of mothers against decapentaplegic |
| **SOX9** | Sex determining region Y-box9 |
| **SZ** | Superficial zone |
| **TBE** | Tris/Borate/EDTA |
| **TEF** | Thyrotrophic Embryonic Factor |
| **TGF-β** | Transforming growth factor beta |
| **TIMP** | Tissue inhibitor of metalloprotease |
| **TNF-α** | Tumour necrosis factor-alpha |
| **TRPV** | Transient receptor potential vanilloid |
| **WNTs** | Wingless-type MMTV integration site family members |
| **YWHAZ** | Tyrosine 3-monooxygenase/tryptophan 5-monooxygenase activation protein zeta |
| **ZT** | Zeitgeber time |

**Units of measurement abbreviations:**

| | |
|---|---|
| **bp** | Base pairs |
| **cm** | Centimetre |
| **$C_T$** | Cycle threshold |
| **g** | Gram |
| **Hz** | Hertz |
| **kDa** | Kilo Dalton |
| **km** | Kilometre |
| **m** | Metre |
| **mg** | Milligram |
| **min** | Minute |
| **ml** | Millilitre |
| **mm** | Millimetre |
| **mM** | Millimolar |
| **mOSM** | Milliosmoles |
| **MPa** | Mega Pascal |
| **N** | Newton |
| **ng** | Nanogram |
| **RFU** | Relative fluorescence units |
| **rpm** | Revolutions per minute |
| **s** | Second |
| **SD** | Standard deviation |
| **$T_m$** | Melting temperature |
| **V** | Volt |
| **µg** | Microgram |
| **µl** | Microlitre |
| **µm** | Micrometre |
| **µM** | Micromolar |

**Abstract**

**Introduction:** Cartilage resident cells, chondrocytes are responsible for sustaining tissue homeostasis by maintaining a balance between biosynthesis and degradative activities in response to mechanical loading and other cues. Previous studies revealed that mechanical loading is imperative for normal cartilage function with physiological loads maintaining tissue homeostasis; in contrast, non-physiological loads, i.e., static, insufficient or excessive, induces maladaptive chondrocyte responses, shifting metabolism towards inflammation and extracellular matrix (ECM) catabolism leading to cartilage deterioration and promoting the development of osteoarthritis (OA). OA is a prevalent joint disease characterised by progressive degeneration of articular cartilage, synovial inflammation and bone remodelling. There is currently no disease modifying treatment for OA as available modalities mostly alleviate symptoms. Previous studies identified circadian rhythm as one of the most dysregulated pathways in human OA and other model systems. Circadian rhythm is mediated by circadian clocks which are endogenous cellular oscillators with an ~24-hour rhythmic cycle ensuring that organisms can predict and align their physiology to the daily variations of light and temperature. In mammals, circadian clocks are organised hierarchically with the master clock located in the suprachiasmatic nucleus (SCN) of the anterior hypothalamus in the brain. However, articular cartilage and other peripheral tissues possess subordinate clocks. More recently, studies have suggested that non-photic zeitgeber including exercise also entrains circadian rhythmicity. However, at the start of this PhD, very few studies had been performed on mechano-regulation of circadian clocks, particularly in cartilage. Therefore, the aim of the PhD was to investigate whether (i) bovine primary chondrocytes subjected to mechanical load (simulated using centrifugal force) would exhibit an altered circadian rhythm, and (ii) whether mechanical load could reset a disrupted circadian rhythm in an *in vitro* model of inflammatory OA.

**Results:** This PhD developed and characterised various *in vitro* 3D pellet models for studying chondrocyte mechanobiology including chondrocyte pellets, with or without pericellular matrix (PCM), exposed to centrifugal force predicted to simulate the compressive, hydrostatic and shear forces observed *in vivo*. In the absence of PCM, 15- and 60-minutes of centrifugation induced transcription of early mechano-responsive genes *c-fos* and *c-jun*, late mechano-responsive catabolic genes *adamts-4*, *adamts-5* and *mmp-3*, and the chondrocyte phenotype gene marker *sox9*. However, delayed transcription of the early and late mechano-responsive genes was observed in 3D pellets with PCM

subjected to 15 minutes of load (770xg force). Overall, a 770xg force induced robust mechano-signalling as compared to the 200- and 1000-xg centrifugal forces and 60 minutes mediated stronger responses as evidenced by higher transcript levels of select early and late response genes as compared to the 15 minutes regimen; thus, this regimen (60 minutes of 770xg force) was utilised in subsequent loading experiments. Overall, application of 60 minutes of load induced quicker transcription of the early and late mechano-responsive genes*,* but dampened the transcription of *sox9,* delayed *adamts-5* transcription and did not alter maximal induction of *mmp-3.*

Assessment of the clock genes in control pellets with no PCM demonstrated rhythmic expression of *bmal1*, *clock*, *cry1, dbp*, *npas2*, *nr1d1, nr1d2*, *per1* and *per2*, and the ECM catabolic gene *adamts-4* in at least one LD cycle; however, catabolic genes including *adamts-5*, *mmp-3* and *mmp-13*, and anabolic genes *acan* and *col2a1*, and the chondrocyte phenotype gene marker *sox9* were not expressed in a rhythmic manner. Circadian expression of *bmal1*, *clock* (though a transient disruption was observed only in the first LD cycle) and *per2* mRNAs was unaffected in 2 consecutive LD cycles following application of one episode of 770xg force (60 minutes) in the absence and/or presence of PCM whilst *acan* and *col2a1* demonstrated arrhythmicity in both the controls and loaded pellets with or without PCM. However, *adamts-4* mRNA rhythmicity in pellets with no PCM was sustained following application of a single episode of load while no circadian oscillations in *adamts-4* mRNA were observed in both controls and loaded (a single episode of 770xg force) pellets with PCM. This PhD also utilised an inflammatory OA model, with exposure of 3D pellets with no PCM to 5 ng/ml IL-1α/β in combination with 10 ng/ml OSM; as expected, proinflammatory cytokine stimulus reduced expression of *acan* and *sox9* and increased expression of *adamts-4*, *adamts-5*, *mmp-3* and *mmp-13* at T24 hours; this was concomitant with disruption of circadian rhythmicity of *bmal1*, *clock*, *cry1*, *npas2*, *nr1d1, nr1d2*, *per1* and *per2* genes. Application of dexamethasone, a known anti-inflammatory and clock synchronisation agent, to cytokine-treated cultures synchronised *bmal1* and *per2* transcription concomitant with the return of *acan* and *mmp-3* mRNA transcripts to control levels at T24 hours. However, application of 770xg force (60 minutes) either once daily for 3-days, twice daily for 1-day or twice daily for 2-days did not reset the cytokine-induced disrupted circadian rhythms of clock gene transcription (*bmal1*, *npas2*, *per2*) and did not return the cytokine-induced reductions in anabolic gene transcription (*acan*, *col2a1*) and cytokine-induced increases in catabolic gene transcription to control levels at T24 hours (*mmp-3*, *adamts-4*).

**Conclusion:** This thesis demonstrates the capacity of centrifugal force to simulate mechanical load in 3D chondrocyte pellets with or without PCM with 60 minutes of 770xg force inducing stronger mechano-signalling suggestive of its potential suitability for utilisation in mechanobiology investigations though loading regimen may need further optimisation. A single episode of 770xg load did not alter the circadian rhythm of clock gene expression (except for a transient disruption of *clock* rhythmicity in the first LD cycle in pellets with no PCM) nor a gene marker of a catabolic phenotype in 3D pellets with/without PCM suggesting that the employed load regimens had no impact on circadian clocks in healthy cartilage. This study also corroborates the capacity of proinflammatory cytokines to disrupt circadian clocks in primary chondrocytes and the capability of dexamethasone to reverse this inflammatory phenotype by synchronising these cytokine-disrupted circadian clocks. However, the inability of mechanical load (770xg force either once daily for 3-days, twice daily for 1-day or twice daily for 2-days) to reset circadian oscillations of clock genes in cytokine-treated pellets suggest that these loading regimens have no effect on disrupted circadian clocks, thus they possess no clock synchronisation properties. Moreover, the inability of mechanical load to reverse the inflammatory state of cytokine-treated cultures suggests that these load regimen does not possess anti-inflammatory properties and requires further optimisation. Overall, the findings of this thesis may aid refinement of future studies aimed at exploring mechano-regulation of the cartilage clock to identify potential therapeutic mechanical loading regimens and optimal times for administering exercise or physiotherapy to patients suffering from OA.

**List of Figures**

***Chapter 1***



***Chapter 3***

***Chapter 4***

***Chapter 5***

## List of Tables

### *Chapter 2*

# Table of Contents

# Chapter 1

## General introduction

## 1.1. Articular cartilage

Articulating surfaces at the end of long bones of diarthrodial joints such as hip, shoulder, ankle and knee are covered by a layer of resilient, highly specialised connective tissue called articular cartilage. This is a specialised form of hyaline cartilage which is about 2-4mm thick in humans (Quinn et al. 2005; Fox et al. 2009) and exposed to various magnitudes of mechanical loads during articulation (Fox et al. 2009; Mow et al. 1992). The tissue consists of the sparsely distributed constituent cells, called chondrocytes residing in a dense extracellular matrix (ECM). Chondrocytes occupy about 5-10% of the total volume of cartilage in humans (Bačenková et al. 2023). Cartilage has been described as having a biphasic nature whereby water and electrolytes account for the fluid phase whereas cells, collagen, proteoglycans, glycoproteins and non-collagenous proteins form the solid phase (Urban 1994). Articular cartilage is alymphatic, aneural and avascular therefore the tissue relies on the diffusion of nutrients, oxygen, waste metabolites and other substances to and from the synovial fluid (Ahmed and Hincke 2010; Frisbie and Johnson 2019; Mow et al. 1992). Chondrocytes are responsible for sustaining tissue homeostasis by maintaining a balance between the synthesis and degradation (remodelling) of the cartilaginous matrix in response to mechanical loading and other cues (Buckwalter et al. 2005; Responte et al. 2007).

### 1.1.1. Zonal arrangement of cartilage

The microscopic appearance of articular cartilage can be divided into four contiguous zones that vary in biomechanical properties, collagen fibril and chondrocyte orientation as well as proteoglycan content [Fig. 1.1] (Hu and Athanasiou 2003).

#### 1.1.1.1. Superficial zone (SZ)

The superficial zone represents about 10-20% of articular cartilage volume (Fox et al. 2009). Chondrocytes in this zone appear flattened with their long axis oriented parallel to the articular surface [Fig. 1.1 left panel] (Mansfield et al. 2015). Collagen and proteoglycan content in this zone are approximately 86% and 15% dry weight, respectively (Hu and Athanasiou 2003). Collagen fibrils in this zone are more densely packed and arranged

parallel to the joint surface so that they can withstand compressive, tensile and shear forces subjected to cartilage during articulation [Fig. 1.1 middle panel] (Fox et al. 2009).

#### 1.1.1.2. Middle zone (MZ)

The MZ contributes 40-60% of articular cartilage volume. Chondrocytes in this zone have an ovoid to round morphology [Fig. 1.1 left panel] (Fox et al. 2009). This zone is rich in proteoglycans accounting for 25% dry weight. Collagen fibrils in the MZ are arranged obliquely relative to the articular surface [Fig. 1.1 middle panel] (Frisbie and Johnson 2019; Hu and Athanasiou 2003). The MZ is considered to be the first line of resistance to compressive forces during joint loading (Hosseini et al. 2014).

#### 1.1.1.3. Deep zone (DZ)

The deep zone represents about 30% of total articular cartilage volume with proteoglycan and collagen contents of 20% and 67% dry weight respectively (Hu and Athanasiou 2003). Chondrocytes in this zone are oriented in a columnar fashion perpendicular to the joint surface [Fig. 1.1 left panel]. Collagen fibrils are also arranged parallel to chondrocytes and oriented perpendicular to the joint surface [Fig. 1.1 middle panel]. The largest magnitude of compression resistance in cartilage is provided by this zone (Fox et al. 2009; Frisbie and Johnson 2019).

#### 1.1.1.4. Calcified zone (CZ)

The CZ is separated from the DZ by a tide mark [Fig. 1.1] (Frisbie and Johnson 2019). The zone is characterised by a low density of hypertrophic chondrocytes and a mineralised matrix aiding in attachment of cartilage to the underlying bone (Huber et al. 2000).

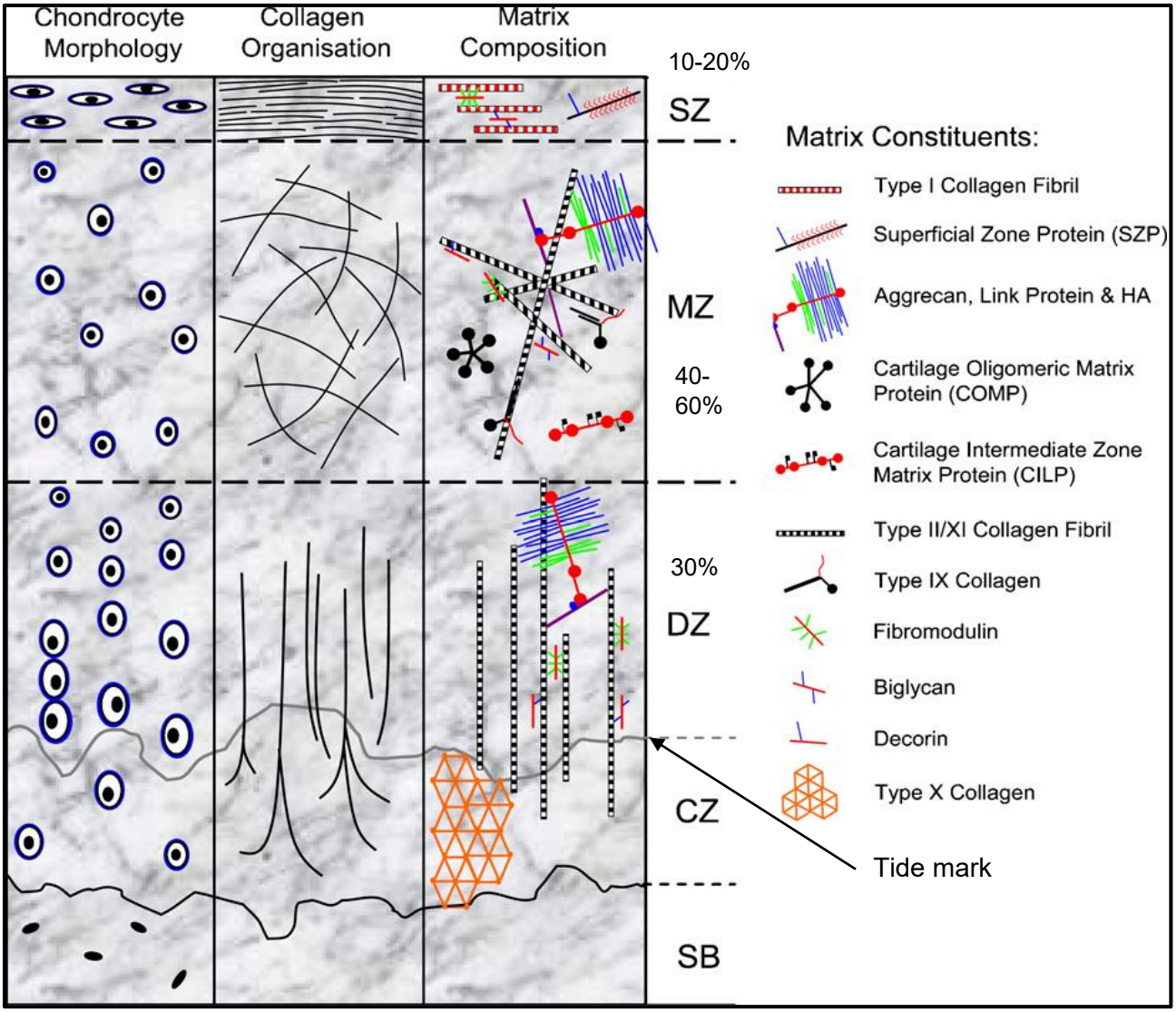


**Figure 1.1. Schematic illustration of the zonal arrangement of mature articular cartilage, composition of ECM components and collagen orientation**. Four continuous zones namely, superficial (SZ), middle (MZ), deep (DZ), and calcified zone (CZ), below which lies the subchondral bone (SB) are shown together with their approximate percentage contribution to total cartilage volume. Chondrocyte morphology (left panel), collagen fibre orientation (middle panel) and biochemical composition of the ECM (right panel) across the four zones of cartilage are also illustrated. The schematic diagram also indicates the tide mark separating the deep zone and the zone of calcified cartilage (Adapted from Hayes et al. 2007 with permission from Sage Publications).

### 1.1.2. Matrix regions

The cartilage ECM is divided into three regions, namely, pericellular, territorial and interterritorial based on composition, and the proximity to chondrocytes [Fig. 1.2] (Fox et al. 2009).

#### 1.1.2.1. Pericellular region (PCM)

The PCM is found adjacent to chondrocyte surface membranes, and it comprises of type VI collagen, proteoglycans, glycoproteins and non-collagenous proteins. The PCM is responsible for initiating signal transduction during mechanical loading in cartilage [Fig. 1.2] (Eggli et al. 1985).

#### 1.1.2.2. Territorial region

The territorial region lies adjacent to the PCM and is dominated by collagen fibrils with a basket-like organisation formed around the PCM [Fig.1.2] (Guilak and Mow 2000; Muir 1995). This region is proposed to play an important role in protecting chondrocytes against mechanical stresses (Szirmai 1969, in Fox et al. 2009).

#### 1.1.2.3. Interterritorial region

Immediately following the territorial region lies the interterritorial region (furthest from chondrocytes) which is rich in proteoglycans; therefore, the majority of the biomechanical properties of articular cartilage (i.e., compression resistance) is imparted by the interterritorial region [Fig. 1.2] (Fox et al. 2009; Mow and Guo 2002).

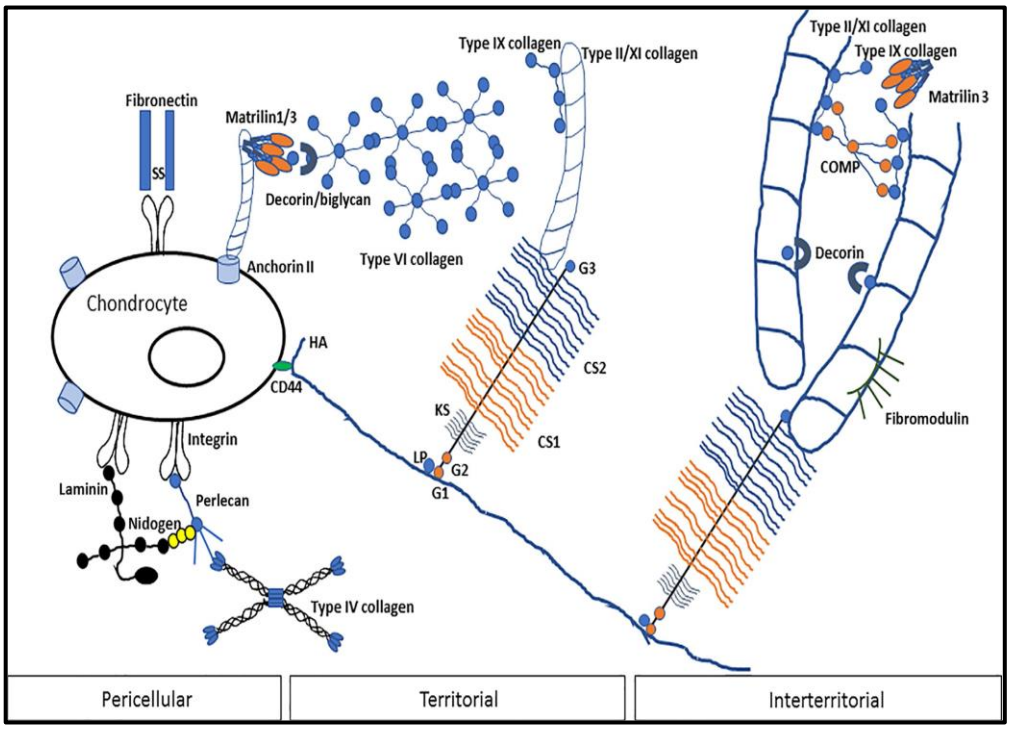


**Figure 1.2. Schematic diagram indicating the regional composition of cartilage ECM**. The three regions of cartilage ECM namely, pericellular, territorial and interterritorial matrix are shown together with the constituents of matrix in these regions and proximity to chondrocytes (Taken from Gilbert and Blain 2018 with permission from Elsevier).

### 1.1.3. Cartilage ECM composition

The ECM of articular cartilage is predominantly composed of proteoglycans, collagens and water. Additionally, non-collagenous proteins and glycoproteins are present in the ECM but in lesser quantities [Fig. 1.1] (Urban 1994).

#### 1.1.3.1. Large aggregating proteoglycans

Large aggregating proteoglycans comprise the second largest group of macromolecules in cartilage contributing about 10-15% of the wet weight (Frisbie and Johnson 2019). Proteoglycans consist of a protein core which is covalently attached to a different number of glycosaminoglycan (GAG) side chains. Sulphated GAG (sGAG) side chains found in cartilage include chondroitin sulphate (CS) (C-4-S and C-6-S in aggrecan), dermatan sulphate (DS) and keratan sulphate (KS); these are long chain repeating linear

polysaccharides consisting of hexosamine sugars and either a galactose or uronic acid sugar (Fox et al. 2009; Frisbie and Johnson 2019; Kiani et al. 2002) [Fig. 1.3]. Aggrecan is the most abundant proteoglycan in articular cartilage with a core protein ~ 250 Kilo daltons (kDa) in size through which ~100 CS molecules preferentially attach to its carboxyl end while ~50 KS molecules preferentially attach to the N-terminal (amino-terminus) region in a monomer [Fig. 1.1] (McIlwraith 2002; Watanabe et al. 1998).

#### 1.1.3.2. Non-aggregating proteoglycans

Non-aggregating proteoglycans also consist of a core protein to which GAG are covalently attached. Non-aggregating proteoglycans in cartilage include biglycan, decorin, fibromodulin, and perlecan [Figs. 1.1 and 1.2]. Apart from perlecan, the above-mentioned molecules have been termed small leucine rich proteoglycans (SLRPs) [Fig. 1.3] (Fox et al. 2009; Frisbie and Johnson 2019). 2 CS/DS chains covalently attach to biglycan core protein (38 kDa). Biglycan interacts with type VI collagen in the PCM and is involved in fibril formation (Hayes et al. 2007; Roughley and Lee 1994; Wiberg et al. 2002). Decorin consist of a core protein ~36 kDa covalently attached to 1 CS/DS chain. Decorin interacts with type I, II and IV collagens and regulate fibrillogenesis (Hayes et al. 2007; Roughley and White 1989). Fibromodulin comprises of a core protein ~42 kDa covalently attached to 4 KS chains, and it play a vital role in fibrillogenesis and interfibrillar interactions (Hayes et al. 2007; Plaas et al. 1990).

#### 1.1.3.3. Collagens

Collagen is the main structural protein found in cartilage ECM with the most abundant being type II collagen (Eyre et al. 2006; Fox et al. 2009). Minor collagens found in cartilage include type I, III, IV, V, VI, IX, X, XI, XII/XIV and XIII which are present in lesser quantities (Bland and Ashhurst 2001; Eyre et al. 2006; Fox et al. 2009). Type VI collagen is localised in the chondron basket, and it is a critical structural feature of the PCM playing a role in mechanotransduction (Eyre et al. 2006; Guilak et al. 2006; Marcelino and McDevitt 1995). Type II, IX and XI collagens are found in the superficial, middle, and deep zones [Fig. 1.1] and they cross-link to form a hetero-polymeric fibrillar network which confers tensile strength to cartilage under different loading conditions (Eyre et al. 2006; Fox et al. 2009). Type II collagen makes up 90-95% of total collagens in adult human cartilage contributing

hugely to the tensile properties of cartilage (Eyre et al. 2006; Fox et al. 2009). Type XI collagen contributes ~1% to total collagens in adult human cartilage, and it plays a crucial role in the development of normal articular cartilage structure as well as the integrity of this tissue (Eyre et al. 2006; Responte et al. 2007). However, type IX collagen makes up ~3% of total collagens in adult human cartilage, and it forms a template which hinders the lateral growth of the hetero-polymeric collagen network therefore regulating fibril diameter (Blaschke et al. 2000; Eyre et al. 2006).

#### 1.1.3.4. Glycoproteins and non-collagenous proteins

Glycoproteins and non-collagenous proteins present in articular cartilage (Cohen et al. 1998) include anchorin CII (Buckwalter et al. 2005), chondroadherin [a member of SLRPs] (Camper et al. 1997), cartilage intermediate layered protein (CILP) (Bernardo et al. 2011), cartilage oligomeric matrix protein (COMP) (Acharyaa et al. 2014), fibronectin (Martin and Buckwalter 1998), lubricin (Jones et al. 2009), matrilin-3 (Muttigi et al. 2016), tenascin-C (Savarese et al. 1996), and thrombospondin-3 [Figs. 1.1 and 1.2] (Tan and Lawler (2009).

#### 1.1.3.5. Water content

Water and electrolytes constitute the liquid phase of articular cartilage with water accounting for about 70% of the wet weight of the tissue in adults (Frisbie and Johnson 2019). The relative concentration of water varies within the zones of cartilage, and it decreases with depth. The superficial zone contains approximately 80% but the concentration decreases to about 65% in the deep zone (Buckwalter and Mankin 1997). Interstitial water quantity in cartilage is determined by several factors such as: (i) Fixed charge density (FCD) associated with proteoglycans, which refers to the measure/total number of charged sulphate ($SO_4^{2-}$) and carboxyl ($COO^-$) groups and the concentration of dissolved ions which contribute to the Donnan osmotic pressure effect; the combined effect is called swelling pressure (Lai et al. 1989; Mow et al. 1990), (ii) strength and stiffness of collagen networks and their organisation, and (iii) material properties of the solid phase of cartilage matrix (Akizuki et al. 1986; Schmidt et al. 1987). Fluids also flow within the matrix and across the articular surface providing lubrication as well as transporting and distributing nutrients to resident cells (Fox et al. 2009; Torzilli et al. 1990).

The fluid is primarily moved through the matrix by compression of the solid matrix or due to the application of pressure gradients across the tissue (Mow et al. 1980; Mow et al. 1992).

### 1.1.4. Biomechanical functions of articular cartilage

The two major biomechanical functions of articular cartilage are to: (i) ensure a smooth, lubricated articulating surface between bones at a diarthrodial joint with a low coefficient of friction, and (ii) provide support and transfer of mechanical loads across the joint when performing daily activities (Khan et al. 2008). Aggrecan permits cartilage to perform these functions as it resists compressive loads during joint motion by binding to water and occupying space. Specifically, carboxyl and sulphate functional groups within the repeating disaccharide units of sGAG found in aggrecan carry net negative charges resulting in the recruitment of cations which subsequently attract water molecules into the cartilage matrix (section 1.1.3.1) (Mow et al. 1992; Rosenberg 1978). Articular cartilage acquires its ability to withstand significant biomechanical loads from a combination of two basic mechanisms, being: (i) pressurization of water and (ii) frictional resistance to water flow within the cartilage matrix (Fox et al. 2009). Additionally, the hetero-polymeric fibrillar collagen network plays a significant role in cartilage function as it provides the tissue with high tensile strength and stiffness hence permitting the resistance of swelling forces during joint articulation (Lane and Weiss 1975) (section 1.1.3.5) [Fig. 1.3].

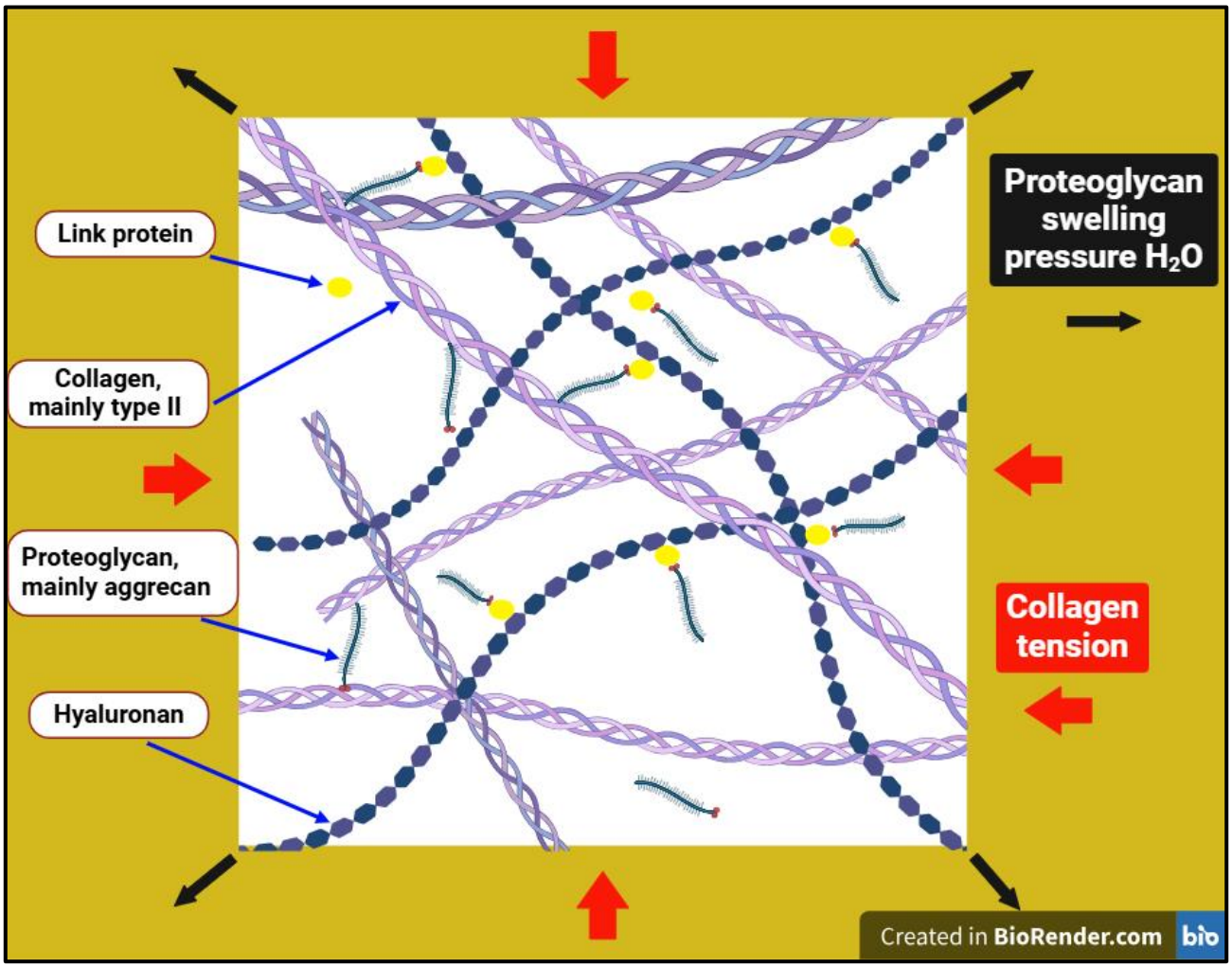


**Figure 1.3. Schematic illustration of the biomechanical function of articular cartilage facilitated by the major ECM constituents, namely collagen, proteoglycan, and water.** The diagram indicates the role of proteoglycan (e.g., aggrecan) in generating swelling pressure by attracting large volumes of water and the ability of collagens (e.g., type II collagen) to resist these swelling pressures. Ultimately, the combined effect of these ECM molecules confers cartilage its high tensile strength and stiffness properties (Created in BioRender using information from Kiani et al. 2002).

## 1.2. Cartilage mechanobiology

Previous studies have demonstrated the importance of biomechanical forces on musculoskeletal tissues including a seminal experiment whereby rats that orbited the Earth for 19.5 days on a satellite exhibited significantly reduced periosteal bone formation (Morey and Baylink 1979); furthermore, limb immobilisation for 6 weeks in a canine model revealed the significance of biomechanical forces on the regulation of cartilage matrix turnover (Palmoski et al. 1979).

Load bearing and locomotion facilitated by diarthrodial joints exposes articular cartilage and its sole resident cells, chondrocytes, to extensive cycles of mechanical load and studies suggest that mechanical loading may be the single most significant external stimulus that regulates chondrocyte behaviour (Arokoski et al. 2000; Sun 2010). Essentially, *in vitro* studies have demonstrated the suppression of proteoglycan synthesis in response to static compressive loading of articular cartilage explants (Guilak et al. 1994; Jones et al. 1982). Moreover, increased transcription of matrix metalloproteinase (*mmp*) -*3*, -*9* and -*13*, as well as a disintegrin and metalloproteinase with thrombospondin-1 like motifs ((*adamts*) -*4* and -*5*, also known as aggrecanase-1 and -2, respectively) and the matrix protease regulator cyclooxygenase-2 (*cox-2*) was observed in bovine cartilage explants subjected to 50% static compressive strains for 24 hours (Fitzgerald et al. 2004). In contrast, physiological mechanical forces applied to chondrocytes regulate tissue homeostasis by eliciting a balance between the chondrocyte phenotype gene marker *sox9*, anabolic (e.g., expression of *acan*, *col2a1*) and catabolic ECM activities (e.g. expression of *adamts-4* and -*5*, as well as *mmp-1*, -*3* and -*13*), hence promoting the maintenance of a slow but consistent turnover of cartilage matrix [Fig. 1.4]. However, exposure of cells to non-physiological mechanical stress i.e., excessive, or injurious, induces maladaptive cellular responses, for instance, shifting cell metabolism towards inflammatory and catabolic events which compromises cartilage integrity (tissue deterioration) subsequently leading to pathological phenotypes such as OA (Quinn et al. 1998; Wong et al. 1999) [Fig. 1.4].

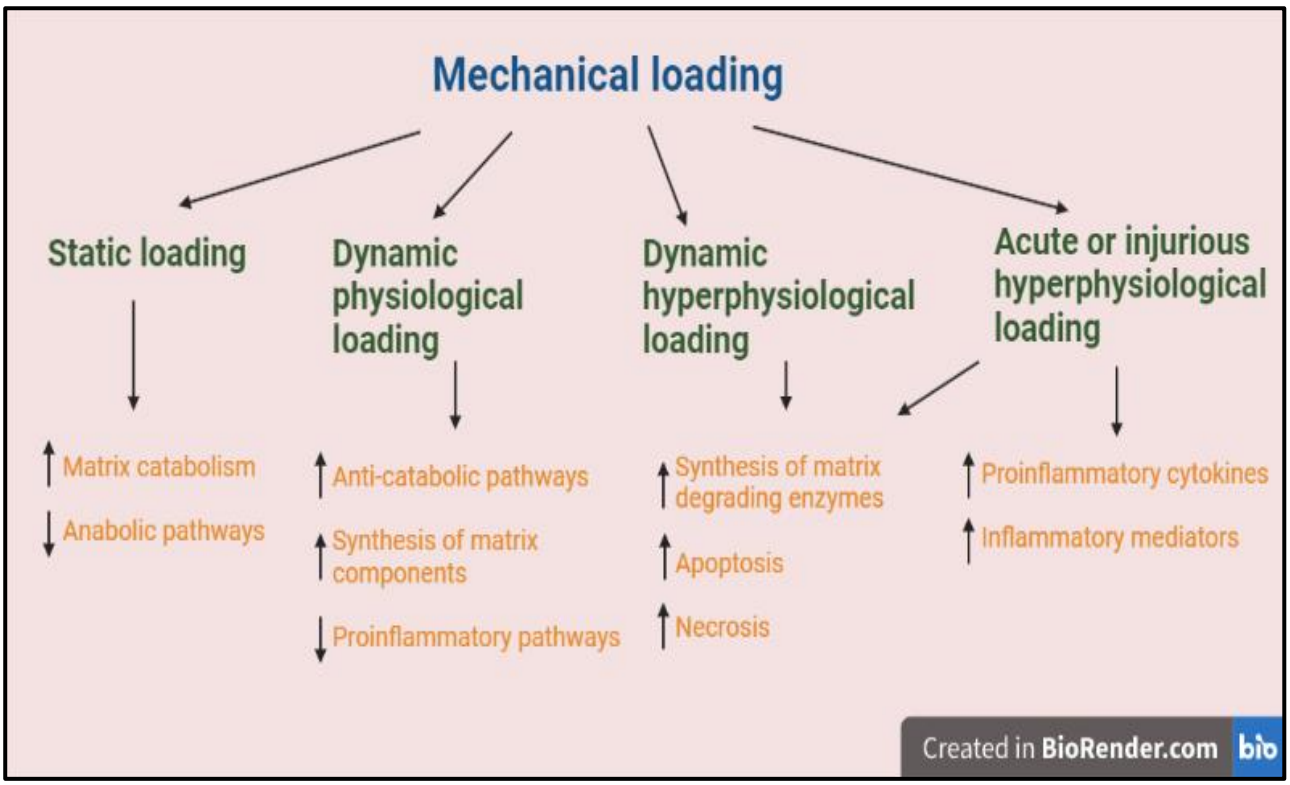


**Figure 1.4. Illustration of diverse metabolic responses of chondrocytes to various modes and magnitudes of mechanical loading**. Static loading induces a decrease in the synthesis of matrix components whilst elevating catabolic activities; however, dynamic physiological loading promotes tissue homeostasis. Excessive loading leads to increased synthesis of matrix degrading enzymes as well as apoptosis and necrosis, while injurious loading elevates the production of proinflammatory cytokines, inflammatory mediators, mediators of matrix catabolism and cell death (Created in Biorender using information from Guilak et al. 1994; Quinn et al. 1998; and Wong et al. 1999).

### 1.2.1. Influence of differing types of physiological mechanical loads on cartilage ECM metabolism

Over the past few decades, various *in vitro* and *in vivo* models have been utilised to study cartilage/chondrocyte mechanobiology instrumental in the assessment of the effect of mechanical forces on cell function and matrix molecule production. During joint loading, chondrocytes embedded in a dense matrix are subjected to a dynamic mechanical environment encompassing the integration of hydrostatic and osmotic pressure, compression, tensile strain, and shear stress to elicit metabolic changes (Anderson and Johnstone 2017; Gilbert et al. 2021; Ramage et al. 2009). For instance, human knee

chondrocytes localised in opposing articulating surfaces can experience dynamic compressive stresses of 5-6 MPa during walking, whilst dynamic compressive stresses of 10-20 MPa can be experienced in the knee and hip joints during activities such as climbing stairs (Morrell et al. 2005). Additionally, previous studies reported that under physiological i.e. low-strain, mechanical loading, mechanotransduction pathways are mediated through the transient receptor potential vanilloid 4 (TRPV4) ion channels (Clark et a. 2010; Li et al. 2011; O'Conor et al. 2014; Phan et al. 2009). Application of mechanical loads within a physiological range of intensity, duration and frequency induces anabolic ECM activities in chondrocytes including increased expression of aggrecan and type II collagen as well as elevated proteoglycan synthesis hence maintaining cartilage integrity (Gilbert et al. 2021; Ramage et al. 2009).

#### 1.2.1.1. Dynamic compressive forces

*In vivo*, cartilage in articulating surfaces of diarthrodial joints is subjected to compressive forces during weightbearing. Several previous studies have demonstrated increased biosynthesis of ECM molecules in chondrocytes exposed to physiological magnitudes of dynamic compression (~10-20%), particularly, type II collagen and proteoglycans (Gilbert et al. 2021). In bovine articular cartilage explants, 0.5 MPa dynamic compressive strain (repeated at 2-, and 4-seconds for 1.5 hours) increased proteoglycan production (Parkkinen et al. 1992) and 1 hour of 0.1 MPa dynamic compressive strain increased aggrecan mRNA synthesis (Valhmu et al. 1998). Application of 15% dynamic compressive strain (1 Hz, 48 hours) to skeletally mature bovine chondrocyte-agarose cylinders stimulated sGAG synthesis (Lee and Bader 1997; Shelton et al. 2003). Skeletally immature bovine cartilage explants subjected to a sinusoidal dynamic displacement of amplitude 50 μm (0.01 Hz, 23 hours) exhibited increased aggrecan synthesis correlating with tissue regions experiencing high interstitial fluid velocities as a result of cyclical compressive loading (Buschmann et al. 1999). 10% intermittent compressive stress [1 Hz, 3× (1 hour on, 1 hour off)/day] on chondrocyte-seeded agarose disks resulted in increased sGAG and collagen content at day 21 (Mauck et al. 2000). Another *in vitro* study demonstrated significantly increased proteoglycan synthesis in bovine 3D chondrocyte/agarose constructs subjected to 15% dynamic compressive strain (1 Hz) at differing loading durations with maximal induction following 12 hours of intermittent compression (Chowdhury et al. 2003). Skeletally immature porcine chondrocyte-agarose constructs subjected to 10% dynamic compressive strain (1 Hz, 3 hours/day over a 4-week

period) exhibited significantly increased ECM accumulation evidenced by enhanced total sGAG and collagen synthesis (O'Conor et al. 2014).

#### 1.2.1.2. Cyclical tensile strain (CTS)

*In situ*, articular chondrocytes experience tensile strain primarily due to compression-induced cartilage deformation (Guilak 1995). A review of literature reporting the influence of cyclical tensile strain on chondrocyte metabolism *in vitro* revealed anabolic responses mostly at strain magnitudes ranging from 3-10%, at frequencies between 0.17 and 0.5 Hz and loading durations between 2 and 12 hours (Bleuel et al. 2015). However, 5% cyclical tensile strain (0.17 Hz, 24 hours) increased proteoglycan production in skeletally immature bovine chondrocyte monolayers (Fukuda et al. 1997). Enhanced proteoglycan synthesis was also observed in skeletally immature bovine chondrocyte monolayers following application of 7% cyclical tensile strain (0.167 Hz, 24 hours) (Matsukawa et al. 2004). Skeletally immature porcine chondrocyte monolayers subjected to 10% dynamic tensile strain (0.5 Hz, 3 hours) demonstrated increased expression of type II collagen and aggrecan mRNAs (Huang et al. 2007). Application of 3% intermittent tensile strain (0.5 and 2.5 Hz, 12 hours) to rat rib growth plate chondrocyte monolayers significantly elevated the synthesis of proteoglycans and collagens (Ueki et al. 2008). Thomas et al. (2011) demonstrated significant induction of aggrecan and type II collagen transcription by 4 hours in skeletally immature bovine chondrocyte monolayer cultures following application of 7.5% cyclical tensile strain (1 Hz, 0.5 hours). In another *in vitro* study, exposure of healthy adult human articular chondrocyte monolayers to cyclical pressure-induced strain of 3000 μstrain (0.33Hz, 20 minutes) [equivalent to a pressure pulse of 50 kPa] resulted in the upregulation of aggrecan mRNA transcripts within 1 hour following mechanical stimulation (Millward-Sadler et al. 2000).

#### 1.2.1.3. Dynamic hydrostatic/osmotic pressure

During joint articulation, the interplay between proteoglycans, collagens and water in the cartilage matrix generates hydrostatic pressure in the tissue, whilst the exudation of water and ions during loading can alter the biophysical environment resulting in alterations of local pH and osmolarity (creating osmotic pressure gradients) (Gilbert et al. 2021). Reviews on the effect of hydrostatic pressure on chondrocyte metabolism reported

significantly increased synthesis of proteoglycans following the utilisation of dynamic hydrostatic loading regimens (i.e., magnitudes within the mid-high physiological range [≤5-10 MPa] and a study duration of ≥2 weeks) in articular cartilage explants or chondrocytes (Gilbert et al. 2021; Hodder et al. 2020). In an *in vitro* study, adult bovine articular cartilage explants subjected to 5-15 MPa intermittent hydrostatic pressure (applied for 20 seconds or for 5 minutes over a 2-hour period) as well as 5-10 MPa continuous hydrostatic pressures for 2 hours demonstrated increased proteoglycan synthesis evidenced by sulphate incorporation into GAG (Hall et al. 1991). Another *in vitro* study revealed the induction of sulphate incorporation into GAG in bovine articular cartilage explants subjected to 5 MPa cyclical hydrostatic pressure (0.5 Hz, 1.5 hours) (Parkkinen et al. 1993); chondrocyte monolayer cultures also exhibited increased proteoglycan synthesis following application of 5 MPa cyclical hydrostatic pressure at frequencies of 0.25 and 0.5Hz (20 hours) (Parkkinen et al. 1993). *In vitro* application of 10 MPa intermittent hydrostatic pressure (1 Hz, 4 hours) to adult bovine articular chondrocyte monolayer cultures resulted in significant increases in proteoglycan synthesis as well as mRNA and protein levels for aggrecan and type II collagen (Smith et al. 1996). Moreover, Ikenoue et al. (2003) demonstrated significantly increased mRNA levels for aggrecan and type II collagen in healthy adult human knee articular chondrocyte monolayer cultures in response to 5 and 10 MPa intermittent hydrostatic pressure (1 Hz, 4 hours per day over a 4-days period [4 x 4] (increased aggrecan transcription was also observed following the 4 x 1 regimen). Exposure of skeletally immature bovine chondrocyte monolayer cultures (derived from wrist joint cartilage; 4-6 months old) to -200 milliosmoles (mOSM) intermittent osmotic pressure (0.1 Hz, 2 hours) also significantly increased expression of aggrecan and type II collagen mRNAs (Chao et al. 2006).

#### 1.2.1.4. Intermittent shear stress

Principally, the movement of synovial fluid over articular cartilage during articulation in diarthrodial joints generates pressure against these tissues resulting in fluid shear stress; however, pressure generated upon joint movement entailing solid-on-solid contact (e.g., femoral condyle and tibial plateau cartilage in the knee joint) is known as contact or tissue shear stress (Gilbert et al. 2021). A study which systematically reviewed the influence of shear stress on chondrocytes demonstrated enhanced synthesis of proteoglycans and collagens in response to physiological shear force regimens mostly at 1-3% amplitudes and frequencies between 0.01 and 1 Hz (Sharifi and Gharravi 2019). Using a spinner flask bioreactor, application of fluid shear at a turbulent mixing intensity resulting from 80 rpm

stress to skeletally immature bovine chondrocytes seeded in fibrous polyglycolic acid meshes induced significant increases in sGAG release and collagen synthesis over a 6-week period (Gooch et al. 2001). In another *in vitro* study, collagen and proteoglycan synthesis was stimulated by application of 1-3% sinusoidal fluid shear strain (0.01-1.0 Hz) in skeletally immature bovine cartilage explants (Jin et al. 2001). Increased production of collagen and sGAG was observed in skeletally immature bovine chondrocytes seeded in polyglycolic acid scaffolds cultivated in wavy-walled bioreactors creating a high-axial mixing environment simulating fluid shear stress (Bueno et al. 2005). Application of 3% dynamic shear stress (0.1 Hz; 24 hours) to immature bovine cartilage explants resulted in significantly increased production of lubricin (Nugent et al. 2006). A significant increase in collagen content as well as mRNA levels for type II collagen and aggrecan were observed at week 2 and 4 in the integration zones of skeletally mature bovine articular cartilage constructs implanted into host cartilage prior to incubation in spinner bioreactors with magnetic stir plate maintained at 90 rpm generating dynamic fluid shear stress (Theodoropoulos et al. 2016). Other studies have demonstrated increased biosynthesis following application of dynamic contact shear stress to chondrocytes. Waldman et al. (2003) reported enhanced collagen and proteoglycan synthesis 1 and 4 weeks after application of 2% intermittent shear strain (1 Hz) to bovine articular cartilage constructs derived from metacarpophalangeal joint chondrocytes seeded in porous calcium polyphosphate scaffolds. Magnitudes of dynamic tissue shear stress between 1.5 and 6% (0.1 Hz, 24 hour) induced significant increases in collagen and proteoglycan synthesis in skeletally immature bovine femoropatellar cartilage disks (Jin et al. 2003).

### 1.2.2. Anti-inflammatory effects of physiological mechanical loads

Application of mechanical loads within a physiological range of intensity, duration and frequency has also been demonstrated to elicit potent anti-inflammatory actions as evidenced by the counteraction of catabolic effects of proinflammatory cytokines such as interleukin-1 (IL-1) or tumour necrosis factor-$\alpha$ (TNFα) (Bleuel et al. 2015). Exposure of IL-1$\beta$ (1 ng/ml) stimulated rabbit chondrocyte monolayers to 20% cyclical tensile strain (0.05 Hz, 96-hour period) resulted in reduced mRNA and protein expression levels for inducible nitric oxide (NO) synthase (*inos*) concomitant with significant increases in proteoglycan synthesis (Gassner et al. 1999). Xu et al. (2000) also demonstrated that in rabbit chondrocyte monolayers stimulated with 1 ng/ml IL-1$\beta$, exposure to either 2.5-, 3.75-, 5-, 6.25- or 7.5-% equibiaxial CTS (0.05 Hz, either 4-,8-,24- and 48-hours) reduced

transcription of catabolic mediators including *inos*, *cox-2* and *mmp-1* concomitant with increased transcription of tissue inhibitor of metalloproteases (*timps*) and *col2a1* as well as a rescue of IL-1*β*-induced inhibition of proteoglycan synthesis (Xu et al. 2000). Moreover, TNF*α* (1 ng/ml) stimulated rabbit chondrocyte monolayers subjected to 6% CTS (0.05 Hz; 4-, 8-, 24- or 48-hours) exhibited suppressed TNF*α*-induced transcription of catabolic mediators such as *inos*, *cox-2* and *mmp-1* concomitant with increased transcription of *timp2*, and the rescue of TNF*α*-induced inhibition of proteoglycan production (Long et al. 2001). Other *in vitro* studies corroborated the inhibition of IL-1β-induced (10 ng/ml) *inos* and *cox*-2 expression as well as NO and $PGE_2$ production in 3D bovine chondrocyte cultures following application of 15% dynamic compression (1 Hz; 6-, 12- or 48-hours) (Chowdhury et al. 2001; Chowdhury et al. 2008). Application of 3-8% cyclic tensile strain (0.25 Hz, 8- or 16-hours) to skeletally mature rat articular chondrocyte monolayers inhibited transcription of *inos*, *cox-2*, *mmp-9* and *-13*, whilst increasing *timp-II* synthesis (Madhavan et al. 2006). The suppression of *inos*, *cox-2* and *mmp* gene expression following exposure of chondrocytes to compressive and tensile mechanical stimuli is reported to be mediated through the inhibition of the nuclear factor-kappa B (NF*κ*B) signal transduction pathway (Agarwal et al. 2004; Akanji et al. 2010). Another mechanism through which mechanical loading enhances anabolic pathways is by inhibiting cytoplasmic dissociation of NF*κ*B from inhibitory *κ*B-*α* (I*κ*B-*α*); this prevents the nuclear translocation of the p65/p50 dimers and/or proteolytic degradation of I*κ*B-*α* by two I*κ*B-specific kinases (IKK*α* and IKK*β*), therefore repressing proinflammatory gene transcription (Bader et al. 2011). However, the NF*κ*B cascade is affected by both proinflammatory cytokines and mechanical signals which either exacerbate or hinder transcriptional induction of various gene markers for ECM catabolism following cytokine stimulation. Studies also revealed NF*κ*B-dependent and independent mechanisms through which mechanical signals suppress proinflammatory responses suggesting crosstalk with other signalling pathways as evidenced by induction overlap of several genes known to be involved in both the NF*κ*B and mitogen-activated protein kinase (MAPK) signal transduction pathways (Bader et al. 2011).

### 1.2.3. Influence of non-physiological loading on catabolic pathways implicated in OA pathology

#### 1.2.3.1. Excessive/injurious mechanical loading

Exposure of cartilage to excessive or non-physiological mechanical loads triggers a shift in equilibrium between anabolic and catabolic events resulting in the disruption of ECM structure and composition reducing the tissue's biomechanical integrity (Gilbert et al. 2021). *In vitro* loading studies have demonstrated that hyper-physiological compressive loads of magnitudes exceeding 20 MPa (or exceeding 10% CTS) inhibits proteoglycan production concomitant with the rapid loss of endogenous proteoglycans, accompanied by reduced collagen synthesis and the degradation of the collagen network in bovine cartilage explants (Bleuel et al. 2015; Torzilli et al. 1999). A significant reduction in proteoglycan synthesis was observed in skeletally immature bovine articular chondrocyte monolayers subjected to 15% cyclical tensile strain (0.17 Hz; 24 hours) (Fukuda et al. 1997). 2D skeletally immature rabbit articular chondrocyte cultures subjected to 23% cyclical tensile strain (0.5 Hz, 12 hours) demonstrated enhanced transcription of *mmp-1*, *-3* and *-9*, as well as *IL-1β*, and *TNFα* (Honda et al. 2000). Significant reductions in proteoglycan and total protein biosynthesis were also observed in skeletally immature bovine articular cartilage explants exposed to dynamic compression with strain rates of 0.1 and 1 $s^{-1}$ resulting in peak stresses of ~18- and 24-MPa, respectively (Kurz et al. 2001). However, application of 10% dynamic tensile strain (0.5 Hz, 24 hours) to skeletally immature porcine chondrocyte monolayers significantly increased in *mmp-1* mRNA, signifying a shift towards matrix remodelling (Huang et al. 2007). Application of 16% cyclical tensile strain (0.5 Hz, 48 hours) to skeletally mature bovine chondrocyte monolayers significantly increased *mmp-3* and *-13*, as well as *adamts-4* and *-5* mRNA levels concomitant with reduced *col2a1* mRNAs [whilst aggrecan transcription was unaffected] (Wang et al. 2011). Moreover, this excessive loading regimen also enhanced transcription of inducible enzymes, *inos* and *cox-2* and their respective mediators, NO and $PGE_2$ as well as hypertrophy-associated genes, type X collagen (*col10a1*) and runt-related transcription factor 2 (*runx2*) (Wang et al. 2011). Significantly reduced aggrecan and type II collagen mRNA levels were observed in skeletally immature rat articular chondrocyte monolayers subjected to 10% cyclical tensile strain (0.167 Hz, 12- and 24-hours) (Ru-song et al. 2012).

*In vivo* models have also demonstrated the catabolic effects of excessive mechanical loading regimen in regulating cartilage ECM metabolism. A strenuous treadmill running regimen (up to 20 km/day for one year) in young female beagle dogs (started at 15 weeks old) reduced articular cartilage thickness in the medial femoral condyle concomitant with decreased proteoglycan content in the summits of the femoral condyles with more prominent reductions in the superficial zone (Kiviranta et al. 1992). Significant reductions in proteoglycan content were also observed in the weightbearing regions (e.g., summits of the femoral condyles, lateral condyle of the femur, lateral condyle of the tibia and the head of the humerus) of young pure breed beagle dogs' articular cartilage particularly prominent in the superficial zone following a strenuous treadmill running regimen (up to 40 km/day for one year; started at 15 weeks old) (Arokoski et al. 1993). Induction of post-traumatic OA (PTOA) in mice, via the rupture of the anterior cruciate ligament (ACL) following application of a single compressive load (12N, 1.4 mm/s) significantly increased mRNA levels for acute proinflammatory markers, *inos*, and *il-6*, and matrix degrading enzymes, *adamts-4* and *mmp-3*, in femoral cartilage at 4 hours post ACL rupture as well as extensive loss of proteoglycans and collagen over 21-days post-injury (Gilbert et al. 2018). Previous studies have reported the involvement of the mechano-sensitive piezo1 and piezo2 channels in the mechano-regulation of chondrocyte metabolism following hyper-physiological loading regimens ~>45% strain (Du et al. 2020; Lee et al. 2005; Lee et al. 2017).

Injurious/traumatic mechanical signals have previously been demonstrated to induce the production of proinflammatory cytokines including IL-1 and TNF*α* (Goldring and Marcu 2009). Upon proinflammatory cytokine release, increased production and activation of proteolytic enzymes occur, reported to be mediated by inductive stimuli including NO, $PGE_2$ and reactive oxygen species (ROS) (Fernandes et al. 2002; Henrotin et al. 2003; Kim and Blanco 2007; Martel-Pelletier et al. 2008). MMPs and aggrecanases are well defined proteolytic enzymes capable of degrading native collagen and proteoglycans in cartilage (Cawston and Wilson 2006; Rengel et al. 2007; Sandy 2006). Enhanced levels of proteinases result in the cleavage of ECM components leading to the accumulation of matrix fragments. These matrix fragments augment catabolic protease-driven pathways which ultimately override anabolic events resulting in cartilage degeneration and this shift of cell metabolism contributes to the onset of OA (Del Carlo et al. 2007; Guo et al. 2009; Homandberg 1999; Stanton et al. 2002; Xie et al. 1994). Matrix degrading proteinase enzymes in joint diseases include the collagenases (MMP-1, MMP-8 and MMP-13),

gelatinases (MMP-2 and MMP-9), stromelysin-1 (MMP-3) and membrane type I (MT1) MMP (MMP-14) (Murphy and Nagase 2008). Other MMPs such as MMP-10, which is similar to MMP-3, are also detectable in joint tissues, OA and rheumatoid arthritis (RA) synovial fluids, as well as synovium and *in vitro* chondrocyte cultures in response to inflammatory cytokines (Barksby et al. 2006). In RA, MMP-14 is predominantly synthesised by synovial tissue, and it plays a role in synovial invasiveness (Rutkauskaite et al. 2005), whilst in OA, MMP-14 activates pro-MMP-13 prior to its production by chondrocytes. Pro-MMP-13 has a role in proteolytic cleavage of pro-MMP-9 (Dreier et al. 2004). Despite the capability of select MMPs such as MMP-3, MMP-8, and MMP-14, to degrade proteoglycans, it has been established that ADAMTS-4 and -5 are the main aggrecan-degrading enzymes in cartilage (Arner 2002; Plaas et al. 2007).

#### 1.2.3.2. Static mechanical loading

*In vivo*, articular cartilage at various diarthrodial joints can experience static compressive strains depending on the type of activity performed. Fundamentally, prolonged static compression induces indirect physicochemical effects such as streaming potentials, changes in pericellular pH, osmolarity, fixed charge density and osmotic pressure due to the expulsion of water and ions from the cartilage ECM which ultimately triggers the suppression of ECM synthesis (Gilbert et al. 2021). Application of 25% static compressive strain (12 hours) to skeletally immature bovine articular cartilage explants inhibited proteoglycan and collagen synthesis, whilst 50% static compression only inhibited collagen synthesis (Sah et al. 1989). Sah et al. (1991) also demonstrated significantly reduced proteoglycan and collagen content in skeletally immature bovine articular cartilage explants subjected to ~60% static compressive strain (12 hours). 0.057-, 0.1-, 0.5- and 1.0-MPa static compressive stresses (24 hours) suppressed proteoglycan synthesis in skeletally mature bovine articular cartilage explants (Guilak et al. 1994). Using the same *in vitro* model and compression system described by Sah et al. (1989), another study also demonstrated that 50% static compression (12 hours) inhibited the production of aggrecan and link protein but not hyaluronan suggesting that static compression induces selective inhibition of ECM biosynthetic pathways potentially in a spatial-temporal manner (Kim et al. 1996). Utilising the same model and compression system described by Sah et al. (1989), significantly reduced aggrecan and type II collagen mRNA and protein levels were observed following application of 50% static compression (4 and 24 hours) (Ragan et al. 1999).

### 1.2.4. Mechanotransduction in chondrocytes

The process through which chondrocytes sense the physical forces together with subsequent intracellular biochemical pathways which ensues before the cells can produce appropriate adaptive responses (e.g., growth regulation, cellular differentiation, gene expression and metabolism) is called mechanotransduction (Sanchez-Adams et al. 2014). Mechanistically, the type of mechanical stimuli transmitted or subjected to cells hugely influences the mechanotransduction pathways by which chondrocytes respond to adapt to their biomechanical environment (Harris et al. 2012; Hodge et al. 1986; Urban 1994). Chondrocytes in cartilage are found encapsulated within a thin layer of PCM known as the ‘‘chondron’’ (Poole 1997). It has been reported that the chondron in different zones of cartilage show variable deformation when the tissue is exposed to compressive forces (Choi et al. 2007). Chondrocytes within SZ chondrons are reported to be shielded from ECM strains since SZ ECM has the lowest elastic modulus in comparison to those of deeper zones, where the PCM is responsible for amplifying strain magnitudes relative to those of the ECM (Poole et al. 1987). This demonstrates that the PCM is involved in modulating cellular strains across all cartilage zones, thereby providing a more uniform environment for the resident cells and possibly protecting chondrocytes from excessive strains which may cause injury (Poole et al. 1987; Poole et al. 1988). The PCM in articular cartilage has emerged as a potential transducer of mechanical signals since it is capable of either amplifying or attenuating local mechanical strains, and consequently converting cartilage deformations into biochemical or physicochemical changes within the chondrocyte microenvironment (Haider et al. 2006; Sanchez-Adams et al. 2014; Vincent et al. 2004). The unique structure and biochemical make-up of the PCM allows it to act as a transducer of mechanical signals (section 1.1.2.1).

Several key mechanisms have been identified including soluble mediators, integrin receptors, mechanosensitive ion channels, and primary cilia which are involved in mechano-coupling [Fig. 1.5]. These mechanoreceptors are situated on chondrocyte membranes, and they have the capacity to effect cellular responses following mechanical stimulation thus allowing cartilage to adapt to the new mechanical environment (Gilbert and Blain 2018; Sanchez-Adams et al. 2014). Moreover, some of the intracellular signalling pathways downstream of mechano-coupling include Wnts (wingless-type MMTV

integration site family members), MAPK and transforming growth factor beta (TGF-β) signalling which can regulate tissue remodelling [Fig. 1.5] (Gilbert and Blain 2018).

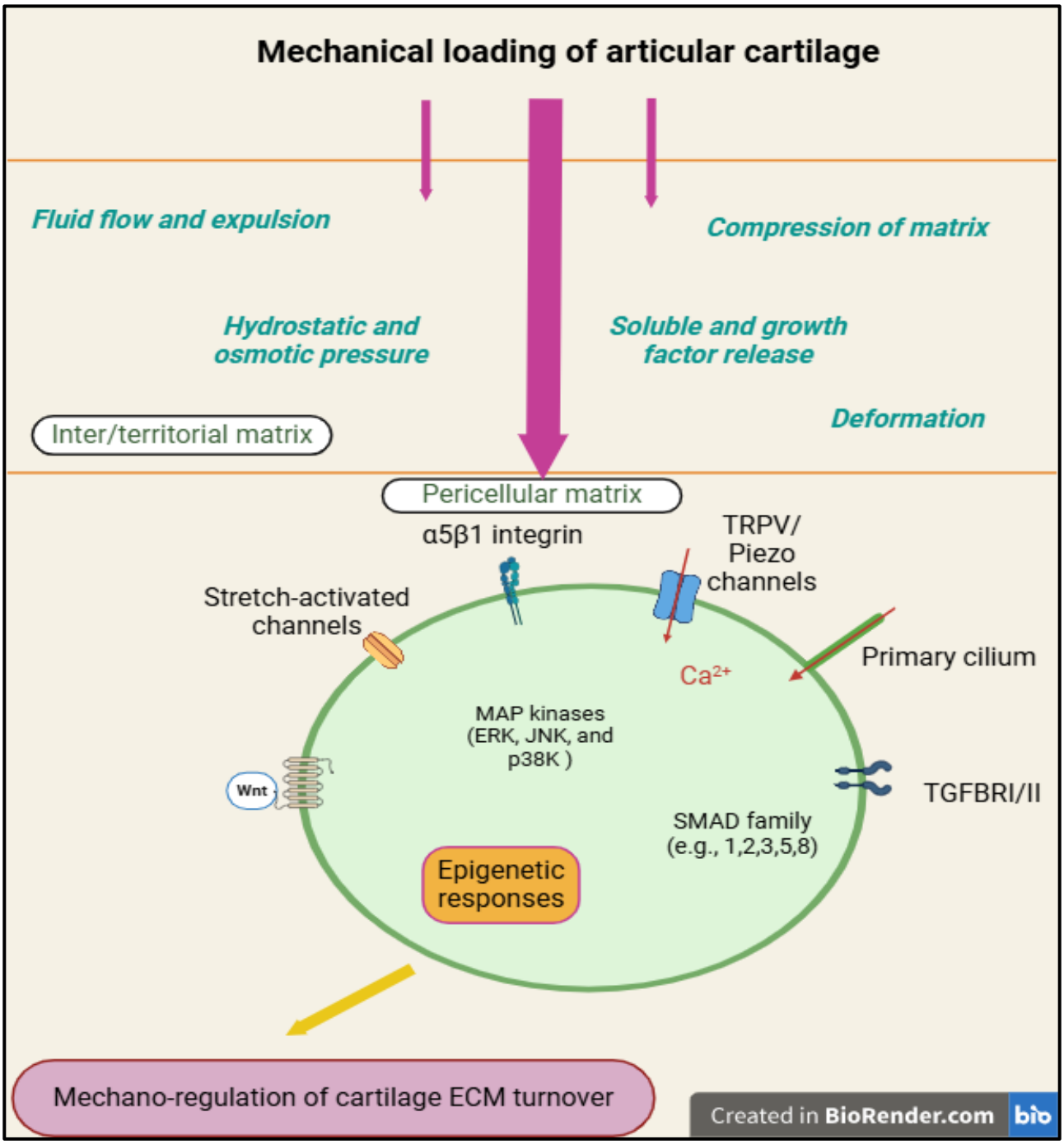


**Figure 1.5. Schematic illustration of mechano-coupling, mechanoreceptors and cascades of intracellular events activated by mechanical stimulation of articular cartilage leading to diverse chondrocyte responses.** Mechanical forces subject cartilage ECM to various stresses which are transmitted to chondrocytes via the PCM. The signals activate mechanoreceptors at the surface of chondrocytes which then initiate their transduction into intracellular signalling events. Ultimately, chondrocytes adapt to the new mechanical environment by remodelling the ECM through regulation of transcription, translation, and/or molecule secretion (Created in BioRender using information from Blain 2011, and Zhao et al. 2020).

## 1.3. Circadian biology

The majority of physiological processes in light-sensitive living organisms, from cyanobacteria to humans are controlled by the circadian clock which is a collection of endogenous cellular oscillators with an approximate 24-hour rhythmic cycle; this ensures that organisms can predict and align their physiological processes to the daily variations of light and temperature synchronised to the Earth's rotation hence driving circadian rhythms (Reppert and Weaver 2002; Roenneberg and Merrow 2005). Circadian rhythmicity is normally exemplified by the sleep/wake cycle, but it is also noticeable in feeding behaviour, blood pressure regulation, metabolism, body temperature and many other processes (Reppert and Weaver 2002; Takahashi et al. 2008). Oscillators of the mammalian circadian clock are ubiquitous and autonomously function at a cellular, tissue and systems level (Mohawk et al. 2012). There are three core characteristics of a circadian rhythm which states that it must be: (i) endogenous [free running with a period of ~24 hours], (ii) entrainable [i.e., capable of being synchronised to the outside world by external stimuli], and (iii) temperature compensated [i.e., within a physiological temperature range the rhythms must remain relatively constant] (Carroll et al. 2019). The mammalian circadian clock is organised hierarchically with the central circadian pacemaker (master clock) situated in the suprachiasmatic nucleus (SCN) of the anterior hypothalamus in the brain [Fig. 1.6]. Subordinate clocks are present in almost all peripheral tissues including articular cartilage (Jacob et al. 2020). Light (representing a photic Zeitgeber) is the primary signal used by the SCN to synchronise the body time to the external day through neural and hormonal signals. Circadian rhythm can also be entrained by non-photic Zeitgeber including exercise, temperature, sleep-wake cycle and the feeding-fasting rhythms [Fig. 1.6] (Jacob et al. 2020). Previous studies have shown that the robustness of circadian rhythms deteriorate during ageing in various tissues resulting in the disturbance in the temporal control of physiology (Nakamura et al. 2011; Orozco-Solis and Sassone-Corsi 2014).

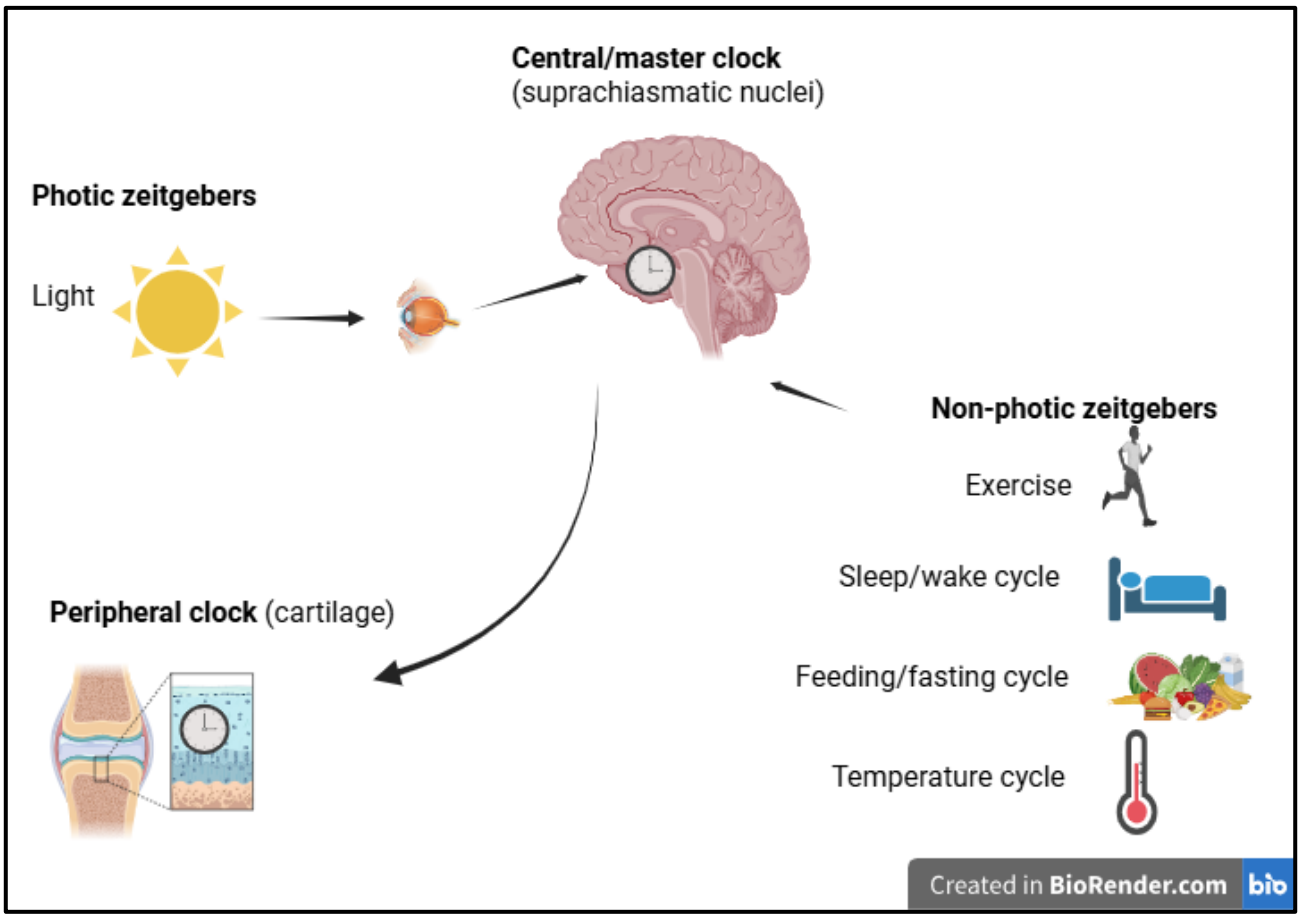


**Figure 1.6. Schematic illustration of the hierarchical organisation and cues which entrain the human circadian system**. The SCN is the master clock (localised in the anterior hypothalamus of the brain) which uses light as the most powerful external cue to entrain the internal timing system, but non-photic signals such as exercise, sleep/wake cycle, feeding/fasting cycle, and temperature cycle also entrain circadian clocks hence coordinating tissue-specific temporal physiology (Created in BioRender using information from Jacob et al. 2020).

### 1.3.1. The molecular mechanism of the circadian clock in mammals

At the molecular level, a core clock mechanism of interlocking autoregulatory transcriptional/translational feedback loops of clock genes and proteins drives the rhythmic circadian oscillators in mammalian cells. The primary feedback loop of the circadian clock is made up of the positive arm consisting of *BMAL1* (brain and muscle ARNT-Like 1/aryl hydrocarbon receptor nuclear translocator-like protein 1 (*ARNTL1*)) and *CLOCK* (circadian locomotor output cycles kaput) and/or the *CLOCK* paralog *NPAS2* [neuronal PAS domain protein 2]) and the negative arm comprising of *PER-1/2* (period circadian regulator -

1/2), and *CRY-1/2* (cryptochrome circadian regulator -1/2) [Fig. 1.7] (Jacob et al. 2020; Mohawk et al. 2012). Upon transcriptional activation of members of the positive arm in the nucleus, e.g. *BMAL1* activation by the binding of RORs (retinoic acid receptor-related orphan receptor) to Rev-responsive element (RRE) in its promoters, BMAL1 heterodimerises with CLOCK to form a BMAL1/CLOCK complex during the day which activates the transcription of their target genes such as *PER-1/2*, and *CRY*-1/2 by binding to the cis-regulatory element E-box (enhancer box) in their promoters (Jacob et al. 2020) [Fig. 1.7]. After translation in the cytoplasm, PER and CRY proteins translocate to the nucleus to bind to the BMAL1/CLOCK complex hence repressing its activity [Fig. 1.7]. During the night, the remaining proteins undergo gradual phosphorylation by casein kinase Iε/δ (CK Iε/δ) and AMP kinase (AMPK) for PER-1/2 and CRY-1/2, respectively. This induces polyubiquitination by Skp1-Cullin-F-box protein (SCF) E3 ubiquitin ligase complexes involving FBXL3 (F-box and leucine rich repeat protein) and β-TrCP (Beta-transducin repeat-containing protein) for CRY-1/2 and PER-1/2 before they are degraded by the 26S proteasome complex, therefore the CLOCK/BMAL1 complex can start another rhythmic cycle of transcription activation (Partch et al. 2014; Takahashi et al. 2008) [Fig. 1.7].

Additional feedback loops exist which also interlock with the core CLOCK-BMAL1/PER-CRY feedback loop to fine-tune the precision of the clock (Mohawk et al. 2012). The most conspicuous stabilising loops directly targeted by CLOCK-BMAL1 involves several nuclear hormone receptors, whereby interaction occurs via E-box elements (for genes such as *RORs* (*RORα*, *RORβ* & *RORγ*, which are activators) and *REV-ERBs -α & β* (reverse strand of *ERB*/*THR-A and -B* [thyroid hormone receptor-α and -β {also known as nuclear receptor subfamily 1 group D member -1 & -2 (*NR1D1 & NR1D2*}, which are repressors] [Fig. 1.7]. Proteins of clock-controlled genes of the PAR-bZip family such as *DBP* (albumin D box-binding protein) bind to the D-box (DNA cis-element box) regulatory elements of core clock genes (e.g., *PER1*) to activate their expression and can be repressed by the bZip protein, *NFIL3* (nuclear factor, interleukin 3 regulated; also known as E4BP4 [E4 Promoter-Binding Protein 4]) in an auxiliary stabilizing loop [Fig. 1.7]. Other auxiliary loops which are transcriptional targets of the CLOCK-BMAL1 complex have been described such as the basic helix-loop-helix proteins, *BHLHE-40* and *BHLHE-41* (also called *DEC1* and *DEC2* or *BHLHB2* and *BHLHB3*), *HLF* (hepatic leukemia factor) and *TEF* (Thyrotrophic Embryonic Factor) (Gachon 2007; Lowrey & Takahashi 2004; Schroeder and

Colwell 2013; Takahashi et al. 2008). Moreover, the CLOCK/BMAL1 complex also binds to the E-box elements in the promoters of clock controlled/output genes (CCGs) which are responsible for driving ~24-hour rhythms in distinct time of day dependent biological processes (e.g., kinase activity, cell signalling, electrical activity and adenosine triphosphate [ATP] production) (Reppert and Weaver 2002; Schibler 2007; Yang and Meng 2016) [Fig. 1.7].

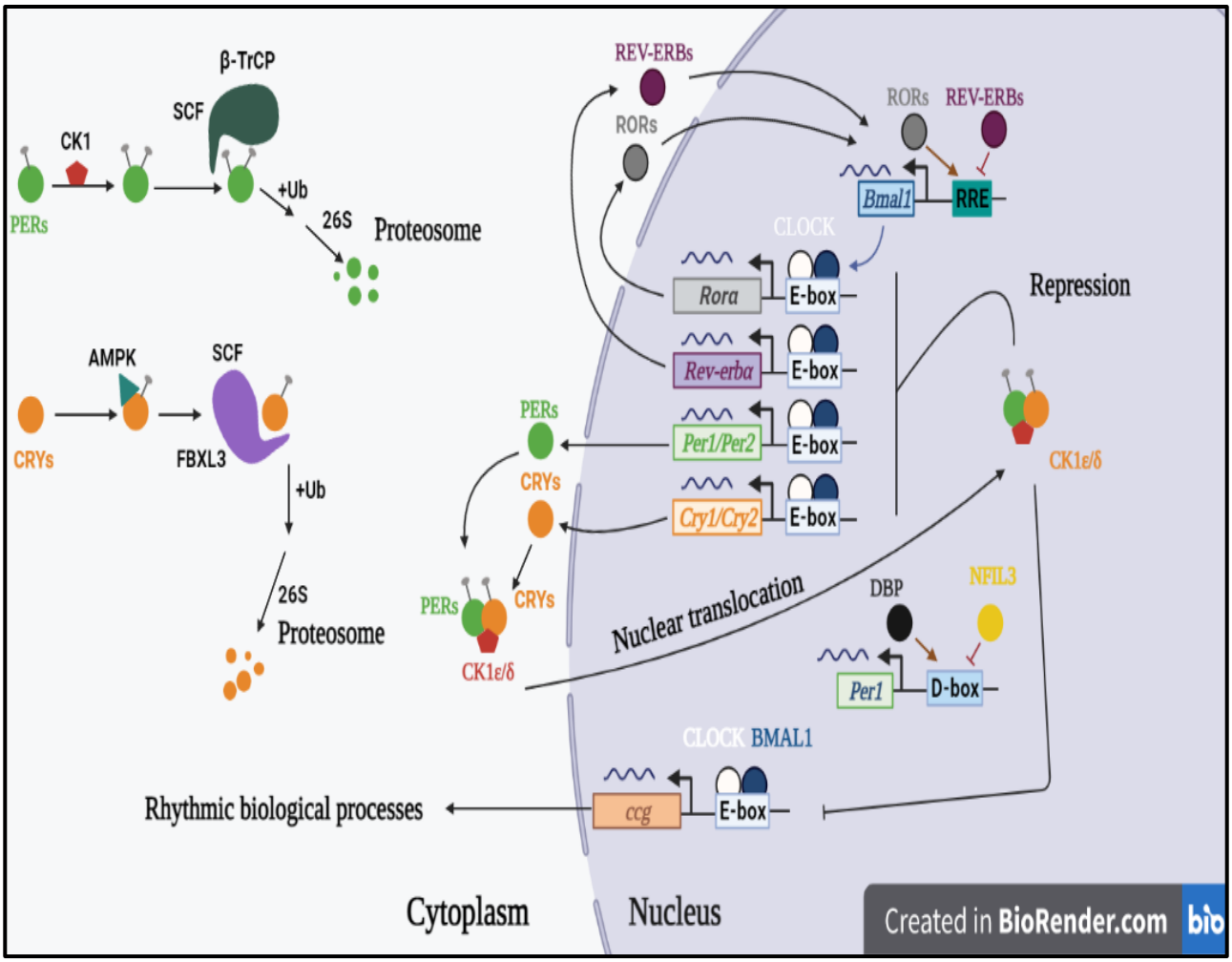


**Figure 1.7. Schematic representation of the molecular mechanism of the mammalian circadian clock.** Transcriptional/translational feedback loops of clock genes and proteins driving circadian oscillations in various 24-hour rhythmic processes. Transcriptional activation through the binding of the BMAL1/CLOCK heterodimeric complex (prior to their transcriptional activation after RORs bind to their RRE elements, cytoplasmic translation then nuclear translocation) to D-, and E-box in the promoters of genes such as *DBP*, *CRY-1/2*, *PER-1/2*, *REV-ERB-α/β*, and *RORα/β/γ* at specific times within a 24-hour day, prior to their appropriate time-of-day dependent cytoplasmic translation and repression to regulate distinct rhythmic biological processes. Specific polyubiquitination events occur to target specific proteins/complexes for degradation by the 26S proteosome hence significantly reducing the amounts of specific proteins in cells before their genes can be re-activated in a continuous 24-hour cycle. Specific genes and proteins encoded by those genes are represented by identical colours. The schematic also illustrates nuclear, and cytoplasm localised cellular processes which ultimately regulate circadian rhythms in mammalian physiology (Created in BioRender using information from Mohawk et al. 2012).

### 1.3.2. Peripheral clocks in cartilage

Over the past decade, various studies have characterised the existence of *ex vivo* functional circadian clocks in cartilage cultured in the absence of external stimuli (Bekki et al. 2020; Dudek et al. 2016; Dudek et al. 2023; Gossan et al. 2013; Guo et al. 2015; Pferdehirt et al. 2022; Snelling et al. 2016). Cartilage tissue dissected from adult and young PER2::luc reporter mice (xiphoid and femoral head cartilage, respectively) exhibited robust circadian rhythm with an ~24.5-hour period, persisting for 1-3 weeks indicative of the existence of intrinsic molecular circadian clocks in murine cartilage (Gossan et al. 2013). Moreover, transcriptome analysis of control (unstimulated) mouse xiphoid cartilage revealed circadian expression of clock genes such as *bmal1*, *cry1*, *dbp*, *e4bp4*, *npas2, nr1d1/2, per2* and *rorα* as well as selected cartilage genes involved in ECM catabolic activities (*adamts-4*, *adamts-9* and *mmp-14*) and an inhibitor of metalloproteinases (*timp4*) (Gossan et al. 2013). Furthermore, robust circadian oscillations in *cry1*-luc and per2::luc activity were observed with an ~24.3 ± 0.3-hour period in control (unstimulated) xiphoid mouse cartilage explants hence verifying that cartilage possesses *ex vivo* functional circadian clocks (Guo et al. 2015). Circadian rhythm in per2::luc activity were observed in femoral head and xiphoid cartilage obtained from wild-type mice hence further confirming the intrinsic circadian clocks found in cartilage (Dudek et al. 2016). Unloaded (control) mice femoral head cartilage, and IVD tissues demonstrated circadian regulation of per2::luc activity in at least 3 LD cycles indicating the *ex vivo* functionality of circadian clocks in mice tissues (Dudek et al. 2023). Rhythmic oscillations in per2::luc activity was also observed in mouse femoral head cartilage explants verifying the presence of self-sustained circadian clocks in murine cartilage (Pferdehirt et al. 2022). Moreover, transduction of porcine primary knee articular chondrocytes (seeded in agarose) with per2-luciferase lentivirus resulted in the observation of sustained circadian expression of per2 within a 48-hour period indicative of *ex vivo* functional circadian clocks in porcine cartilage (Pferdehirt et al. 2022). Moreover, circadian rhythmicity of *CRY-1* and *-2* mRNA transcripts were observed in healthy (non-osteoarthritic) human femoral head chondrocytes within a 46-hour period indicative of the *ex vivo* functionality of circadian clocks in human cartilage (Bekki et al. 2020). A circadian pattern of expression of core clock genes including *BMAL1*, *CLOCK*, *CRY1*, *CRY2*, *PER1* and *PER2* was observed over a 24-hour period in chondrocyte monolayers derived from healthy human tibial plateau cartilage, hence corroborating the existence of autonomous circadian clocks in human cartilage (Snelling et al. 2016).

### 1.3.3. Interplay of peripheral clocks and primary cilia

Emerging evidence has indicated an interplay of peripheral clocks and regulation of primary cilium features; this is highly relevant to cartilage chondrocytes as the primary cilium are important ‘mechanosensors’ at the cell surface. For example, in murine fibroblasts, circadian clocks control oscillation in primary cilia length as evidenced by the synchronisation of clock gene expression using a 2-hour pulse of 100 nM dexamethasone in NIH/3T3 mouse embryonic fibroblasts which had had ciliogenesis induction through serum starvation-mediated cell cycle arrest (Nakazato et al. 2023; Nagoshi et al. 2004; Tucker et al. 1979). per1-luciferase transduced fibroblasts revealed a circadian pattern of luciferase activity following Dex exposure concomitant with rhythmicity in primary cilia length which persisted for more than 48 hours (Nakazato et al. 2023). Introduction of SR9011 (a synthetic agonist for REV-ERB) to Dex treated NIH/3T3 fibroblasts significantly disrupted the rhythmicity of *bmal1* mRNA expression and primary cilium length suggesting that circadian oscillations in the length of fibroblast primary cilium is regulated by clock genes. Such a phenomenon has also been observed following CRISPR/Cas9-induced bmal1 knockout (KO) in NIH/3T3 cells (Nakazato et al. 2023), hence providing a direct link between rhythmic expression of clock genes and primary cilia length. Mechanistically, changes in subcellular localisation of pericentrin (PCNT) to centriolar satellites has been implicated in circadian rhythm-dependent changes in primary cilium length through the control of IFT protein recruitment to primary cilia in murine fibroblasts (Nakazato et al. 2023).

*In vivo* investigations also demonstrated that astrocytes and hippocampal dentate gyrus neurones exhibit a circadian pattern in primary cilium length: in adult murine brain samples collected at zeitgeber time ZT5 and ZT17, significantly longer primary cilia were observed in both the neurones and astrocytes at ZT17 than at ZT5, indicative of circadian rhythm in brain primary cilia length *in vivo* (Nakazato et al. 2023).

In conjunction, circadian regulation of primary cilium length has also been implicated in the wound healing response; synchronised NIH/3T3 fibroblasts with shorter primary cilia were observed to migrate faster in a straight line towards the wound site resulting in faster wound healing after 24 hours, as compared to those with longer primary cilia (Nakazato et al. 2023).

### 1.3.4. Circadian rhythm parameters or characteristics

Four major circadian rhythm parameters normally used to describe rhythmicity in diverse biological processes are the MESOR (midline estimating statistic of rhythm), amplitude, period and phase (Hou et al. 2021; Refinetti et al. 2007; Reid 2019) and they are described as follows:

- **Period** is the duration of a full cycle (that is, the time distance between one peak and the next. Clock gene rhythms have a period of ~24 hours) (Refinetti et al. 2007) [Fig. 1.8].

- **MESOR** is the central value around which the oscillation occurs (Refinetti et al. 2007), i.e., a rhythm-adjusted mean. It represents mean level of rhythmic activity (Hou et al. 2021) [Fig. 1.8].

- **Amplitude** is half the range of excursion of the cycle within the given period; in a symmetrical oscillation, the amplitude corresponds to the distance between the **MESOR** and the peak (or trough) of the wave (Refinetti et al. 2007) [Fig. 1.8]. The amplitude of a rhythm reflects its strength, and it is normally used to assess the robustness of the biological clock (Reid 2019).

- **Phase** is the time corresponding to the first peak of an oscillation within a given period; in the study of circadian rhythms, the phase of a rhythm is often determined in reference to the environmental LD cycle (Refinetti et al. 2007) [Fig. 1.8]. Phase shift is described either in terms of advance or delay. For example, in the sleep-wake cycle, a phase advance indicates an earlier sleep time while a phase delay means a later sleep time (Leng et al. 2019).

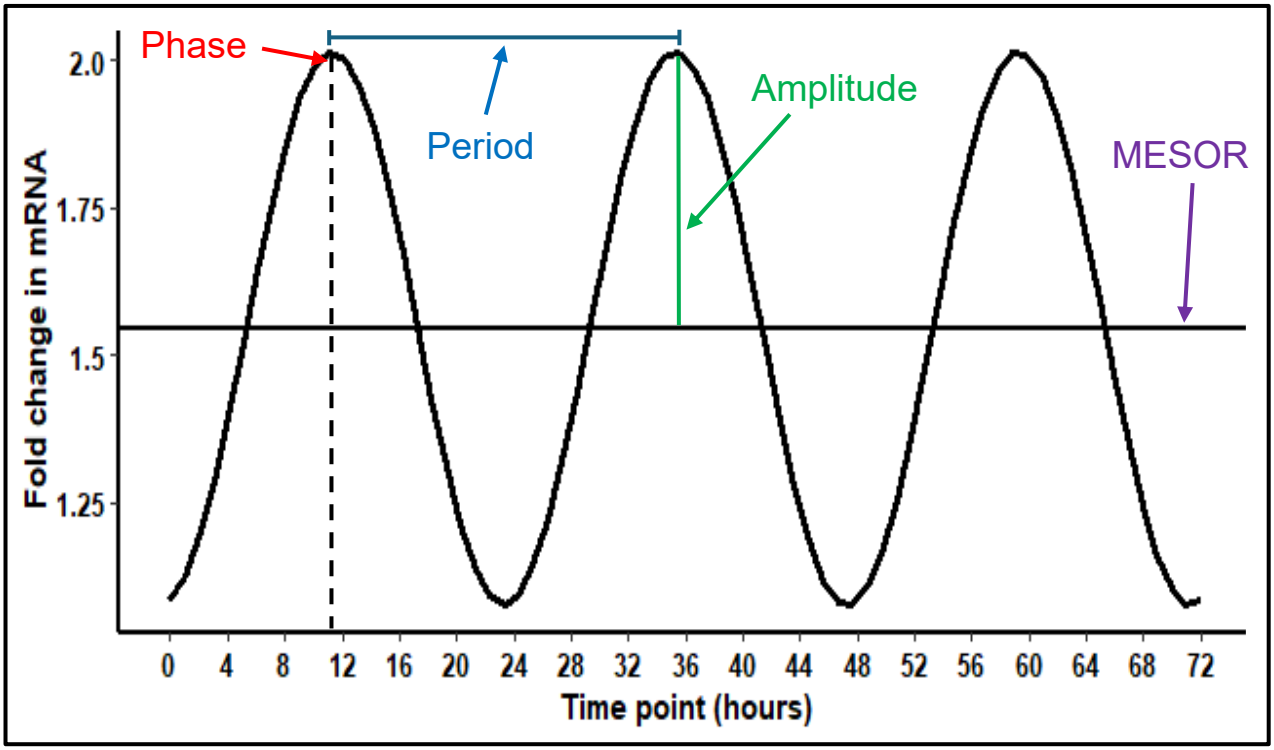


**Figure 1.8. Illustration of the main circadian rhythm features used in chronobiology.** The graph shows an example of a sinusoidal wave representing rhythmic expression of a clock gene within 3 LD cycles with annotations for the amplitude (= 0.469), period (= 24-hours), phase (= 11.5 hours) and MESOR (= 1.55), plotted in R software using the ggplot2 package and annotated using Microsoft PowerPoint.

### 1.4. OA pathology

The avascular nature of articular cartilage has been attributed to its poor intrinsic healing response. Cartilage injury or exposure to non-physiological loads leads to a disturbance in tissue homeostasis and consequently pathological conditions such as OA develop (Hosseinzadeh et al. 2016; Hunziker 1999; Im et al. 2008) (section 1.2.3). OA is a chronic degenerative joint disease characterised by the progressive deterioration of articular cartilage accompanied by changes in the structure and function of the entire diarthrodial joint (van der Kraan et al. 2017) [Fig. 1.9]. This complex disease has a multifactorial aetiology including joint destabilisation, joint trauma, obesity, age, genetics, gender and occupation. One of the hallmarks of OA is reduced mechanical integrity of cartilage that eventually leads to disability, pain and the necessity of total joint arthroplasty (Cooper et al. 2000). It has been estimated that approximately 303 million people worldwide were affected by OA between 1990 and 2017 (GBD 2018). Dealing with OA poses a great socioeconomic burden, especially in developed countries where it has been estimated that 2.5% of the gross national product (GNP) is spent on arthritis (Reginster 2002). Recently, in the UK, an estimate of 10 million people (i.e., 6 million women, 4 million men) have been reported to have OA; an estimated 5.4 million people are reported to be affected by knee OA whilst 3.2 million people are affected by hip OA (Versus Arthritis 2024). Moreover, the report estimated that every year 350,000 people are diagnosed with OA. Economically, treatment of the two most common forms of arthritis (OA and RA) is reported to have cost the NHS and wider UK healthcare system an estimated £10.2 billion in direct costs in 2017 (Versus Arthritis 2024). Despite the financial costs and reduced patient quality of life, a breakthrough in the discovery of efficacious (disease modifying) treatment for OA is yet to be attained since most of the currently available treatment modalities focusses on the alleviation of symptoms (Dernie and Adeyoju 2021).

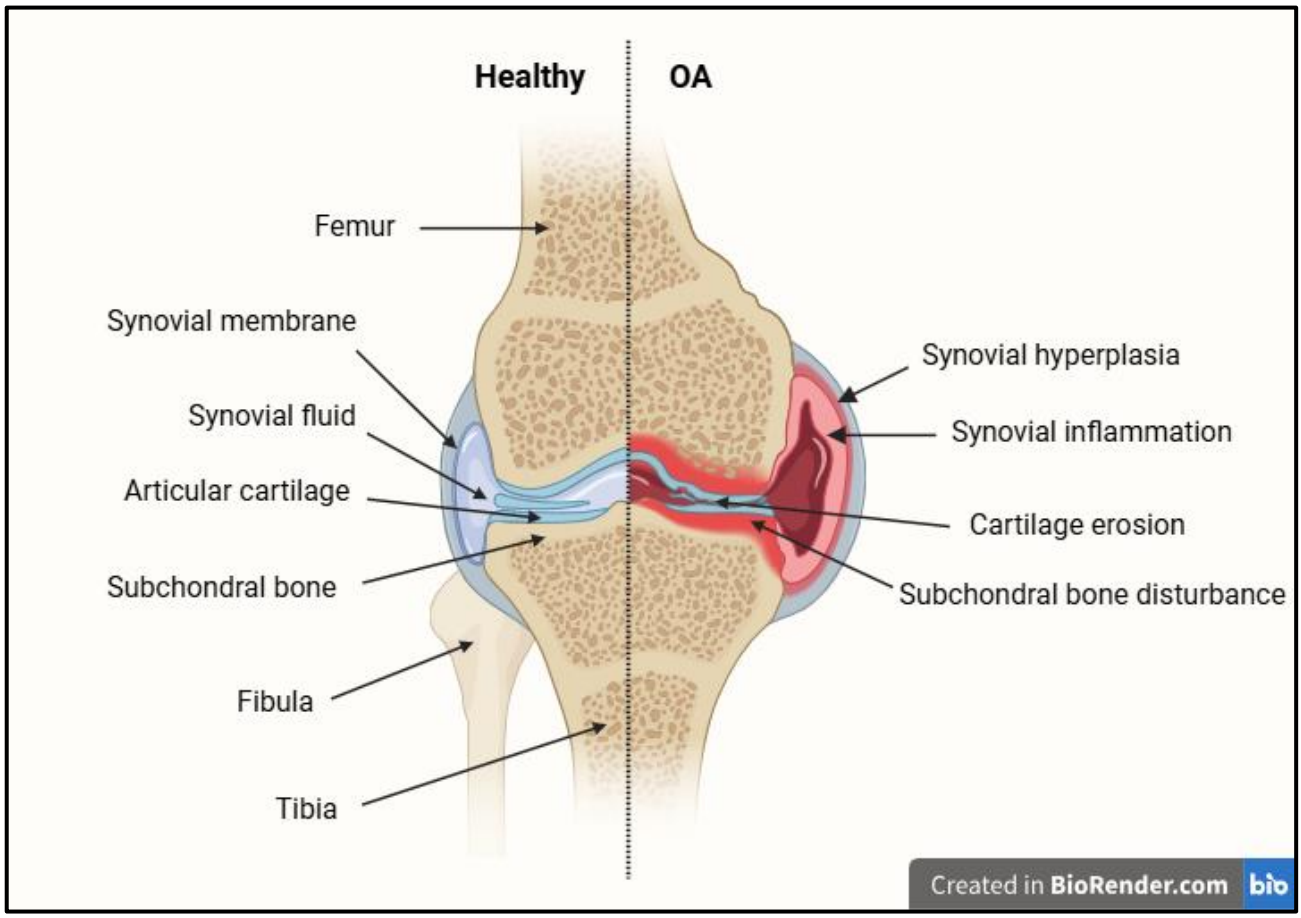


**Figure 1.9. Schematic cross section of a healthy versus osteoarthritic knee joint**. The left part of the illustration shows healthy articular cartilage, synovial cavity and subchondral bone. The right part of the illustration demonstrates possible changes of synovial joint structure and symptoms of osteoarthritis such as cartilage erosion, synovial inflammation, synovial hyperplasia, and loss of intact subchondral bone (BioRender template annotated on-site using information from Yao et al. 2023).

### 1.4.1. Dysregulated circadian rhythm in OA

*In vitro* studies have revealed the existence of self-sustained circadian clocks in cartilage/ chondrocytes regulating rhythmic biological processes in various mammalian tissues (described in more details in section 1.3.2). However, other studies have demonstrated the disruption of these chondrocyte-intrinsic circadian clocks in osteoarthritic cartilage and differing models of OA (Kanbe et al. 2006; Bekki et al. 2020; Kc et al. 2015; Dudek et al. 2016; Snelling et al. 2016); RNA sequencing identified circadian rhythm as the most dysregulated pathway in human OA cartilage (Akagi et al. 2017). Immunoblotting revealed the suppression of *clock* proteins in human knee chondrocytes exhibiting a severe OA phenotype indicative of the disruption of circadian rhythm in these cells (Kanbe et al. 2006). In an *in vivo* model of environmental circadian rhythm disruption (induced by weekly 12-hour phase shifts in the light-dark (LD) cycle of mice to replicate night shift occupations), significantly reduced proteoglycan content concomitant with fibrillation and mast cell infiltration of the synovium as well as the upregulation of catabolic enzymes (*mmp-13* and *adamts-5*) were observed in murine knee cartilage over a 22-week period (Kc et al. 2015). This is indicative of circadian rhythm disruption as a potential risk factor for OA pathogenesis (Kc et al. 2015). In an *in vitro* human study, significantly increased expression of *PER2* concomitant with reduced expression of *BMAL1* were observed in OA chondrocytes (Snelling et al. 2016). Moreover, *BMAL1* knockdown in healthy chondrocytes was associated with enhanced cell proliferation and *MMP13* transcription recapitulating an OA phenotype suggesting that circadian regulation of BMAL1 expression might play a vital role in maintaining the chondrocyte phenotype in human cartilage, and that reduced *BMAL1* expression may contribute to early OA pathogenesis (Snelling et al. 2016). However, genetic disruption of circadian rhythm in mouse femoral head and xiphoid cartilage through chondrocyte specific conditional *bmal1* knockout (*bmal1*$^{-/-}$) induced progressive cartilage degeneration with age concomitant with reduced expression of chondrocyte-specific genes whilst activating catabolic pathways (Dudek et al. 2016). This provides direct evidence implicating circadian rhythm in the onset of OA pathology in murine cartilage (Dudek et al. 2016). Another *in vitro* human study also demonstrated significantly reduced mRNA and protein levels for *NR1D1* and *BMAL1* in human knee OA cartilage with RNA sequencing revealing “circadian rhythm” as the most dysregulated pathway in human OA cartilage compared to healthy cartilage (Akagi et al. 2017). This also provides a mechanistic link between a dysregulated circadian clock and OA pathology in human OA cartilage (Akagi et al. 2017). Disrupted circadian rhythm was also observed

in osteoarthritic human knee chondrocytes evidenced by significantly reduced mRNA levels and amplitudes of *CRY1* and *CRY2* oscillations (Bekki et al. 2020), further verifying the involvement of circadian clock dysregulation in OA pathology in human cartilage.

### 1.5. Hypothesis and aims of the study

Despite the knowledge that (i) mechanical loading is imperative for cartilage function, (ii) proinflammatory cytokines trigger inflammation and subsequently contribute to the initiation and/or progression of OA and (iii) circadian rhythm is one of the most dysregulated pathways in OA pathology, very few studies to date have assessed the effect of mechanical loading on cartilage clocks (Dudek et al. 2023; Heywood et al. 2022; Kanbe et al. 2006). This clearly warrants more research to gain further insight into the interplay between mechanical forces and circadian rhythm in cartilage/chondrocytes and how this might impact tissue homeostasis.

#### 1.5.1 Hypotheses

Thus, the hypotheses of this study were:

- **cartilage chondrocytes subjected to centrifugal force (used to simulate mechanical loading) will exhibit an altered circadian rhythm (e.g., change in amplitude and/or phase) which will potentially influence cartilage metabolism**

- **centrifugal force will reset disrupted chondrocyte circadian rhythm in an *in vitro* model of inflammatory OA and ultimately counteract the cytokine-induced catabolic pathways**

#### 1.5.2. Specific Aims

- To establish a centrifugal force protocol to simulate mechanical loading mimicking physiological forces in skeletally immature bovine chondrocytes cultured as 3D pellets. Gene expression of the early response mechano-sensitive genes as well as anabolic and catabolic markers of chondrocyte metabolism will provide the characteristics for physiological mechanical loading.

- To determine the influence of increasing load duration on mechano-responses of 3D chondrocyte pellets with or without PCM to a select loading regime
- To characterise circadian clocks in control 3D chondrocyte pellet cultures within a 72-hour period
- To investigate the effect of centrifugal force (one episode of 770xg force (60 minutes)) on the expression of clock genes and markers of ECM metabolism in 3D chondrocyte pellets with or without PCM
- To investigate the response of primary chondrocytes (pellets with no PCM) to stimulation with the proinflammatory cytokine IL-1 in combination with OSM within 3 LD cycles to determine (i) the impact of cytokines on cartilage circadian clocks, and (ii) whether markers of ECM metabolism possess and/or lose circadian rhythmicity
- To assess the response of inflammatory OA 3D pellets with no PCM to constant dexamethasone stimulation as well as application of 770xg force either once daily for 3-days, twice daily for 1-day or twice daily for 2-days to determine (i) how dexamethasone/centrifugal force influences disrupted circadian rhythm within 2 LD cycles, and (ii) whether markers of ECM metabolism are affected

# Chapter 2

## General materials and methods

All reagents, plasticware and equipment were obtained from Thermo Fisher Scientific (Paisley, UK) unless otherwise indicated. All plasticware and reagents were certified RNase and DNase free for all molecular biology analyses. A standard “chondrogenic culture medium” consisting of Dulbecco’s Modified Eagle’s Medium/Nutrient Mixture Ham’s F-12 (DMEM/F12) GlutaMAX™ supplemented with 50 µg/ml ascorbate-2-phosphate (Sigma Aldrich, Southampton, UK), 100 U/ml penicillin and 100 µg/ml streptomycin and 1X Insulin-Transferrin-Selenium (ITS) was used for all *in vitro* cultures unless specified otherwise (referred to hereon in as standard culture media).

### 2.1. Harvesting of bovine articular cartilage

Articular cartilage was harvested from the *metacarpophalangeal* joint of skeletally immature bovine calves’ legs [< 3 weeks old] obtained from a local abattoir (Drury and Sons, Swindon, UK) within 6 hours of slaughter as described previously (Thomas et al. 2011). In brief, legs were thoroughly cleaned with disinfectant and water prior to skinning and before the joint was opened using a sterile scalpel. Full-depth articular cartilage explants were harvested using a sterile scalpel and temporarily kept in standard culture media before chondrocytes were isolated using an enzymatic preparation.

#### 2.1.1. Chondrocyte isolation using enzymatic digestion

Chondrocyte isolation was performed as described previously (Vaughan-Thomas et al. 2001); freshly harvested cartilage explants (pooled from 5-15 legs, hence different animals) were washed three times (for 15 minutes) with Hanks Balanced Salt Solution (HBSS) supplemented with 400 U/ml penicillin and 400 µg/ml streptomycin. Explants were then washed with HBSS containing 100 U/ml penicillin and 100 µg/ml streptomycin for 15 minutes under sterile conditions. The 1x wash was removed before explants were incubated for 40 minutes at 37$^{o}$C, with gentle agitation, in 0.1% (w/v) pronase [Roche Diagnostics, Germany] in DMEM/F12 GlutaMAX™ supplemented with 100 U/ml penicillin, 100 µg/ml streptomycin and 5% (v/v) foetal bovine serum (FBS). Pronase was then removed and replaced with 0.04% (w/v) collagenase type II and incubated at 37$^{o}$C, with gentle agitation, for 16-18 hours. The resulting cell suspension was centrifuged for 5 minutes at 500xg (Boeco U-32R, Hettich Zentifugen-D-78532, Germany) to pellet the chondrocytes. The pellet was resuspended in 10 ml of a standard culture media followed

by filtration through a 40 µm cell strainer before the number of cells was counted using a haemocytometer. After counting, cells were seeded as described in 2.1.2.

### 2.1.2. Chondrocyte seeding in a 3D pellet model

Chondrocytes were seeded at a final density of $4x10^6$ cells/ml in 1.5 ml microcentrifuge tubes and pelleted by centrifugation at 500xg for 5 minutes (Thermo Scientific™ Sorvall™ ST8R centrifuge, Thermo Fisher Scientific, Paisley, UK) to create a 3D pellet model; cells were incubated at 37°C in a humidified atmosphere of 5% $CO_2$ - 95% air for ~65 hours to allow for equilibration. Culture media was changed immediately after the equilibration period (1 ml removal and replenishment with standard culture media) before pellets were either cultured devoid of stimulation and collected in circadian time series experiments (section 4.2.1) or subjected to relevant treatments (centrifugal force: sections 3.2.1, 3.2.2, 4.2.2, 6.2.1, and 6.2.2; proinflammatory cytokines: section 5.2.1; proinflammatory cytokines and centrifugal force/dexamethasone: sections 5.2.2, and 5.2.3).

## 2.2. RNA isolation using 2-propanol precipitation

Total RNA was isolated from 3D chondrocyte pellets lysed in TRIzol™ reagent at sample collection as described previously (Blain et al. 2006). The TRIzol™ reagent/chondrocyte mixture was allowed to thaw before mixing to maximise the release of cell contents; 200 µl 1-bromo-3-chloropropane was added to the mixture, shaken vigorously for 15 seconds, and allowed to stand for 10 minutes on ice before centrifugation at 12 000xg for 15 minutes at 4°C (Boeco U-32R, Hettich Zentifugen-D-78532, Germany). The upper aqueous phase containing RNA was transferred to a fresh 1.5 ml Eppendorf tube and a 1:1 volume of 2-propanol (Sigma-Aldrich, Dorset, UK) added to precipitate RNA at -20°C overnight. This was followed by centrifugation at 12 000xg for 15 minutes at 4°C resulting in the formation of an RNA pellet. The supernatant was pipetted out and 1 ml of 75% ethanol added to wash the pellet before centrifugation at 12 000xg for 5 minutes at 4°C. The supernatant was removed, and the RNA pellet was briefly air dried for 15-30 minutes; 26 µl nuclease free water was added to the pellet and RNA temporarily stored on ice.

### 2.3. Genomic DNA digestion using DNase

Genomic DNA was removed by performing a DNase treatment whereby 2 Units DNase and 3 µl 10X DNase buffer were added to RNA and incubated at 37°C for 30 minutes. 0.1 volumes of DNase inactivation reagent were then added to the RNA solution to remove impurities, salts and other contaminants followed by centrifugation at 10 000xg for 2 minutes at room temperature. Pure RNA was transferred to a new Eppendorf tube and stored at -80°C.

### 2.4. Measurement of RNA quality and quantity

The purity (A260:A280 ratio) and concentration (ng/µl) of RNA samples was quantified using the Nanodrop$^{s}$ Lite Spectrophotometer (Thermo Fisher Scientific, Paisley, UK). The instrument was cleaned with lens tissue, blanked against 1 µl of nuclease free water, cleaned again before placing 1 µl of each sample on the sensor. An A260:A280 ratio between 1.8 and 2 represents pure RNA.

### 2.5. Complementary DNA (cDNA) synthesis using Superscript IV$^{TM}$ reverse transcriptase

cDNA was synthesised as described previously (Blain et al. 2006) with a few modifications. 500 ng of total RNA was added to 250 ng of random primers (Promega, Southampton, UK) and 500 µM deoxynucleotide triphosphates (dNTPs) and made up to 20 µl with nuclease free water. Components were incubated at 60°C for 5 minutes to promote annealing of primers to template RNA in a Techne$^{TM}$ TC-3000 Thermal cycler (Bibby Scientific Ltd, UK) before cooling on ice. A reverse transcription (RT) master mix comprising 6 µl 5x 1$^{st}$ Strand buffer (250 mM Tris pH 8.3, 375 mM KCl, 25 mM $MgCl_2$), 30 mM DTT, 20 U recombinant RNasin RNase inhibitor (Promega, Southampton, UK) and 100 U Superscript IV$^{TM}$ reverse transcriptase was prepared, and 10 µl of the RT master mix added to the RNA/random primer/dNTPs mixture. Samples were incubated at 23°C for 10 minutes prior to incubation for 50 minutes at 50°C to allow extension of nucleotide sequences, then 15 minutes at 70°C to inactivate the reaction before storage at -20°C.

## 2.6. Real-time quantitative polymerase chain reaction (RT-qPCR)

### 2.6.1. Design and optimisation of clock gene primers

Accession numbers for bovine target genes were acquired from the Nucleotide database (National Centre for Biotechnology Information (NCBI) website). Each accession number was pasted onto the Primer-BLAST tool (utilises Primer3 and BLAST) where the following parameters were defined; minimum melting temperature ($T_m$), optimum $T_m$ and maximum $T_m$ were 57, 60 and 63$^o$C respectively, with the maximum $T_m$ difference between primer pairs being 1$^o$C. The minimum and maximum product sizes were 70 and 200 base pairs (bp), respectively and exon junction span specification was such that primers must span an exon-exon junction and must be separated by at least one intron on the genomic DNA with intron length ranging from 1 000 to 1 000 000 bp. Refseq mRNA was selected to automatically check the specificity of primer pairs to the intended PCR template. The design was restricted to *Bos Taurus*(taxid:9913) allowing amplification of mRNA splice variants. The criteria used to select appropriate primer pairs was low self-complementarity, percentage GC content difference of 5 or less, no possibility of self-looping and primer-dimer formation. The nucleotide-Blast (blastn) tool was then used to confirm selected primer specificity. Primers were purchased from Eurofins Genomics (Ebersberg, Germany), 200 µM primer stock solutions prepared in nuclease-free water and working stocks of 10 µM prepared for use.

**Table 2.1. Bovine clock gene forward and reverse primer sequences and their respective product sizes validated in this study.** The accession number for each gene is also shown.

| Gene | Accession number | Forward sequence 5'-3' | Reverse sequence 5'-3' | Product size (bp) |
|---|---|---|---|---|
| ***bhlhe40*** | NM_001024929.1 | CGAGGACAGCAAGGAGACCTA | CACTGCTTTTTCCAAGTGCCC | 148 |
| ***bhlhe41*** | NM_001076297.1 | AGGAGCATGAAGCGAGACGA | TCCAGATGCCCCAGAGTTGTC | 152 |
| ***bmal1*** | NM_001191170.1 | ACCTTATTCTCAGGGCAGCA | GCTCCTTGACTTTGGCGATA | 174 |
| ***clock*** | NM_001289769.1 | TGGTGGAAGAAGATGACAAGG | GACTGTGCAGTGATTTCTTTATGT | 199 |
| ***cry1*** | NM_001105415.1 | GATCAACAGGTGGCGATTT | TTCCAAAGGGCTCAGAATCA | 176 |
| ***dbp*** | NM_001037445.1 | AACTCAAGCCCCAGCCAATC | GTCGGCTCCAGTATTTCTCGT | 84 |
| ***nfil3*** | NM_001075240.1 | TTTGTGGATGAGCATGAGCC | GGAACTTGCTTTCTGGGCTT | 163 |
| ***npas2*** | NM_001083763.1 | GGACGGCAAGTCAAGTA | ACCTGAAGAAAGTGCGG | 182 |
| ***nr1d1*** | NM_001078100.2 | CAGCTGCAACTGTAACCTCCA | CTGCCATTCGAGCTGTCACT | 187 |
| ***nr1d2*** | NM_001289793.1 | CTTGTGAAGGCTGTAAGGGTTT | AGGAATACGCCCAAACCGAA | 185 |
| ***per1*** | NM_001289772.1 | GTCTCCCACCTCCCTCCTCTA | CCTCCAGGACAAAAGGGTTCC | 178 |
| ***per2*** | NM_001192317.1 | GATGCCCGCACGAGACTTA | GGTTGTCCTCTCCCTCGTTT | 200 |
| ***rorα*** | NM_001192861.1 | CCAGCACCAGCAGAGGTATC | TGACGAGGACAGGAGTAGGT | 184 |
| ***rorγ*** | NM_001083451.2 | CCCCACAGAGACATCACCGA | CGGAAGAAGCCCTTGCACC | 157 |

**Table 2.2. Previously validated primer pairs for gene markers of chondrocyte remodelling and mechano-responsive genes used in this study.** The accession number for each gene and their respective amplicon sizes are also shown.

| Gene | Accession number | Product size (bp) | Forward sequence 5'-3' | Reverse sequence 5'-3' | Reference |
|---|---|---|---|---|---|
| ***acan*** | NM_173981.2 | 74 | CAGCCAGGCCACCCTAGAG | GGGTGTAGCGCGTGGAGAT | Park et al. (2005) |
| ***col2a1*** | NM_001001135.3 | 73 | AGCAGGTTCACATATACCGTTCTG | CGATCATAGTCTTGCCCCACTT | Park et al. (2005) |
| ***sox9*** | XM_024981096.1 | 434 | TGAAGATGACCGACGAGCAGG | CCGCTTCTCGCTCTCGTTCAG | Park et al. (2005) |
| ***c-fos*** | NM_182786.2 | 192 | CGGCTTTGCAGACAGAGATTG | GGGTGAAGGCCTCCTCAGATT | Thomas et al. (2011) |
| ***c-jun*** | NM_001077827.1 | 100 | TAAACTAAGCCCACGCGAAG | CTCAGACTGGAGGAACGAGG | Thomas et al. (2011) |
| ***mmp-3*** | XM_586521 | 221 | TGGAGATGCTCACTTTGATGATG | GAGACCCGTACAGGAACTGAATG | Nachar et al. (2014) |
| ***mmp-13*** | NM_174389.2 | 202 | CCCTTGATGCCATAACCAGT | GCCCAAAATTTTCTGCCTCT | Blain et al. (2010) |
| ***adamts-4*** | NM_181667.1 | 169 | CTCCATGACAACTCGAAGCA | CTAGGAGACAGTGCCCGAAG | Blain et al. (2010) |
| ***adamts-5*** | NM_001166515.1 | 155 | CTCCCATGACGATTCCAAGT | TACCGTGACCATCATCCAGA | Blain et al. (2010) |

**Table 2.3. Reference gene primer pairs tested in this study.** mRNA accession number for each bovine gene and their respective amplicon sizes are also shown (Al-Sabah et al. 2016).

| Gene | Accession number | Forward sequence 5'-3' | Reverse sequence 5'-3' | Product size (bp) | Reference |
|---|---|---|---|---|---|
| ***18s*** | NR_036642 | GCAATTATTCCCCATGAACG | GCCTCACTAAACCATCCAA | 123 | Frye et al. (2005) |
| ***β-actin*** | NM_173979 | CATCGCGGACAGGATGCAGAAA | CCTGCTTGCTGATCCACATCTGCT | 157 | Anstaett et al. (2010) |
| ***gapdh*** | NM_001034034 | TTGTCTCCTGCGACTTCAACAGCG | CACCACCCTGTTGCTGTAGCCAAAT | 133 | Darling et al. (2005) |
| ***hprt*** | NM_001034035 | TAATTATGGACAGGACCGAACGGCT | TTGATGTAATCCAACAGGTCGGCA | 127 | Anstaett et al. (2010) |
| ***ppia*** | NM_178320 | GGTGGTGACTTCACACGCCATAATG | TTGATGTAATCCAACAGGTCGGCA | 186 | Anstaett et al. (2010) |
| ***rpl4*** | NM_001014894 | TTTGAAACTTGCTCCTGGTGGTCAC | TCGGAGTGCTCTTTGGATTTCTGG | 199 | Anstaett et al. (2010) |
| ***sdha*** | NM_175814 | GATGTGGGATCTAGGAAAAGGCCTG | ACATGGCTGCCAGCCCTACAGA | 104 | Anstaett et al. (2010) |
| ***ywhaz*** | NM_174814 | CTGAGGTTGCAGCTGGTGATGACA | AGCAGGCTTTCTCAGGGGAGTTCA | 180 | Anstaett et al. (2010) |

### 2.6.2. Assessment of qPCR primer efficiency

The efficiencies of primers designed to amplify target clock genes were measured as described previously (Svec et al. 2015). To create a standard curve, a 10-fold serial dilution of chondrocyte cDNA was performed to serve as templates hence resulting in the following cDNA sample quantities; 1, 0.1, 0.01, 0.001, and 0.0001.

Quantitative PCR was carried out as described previously (Stephens et al. 2004) with a few variations. 1 µl of cDNA template at appropriate sample quantity was added to 19 µl of a qPCR reaction master mix made up of 7.8 µl nuclease free water, 1X Brilliant III Ultra-fast SYBR Green qPCR master mix (Agilent Technologies, Cheshire, UK), and 300 nM gene specific forward and reverse primers in AriaMx Tube Strips (Agilent Technologies, Cheshire, UK) capped with Mx3000P Optical Strip Caps (Agilent Technologies, Cheshire, UK). The resulting 20 µl reaction volumes were incubated in an AriaMx Real-Time qPCR machine (Agilent Technologies, Cheshire, UK) under the following cycling conditions; heating at 95°C for 3 minutes in one cycle to activate DNA polymerase, before performing 40 cycles of denaturation at 95°C for 15 seconds and incubation at 60°C for 30 seconds to allow the annealing of primers to template DNA and extension of nucleotide sequences. One more cycle of incubation at 95°C for 1 minute, then 65°C for 30 seconds and 95°C for a minute was performed to generate standard melting curves. Comparative threshold values, dissociation and melting curves were generated by the AriaMx Real-Time qPCR software.

Microsoft Excel was used to calculate average $C_T$ values for each of the technical replicates and the log of each sample quantity. The slope was taken as the gradient of the regression equation in a graph where average $C_T$ values were plotted as a function of log sample quantity before use in the efficiency equation below:

$$Efficiency\ (\%) = \left(10^{\frac{-1}{Slope}} - 1\right) \times 100$$

### 2.6.3. Validation of primer specificity using agarose gel electrophoresis

To determine primer specificity and confirm qPCR product sizes, amplicons were separated by agarose gel electrophoresis. Briefly, 2% (w/v) agarose (Promega, Southampton, UK) was added to 50 ml 1X Tris/Borate/EDTA (TBE) buffer (Promega, Southampton, UK), mixed and heated for a minute in a microwave to fully dissolve the powder; 5 µl SafeView dye (NBS Biologicals, Cambridgeshire, UK) was added before the solution was poured into a casting chamber and left for 30 minutes to set. The gel was placed in an electrophoresis tank, filled with 1X TBE buffer and 10 µl of qPCR products (amplicons mixed with 2 µl of loading dye) loaded. A 100 bp DNA Ladder (6 µl; Promega, Southampton, UK) was also loaded to determine the molecular weight of amplicons. Electrophoresis was performed at 80 volts (V) using the Anachem Origo Gel Electrophoresis System (Anachem, Luton, UK) and stopped before samples ran off the gel. The Uvidoc HD6 Transilluminator (UVITEC, Cambridge, UK) was used to visualise DNA under ultraviolet (UV) illumination before an image was captured and printed using a digital monochrome printer (Mitsubishi Electric, Kyoto, Japan).

### 2.6.4. Assessment of housekeeping genes stability using refFinder software

RefFinder - a web-based tool (https://www.ciidirsinaloa.com.mx/RefFinder-master/) was used to screen and evaluate suitable housekeeping genes (HKGs) for qPCR normalisation of target genes under distinct experimental conditions. RefFinder software consolidates the four main accessible computational programs; BestKeeper (Pfaffl et al. 2004), comparative delta-$C_T$ method (Silver et al. 2006), geNorm (Vandesompele et al. 2002) and Normfinder (Andersen et al. 2004). The $C_T$ values of experimental samples (including controls) in which eight housekeeping genes were amplified (*18s, β-actin, gapdh, hprt, ppia, rlp4*, *sdha* and *ywhaz*) were exported into the refFinder software which analysed and compared the data, before ranking the candidate genes by assigning an appropriate weighting to a gene based on the scores from each program; this enabled the geometric mean of candidate gene weightings to be calculated to generate an overall gene stability ranking (Xie et al. 2012).

### 2.6.5. Quantitative PCR using SYBR® green chemistry

To measure the relative expression of specific target genes in relevant experimental samples, template cDNAs were amplified using the real-time qPCR method as described previously (Section 2.1.6.2), with 1 µl cDNA or equivalent volume of water (non-template control) added for analyses. Comparative threshold values, dissociation and melting curves were generated by the AriaMx Real-Time qPCR software before downstream analysis.

### 2.6.6. Analysis of gene expression using the $\Delta\Delta C_T$ method

To measure relative gene expression at the mRNA transcript level, the $\Delta\Delta C_T$ method was employed as described by Livak and Schmittgen (2001). Briefly, in Microsoft Excel, the geometric mean (GEO mean) of the selected two most stable housekeeping genes (*hprt* and *18s*) was calculated per cDNA sample before $\Delta C_T$ (change in cycle threshold) was determined for the normalisation of target gene expression.
$\Delta C_T$ was calculated as target gene $C_T$ minus the GEO mean;

$\Delta C_T$ = raw $C_T$ value - GEO mean

In preparation for circadian rhythmicity assessment, $\Delta\Delta C_T$ at specific time points were calculated by deducting the mean $\Delta C_T$ of T0 hours from each successive time point's $\Delta C_T$ value within a 24-, 48-, or 72-hour period.

$\Delta\Delta C_T$ = time point $\Delta C_T$ - mean $\Delta C_T$ for T0 hours

Fold change in mRNA transcripts was calculated by raising -($\Delta\Delta C_T$) to base 2;

Fold change in mRNA transcripts = $2^{-\Delta\Delta C_T}$

For relative gene expression of markers of chondrocyte remodelling in response to relevant stimuli, $\Delta\Delta C_T$ was calculated by deducting the mean $\Delta C_T$ of the untreated (control) group from that of a relevant treatment group at that time point.

$\Delta\Delta C_T$ = treated group $\Delta C_T$ - mean $\Delta C_T$ for untreated group

Fold change in mRNA transcripts = $2^{-\Delta\Delta C_T}$

Relative gene expression data was expressed as fold change in mRNA transcripts ± standard deviation (SD).

An example of an R script for creating boxplots depicting mechano-responses of 3D pellets to mechanical load (simulated through either 200-, 770- or 1000-xg centrifugal forces) is shown in Appendix 1.

### 2.7. Determination of circadian rhythmicity within a 48 or 72-hour period using the CircWaveBatch software

Fold change in mRNA transcript data was imported into the CircWaveBatch version 3.3 software (Programmed by Roelof A. Hut and Leon Steijvers, University of Groningen, Netherlands; downloaded for free online: *https://clocktool.org/index.php/clock-modules/clock-tools/item/circ-wave-batch.html*) equipped with an analytical tool for simultaneously determining circadian rhythmicity profiles of multiple genes across a wide time scale and their significance using harmonic regression in combination with the statistical F-test. In brief, the program is based upon forward linear harmonic regression which calculates the shape of the profile wave form and fits a fundamental sinusoidal wave through the data points with its significance being tested against a fitted horizontal line through the overall average. This fundamental sinusoidal wave is described by the function:

$f(t) = M + \alpha \sin((2 \pi t)/\gamma) + \beta \cos((2 \pi t)/\gamma)$

where: M = MESOR (midline estimating statistic of rhythm); α = sine coefficient; β = cosine coefficient; t = time point; γ = period.

By default, the CircWaveBatch software sets the period (*tau*) at 24-hours, but the period parameters used when analysing data in this thesis ranged between 20-28 hours to accommodate genes with periods slightly greater or less than 24-hours. The software then

generated an output file which provided amongst others, values for the major rhythm characteristics including the period, MESOR, regression coefficient ($r^2$), sine and cosine coefficients and p-values for each target gene.

Overall, a gene was considered to exhibit circadian rhythmicity if its dataset met the following criteria: both an $r^2 \geq 0.8$, and a p-value < 0.05, and a period of ~24 hours.

### 2.7.1. Fitting of sinusoidal waves onto data points using the R software

For the visualisation of data points and fitting of sinusoidal waves onto the data points for a given rhythmic gene, a linear model consisting of both the sine and cosine terms was modelled in the R software and plotted using the ggplot2 package (Wickham 2016; R Core Team 2022). An example of an R script for plotting circadian rhythmicity curves is shown in Appendix 2.

### 2.7.2. Assessment of circadian rhythmicity in individual LD cycles using the CircWaveBatch software

In preparation for the determination of statistical significance of differences in amplitude, period, and phase of mRNA circadian rhythm between two experimental groups (e.g., control and 770xg loaded groups in a 3D model), fold change (relative expression) data was imported into the CircWaveBatch software as individual LD cycles within either a 48 or 72-hour period to generate an n = 2, or n = 3 datasets, respectively, per rhythm characteristic. i.e., separately importing T0-24 hours, T24-48 hours, and T48-72 hours to compare rhythm features between individual LD cycles since no statistical tests could be performed in datasets with an n = 1.

## 2.8. Assessment of cell viability in 3D pellet cultures

To evaluate cell viability in the employed 3D chondrocyte pellet model, live/dead staining was performed using fluorescein diacetate (FDA) and propidium iodide (PI) (Sigma Aldrich, Southampton, UK) according to the Ibidi GmbH protocol (Application Note 33, 2015).

Briefly, the staining solutions were prepared comprising DMEM/F12 GlutaMAX™ (FBS and phenol red free), 7.91 µg/ml FDA solution (from a 5 mg/ml FDA stock resuspended in acetone) and 19.8 µg/ml PI (from a 2 mg/ml PI stock in phosphate buffer saline [PBS]). Media was removed from the cell pellets prior to the addition of 1 ml staining solution; samples were incubated at room temperature for 30 minutes in the dark, staining solution removed and pellets washed with 1X PBS. Pellet samples were transferred into 30 mm diameter petri dishes, DMEM (FBS and phenol red free; to avoid interference with the fluorescence of live/dead stains) added and fluorescent images acquired using the ZEISS Celldiscoverer 7 (CD7) microscope (Bioimaging Hub, School of Biosciences).

### 2.9. Biochemical analysis of culture media samples

#### 2.9.1. Measurement of sulphated glycosaminoglycan content

To quantify the amount of sulphated glycosaminoglycans (sGAG) secreted into culture media by 3D chondrocyte cultures, the 1,9-dimethylmethylene blue assay (DMMB) was employed as previously described (Farndale et al. 1986). A standard curve was prepared using Chondroitin-6-Sulphate (C-6-S) from shark cartilage (Sigma-Aldrich, Southampton, UK) at concentrations of 0, 10, 20, 30 and 40 µg/ml. 50 µl of each standard was pipetted into triplicate wells of a 96-well microplate whereas experimental samples were pipetted into quadruplicate wells; 200 µl of DMMB solution was added to all wells and the plate read immediately at 525 nm in a CLARIOstar Plus plate reader (BMG LABTECH, Bucks, Great Britain). In Microsoft Excel, C-6-S absorbance was plotted as a function of C-6-S concentration hence generating a regression line and the equation used to calculate sGAG concentration in experimental samples. Appropriate dilutions of media samples which demonstrated absorbances exceeding those for the 40 µg/ml standards were performed where relevant. Data represented total sGAG release ± SD.

#### 2.9.2. Quantification of nitrite as a measure of NO

To measure the concentration of nitrite ($NO_2^-$) in experimental samples, the Griess assay was performed according to manufacturers' protocol (Promega, Southampton, UK). The assay determines NO production indirectly through the measurement of $NO_2^-$ concentration, a stable and non-volatile breakdown product of NO (Griess 1879). In brief,

50 µl of nitrite standards were prepared in triplicate wells of a 96-well microplate by creating a series of doubling dilutions (using standard culture media) of a 100 µM nitrite stock, hence obtaining final $NO_2^-$ concentrations of 100, 50, 25, 12.5, 6.25, 3.13, 1.56 and 0 µM. 50 µl of experimental media samples were then added into appropriate wells of the same 96-well microplate, 50 µl sulfanilamide solution added to all wells and the plate incubated for 10 minutes in the dark. Subsequently, 50 µl of N-1-napthylethylenediamine dihydrochloride (NED) solution was dispensed into each well before incubation for 10 minutes protected from light; the plate was immediately read at 540 nm in a CLARIOstar Plus plate reader (BMG LABTECH, Bucks, Great Britain). The regression equation obtained from plotting the standards' absorbances against $NO_2^-$ concentration was used to calculate the concentration of $NO_2^-$, i.e. NO, in experimental samples in Microsoft Excel. Data represented total NO release ± SD.

## 2.10. Enzyme activity analysis

### 2.10.1. Detection of aggrecanase-1 (adamts-4) enzyme activity

To determine whether changes in the expression of the catabolic gene, *adamts-4* leads to alterations in protein levels (active enzymes) secreted into culture media by chondrocytes in a 3D pellet model, the SensoLyte® 520 aggrecanase-1 fluorimetric assay was employed according to manufacturers' protocol (Eurogentec, Camberley, UK). The assay is based on a fluorescence resonance energy transfer (FRET) principle utilising a novel internally quenched peptide substrate consisting of the 5-FAM/TAMRA pair. This FRET peptide is cleaved into two separate fragments specifically by active adamts-4 enzymes hence unlocking the fluorescence signal of 5-FAM monitorable at excitation/emission (Ex/Em) wavelengths of 490/520 nm.

In brief, 50 µl of culture media obtained from 770xg centrifuged pellet cultures and corresponding controls (section 3.3.2.3) or cytokine-stimulated pellet cultures and controls (section 5.3.1.3) were added into the wells of a black, flat-bottomed, non-binding 96-well microplate; 50 µl of diluted aggrecanase-1 substrate was added to the wells, prior to the incubation of reactions away from direct light for 45 minutes. 50 µl of substrate controls (assay buffer) were also set up. In duplicate wells, a doubling dilution series of 5-FAM in assay buffer containing aggrecanase-1 substrate was performed culminating in 5-FAM

final concentrations as follows: 5000, 2500, 1250, 625, 312.5, 156, 78, and 0 nM. Subsequently, 50 µl of stop solution was added to all wells and the fluorescence intensity measured at Ex/Em=490/520 nm using a CLARIOstar Plus microplate reader (BMG LABTECH, Bucks, Great Britain). Fluorescence readings were corrected by deducting the background fluorescence (substrate controls) and subsequently expressing the readings in relative fluorescence units (RFU). The regression equation obtained from plotting standards' RFU against 5-FAM concentration in Microsoft Excel was used to calculate the concentration of 5-FAM in experimental samples following the cleavage of the FRET peptide by active adamts-4 enzymes, hence indicating the activity of aggrecanase-1 in media samples. Data represented total 5-FAM concentration, i.e., total aggrecanase-1 activity ± SD.

### 2.10.2. Detection of mmp-13 enzyme activity

To determine whether changes in the expression of the catabolic gene, *mmp-13* leads to alterations in protein levels (active enzymes) secreted into culture media by chondrocytes in a 3D pellet model, the SensoLyte® 520 generic MMP fluorimetric assay was employed according to manufacturers' protocol (Eurogentec, Camberley, UK). In this assay, the 5-FAM fluorescence of an intact FRET peptide is internally quenched by QXL$^{TM}$520 (5-FAM/QXL$^{TM}$520 FRET peptide, acting as an mmp-13 substrate). However, the fluorescence of 5-FAM is recovered upon the cleavage of the substrate into two fragments by active mmp-13 enzymes and can be monitored at Ex/Em wavelengths of 490/520 nm.

In brief, 50 µl of culture media samples obtained from 770xg centrifuged pellet cultures and corresponding controls (section 3.3.2.3) or cytokine-stimulated pellet cultures and controls (section 5.3.1.3) were added into the wells of a black, flat-bottomed, non-binding 96-well microplate; 50 µl of 1 mM 4-aminophenylmercuric acetate (APMA) was added to mmp containing media samples and incubated for 40 minutes to activate mmp-13 enzymes. 50 µl of dilute generic mmp substrate was then added into each well before incubation at room temperature for 45 minutes in the absence of direct light. 50 µl of substrate controls (assay buffer) were also set up. In duplicate wells, a doubling dilution series of 5-FAM-Pro-Leu-OH in assay buffer containing mmp generic substrate was performed culminating in the preparation of 5-FAM final concentrations as follows: 2500, 1250, 625, 312.5, 156, 78, 39, and 0 nM. Subsequently, 50 µl of stop solution was added

to all wells before the fluorescence intensity was measured at Ex/Em = 490/520 nm using a CLARIOstar Plus microplate reader (BMG LABTECH, Bucks, Great Britain).

Fluorescence readings were corrected by deducting the background fluorescence and subsequently expressing the readings in RFU. The regression equation obtained from plotting standards' RFU against 5-FAM-Pro-Leu-OH concentration in Microsoft Excel was used to calculate the concentration of 5-FAM-Pro-Leu-OH in experimental samples following the cleavage of the FRET peptide by active mmp-13 enzymes, hence indicating mmp-13 activity in media samples. Data represented total 5-FAM-Pro-Leu-OH concentration, i.e., total mmp-13 activity ± SD.

### 2.11. Statistical analysis

Data was checked for normality using the Shapiro-Wilk test in the R software (data was considered normal if p-value > 0.05) and non-normal data was log-transformed ($log_{10}$) in Microsoft Excel. The Shapiro-Wilk test was then utilised to determine the normality of log transformed data before the Bartlett's test was employed to check the homogeneity of variances (data was considered to have equal variances if p-value > 0.05). Parametric tests were used to investigate statistical significance of differences between means of different groups if the dataset met both the normality and equality of variances criteria, e.g., ‘‘one-way ANOVA'' followed by a ‘‘TukeyHSD *post-hoc* test'' for multiple groups or a ‘‘Welch Two Sample t-test'' for comparing two groups. The non-parametric tests: ‘‘Kruskal-Wallis test'' followed by a ‘‘Wilcoxon rank sum test'' were used otherwise (R Core Team 2022). Data was considered statistically significant if $p < 0.05$.

# Chapter 3

## Characterisation of the responses of 3D chondrocyte pellets to mechanical loading mimicked by centrifugation

## 3.1. Introduction

### 3.1.1. Simulation of mechanical loading using centrifugal force

It has long been established that mechanical load plays a significant role in the regulation of chondrocyte metabolism and contributes to OA progression. Indeed, it has been widely reported that mechanical stimulation regulates ECM turnover (section 1.2), and previous investigations have reported the use of centrifugal force in various regimens in diverse cell types to determine its mechano-regulatory potential. Centrifugation predominantly simulates compressive stress in cells, whilst the surrounding culture media contributes hydrostatic pressure and/or fluid shear stress (Grimm et al. 2020; Jang et al. 2016; Prittinen et al. 2019; Redlich et al. 2004). Human periodontal ligament (PDL) fibroblasts subjected to centrifugation at 167xg for either 10-, 20-, 30-, 60-, 90- or 120-minutes revealed significant increases in mRNA transcripts for *MMP-1*, *COL1α1*, *TIMP-1* and *TIMP-2* in the first 60 minutes post centrifugation; *MMP-1* demonstrated the greatest induction before its mRNA levels dropped to almost control levels 90 minutes post force application (Redlich et al. 2004). This suggests that the force-induced remodelling of PDL tissue via fibroblast activities could partially be linked to the direct effect of mechanical force on *MMP-1* expression (Redlich et al. 2004). Moreover, hydrostatic, compressive and shear forces as simulated by centrifugation of human PDL fibroblasts at 124xg for 3 hours (equivalent to a 34.9 g/cm$^2$ force) significantly increased *MMP-8* mRNA, whereas *TIMP-1* mRNA was significantly reduced suggesting that centrifugal force had an impact on periodontal tissue remodelling (Grimm et al. 2020). Moreover, human adipose-derived stem cells (ASCs) subjected to centrifugation at 2400xg for 30 minutes exhibited upregulation of a gene marker for the chondrocyte phenotype *SOX9* and ECM anabolism *ACAN* and *COL2A1*, as well as an upstream stimulator of *SOX9*, bone morphogenetic protein 4 (*BMP-4*), whilst type X collagen (*COL10A1*) was downregulated (Jang et al. 2016). This suggests that centrifugal force can induce chondrogenic differentiation of ASCs through increasing BMP4 expression (Jang et al. 2016).

Taken together, this indicates the capacity of centrifugal force in inducing mechano-responses in various cell types, hence suggesting its suitability as a model system to study chondrocyte mechanobiology. Despite the lack of previous literature describing the optimisation of a physiological centrifugation regimen to regulate mechano-signalling in cartilage chondrocyte metabolism, several studies have been identified which demonstrated the impact of centrifugal force at distinct magnitudes and durations on

cartilage turnover. Application of 3xg centrifugal force (12-32 hours) to 3D skeletally immature rabbit growth plate chondrocyte pellet cultures induced a 2-fold increase in [$^{35}$S] sulphate incorporation into proteoglycans (Inoue et al. 1990). Moreover, Inoue et al. (1990) demonstrated increased [$^{35}$S] sulphate incorporation into proteoglycans and [$^{3}$H] thymidine incorporation into DNA in skeletally immature rabbit 3D articular chondrocyte pellet cultures subjected to 3xg centrifugal force (12-32 hours) (Inoue et al. 1990). An increase in radiolabelled thymidine incorporation into DNA only in centrifuged articular chondrocytes suggests divergent centrifugal force-induced alterations in cell proliferation between articular and growth-plate chondrocytes (Inoue et al. 1990). Another study demonstrated cluster formation and a columnar arrangement of cells in tissue constructs resulting from skeletally immature rabbit articular chondrocyte pellet cultures subjected to 6.9 MPa centrifugal pressure (15 000 rpm; 15 minutes every 24 hours over a 28-day period) (Maeda et al. 2005). Furthermore, Maeda et al. (2005) revealed that collagen fibrils were more abundant in stressed cultures with fibrils running parallel to the surfaces of resultant tissue constructs concomitant with increased type II collagen expression at day 7 and 14. However, centrifugation did not affect aggrecan mRNA expression suggesting that 6.9 MPa induces divergent regulation of key ECM molecules in chondrocyte pellet cultures (Maeda et al. 2005). Taken together, the force-induced increases in cell proliferation over time suggests that mechanical stress affects chondrocyte proliferation from as early as day 7 of culture (Maeda et al. 2005). Skeletally mature bovine chondrocyte 3D cultures, laid on top of defatted bone disks, in agarose constructs exhibited significantly increased sGAG release with culture period following application of 771xg centrifugal force (15 minutes either 1 or 3 times per day for up to 4 weeks) (Prittinen et al. 2019). Furthermore, this centrifugal regimen upregulated procollagen α2(I) mRNA concomitant with unaltered aggrecan and procollagen α1(II) mRNA levels (Prittinen et al. 2019). Failure of the centrifugation regimen to induce gene markers of anabolism in *ex vivo* cultivated chondrocytes imply that either the type, magnitude, frequency or duration of force employed was inadequate in triggering production of hyaline cartilage, while the upregulation of type I procollagen (α2) suggests that the cells were induced to undergo fibroblastic de-differentiation (Prittinen et al. 2019).

### 3.1.2. Employment of the pellet culture model in mechanobiological research

Previous studies have used chondrocyte pellets as a 3D *in vitro* model for studying cartilage tissue engineering and mechanobiology since pellets offer a three-dimensional environment which permits the interaction of congregated cells enhancing cell-cell communication as well as cell-ECM interactions. Moreover, these interactions were observed to be similar to those occurring during embryonic chondrogenesis where mesenchymal cells are condensed (a critical step in the process), initiating cell-cell communication and consequently resulting in the development of chondrocytes (Ballock et al. 1993; DeLise et al. 2000; Fedewa et al. 1998; Lübke et al. 2005; Kato et al. 1988; Zhang et al. 2010). Furthermore, porcine chondrocyte pellet cultures elicited superior chondrogenic redifferentiation as compared to chondrocytes encapsulated in alginate beads (Bernstein et al. 2009). Pellet cultures consisting of chick embryo sternal chondrocytes maintained their cell phenotype and ultimately produced hyaline cartilage with native-like structural characteristics such as matrix composition and density, zonal distribution of cells and tissue ultrastructure (Zhang et al. 2004).

### 3.1.3. PCM deposition in 3D chondrocyte pellet cultures

As previously described (section 1.1.2.1), chondrocytes in healthy cartilage are surrounded by the PCM, rich in a number of ECM molecules including type VI collagen, which modulates biophysical, biomechanical and biochemical signals (Alexopoulos et al. 2009; Guilak et al. 2006). The PCM has a chondroprotective role and facilitates mechanotransduction. Additionally, the stiffness of the PCM has a critical role in the transmission of biomechanical signals to chondrocytes, possibly via the interaction between type VI collagen and integrins or other cell surface receptors (Brahmachary et al. 2024). Moreover, previous studies demonstrated that chondrocyte pellets deposit variable quantities of PCM components with extended periods of *ex vivo* culture. In a study employing chondrocytes from immature bovine femoral condyles, no type VI collagen staining was observed immediately following the embedding of isolated chondrocytes into agarose gels; in contrast, type VI collagen staining was observed around cell peripheries by day 7 suggesting the deposition of substantial amounts of PCM after a week of culture (DiMicco et al. 2007). Furthermore, immunofluorescence staining revealed no type VI collagen expression at day 1 after cell seeding, but significant type VI collagen was observed from day 7 onwards in a study utilising skeletally mature bovine articular

chondrocytes seeded in 3D cultures (either hyaluronic acid or agarose hydrogels) (Owida et al. 2021).

### 3.1.4. Major mechano-sensitive genes showing responses to mechanical loads

To detect, at the molecular level, cellular responses following the application of differing mechanical loads, the expression of reported mechano-sensitive genes is monitored post mechanical stimulation with timepoints of analysis ranging from minutes to ~24 hours post loading. The major early stress response genes used to test the modulation of cellular response by mechanical loading in various cell types including chondrocytes are *c-fos* and *c-jun* (Ferraro et al. 2004; Janssen et al. 1995; Kumahashi et al. 2004; Peake et al. 2000; Ranjan et al. 1996; Shiu et al. 2003; Thomas et al. 2011). Proteins encoded by the *c-fos* and *c-jun* genes are members of the activator protein-1 (AP-1) transcription factor family, revealed to partake in the early mechano-regulation of downstream target genes involved in cell differentiation and division (Holt et al. 1986; Janknecht et al. 1995). Due to the scarcity of publications characterising centrifugal forces capable of simulating mechanical loading within a physiological range, it is imperative to test the mechano-regulatory potential of distinct centrifugal forces on early mechano-responsive genes (e.g., *c-fos* and *c-jun*) as well as mechano-responsive catabolic genes (e.g., *mmp-3*, *adamts-4* and *adamts-5*) also representative of late responses (Lee et al. 2005b; Monfort et al. 2006; Patwari et al. 2003); this knowledge will facilitate the selection of a force eliciting more prominent mechano-responses followed by the utilisation of the selected force in mechanobiology and chronobiology experiments in this PhD project.

### 3.1.5. Aims

The aim of the work presented in this chapter is to establish a centrifugal force protocol that simulates mechanical loading mimicking physiological forces (predicted to mimic hydrostatic pressure, compressive and shear forces as experienced by chondrocytes *in vivo*) in a 3D model described in section 2.1.2 (i.e., 3D pellets with an immature [minimal or no] PCM, hereon termed 3D chondrocyte pellets). Furthermore, it is the aim of chapter 3 to provide an extensive characterisation for the optimal magnitude and duration (15- versus 60-minutes) of centrifugal force application to elicit mechano-responses and/or metabolic changes in 3D chondrocyte pellets. The final aim of chapter 3 is to compare the

mechano-responses of 3D chondrocytes pellets (with minimal or no PCM) to 3D chondrocyte pellets with an established PCM, henceforth referred to as '3D pellets with PCM' (i.e., *ex vivo* cultivated for 9 days before commencement of specified loading regimen) to determine the importance of the PCM in this model system. Hence, chapter 3 aims to further optimise a suitable model system for use in mechanobiology experiments where mechanical loads are simulated by centrifugation. The outcome of these investigations will be utilised in chapter 4 within experimental set-ups aimed to investigate the effects of mechanical loading (magnitude and duration selected from the above-mentioned experiments) on chondrocyte circadian clocks and ECM metabolism in 3D pellets with or without PCM.

**Drawing from previous studies,** a panel of three candidate centrifugal forces namely, 200-, 770- and 1000-xg were tested for eliciting mechano-responses (15 minutes loading duration was used for all regimens). A 200xg regimen was used to approximate 167xg, previously utilised in a human periodontal ligament fibroblast study (Redlich et al. 2004), whilst 770xg force was selected from a bovine knee primary chondrocyte publication (which used 771xg, Prittinen et al. 2019), and a 1000xg regimen was obtained as an approximate sum of the two-regimens mentioned above. In addition, to determine the impact of increasing the duration of centrifugal force exposure on chondrocyte's responsiveness, 3D chondrocyte pellets were subjected either to 15- or 60-minutes of a predicted 'physiological force'.

#### 3.1.5.1 Specific chapter objectives

- To evaluate the effects of three centrifugal force applications (200-, 770- and 1000-xg) on chondrocyte viability, sGAG and NO release, the stability of housekeeping genes as well as known mechano-response genes, i.e., early mechano-responsive genes (*c-fos* and *c-jun*) and, late mechano-responsive catabolic genes (*adamts-4*, *adamts-5*, and *mmp-3*) in 3D chondrocyte pellets (without PCM)
- To determine the influence of increasing load duration from 15- to 60-minutes on chondrocyte responsiveness to a select centrifugal regimen (established in objective 1) in 3D chondrocyte pellets with or without a PCM by evaluating centrifugal force-induced changes in sGAG and NO release and expression of early mechano-responsive genes (*c-fos* and *c-jun*), late mechano-responsive catabolic

genes (*adamts4*- and -*5* and *mmp*-*3*) and a chondrocyte phenotype gene marker (*sox9*)

### 3.2. Experimental protocols

#### 3.2.1. Optimisation of centrifugal force to simulate mechanical load in a 3D pellet model

To assess the mechano-regulatory potential of centrifugal force on chondrocyte pellet cultures and to determine a force which elicits pronounced mechano-responses, 3D chondrocyte pellets were subjected to centrifugation as described previously (Prittinen et al. 2019). Specifically, 3D cultures were subjected either to 200-, 770- or 1000-xg centrifugal force for 15 minutes; culture media was then collected prior to the harvesting of chondrocyte pellets at 0.5-, 4-, 8- and 24-hours post-cessation of force application by adding 1 ml of TRIzol$^{TM}$ reagent before storage at -80$^{o}$C until further processing (sections 2.2 - 2.10). Control 3D chondrocyte pellets were also set up with no exposure to centrifugal force but kept under identical culture conditions as the centrifuged groups. Two biological repeat experiments were conducted (i.e., N = 2); each consisting of four technical repeats (i.e., n = 4 per time point). Mechanical loading was always performed at the same time of day (i.e., 10:00 am).

#### 3.2.2. Investigating whether increasing load duration influences chondrocyte mechano-responses in 3D chondrocyte pellets with or without PCM

To determine whether increasing the duration of centrifugation influences chondrocyte mechano-responsiveness in 3D pellets with differing PCM amounts, relevant 3D chondrocyte pellets (either with or without PCM) were subjected to centrifugal force determined from the outcomes of section 3.2.1 (i.e., 770xg force) for either 15- or 60-minutes. In each experiment, culture media was changed daily (1 ml removal and replenishment with standard culture media as described in section 2.1.2). In each experiment, culture media was harvested prior to pellet harvesting at 1-, 4-, 8- and 24-hours following the cessation of centrifugation by adding 1 ml of TRIzol$^{TM}$ reagent before storage at -80$^{o}$C until further processing (sections 2.2 - 2.10). One experiment was conducted using each 3D model and load duration, i.e., 3D pellets with and without PCM loaded for either 15- or 60-minutes (i.e., N = 1) each consisting of four technical repeats per time point (i.e., n = 4). Mechanical loading was always performed at the same time of day (i.e., 10:00 am). Control 3D chondrocyte pellets (either with or without PCM) also were set up with no exposure to centrifugal force but kept under identical culture conditions as

the centrifuged groups in each experiment, before harvesting and processing at similar time points.

## 3.3. Results

### 3.3.1. Responses of 3D chondrocyte pellet cultures (without PCM) to centrifugal force

#### 3.3.1.1. Live/dead staining demonstrated high cell viability in 3D chondrocyte pellet cultures

To assess the viability of chondrocytes in 3D pellet cultures, live/dead staining was performed using FDA (green) and PI (red) in control pellet cultures and those subjected to 770xg force for 15 minutes before harvesting at T24- and 72-hours (sampling at T72 hours was performed on a different experimental set-up specifically to assess cell viability as other experiments in this PhD project ran up to 72 hours post cessation of centrifugation). Control chondrocyte pellets exhibited conspicuous FDA staining [Fig. 3.1.A], with a lower intensity of PI stain [Fig. 3.1.B] at T24 hours, suggesting that most chondrocytes in these pellets were viable [Fig. 3.1.C]. High cell viability was also observed 24 hours following cessation of 15 minutes of 770xg force [Fig. 3.1.D & F]. Furthermore, the observed FDA fluorescence was more prominent in the pellets' periphery whereas the limited PI staining was predominantly identified towards the centre of the pellets, indicative of a potential necrotic core [Fig. 3.1.E]. Similar labelling was observed at 72-hours post cessation of centrifugation, with high FDA fluorescence mainly towards the periphery of the pellet [Fig. 3.1.G] relative to the PI fluorescence which was predominantly in the pellet centre [Fig. 3.1.H], suggestive of a persistence of high cell viability following this culture period [Fig. 3.1.I].

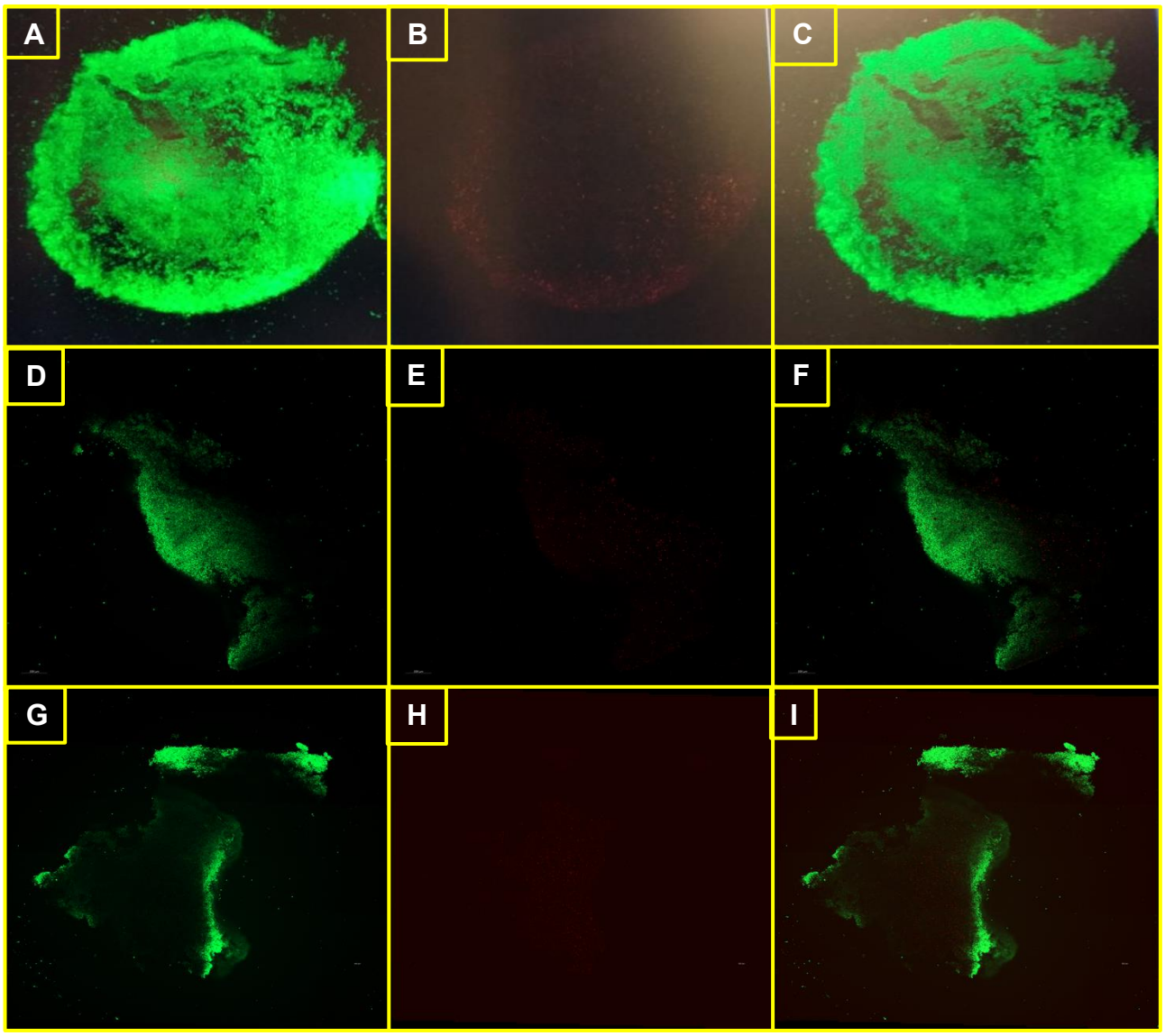


**Figure 3.1. Live/dead staining of 3D chondrocyte pellets to determine the influence of 770xg force on cell viability**. Images illustrate live/dead stain using fluorescein diacetate (FDA - green) and propidium iodide (PI - red) dyes, respectively, in control pellets as well as those subjected to 770xg force for 15 minutes before collection either at T24- or T72-hours; images demonstrate: **A)** control pellet; FDA live cells stain at T24 hours, **B)** control pellet; PI dead cells stain at T24 hours, **C)** control pellet; composite image for FDA & PI stains at T24 hours, **D)** 770xg loaded pellet; FDA live cells stain at T24 hours, **E)** 770xg loaded pellet; PI dead cells stain at T24 hours, **F)** 770xg loaded pellet; composite image for FDA & PI stains at T24 hours, **G)** 770xg loaded pellet; FDA live cells stain at T72 hours, **H)** 770xg loaded pellet; PI dead cells stain at T72 hours, and **I)** 770xg loaded pellet; composite image for FDA & PI stains at T72 hours. Images showing irregular shapes represent pellets which disintegrated during transfer from microcentrifuge tubes to petri dishes prior to microscopic imaging using the ZEISS Plan-APOCHROMAT 20X/0.95 Autocorr Objective in the Celldiscoverer 7 microscope [Bioimaging Hub]; images are not illustrated to a specific scale.

### 3.3.1.2. Application of 200- and 1000-xg forces had no effect on sGAG release within a 24-hour window, while 770xg force induced subtle reductions in sGAG release at T24 hours in 3D chondrocyte pellets

**200xg** Control pellet cultures exhibited significant increases in sGAG concentration within a 24-hour window of investigation measured at T0.5- and T24-hours (T0.5 vs 24 hours: 1.18±0.88 µg/ml, 20.3±3.77 µg/ml [p = 0.0294]). Likewise, a significant increase in sGAG concentration was observed between T0.5- and T24-hours in pellet cultures subjected to 15 minutes of 200xg force (T0.5 vs 24 hours: 1.22±0.84 µg/ml, 19.8±1.26 µg/ml [p = 0.0294]). However, no significant differences were observed between controls and 200xg loaded pellets at both time points (T0.5 hours [p = 0.9999], T24 hours [p = 0.6612]) (data not shown).

**770xg** A significant increase in sGAG concentration was observed in control pellet cultures within a 24-hour window measured at T0.5- and T24-hours (T0.5 vs 24 hours: 1.45±0.23 µg/ml, 15.7±0.77 µg/ml [p = 0.0294]). Likewise, significantly increased concentration of sGAG was observed between T0.5- and T24-hours following application of 15 minutes of 770xg force (T0.5 vs 24 hours: 1.53±1.05 µg/ml, 14.5±0.19 µg/ml [p = 0.0294]). However, no significant differences were observed between controls and 770xg loaded pellets at T0.5 hours (p = 0.9999). Surprisingly, application of 770xg force elicited a subtle but statistically significant reduction at T24 hours (p = 0.0294) (data not shown).

**1000xg** Control pellet cultures exhibited significant increases in sGAG concentration within a 24-hour window measured at T0.5- and T24-hours (T0.5 vs 24 hours: 1.18±0.45 µg/ml, 13.3±0.51 µg/ml [p = 0.03038]). Likewise, a significant increase in sGAG concentration was observed between T0.5- and T24-hours in pellet cultures subjected to 15 minutes of 1000xg force (T0.5 vs 24 hours: 1.03±0.45 µg/ml, 12.8±1.13µg/ml [p = 0.03038]). However, no significant differences were observed between controls and 1000xg loaded pellets at both time points (T0.5 hours [p =0.8839], T24 hours [p = 0.5614]) (data not shown).

### 3.3.1.3. Application of 200-, 770- and 1000-xg forces had no effect on NO release in 3D chondrocyte pellets

No detectable nitrite/NO was observed at T0.5 hours in both the controls and loaded pellet cultures (i.e., following 200-, 770- and 1000-xg force).

**200xg** Control pellet cultures exhibited significant increases in nitrite concentration between T8- and T24-hours (T8 vs 24 hours: 7.51±0.06 μM, 11.0±1.08 μM [p = 0.02558]). In contrast, application of 200xg force had no effect on nitrite production between T8- and T24-hours (T8 vs 24 hours: 7.87±2.24 μM, 11.8±1.84 μM [p = 0.0606]). Also, no significant differences were observed between controls and 200xg loaded pellets at both time points (T8 hours [p = 0.9999], T24 hours [p = 0.5590]).

**770xg** A significant increase in nitrite concentration was observed in control pellet cultures between T8- and T24-hours (T8 vs 24 hours: 3.53±0.89 μM, 9.59±0.89 μM [p = 7.1e-05]). Likewise, a significantly increased concentration of nitrite was observed between T8- and T24-hours following application of 15 minutes of 770xg force (T8 vs 24 hours: 4.45±1.31 μM, 10.3±1.24 μM [p = 0.000620]). Overall, no significant differences were observed between controls and 770xg loaded pellets at both time points (T8 hours [p = 0.290], T24 hours [p = 0.370]).

**1000xg** Control pellet cultures produced significant increases in nitrite between T8- and T24-hours (T8 vs 24 hours: 6.43±0.40 μM, 12.4±2.54 μM [p = 0.0290]). Likewise, a significant increase in nitrite production was observed between T8- and T24-hours in pellet cultures subjected to 15 minutes of 1000xg force (T8 vs 24 hours: 7.03±0.89 μM, 12.5±2.65 μM [p = 0.0290]). However, no significant differences were observed between controls and 1000xg loaded pellets at both time points (T8 hours [p = 0.340], T24 hours [p = 0.999]).

#### 3.3.1.4. Assessment of HKG stability using refFinder software identified *hprt* and *18s* to be the most stable HKGs in 3D chondrocyte pellets following load

To determine the two most suitable HKGs for qPCR normalisation of target gene expression following exposure of chondrocyte pellets to 15 minutes of centrifugal force (200-, 770- or 1000-xg) within a 24-hour window of investigation, refFinder software was employed. BestKeeper analysis identified *18s* and *ppia* [Fig. 3.2A], comparative Delta Ct identified *hprt* and *ppia* [Fig. 3.2B], Genorm revealed *18s* and *hprt* [Fig. 3.2C] and normFinder selected *hprt* and *ppia* as the two most stable housekeeping genes following force application [Fig. 3.2D]. Ultimately, the refFinder software integrated the ranking scores from all four programmes and provided a comprehensive overall gene stability ranking which demonstrated *hprt* and *18s* to be the two most suitable HKGs for qPCR normalisation of target gene expression in further centrifugation experiments [Fig. 3.2E].

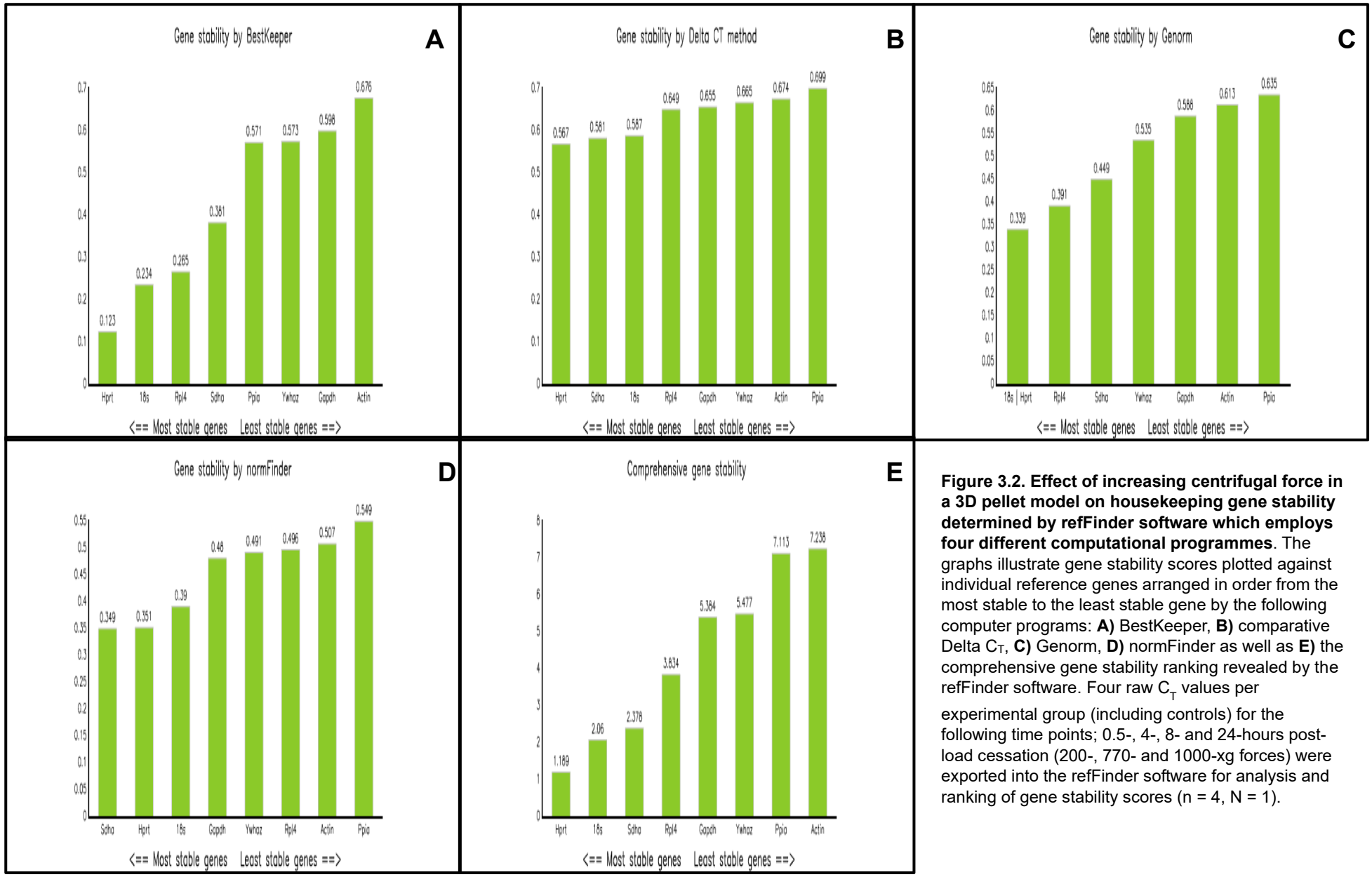


**Figure 3.2. Effect of increasing centrifugal force in a 3D pellet model on housekeeping gene stability determined by refFinder software which employs four different computational programmes**. The graphs illustrate gene stability scores plotted against individual reference genes arranged in order from the most stable to the least stable gene by the following computer programs: **A)** BestKeeper, **B)** comparative Delta $C_T$, **C)** Genorm, **D)** normFinder as well as **E)** the comprehensive gene stability ranking revealed by the refFinder software. Four raw $C_T$ values per experimental group (including controls) for the following time points; 0.5-, 4-, 8- and 24-hours post-load cessation (200-, 770- and 1000-xg forces) were exported into the refFinder software for analysis and ranking of gene stability scores (n = 4, N = 1).

### 3.3.1.5. The impact of centrifugal force on the expression of mechano-responsive genes in 3D chondrocyte pellets

mRNA transcripts for the early mechano-responsive genes, *c-fos* and *c-jun*, and late mechano-responsive catabolic genes *adamts-4*, *adamts-5* and *mmp-3* were analysed at 0.5-, 4-, 8- and 24-hours post cessation of centrifugation of pellets with no PCM. Analysis was carried out as described in Chapter 2 (sections 2.6.5 and 2.6.6) where fold change was calculated relative to the control for each time point.

#### 3.3.1.5.1. Early increases in *c-fos* transcription in response to centrifugal force

**200xg force**

No significant changes in mRNA transcripts for the early mechano-responsive gene *c-fos* were observed at T0.5 hours following application of 200xg force, however, *c-fos* mRNA transcripts were significantly upregulated at T4 hours (1.59-fold, p = 0.03038) [Fig. 3.3A]. Interestingly, a significant reduction in *c-fos* mRNA transcripts was then observed at T8 hours (2.2-fold, p = 0.03038) which returned to basal levels at T24 hours [Fig. 3.3A].

**770xg force**

3D chondrocyte cultures subjected to 770xg force exhibited significant increases in *c-fos* mRNA transcripts at T0.5 hours (1.32-fold, p = 0.0294) and T4 hours (1.53-fold, p = 0.03038) [Fig. 3.3B]; however, *c-fos* mRNA expression returned to basal levels at T8 hours [Fig. 3.3B], suggesting the chondrocytes' early, but transient mechano-response to 770xg force.

**1000xg force**

Following application of 1000xg force, *c-fos* mRNA levels were significantly upregulated at 0.5 hours post cessation of centrifugation (1.89-fold, p = 0.0014) [Fig. 3.3C] before becoming downregulated at T4- (1.42-fold, p = 0.018), T8- (1.31-fold, p = 0.039) and T24-hours (1.78-fold, p = 7.2e-05) [Fig. 3.3C].

Collectively, this data demonstrates that at all centrifugal forces tested there was an initial up-regulation of *c-fos* gene expression which returned to control level or below within a 24-hour window post-cessation of centrifugation.

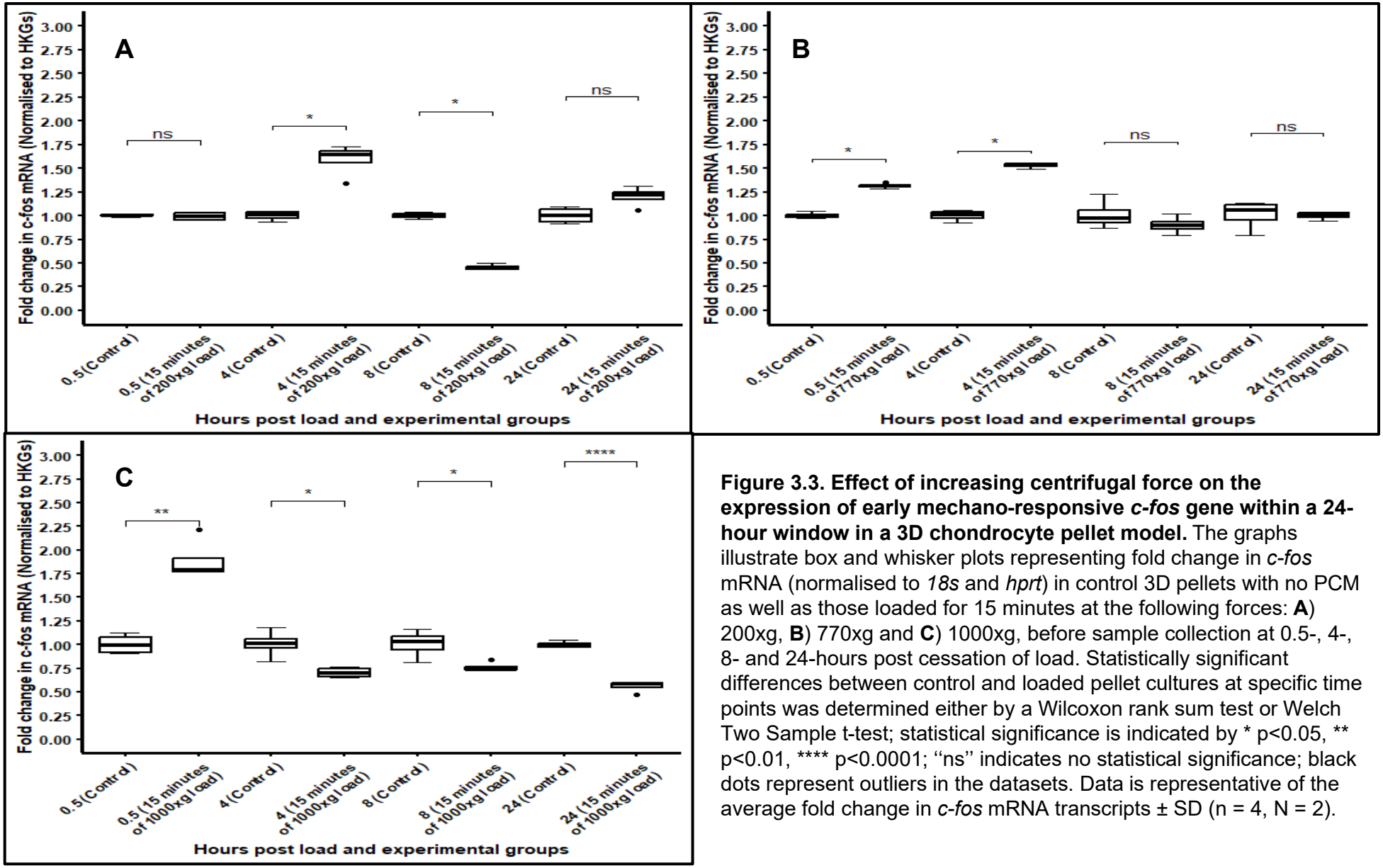


**Figure 3.3. Effect of increasing centrifugal force on the expression of early mechano-responsive *c-fos* gene within a 24-hour window in a 3D chondrocyte pellet model.** The graphs illustrate box and whisker plots representing fold change in *c-fos* mRNA (normalised to *18s* and *hprt*) in control 3D pellets with no PCM as well as those loaded for 15 minutes at the following forces: **A**) 200xg, **B**) 770xg and **C**) 1000xg, before sample collection at 0.5-, 4-, 8- and 24-hours post cessation of load. Statistically significant differences between control and loaded pellet cultures at specific time points was determined either by a Wilcoxon rank sum test or Welch Two Sample t-test; statistical significance is indicated by * $p<0.05$, ** $p<0.01$, **** $p<0.0001$; ‘‘ns’’ indicates no statistical significance; black dots represent outliers in the datasets. Data is representative of the average fold change in *c-fos* mRNA transcripts ± SD (n = 4, N = 2).

#### 3.3.1.5.2. Application of 200- and 770-xg force transiently increases *c-jun* mRNA transcription

**200xg force**

As observed with *c-fos*, it was only at T4 hours that 200xg force significantly increased *c-jun* expression (1.64-fold, p = 0.03038) [Fig. 3.4A]; no differences were observed at the later time points.

**770xg force**

A 770xg force significantly induced *c-jun* transcription at T0.5 hours (1.67-fold, p = 0.03038) [Fig. 3.4B]; however, no changes were observed in *c-jun* mRNA transcripts at 4-, 8- and 24-hours post 770xg force cessation.

**1000xg force**

Following 1000xg force, there was no effect on *c-jun* transcription at T0.5- and 4-hours; however, a significant 1.27-fold downregulation was observed 8 hours post cessation of 1000xg force (p = 0.03038) [Fig. 3.4C]. At T24 hours, signals had returned to baseline levels.

#### 3.3.1.5.3. A 770xg force significantly induces expression of mechano-responsive catabolic gene *mmp-3* in a time-dependent manner

**200xg force**

Expression of the mechano-responsive catabolic gene *mmp-3* was significantly induced at 4 hours post cessation of 200xg force (1.25-fold increase, p = 0.00850) [Fig. 3.5A]. However, values returned to baseline at T8 hours [Fig. 3.5A].

**770xg force**

Application of 770xg force appeared to subtly reduce *mmp-3* mRNA transcripts at T0.5 hours (1.10-fold, p = 0.03038) [Fig. 3.5B], before demonstrating an increase at T4 hours (1.26-fold, p = 0.03038); *mmp-3* mRNA expression peaked at 8 hours post 770xg force cessation (1.85-fold increase, p = 0.03038) [Fig. 3.5B]. At T24 hours, *mmp-3* mRNA levels had returned to basal levels.

**1000xg force**

Surprisingly, no significant changes in *mmp-3* mRNA transcription were observed throughout the 24-hour period of investigation (i.e., at T0.5-, T4-, T8- and T24-hours) in 3D chondrocyte pellet cultures subjected to 1000xg force [Fig. 3.5C].

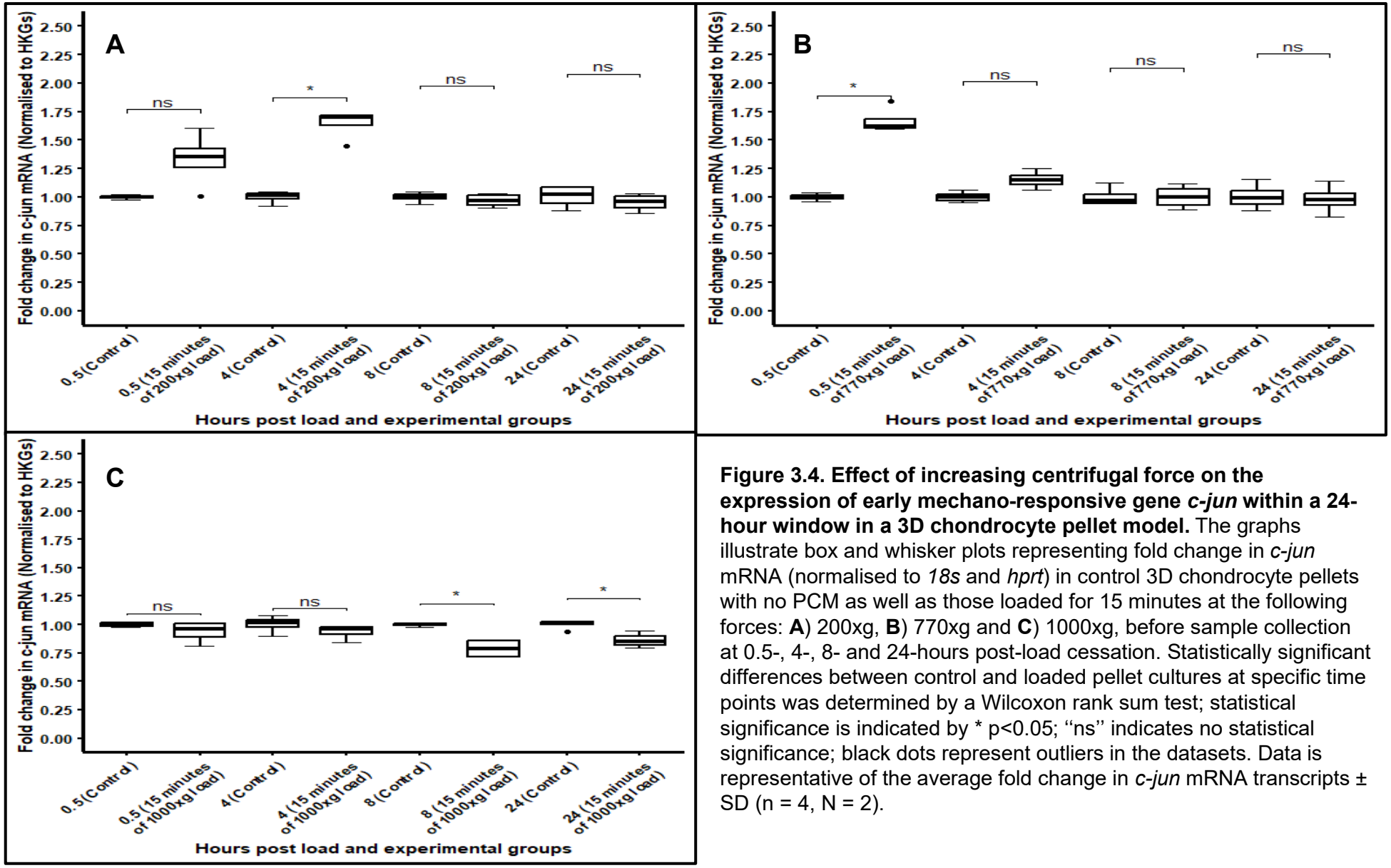


**Figure 3.4. Effect of increasing centrifugal force on the expression of early mechano-responsive gene *c-jun* within a 24-hour window in a 3D chondrocyte pellet model.** The graphs illustrate box and whisker plots representing fold change in *c-jun* mRNA (normalised to *18s* and *hprt*) in control 3D chondrocyte pellets with no PCM as well as those loaded for 15 minutes at the following forces: **A**) 200xg, **B**) 770xg and **C**) 1000xg, before sample collection at 0.5-, 4-, 8- and 24-hours post-load cessation. Statistically significant differences between control and loaded pellet cultures at specific time points was determined by a Wilcoxon rank sum test; statistical significance is indicated by * $p<0.05$; ‘‘ns’’ indicates no statistical significance; black dots represent outliers in the datasets. Data is representative of the average fold change in *c-jun* mRNA transcripts ± SD (n = 4, N = 2).

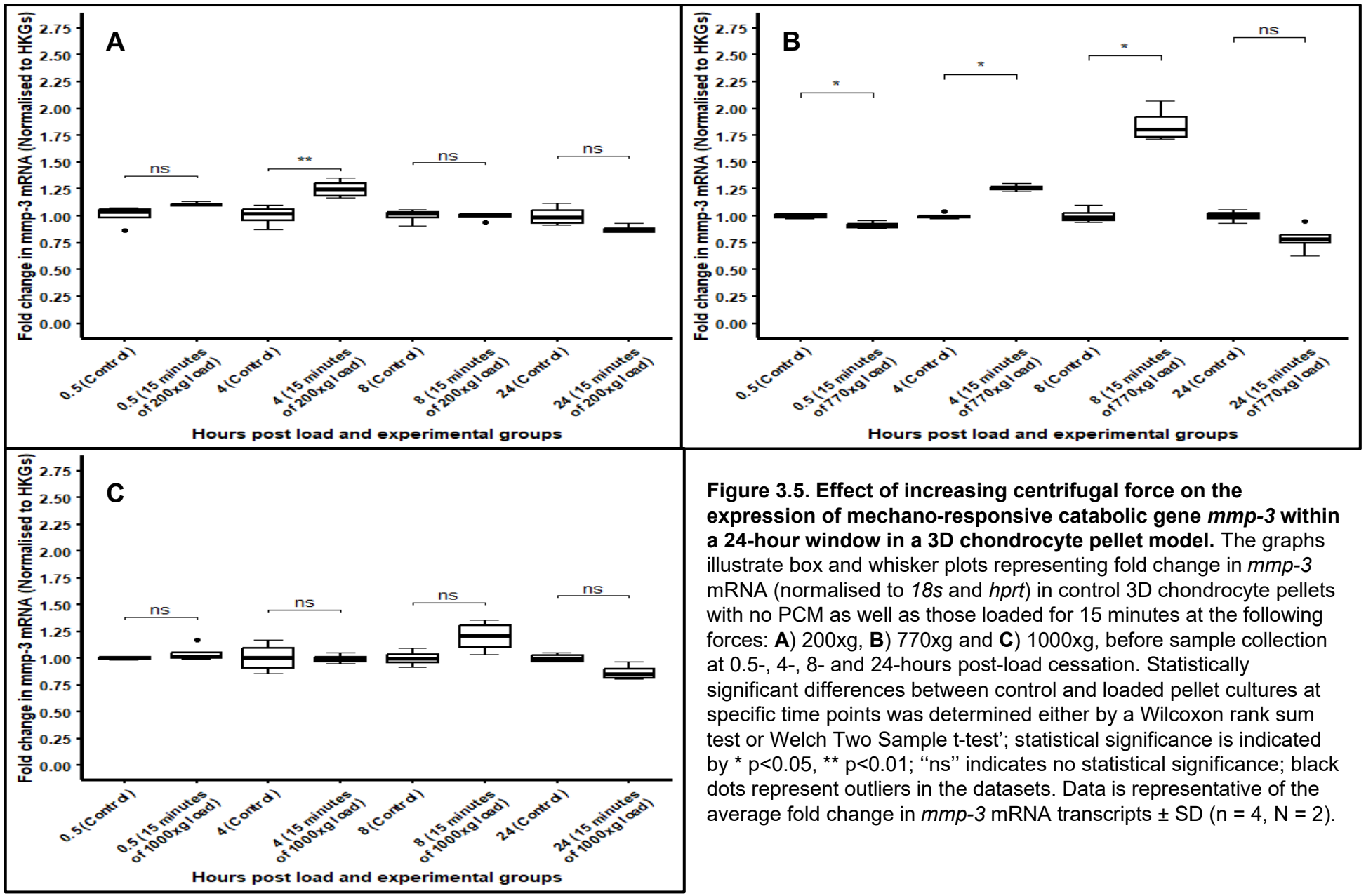


**Figure 3.5. Effect of increasing centrifugal force on the expression of mechano-responsive catabolic gene *mmp-3* within a 24-hour window in a 3D chondrocyte pellet model.** The graphs illustrate box and whisker plots representing fold change in *mmp-3* mRNA (normalised to *18s* and *hprt*) in control 3D chondrocyte pellets with no PCM as well as those loaded for 15 minutes at the following forces: **A**) 200xg, **B**) 770xg and **C**) 1000xg, before sample collection at 0.5-, 4-, 8- and 24-hours post-load cessation. Statistically significant differences between control and loaded pellet cultures at specific time points was determined either by a Wilcoxon rank sum test or Welch Two Sample t-test'; statistical significance is indicated by * $p<0.05$, ** $p<0.01$; ''ns'' indicates no statistical significance; black dots represent outliers in the datasets. Data is representative of the average fold change in *mmp-3* mRNA transcripts ± SD (n = 4, N = 2).

### 3.3.1.5.4. Differential biphasic transcriptional regulation of mechano-responsive catabolic gene *adamts-4* following 770- and 1000-xg force application

#### 200xg force

Overall, chondrocyte pellets subjected to the 200xg force exhibited significantly reduced *adamts*-4 mRNA transcripts, a marker of catabolism; there was a reduction in expression at 0.5 hours post 200xg force cessation (1.21-fold, p = 0.03038) and at T24 hours (1.34-fold, p = 0.03038) [Fig. 3.6A].

#### 770xg force

Expression of *adamts*-4 transcripts appeared to follow a biphasic profile (i.e., a response showing two-phases of induction as there was an initial reduction, before the return to baseline followed by a significant increase and another reduction to baseline) following application of a 770xg force as demonstrated by significant downregulation at T0.5 hours (1.76-fold, p = 0.03038), followed by no effect at T4 hours, then a 2.10-fold increase at T8 hours (p = 0.03038) [Fig. 3.6B]. *adamts*-4 mRNA transcripts had returned to basal levels by 24 hours [Fig. 3.6B].

#### 1000xg force

Although no effects were observed at the earlier time points, there was a significant increase in *adamts*-4 mRNA transcripts 8 hours post 1000xg force cessation (1.40-fold, p = 0.0294) [Fig. 3.6C]. At T24 hours, *adamts-4* mRNA levels had significantly reduced to below basal expression levels (1.52-fold, p = 0.03038) [Fig. 3.6C].

### 3.3.1.5.5. Centrifugal force induces mechano-responsive catabolic gene *adamts-5* expression, which is significantly reduced 24 hours post-force cessation, irrespective of magnitude of centrifugation

#### 200xg force

*adamts-5* mRNA levels were significantly increased 0.5 hours post-200xg force cessation (1.27-fold, p = 0.03038) [Fig. 3.7A]. Although no effects were observed at T4- and 8-hours, there was a significant reduction at 24 hours post-200xg force cessation (1.36-fold, p = 0.03038) [Fig. 3.7A].

### 770xg force

*adamts-5* transcription was not induced at T0.5 hours following application of 770xg force to 3D chondrocyte pellets. Interestingly, application of 770xg force induced significant increases in *adamts-5* mRNAs at 4- (1.43-fold, p = 0.03038) and 8-hours post 770xg force cessation (2.20-fold, p = 0.03038) [Fig. 3.7B]. However, at 24 hours, a significant reduction in *adamts-5* mRNA levels was observed falling below basal expression (1.25-fold, p = 0.03038) [Fig. 3.7B].

### 1000xg force

An early induction of *adamts-5* transcription was detected at 0.5 hours post-1000xg force cessation (1.54-fold increase, p = 0.00062) [Fig. 3.7C]. Levels subsequently returned to baseline levels at T4- and T8-hours. At T24 hours, a significant reduction in *adamts-5* mRNA transcripts was observed following application of 1000xg force (1.27-fold, p = 0.0035) [Fig. 3.7C].

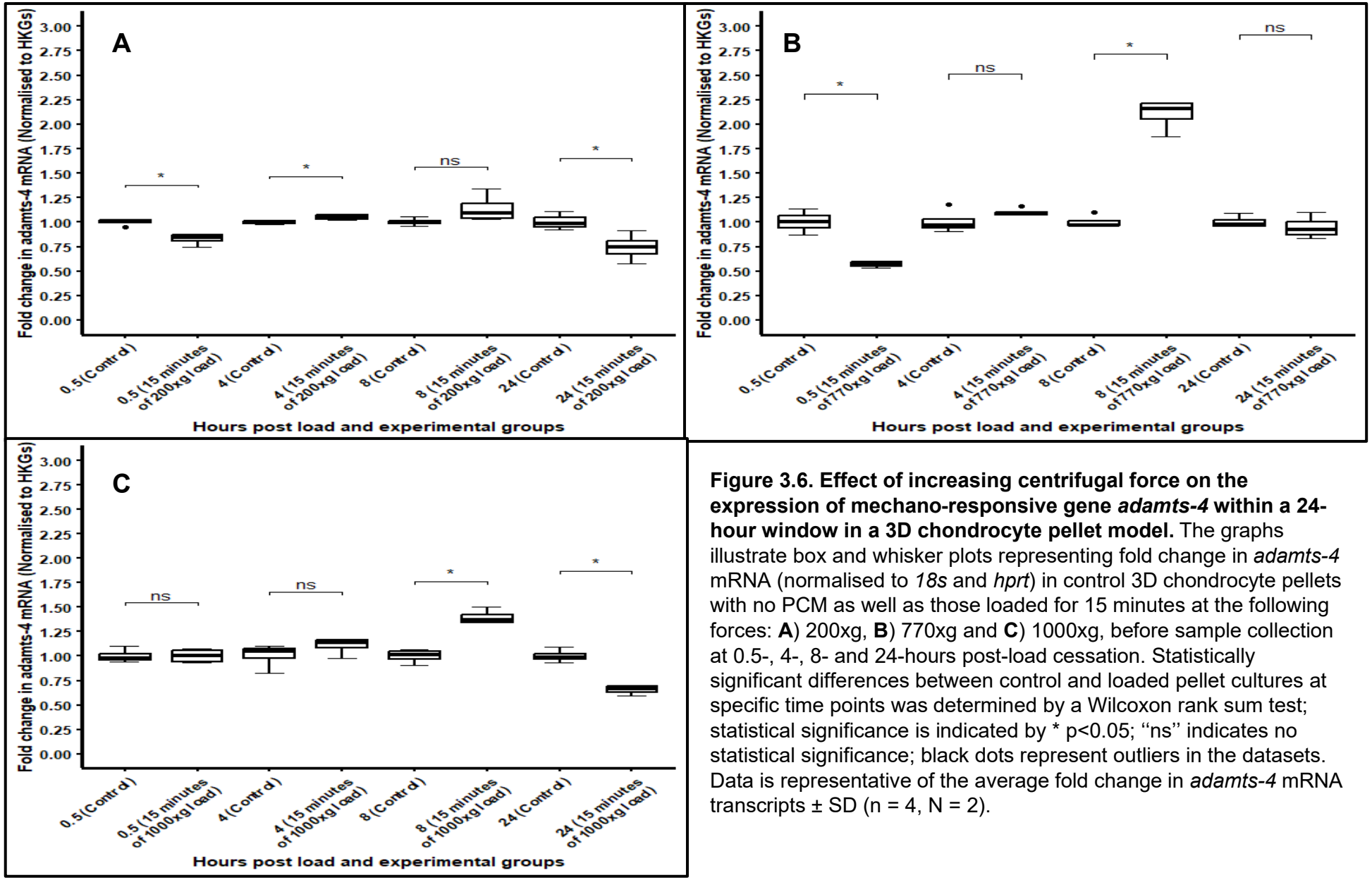


**Figure 3.6. Effect of increasing centrifugal force on the expression of mechano-responsive gene *adamts-4* within a 24-hour window in a 3D chondrocyte pellet model.** The graphs illustrate box and whisker plots representing fold change in *adamts-4* mRNA (normalised to *18s* and *hprt*) in control 3D chondrocyte pellets with no PCM as well as those loaded for 15 minutes at the following forces: **A**) 200xg, **B**) 770xg and **C**) 1000xg, before sample collection at 0.5-, 4-, 8- and 24-hours post-load cessation. Statistically significant differences between control and loaded pellet cultures at specific time points was determined by a Wilcoxon rank sum test; statistical significance is indicated by * $p<0.05$; ‘‘ns’’ indicates no statistical significance; black dots represent outliers in the datasets. Data is representative of the average fold change in *adamts-4* mRNA transcripts ± SD (n = 4, N = 2).

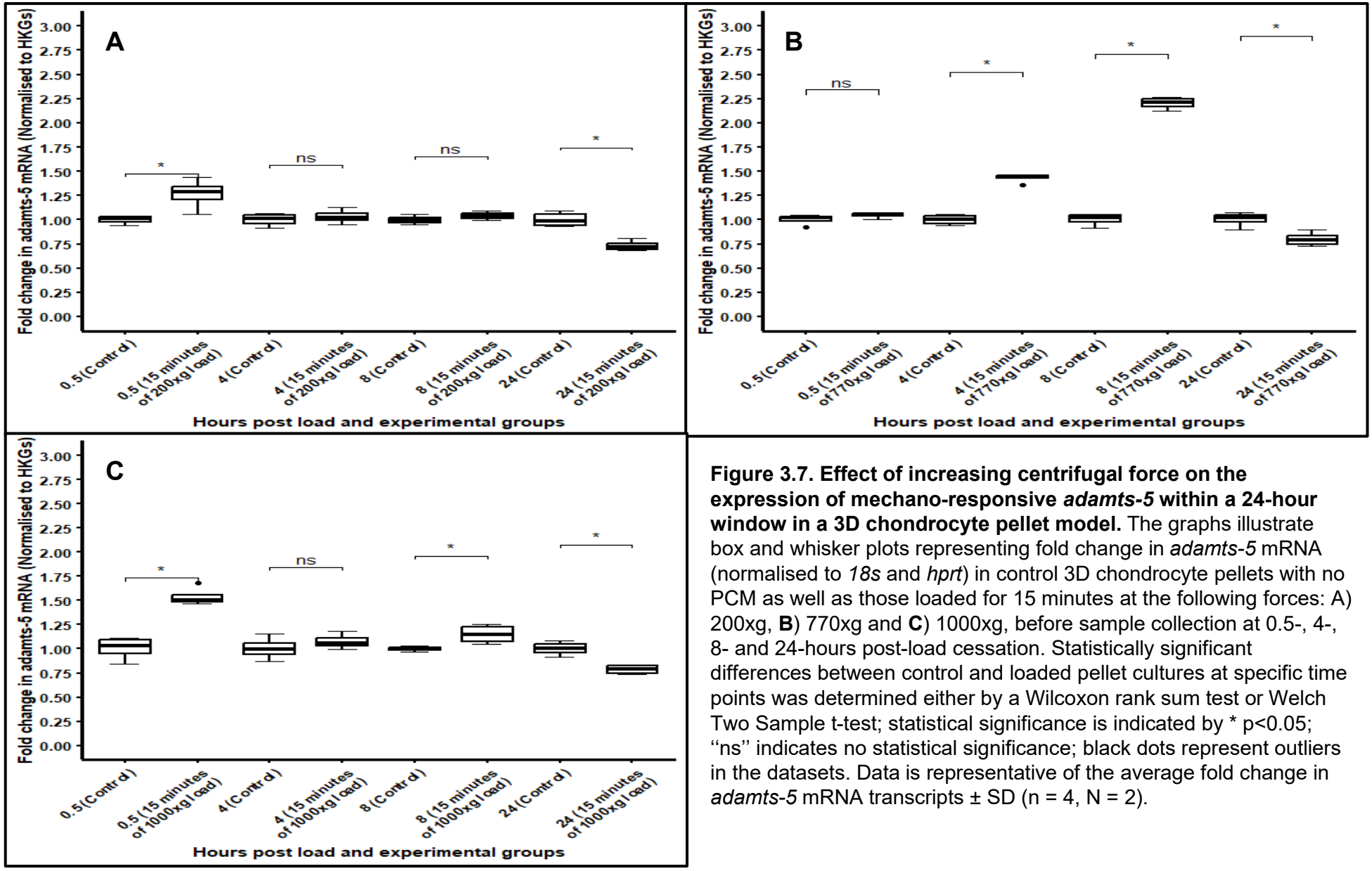


**Figure 3.7. Effect of increasing centrifugal force on the expression of mechano-responsive *adamts-5* within a 24-hour window in a 3D chondrocyte pellet model.** The graphs illustrate box and whisker plots representing fold change in *adamts-5* mRNA (normalised to *18s* and *hprt*) in control 3D chondrocyte pellets with no PCM as well as those loaded for 15 minutes at the following forces: A) 200xg, **B**) 770xg and **C**) 1000xg, before sample collection at 0.5-, 4-, 8- and 24-hours post-load cessation. Statistically significant differences between control and loaded pellet cultures at specific time points was determined either by a Wilcoxon rank sum test or Welch Two Sample t-test; statistical significance is indicated by * $p<0.05$; ‘‘ns’’ indicates no statistical significance; black dots represent outliers in the datasets. Data is representative of the average fold change in *adamts-5* mRNA transcripts ± SD (n = 4, N = 2).

### 3.3.1.6. 15 minutes of 770xg centrifugal force mediates prominent responses in induction of mechano-responsive genes in 3D chondrocyte pellet cultures

Collectively, data revealed the induction of prominent mechano-responses of target genes when mechanical loads were simulated using the 770xg centrifugal force as compared to the 200- and 1000-xg centrifugal forces as evidenced by significant increases in the early mechano-responsive genes, *c-fos* [Fig. 3.3B] and *c-jun* [Fig. 3.4B] at T0.5- or T4-hours following application of 770xg force. Significant increases in mRNA transcripts for the mechano-responsive catabolic genes; *mmp-3* [Fig. 3.5B], *adamts-4* [Fig. 3.6B] and *adamts-5* [Fig. 3.7B] were also observed following the cessation of 770xg force, with fold-increases above those of control cultures observed at late time points, i.e., T8- or T24-hours. This data informed the decision to select this magnitude of centrifugation for further optimisation of a centrifugal regimen to determine the impact of increasing load duration on cell behaviours.

### 3.3.2. Responses of 3D chondrocyte pellets with and without PCM to increases in the duration of centrifugal force application

#### 3.3.2.1. Differential induction of sGAG release within a 72-hour window following application of 15- or 60-minutes of 770xg force to 3D pellets with and without PCM

No sGAG was detectable at T1 hour in both the controls and 770xg loaded pellets with and without PCM following exposure to either 15- or 60-minutes (data not shown).

**15 minutes** Control pellets with no PCM exhibited significant increases in sGAG concentration within a 64-hour window with levels increasing from 17.2±0.070 µg/ml (T8 hours), 28.4±2.63 µg/ml (T24 hours), to 30.3±2.41 µg/ml (T48 hours) before decreasing to 21.6±0.31 µg/ml (T72 hours). Application of 15 minutes of 770xg force to 3D pellets with no PCM induced similar increases in sGAG concentration within a 64-hour window, however, no significant differences were observed when comparing control cultures and those subjected to 15 minutes of 770xg force at T8- [$p = 0.3065$], T24- [$p = 0.3123$], and T48-hours [$p = 0.5614$]. Interestingly, application of 15 minutes of 770xg force to 3D pellets with no PCM significantly reduced sGAG levels at T72 hours [$p = 0.02843$]) (data not shown).

However, a significant decrease in sGAG concentration from 24.1±2.77 µg/ml (T24 hours) to 10.9±4.13 µg/ml (T72 hours) [$p = 0.003$] was observed in control 3D pellets with PCM within a 48-hour window (data not shown). Application of 15 minutes of 770xg force to pellets with PCM induced a similar reduction in sGAG concentration within the same 48-hour window; however, no significant differences were observed when comparing sGAG levels between control cultures and those subjected to 15 minutes of 770xg force at T24- [$p = 0.885$], T48- [$p = 0.772$] and T72-hours [$p = 0.468$] in 3D pellets with PCM (data not shown).

**60 minutes** Significant increases in sGAG concentration were observed in control pellets with no PCM ranging from 16.9±0.62 µg/ml (T8 hours), 30.5±3.99 µg/ml (T24 hours) to 31.5±0.14 µg/ml (T48 hours) before decreasing to 19.2±2.12 µg/ml (T72 hours). Similar increases in sGAG release were observed in pellets with no PCM subjected to 60 minutes of 770xg force, but overall, no significant differences were detected between control cultures and those exposed to 60 minutes of 770xg force (T8- [$p = 0.3094$], T24- [$p = 0.8852$], and T72-hours [$p = 0.4705$]), except at T48 hours where a significant reduction was observed [$p = 0.0294$] (data not shown).

Likewise, sGAG levels were significantly reduced in control pellets with no PCM from 21.9±2.88 µg/ml (T24 hours) to 13.0±1.58 µg/ml (T72 hours) [p = 0.002] within a 48-hour window. Comparable reductions in sGAG concentrations were observed in pellets with PCM following exposure to 60 minutes of 770xg force, but overall, no significant differences were detected relative to control cultures at T24- [p = 0.665], T48-, [p = 0.999] and T72-hours [p = 0.661] (data not shown).

#### 3.3.2.2. Undetectable nitrite/NO was observed within a 72-hour window in both the control 3D pellets with and without PCM and those subjected either to 15- or 60-minutes of 770xg force

No detectable nitrite was observed at T1-, T24-, T48- and T72-hours in both the control and 770xg loaded pellets with and without PCM irrespective of the loading duration (i.e., 15- or 60-minutes) (data not shown).

#### 3.3.2.3. The impact of increasing the duration of centrifugal force application on the expression of mechano-responsive genes in 3D chondrocyte pellets with and without PCM

mRNA transcripts for the early mechano-responsive genes, *c-fos*, *c-jun,* and late mechano-responsive catabolic genes, *adamts-4*, *adamts-5* and *mmp-3* as well as the chondrogenic gene *sox9* (included to assess the chondrocyte phenotype in the utilised 3D pellet model) were analysed at 1-, 4-, 8- and 24-hours post cessation of 15- and 60-minutes centrifugation at 770xg force in pellets with no PCM. Analysis was carried out as described in chapter 2 (sections 2.6.5 and 2.6.6), where fold change was calculated relative to the control for each time point. To ascertain how extensively the PCM contributes to cell mechano-responses, chondrocytes were cultured for a further 7 days and comparable analyses performed.

#### 3.3.2.3.1. Application of 60 minutes of 770xg force induced prominent elevations in *c-fos* mRNA levels in pellets with no PCM, but stronger and earlier mechano-regulation of *c-fos* transcription in pellets with PCM

3D pellets with no PCM subjected to 770xg force for 15 minutes demonstrated significantly elevated mRNA transcripts for the early mechano-responsive gene, *c-fos* 1-hour post 770xg force cessation (1.99-fold, p = 0.0290) [Fig. 3.8A]. At T4 hours, no significant differences were observed in *c-fos* mRNA levels having returned to basal expression [Fig. 3.8A]. This early mechano-responsiveness is comparable to that revealed in section 3.3.1.5.1 where *c-fos* upregulation was observed at T0.5- and T4-hours following application of 15 minutes of 770xg force to 3D pellets.

Likewise, following 60 minutes of 770xg force, a significant increase in *c-fos* mRNA transcripts was also observed 1-hour post-force cessation (3.14-fold, p = 0.0294), before the signal returned to basal expression at T4 hours [Fig. 3.8B]. This indicates that increasing the duration of 770xg force exposure from 15- to 60-minutes induced stronger mechano-regulation of this early response gene (1.58-fold increase) in 3D pellets with no PCM.

In 3D pellets with PCM exposed to 15 minutes of 770xg force, subtle reductions were observed in *c-fos* transcripts at 1- (1.09-fold, p = 0.0294) and 4-hours post-cessation of centrifugation (1.11-fold, p = 0.03038) [Fig. 3.8C]. However, at T8 hours a significant 1.50-fold increase in *c-fos* mRNA transcripts was observed (p = 0.0294) [Fig. 3.8C]; at 24 hours, a significant 1.74-fold reduction in *c-fos* transcripts was observed (p = 0.0294) [Fig. 3.8C].

In contrast, pellet cultures with PCM subjected to 60 minutes of 770xg force exhibited a significant 2.55-fold increase in *c-fos* mRNA levels at T1 hour (p = 0.0294) [Fig. 3.8D]; this mechano-responsiveness was sustained at T4- (2.21-fold, p = 0.03038) and T8-hours (1.71-fold, p = 0.03038) [Fig. 3.8D], before decreasing to basal levels, as observed in control pellets, at T24 hours [Fig. 3.8D]. Overall, this indicates that increasing load duration resulted in stronger and earlier mechano-regulation of this early response gene in the presence of PCM.

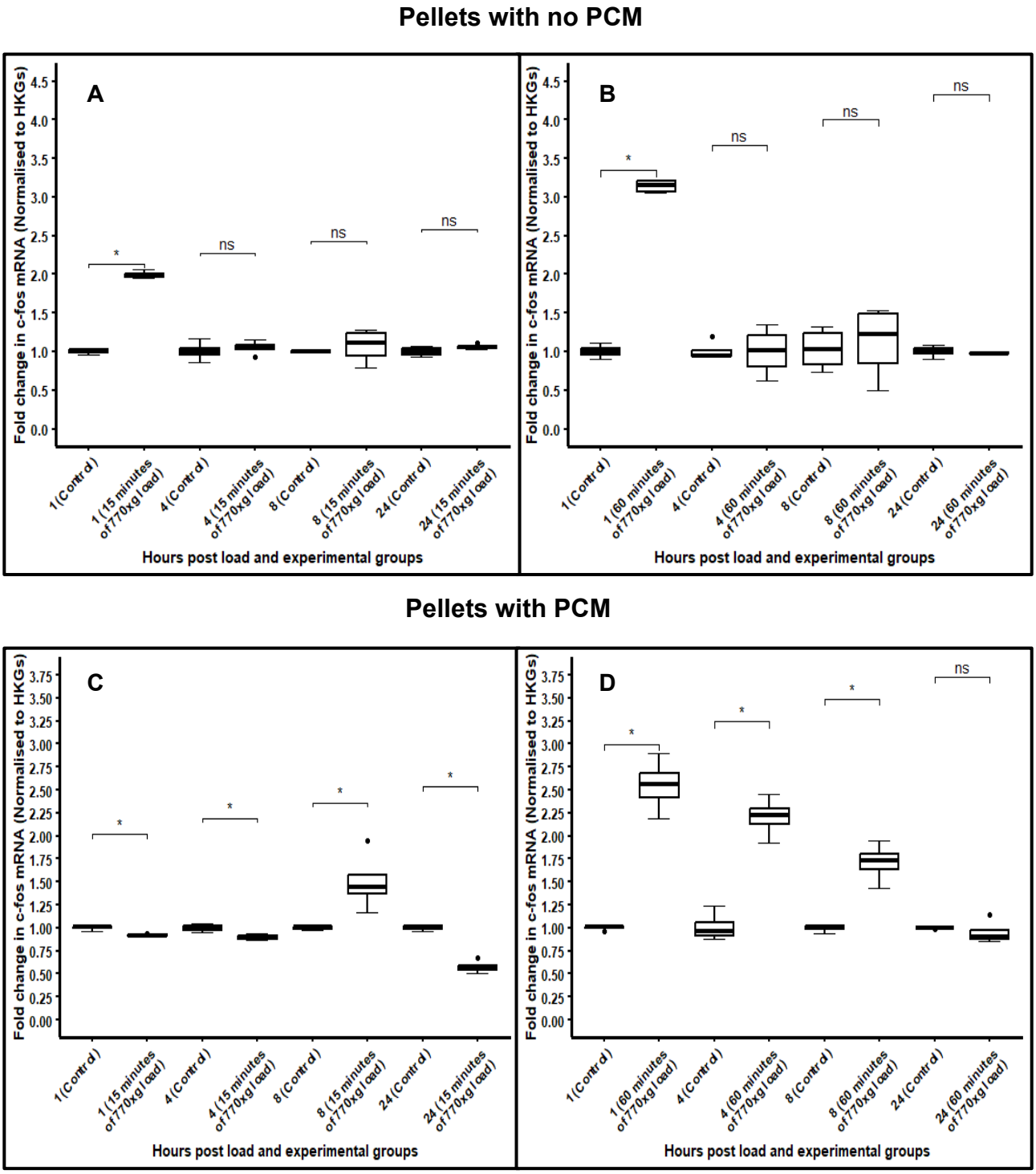


**Figure 3.8. Effect of increasing the duration of 770xg force application on mechano-regulation of *c-fos* transcription in 3D pellets with and without PCM.** *c-fos* transcripts (normalised to *18s* and *hprt*) in control 3D pellets and those subjected to 770xg force for either **A**) 15 minutes in the absence of PCM, **B**) 60 minutes in the absence of PCM, **C**) 15 minutes in the presence of PCM or **D**) 60 minutes in the presence of PCM. Transcript expression was determined at 1-, 4-, 8- and 24-hours post 770xg force cessation. Box and whisker plots represent average fold change ± SD and black dots identify outliers in the datasets (n = 4, N = 1); statistical significance was assessed between control and loaded pellet cultures at specific time points using a Wilcoxon rank sum test (* $p<0.05$, ns = no significance).

#### 3.3.2.3.2. Increasing centrifugal force duration induced no apparent effects on maximal *c-jun* transcription in pellets with no PCM, but mediated early maximal induction of *c-jun* mRNA in pellets with PCM

3D chondrocyte pellets with no PCM subjected to 770xg force for 15 minutes demonstrated a significant 1.94-fold increase in the early mechano-responsive gene *c-jun* mRNA 1-hour post 770xg force cessation ($p = 0.03038$) [Fig. 3.9A]. At 4- and 8-hours post-force cessation, there was a significant reduction in *c-jun* mRNA transcripts observed (T4 hours: 1.19-fold decrease, $p = 0.03038$; T8 hours: 1.31-fold decrease, $p = 0.03038$) [Fig. 3.9A], before the signal returned to near control levels at T24 hours [Fig. 3.9A]. This early mechano-responsiveness is comparable to that revealed in section 3.3.1.5.2 where *c-jun* upregulation was observed at T0.5 hours following application of 15 minutes of 770xg force to 3D pellets with no PCM.

Likewise, following 60 minutes of 770xg force, a significant 2.18-fold increase in *c-jun* mRNA transcripts was observed 1-hour post-force cessation ($p = 0.03038$) [Fig. 3.9B] hence mirroring the response observed with the shorter loading regimen. 3D pellets with no PCM subjected to 60 minutes of 770xg force also revealed marginal downregulation of *c-jun* mRNA transcripts at T4 hours (1.28-fold, $p = 0.03038$), with no significant changes in *c-jun* mRNA levels observed at T8 hours. However, marginal upregulation of *c-jun* mRNA was observed at 24-hours post cessation of 770xg force (1.20-fold, $p = 0.03038$) [Fig. 3.9B]. This indicates that increasing the duration of 770xg force exposure from 15- to 60-minutes induced no alterations in the mechano-regulation of this early response gene in 3D pellets with no PCM.

In 3D pellet cultures with PCM centrifuged at 770xg for 15 minutes, subtle increases were observed in *c-jun* transcripts at T1 hour (1.14-fold, $p = 0.0294$) [Fig. 3.9C], before demonstrating maximal upregulation at 4 hours post-cessation of 770xg force (1.55-fold, $p = 0.03038$) [Fig. 3.9C]. However, at T8- and T24-hours, reductions in *c-jun* transcription relative to the peak were observed (1.26-fold [$p = 0.03038$]; 1.15-fold [$p = 0.03038$], respectively) [Fig. 3.9C].

In contrast, 3D pellets with PCM subjected to 60 minutes of 770xg force exhibited a significant 1.50-fold increase in *c-jun* mRNA levels at T1 hour ($p = 0.0294$) [Fig. 3.9D]; this mechano-responsiveness was also observed at T4- (1.56-fold, $p = 0.0294$) and T8-hours (1.44-fold, $p = 0.03038$), before decreasing to basal levels, as observed in control pellets with PCM, at T24 hours [Fig. 3.9D]. This indicates that increasing load duration induced

quicker mechano-regulation of this early response gene with no apparent differences in maximal induction in response to 60 minutes of 770xg force in the presence of PCM.

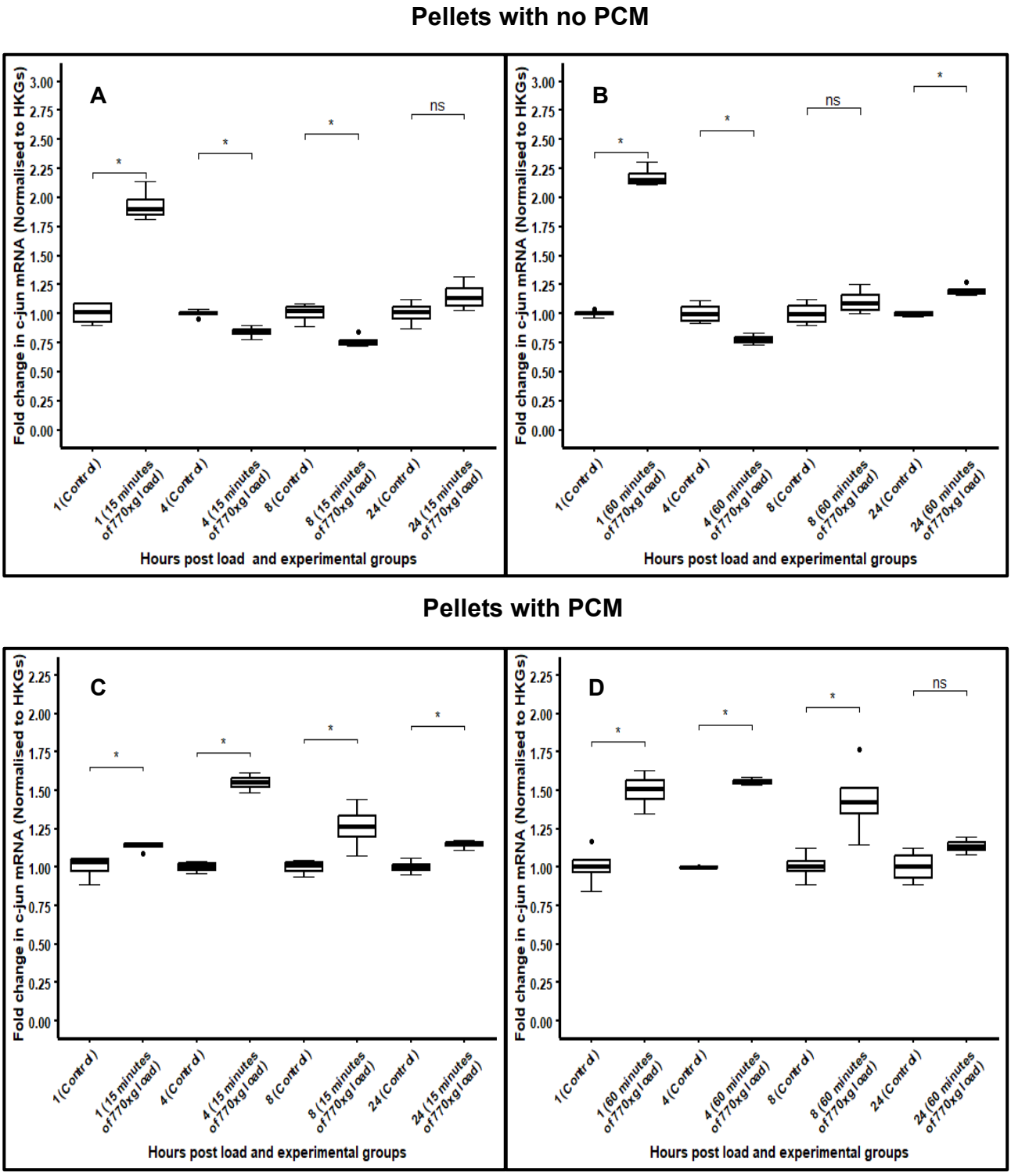


**Figure 3.9. Effect of increasing the duration of 770xg force application on mechano-regulation of *c-jun* transcription in 3D pellets with and without PCM.** *c-jun* transcripts (normalised to *18s* and *hprt*) in control 3D pellets and those subjected to 770xg force for either **A**) 15 minutes in the absence of PCM, **B**) 60 minutes in the absence of PCM, **C**) 15 minutes in the presence of PCM or **D**) 60 minutes in the presence of PCM. Transcript expression was determined at 1-, 4-, 8- and 24-hours post 770xg force cessation. Box and whisker plots represent average fold change ± SD and black dots identify outliers in the datasets (n = 4, N = 1); statistical significance was assessed between control and loaded pellet cultures at specific time points using a Wilcoxon rank sum test (* $p<0.05$, ns = no significance).

#### 3.3.2.3.3. An increase in duration of centrifugal force application delayed mechano-regulation of *mmp-3* transcription, but had no apparent effects on maximal induction of *mmp-3* transcription in pellets with PCM

15 minutes of 770xg force induced significant increases in mRNA transcripts for the mechano-responsive catabolic gene *mmp-3* 1-hour post-force cessation in 3D chondrocyte pellets with no PCM (1.89-fold, p = 0.0294) [Fig. 3.10A]. At T4 hours, no significant differences were observed in *mmp-3* mRNA levels having returned to basal expression [Fig. 3.10A]. Interestingly, this early mechano-responsiveness contradicts the responses demonstrated in section 3.3.1.5.3 where *mmp-3* upregulation was observed at T8 hours following application of 15 minutes of 770xg force to 3D pellets with no PCM.

In contrast, following application of 60 minutes of 770xg force to pellets with no PCM, no significant differences in *mmp-3* transcription were observed 1- and 4-hours post-force cessation [Fig. 3.10B], before significantly reduced *mmp-3* mRNA levels were observed at T8 hours (1.52-fold, p = 0.03038) [Fig. 3.10B]. However, significantly elevated *mmp-3* transcripts were observed at T24 hours (1.23-fold, p = 0.03038) returning levels to above basal levels [Fig. 3.10B]. This indicates that increasing the duration of 770xg force exposure from 15- to 60-minutes delayed regulation of this mechano-responsive catabolic gene in 3D pellets with no PCM.

In 3D pellets with PCM, *mmp-3* mRNA expression appeared to follow a biphasic profile following application of 15 minutes of 770xg force as demonstrated by significant downregulation at 1-hour post-force cessation (1.47-fold, p = 0.03038) [Fig. 3.10C], followed by no effect at T4 hours, then a significant 2.23-fold increase at T8 hours (p = 0.03038) [Fig. 3.10C] before returning to basal levels at T24 hours [Fig. 3.10C].

In contrast, following application of 60 minutes of 770xg force to pellets with PCM, a significant induction of *mmp-3* transcription was observed 1-hour post-770xg force cessation (1.21-fold increase, p = 0.0294) [Fig. 3.10D], followed by no effect at T4 hours, then a 1.90-fold increase at T8 hours (p = 0.0294) [Fig. 3.10D] and ultimately, *mmp-3* mRNA transcripts returned to basal levels at T24 hours [Fig. 3.10D], suggesting a biphasic expression profile as seen following the 15 minutes centrifugation regimen in pellets with PCM. Overall, data indicates that increasing loading duration made no difference to the profile of mechano-regulation of this gene marker for catabolism in the presence of PCM.

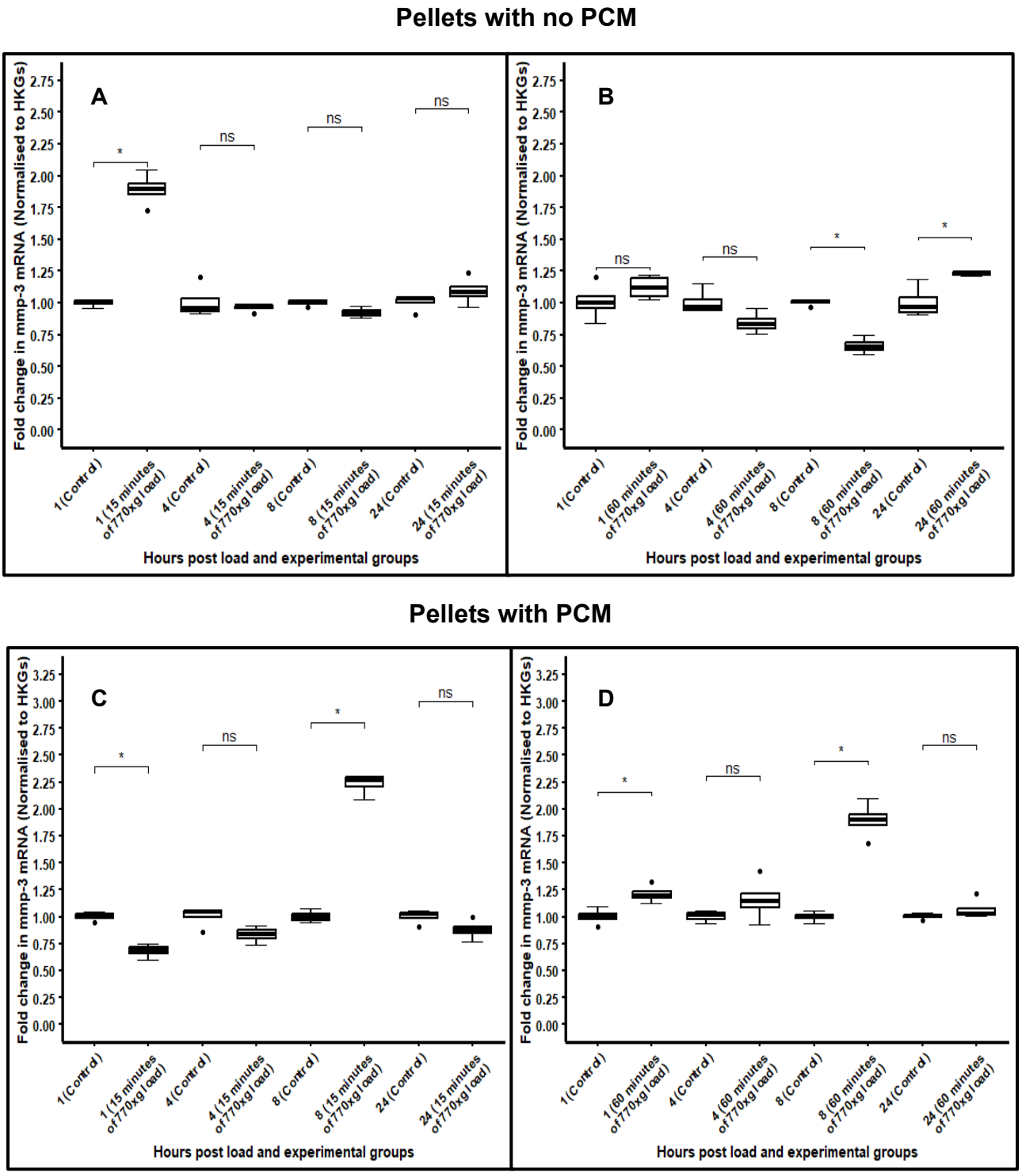


**Figure 3.10. Effect of increasing the duration of 770xg force application on mechano-regulation of *mmp-3* transcription in 3D pellets with and without PCM.** *mmp-3* transcripts (normalised to *18s* and *hprt*) in control 3D pellets and those subjected to 770xg force for either **A**) 15 minutes in the absence of PCM, **B**) 60 minutes in the absence of PCM, **C**) 15 minutes in the presence of PCM or **D**) 60 minutes in the presence of PCM. Transcript expression was determined at 1-, 4-, 8- and 24-hours post 770xg force cessation. Box and whisker plots represent average fold change ± SD and black dots identify outliers in the datasets (n = 4, N = 1); statistical significance was assessed between control and loaded pellet cultures at specific time points using a Wilcoxon rank sum test (* $p<0.05$, ns = no significance).

### 3.3.2.3.4. An increase in duration of centrifugal force application delayed mechano-regulation of *adamts-4* transcription in pellets with no PCM, but mediated early maximal induction of *adamts-4* transcription in pellets with PCM

A very subtle increase in mRNA transcripts for the mechanoresponsive catabolic gene, *adamts-4* were observed 1-hour following the application of 15 minutes of 770xg force to 3D chondrocyte pellets with no PCM (1.09-fold, p = 0.0294) [Fig. 3.11A]. At T4 hours, *adamts-4* mRNA transcripts were significantly downregulated (1.57-fold decrease, p = 0.03038), before returning to basal levels at T8 hours [Fig. 3.11A]. This mechano-responsiveness contradicts that demonstrated in section 3.3.1.5.4 where *adamts-4* induction was observed at T0.5 hours and T8 hours following application of 15 minutes of 770xg force to 3D pellets with no PCM.

In contrast, 60 minutes of 770xg force induced no significant differences in *adamts-4* transcription 1-, 4- and 8-hours post-force cessation in pellets with no PCM [Fig. 3.11B]. However, a 1.65-fold upregulation was observed at T24 hours in these pellets (p = 0.03038) [Fig. 3.11B]. This indicates that increasing the duration of 770xg force exposure from 15- to 60-minutes delayed the regulation of this mechano-sensitive catabolic gene in 3D pellets with no PCM.

Chondrocyte pellets with PCM subjected to 15 minutes of 770xg force revealed significantly reduced *adamts-4* mRNA transcripts 1-hour post cessation of centrifugation (1.31-fold, p = 0.03038) [Fig. 3.11C], followed by no effect at T4 hours, then 1.84-fold upregulation 8 hours post cessation of centrifugation (p = 0.03038) [Fig. 3.11C]. However, at T24 hours, *adamts-4* mRNA transcripts were still significantly upregulated (1.38-fold, p = 0.03038) [Fig. 3.11C].

60 minutes of 770xg force also induced a significant reduction in *adamts-4* transcription 1-hour post cessation of centrifugation in pellets with PCM (1.42-fold, p = 0.02652) [Fig. 3.11D], before eliciting a maximal 1.86-fold induction in *adamts-4* transcription at T4 hours (p = 0.0294) [Fig. 3.11D]. Although there were still elevated *adamts-4* levels beyond T4 hours following application of 60 minutes of 770xg force, these appeared to reduce from T8- to T24-hours (1.44-fold [p = 0.03038] and 1.31-fold [p = 0.0294], respectively) when compared to the peak at T4 hours [Fig. 3.11D]. Overall, data indicates that increasing load duration did not affect overall fold change in *adamts-4* expression in the presence of PCM, but the effect was induced more quickly i.e. at T4 hours compared with T8 hours for 15 minutes of 770xg force in pellets with PCM.

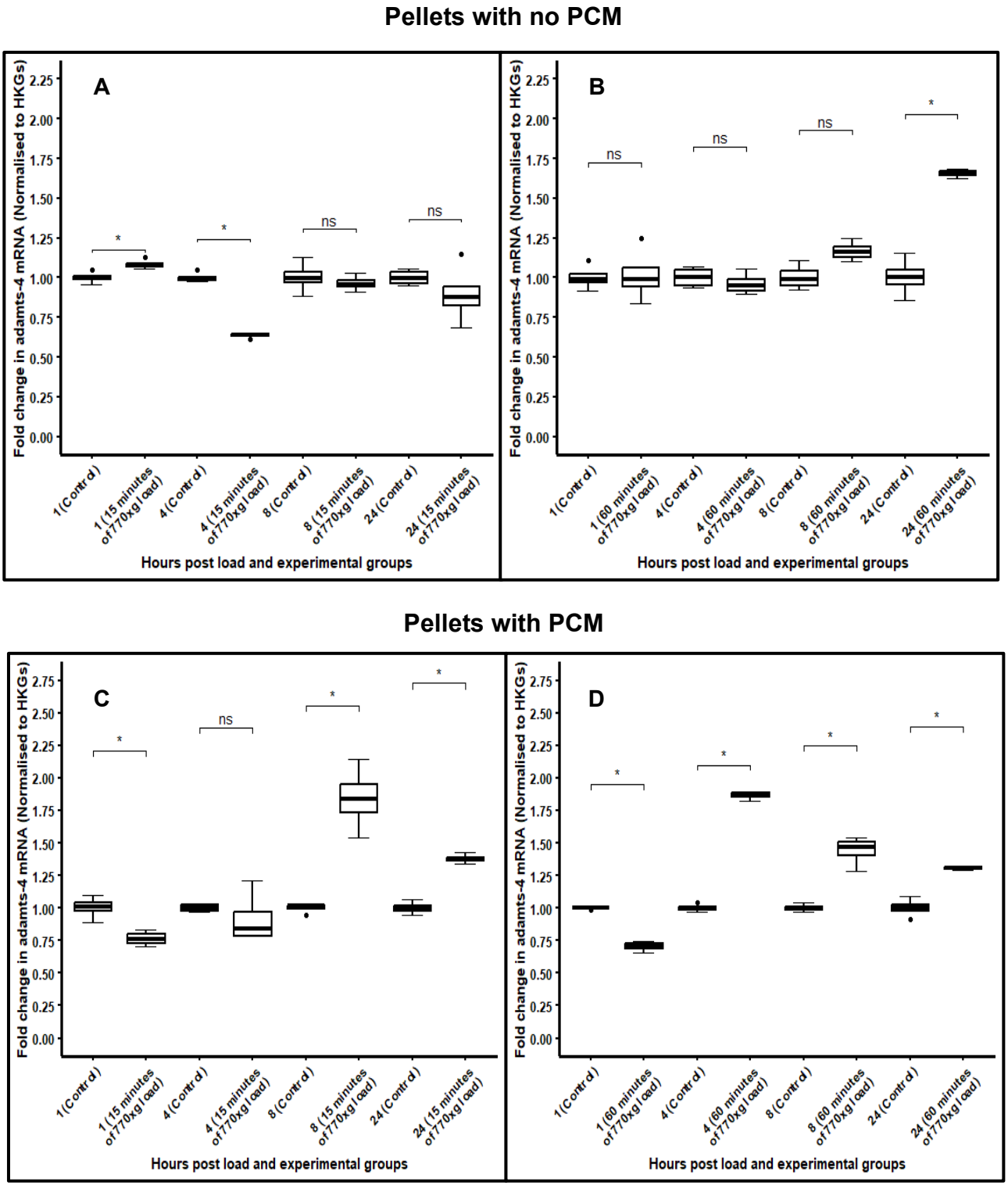


**Figure 3.11. Effect of increasing the duration of 770xg force application on mechano-regulation of *adamts-4* transcription in 3D pellets with and without PCM.** *adamts-4* transcripts (normalised to *18s* and *hprt*) in control 3D pellets and those subjected to 770xg force for either **A**) 15 minutes in the absence of PCM, **B**) 60 minutes in the absence of PCM, **C**) 15 minutes in the presence of PCM or **D**) 60 minutes in the presence of PCM. Transcript expression was determined at 1-, 4-, 8- and 24-hours post 770xg force cessation. Box and whisker plots represent average fold change ± SD and black dots identify outliers in the datasets (n = 4, N = 1); statistical significance was assessed between control and loaded pellet cultures at specific time points using a Wilcoxon rank sum test (* $p<0.05$, ns = no significance).

### 3.3.2.3.5. Increasing load duration had no effect on maximal induction of *adamts-5* transcription in pellets with no PCM, but mediated late maximal mechano-regulation of *adamts-5* transcription in pellets with PCM

Application of 15 minutes of 770xg force had no effect on the mechano-responsive catabolic gene, *adamts-5* 1- and 4-hours post 770xg force cessation when compared to control 3D pellets with no PCM [Fig. 3.12A]. At T8 hours, a 2.81-fold upregulation was observed relative to control cultures following cessation of 15 minutes of 770xg centrifugation ($p = 0.03038$) [Fig. 3.12A]. However, at T24 hours there was a significant decrease (1.86-fold, $p = 0.03038$) [Fig. 3.12A] below that of control cultures. This late mechano-responsiveness is comparable to that revealed in section 3.3.1.5.5 where *adamts-5* upregulation was observed to peak at T8 hours following application of 15 minutes of 770xg force to 3D pellets with no PCM.

Likewise, a 60-minute exposure of 3D pellets with no PCM to 770xg force had limited effect until 8-hours post-force cessation whereby a 2.75-fold increase in *adamts-5* transcription was observed ($p = 0.03038$) [Fig. 3.12B], mirroring the response observed with the shorter loading regimen. However, *adamts-5* mRNA levels returned to almost baseline expression at T24 hours (1.17-fold increase; $p = 0.03038$) [Fig. 3.12B]. This indicates that increasing the duration of 770xg force exposure from 15- to 60-minutes did not alter the regulation of this late mechano-responsive gene at its peak of expression in 3D pellets with no PCM.

Application of 15 minutes of 770xg force to 3D pellets with PCM induced a 1.72-fold increase in *adamts-5* mRNA transcripts at T4 hours ($p = 0.03038$) [Fig. 3.12C], before the signal returned to basal expression at T8 hours [Fig. 3.12C].

Similarly, in pellets with PCM, application of 60 minutes of 770xg force had no effect at 1-hour post-force cessation [Fig. 3.12D]. However, minimal increases in *adamts-5* transcripts were observed at T4 hours (1.06-fold [$p = 0.04083$]) and T8 hours (1.17-fold, $p = 0.03038$) [Fig. 3.12D], before a 1.89-fold upregulation was observed at T24 hours ($p = 0.03038$) [Fig. 3.12D]. This indicates that increasing load duration delayed the maximal regulation of this late mechano-responsive catabolic gene with no apparent differences in peak expression elicited by the two durations of centrifugation in the presence of PCM.

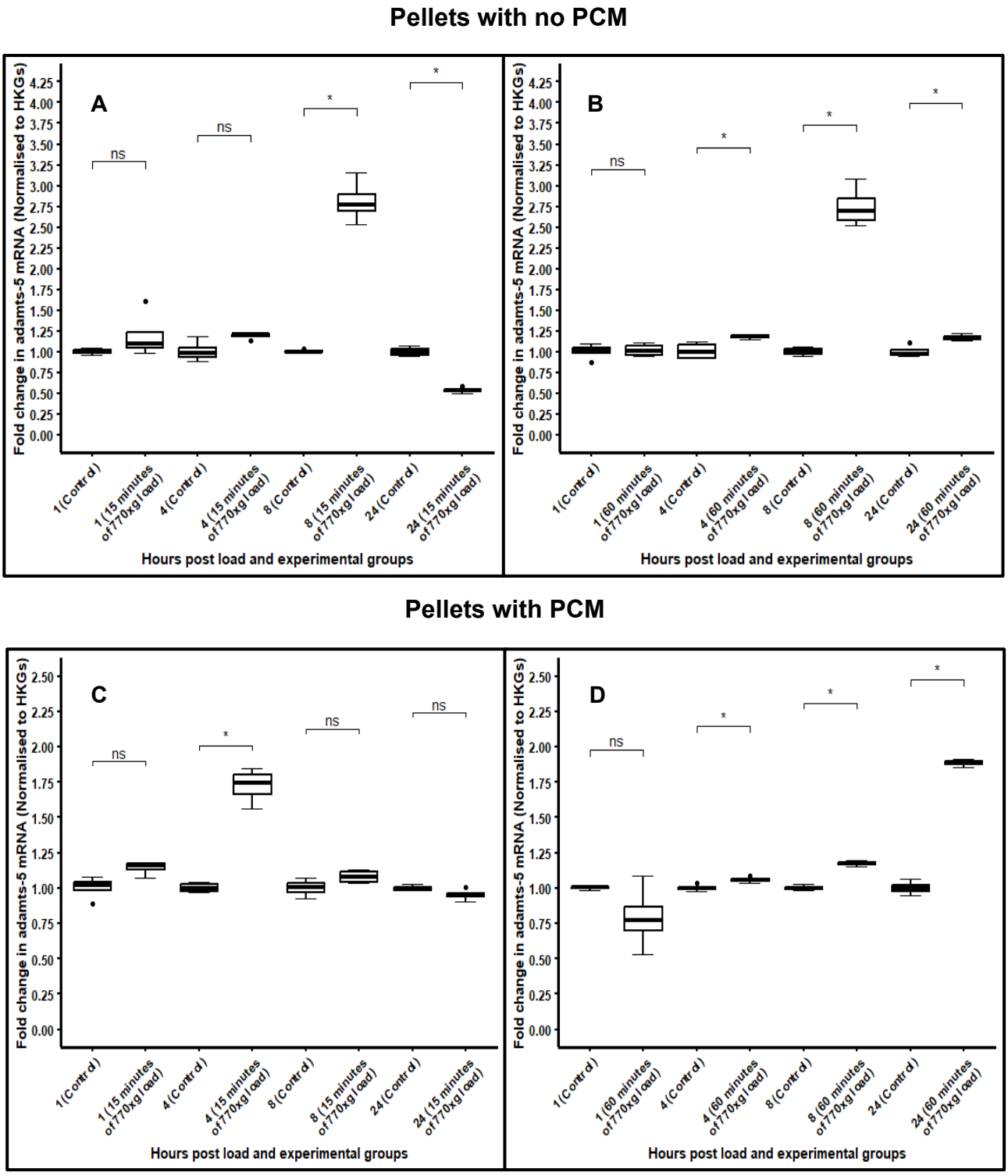


**Figure 3.12. Effect of increasing the duration of 770xg force application on mechano-regulation of *adamts-5* transcription in 3D pellets with and without PCM.** *adamts-5* transcripts (normalised to *18s* and *hprt*) in control 3D pellets and those subjected to 770xg force for either **A**) 15 minutes in the absence of PCM, **B**) 60 minutes in the absence of PCM, **C**) 15 minutes in the presence of PCM or **D**) 60 minutes in the presence of PCM. Transcript expression was determined at 1-, 4-, 8- and 24-hours post 770xg force cessation. Box and whisker plots represent average fold change ± SD and black dots identify outliers in the datasets (n = 4, N = 1); statistical significance was assessed between control and loaded pellet cultures at specific time points using a Wilcoxon rank sum test (* $p<0.05$, ns = no significance).

#### 3.3.2.3.6. Increasing load duration sustained induction of *sox9* transcription in pellets with no PCM, but reduced the mechano-sensitivity of *sox9* transcription in pellets with PCM

Transcript levels of *sox9*, a gene marker for the chondrocyte phenotype were unaffected 1-hour post cessation of 15 minutes of 770xg force in 3D chondrocyte pellets with no PCM [Fig. 3.13A]. At T4 hours, significantly elevated *sox9* mRNA levels were observed (1.32-fold, p = 0.0294); this response was not observed at T8 hours, however, a 1.70-fold increase in *sox9* expression was observed again at 24 hours post-force cessation (p = 0.03038) [Fig. 3.13A].

Following application of 60 minutes of 770xg force to pellets with no PCM, significant increases in *sox9* transcripts were observed 1- (1.33-fold, p = 0.03038), 4- (1.40-fold, p = 0.03038) and 24-hours (1.61-fold, p = 0.03038) post-force cessation [Fig. 3.13B]. Increasing the duration of 770xg force application from 15- to 60-minutes appeared to induce this chondrogenic marker at most time points within a 24-hour window in 3D pellets with no PCM suggesting its capability to sustain the chondrocyte phenotype.

In 3D pellets with PCM, significant elevations of *sox9* transcripts were observed at T1- (1.12-fold, p = 0.03038), T4- (1.49-fold, p = 0.0294) and T8-hours (2.28-fold, p = 0.03038) [Fig. 3.13C] following application of 15 minutes of 770xg force. However, at T24 hours, a 1.77-fold reduction in *sox9* transcription was observed (p = 0.0294) [Fig. 3.13C].

In contrast, 60 minutes of 770xg force to pellets with PCM had minimal effects on *sox9* mRNA levels within the 24-hour period, except for T4 hours where a 1.14-fold increase was observed (p = 0.0294) [Fig. 3.13D]. This indicates that increasing load duration to 60 minutes reduced the mechano-sensitivity of this chondrocyte phenotype gene marker in chondrocyte pellets with a PCM.

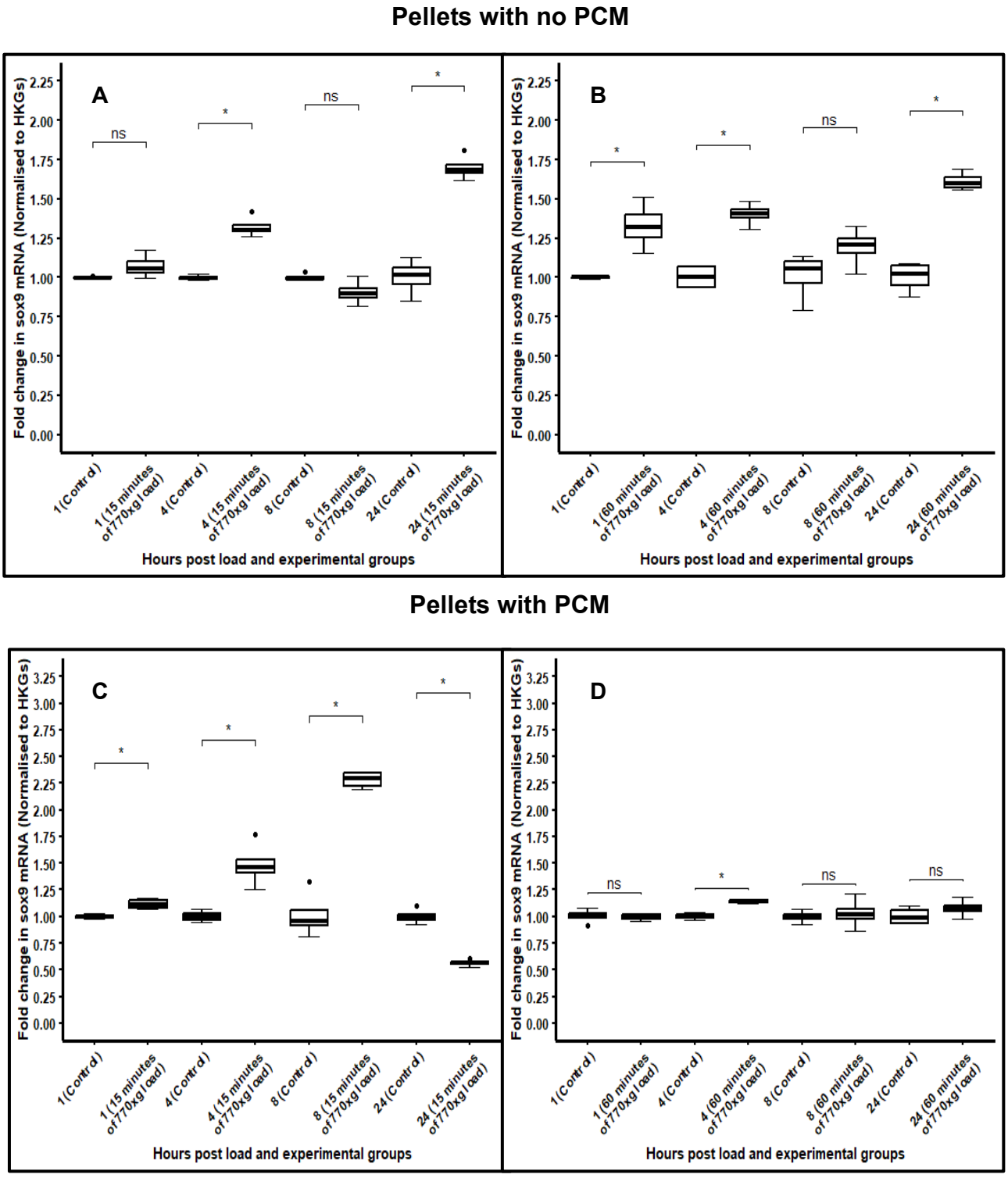


**Figure 3.13. Effect of increasing the duration of 770xg force application on mechano-regulation of *sox9* transcription in 3D pellets with and without PCM.** *sox9* transcripts (normalised to *18s* and *hprt*) in control 3D pellets and those subjected to 770xg force for either **A**) 15 minutes in the absence of PCM, **B**) 60 minutes in the absence of PCM, **C**) 15 minutes in the presence of PCM or **D**) 60 minutes in the presence of PCM. Transcript expression was determined at 1-, 4-, 8- and 24-hours post 770xg force cessation. Box and whisker plots represent average fold change ± SD and black dots identify outliers in the datasets (n = 4, N = 1); statistical significance was assessed between control and loaded pellet cultures at specific time points using a Wilcoxon rank sum test (* $p<0.05$, ns = no significance).

#### 3.3.2.3.7. 60 minutes of 770xg force induced stronger mechano-signalling events in 3D chondrocyte pellets with and without PCM

Taken together, data revealed stronger responses of 3D chondrocyte pellets, with and without PCM, to mechanical loading for 60 minutes as compared to 15 as evidenced by induction of pronounced mechano-responsiveness of *c-fos* gene [Fig. 3.8B] as early as 1-hour post-force cessation, as well as late mechano-responsiveness of *adamts-4* gene [Fig. 3.11B] at T24 hours following application of 60 minutes of 770xg force. Moreover, sustained upregulation of a gene marker for the chondrocyte phenotype *sox9* was also observed within a 24-hour window of investigation in response to 60 minutes of loading in 3D chondrocyte pellets with no PCM [Fig. 3.13B]. Likewise, quicker and/or stronger regulation of mechano-sensitive genes (e.g., T1 hour vs T8 hours for 60- and 15-minutes load induction, respectively for *c-fos* [Fig. 3.8D]; T1 hour vs T4 hours for 60- and 15-minutes load induction, respectively for *c-jun* [Fig. 3.9D]) was observed following application of 60 minutes of 770xg force to 3D pellets with PCM. Overall, this suggests that increasing the duration of 770xg load induced more robust mechano-signalling irrespective of the extent of PCM deposition in 3D chondrocyte pellets; thus, informing the decision to utilise this longer load duration in investigations described in chapter 4 aimed at determining the influence of mechanical load on circadian rhythm employing both the 3D chondrocyte pellets with and without PCM.

### 3.3.2.4. 15 minutes of 770xg force exposure elevated adamts-4 enzyme activity at T48 hours only, whilst adamts-4 enzyme activity was unaffected at T48- and T72-hours following application of 60 minutes of 770xg in 3D pellets with no PCM

No detectable adamts-4 enzyme activity was observed at T24 hours in both the control 3D pellets with no PCM and those subjected either to 15- or 60-minutes of 770xg force (data not shown).

**15 minutes regimen:** A significant reduction in 5-FAM concentration (i.e., aggrecanase-1 or adamts-4 activity) from 680±57.0 nM (T48 hours) to 529±18.2 nM (T72 hours) [p = 0.03038] was observed in control 3D pellets with no PCM [Fig. 3.14A]. Comparable reductions in adamts-4 activity were detected following application of 15 minutes of 770xg force to 3D cultures (i.e. decreasing from 759±13.2 nM at T48 hours to 490±62.9 nM at T72 hours [p = 0.03038]) [Fig. 3.14A]. However, application of 15 minutes of 770xg force appeared to significantly increase adamts-4 activity relative to controls at T48 hours (11.6% increase, p = 0.03038), but not at T72 hours (p = 0.8852) [Fig. 3.14A].

**60 minutes regimen:** Control 3D pellets with no PCM for the 60 minutes experimental set-up demonstrated significant reduction in 5-FAM concentration from 787±51.7 nM (T48 hours) to 471±51.7 nM (T72 hours) [p = 0.03038] [Fig. 3.14B]. Similar decreases in adamts-4 activity were detected following application of 60 minutes of 770xg force to 3D cultures (i.e. decreasing from 824±25.5 nM at T48 hours to 476±31.0 nM at T72 hours [p = 0.03038]) [Fig. 3.14B]. However, no significant differences in adamts-4 activity were observed between control cultures and those subjected to 60 minutes of 770xg at both T48- (p = 0.3124), and T72-hours (p = 0.8852) [Fig. 3.14B].

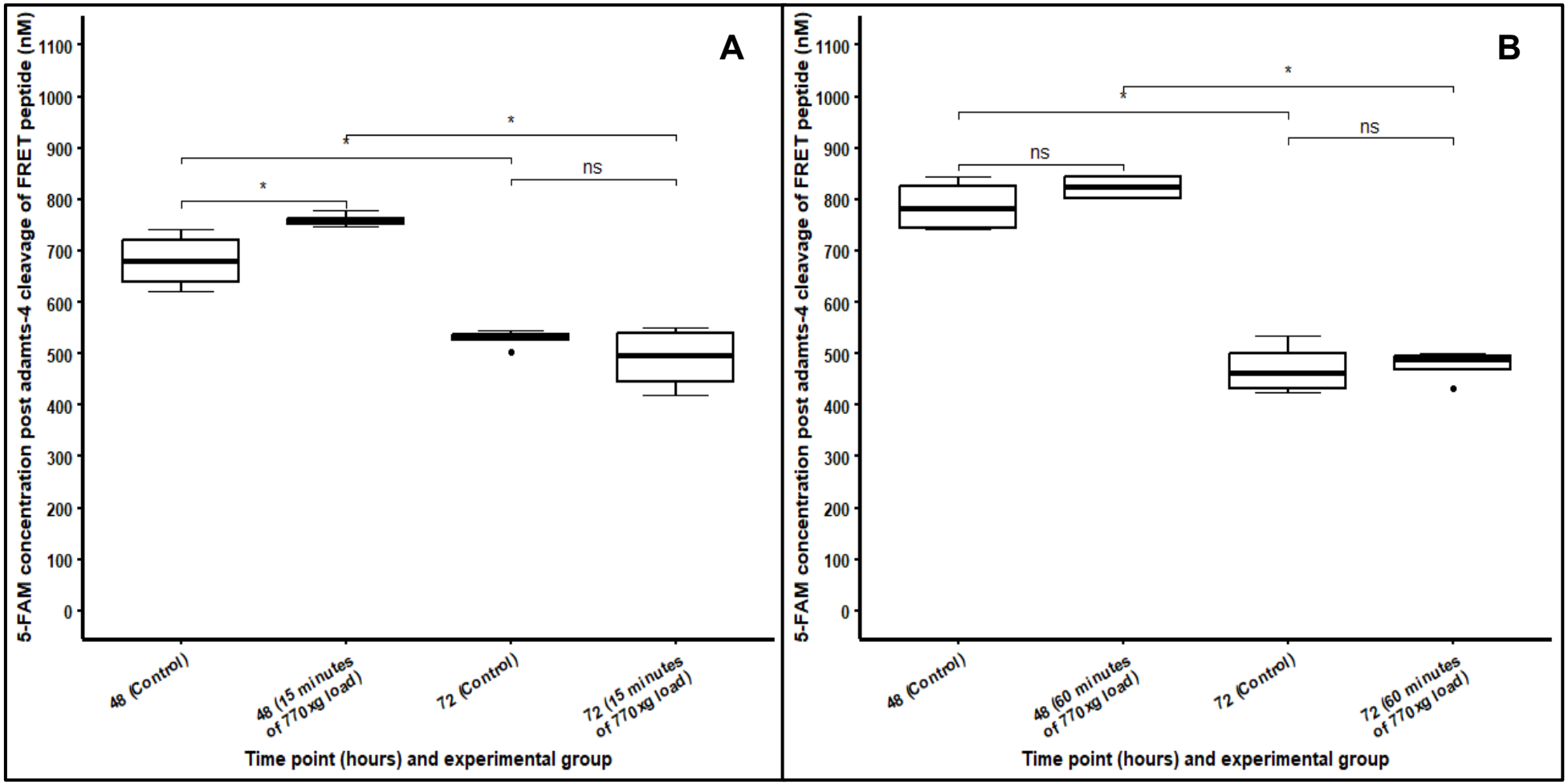


**Figure 3.14. The effect of increasing load duration of 770xg force application on adamts-4 activity in 3D chondrocyte pellets with no PCM.** The graph illustrates box and whisker plots representing the concentration of 5-FAM following the cleavage of adamts-4 substrates (5-FAM/TAMRA FRET peptide) by activated enzymes in culture media collected at T48- and T72-hours from control 3D pellets with no PCM as well as those subjected to 770xg load for the following durations: **A**) 15 minutes or **B**) 60 minutes. Black dots represent outliers in datasets. Statistical significances of differences in 5-FAM concentration (enzyme activity) between control and 770xg loaded cultures at a given time point or two time points within the same experimental group were determined by a Wilcoxon rank sum test in the R software and graphically annotated using the ggpubr package (* $p<0.05$, ns = no significance). Data represent the average total concentration of 5-FAM ± SD (n = 4, N = 1).

### 3.3.2.5. 15 minutes of 770xg force exposure had no effects on mmp-13 enzyme activity, while application of 60 minutes of 770xg force induced significant increases in mmp-13 enzyme activity only at T72 hours in 3D chondrocyte pellets with no PCM

No detectable mmp-13 enzyme activity was observed at T24 hours in both the control 3D chondrocyte pellets with no PCM and those subjected either to 15- or 60-minutes of 770xg force (data not shown).

**15 minutes regimen:** Significant decreases in 5-FAM concentration (i.e., mmp-13 activity) from 881±124 nM (T48 hours) to 478±47.8 nM (T72 hours) [p = 0.0041] was observed in control 3D pellets with no PCM [Fig. 3.15A]. Similar reductions were detected following application of 15 minutes of 770xg force to 3D cultures (i.e., decreasing from 1070±177 nM at T48 hours to 481±165 nM at T72 hours [p = 0.0029]) [Fig. 3.15A]. However, application of 15 minutes of 770xg force induced no significant differences in mmp-13 activity relative to control cultures at T48- (p = 0.1218), and T72-hours (p = 0.851) [Fig. 3.15A].

**60 minutes regimen:** Likewise, control pellets with no PCM revealed a significant reduction in 5-FAM concentration from 743±143 nM (T48 hours) to 278±90 nM (T72 hours) [p = 0.0026] [Fig. 3.15B]. Comparable decreases in mmp-13 activity were observed following application of 60 minutes of 770xg force to 3D cultures (i.e., decreasing from 870±129 nM at T48 hours to 469±92 nM at T72 hours [p = 0.0031]) [Fig. 3.15B]. However, no differences in mmp-13 activity were observed between control cultures and those subjected to 60 minutes of 770xg force at T48 hours (p = 0.228) [Fig. 3.15B]. Interestingly, a significant 68.7% increase in mmp-13 activity was observed at T72 hours following the exposure of 3D chondrocyte cultures to 770xg load for 60 minutes (p = 0.025) [Fig. 3.15B].

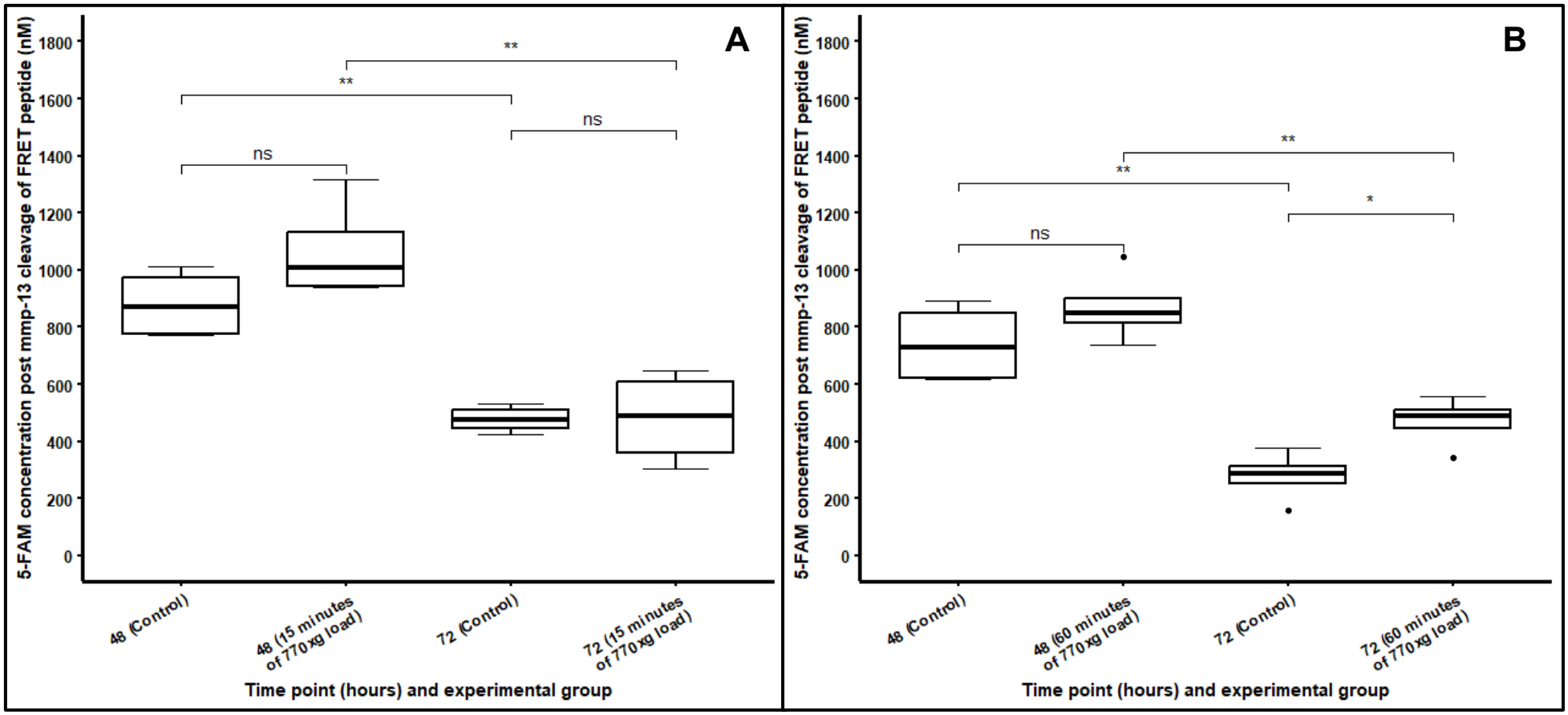


**Figure 3.15. The effect of increasing load duration of 770xg force application on mmp-13 activity in 3D chondrocyte pellets with no PCM.** The graph illustrates box and whisker plots representing the concentration of 5-FAM-Pro-Leu-OH following the cleavage of mmp-13 substrates (5-FAM/QXL™ 520 FRET peptide) by activated enzymes in culture media collected at T48- and T72-hours from control 3D pellets with no PCM as well as those subjected to 770xg load for the following durations: **A**) 15 minutes, or **B**) 60 minutes. Black dots represent outliers in datasets. Statistical significances of differences in 5-FAM concentration between control and 770xg loaded cultures at a given time point or two time points within the same experimental group were determined by a Welch Two Sample t-test in the R software and graphically annotated using the ggpubr package (* $p<0.05$, ** $p<0.01$, ns = no significance). Data represent the average total concentration of 5-FAM ± SD (n = 4, N = 1).

### 3.4. Discussion

The work in this chapter has developed and characterised two *in vitro* 3D model systems for studying chondrocyte mechanobiology i.e., 3D chondrocyte pellets with or without PCM. Cell viability, determined using the live/dead assay employing FDA (showing prominent staining) and PI stains (indicating limited staining), was confirmed on pellets with no PCM. Assessment of sGAG release using the DMMB assay revealed accumulation within a 24-hour window in both the 3D pellet cultures with and without PCM, but overall, no differences were observed either within a 24- or 72-hour window when comparing 770xg loaded cultures to controls at each sampling time point. The Griess assay also demonstrated no significant changes in nitrite/NO following load in comparison to controls in both the 3D pellet cultures with and without PCM. Moreover, *hprt* and *18s* were identified as the most stable and appropriate reference genes for qPCR normalisation of target genes following application of centrifugal force (predicted to simulate mechanical loading of chondrocytes: compression, shear forces, hydrostatic pressure). As compared to the 200- and 1000-xg centrifugal forces, application of 15 minutes of 770xg force to pellets with no PCM induced early mechano-responsive genes *c-fos* and *c-jun* and late mechano-responsive catabolic genes *adamts-4*, *adamts-5* and *mmp-3* within a 24-hour window. Additionally, in pellets with no PCM, increasing the duration of 770xg force application from 15- to 60-minutes led to stronger regulation of the early mechano-responsive gene *c-fos*; the chondrogenic gene *sox9* and the mechano-responsive catabolic gene *adamts-4* within a 24-hour window of investigation. Moreover, a significant increase in adamts-4 but not mmp-13 enzyme activity was observed 48-hours post cessation of 15 minutes of 770xg force application whilst mmp-13, but not adamts-4 enzyme activity was induced 72 hours following cessation of 60 minutes of 770xg force application in pellets with no PCM. However, quicker and/or stronger regulation of *c-fos*, *c-jun* and *adamts-4* transcription, delayed *adamts-5* transcription as well as reduced *sox9* transcription were observed following an increase in load duration from 15- to 60-minutes in 3D pellets with PCM. Collectively, data demonstrates robust mechano-regulation of mechano-responsive genes following an increase in loading duration from 15- to 60-minutes in both the 3D pellets with and without PCM suggesting the suitability of 60 minutes of 770xg force for further use in chapter 4 investigations aimed at determining the influence of mechanical load on chondrocyte circadian clocks.

### 3.4.1. Live/dead staining revealed high chondrocyte viability in 3D chondrocyte pellets (no PCM) following application of centrifugal force

Both the control and loaded 3D pellets with no PCM demonstrated high cell viability irrespective of days of extended *ex vivo* culture (up to 72 hours) suggesting that 15 minutes of 770xg force had minimal effects on chondrocyte death. However, the equivalent analysis was not performed in 3D pellets with no PCM following exposure to 60 minutes of 770xg force as well as pellets with PCM subjected to either 15- or 60-minutes of 770xg force; therefore, this needs to be done to confirm cell viability following increased load duration and PCM deposition. Live/dead assay data revealing minimal cell death in 3D chondrocyte pellets is consistent with the Griess assay outcomes which indicated the production of ~5-10 nM NO at T8- and T24-hours in both the control and 770xg loaded 3D cultures with no significant differences observed between the two groups at either time point; excessive NO production is a potential marker of cell death in pathophysiological disorders (Gross and Wolin 1995; Murphy 1999), thus the low levels detected supports chondrocyte viability in the model system. Despite the lower intensity of PI fluorescence relative to the FDA staining, some of the observed PI staining in this study (especially that localised in pellets' periphery) might be attributed to chondrocytes' physical injury during the transfer of pellets from microcentrifuge tubes into petri dishes or the removal and addition of various solutions.

### 3.4.2. *hprt* and *18s* were identified as the two most stable reference genes for qPCR normalisation following application of centrifugal force to 3D chondrocyte pellets

One of the crucial objectives necessary for achieving chapter 3 aims was to identify the most stable reference genes within a 24-hour period following application of either 200-, 770- or 1000-xg force to 3D chondrocyte pellets (including control cultures). From this, *hprt* and *18s* were identified by refFinder as being the two most stable and suitable reference genes for qPCR normalisation of target genes since they were least affected by centrifugal force. Previous studies have emphasised the importance of qPCR normalisation to at least two reference genes (Kozera and Rapacz 2013; Vandesompele et al. 2002). The identification of *hprt* and *18s* as the two most stable reference genes in this chapter is partially consistent with the findings of Lee et al. (2005a) who identified *18s* and *gapdh* as the two most stable from a panel of 5 putative genes in articular chondrocyte and intervertebral disc tissues subjected to mechanical load (Lee et al. 2005a); whilst Zhai et

al. (2013) identified *hprt* and *ppia* as the two most suitable from a panel of 16 candidate reference genes in the ATDC5 chondrogenic cell line (Zhai et al. 2013). However, identification of *hprt* and *18s* as the two most stable following application of centrifugal force disagrees with the findings of Al-Sabah et al. (2016) who demonstrated that *sdha*, *ywhaz* and *rpl4* were the most stable from a panel of 8 candidate reference genes in bovine articular cartilage explants and primary chondrocytes exposed to compressive loads and tensile strain (Al-Sabah et al. 2016), indicating how important it is to verify reference gene suitability for each individual experimental setup.

### 3.4.3. A 770xg centrifugal force mediated the induction of early mechano-responsive genes in 3D chondrocyte pellet cultures

Most previous studies have reported the repeated application of centrifugal force to chondrocyte pellet cultures ranging from minutes (Maeda et al. 2005; Prittinen et al. 2019) to hours (Inoue et al. 1990) before measuring cell behaviours days or even weeks following application of centrifugal force. However, chapter 3 aimed to develop a model system identifying a centrifugal force capable of inducing early mechano-signalling events detectable at the transcriptional level within a 24-hour period (0.5/1-, 4-, 8- and 24-hours post cessation of centrifugal force) in 3D pellets with and without PCM. To achieve this, 3D chondrocyte pellets were exposed to 15 minutes of centrifugation (either 200-, 770- or 1000-xg forces). A panel of well-known mechano-sensitive genes were selected that were representative of early responses, i.e., members of AP-1 transcription factor (*c-fos* and *c-jun*); the selection criteria of these genes was solely on the basis of previous literature demonstrating their early induction in cartilage or chondrocytes following mechanical load (Bougault et al. 2012; De Croos et al. 2008; Malfait et al. 2002; Scholtes et al. 2018; Sironen et al. 2002; Thomas et al. 2011). Overall, this study revealed a greater induction of early response mechano-sensitive genes following application of 770xg centrifugal force to pellets with no PCM as compared to the 200- and 1000-xg forces. Specifically, 770xg force significantly elevated transcription of the early response genes, *c-fos* and *c-jun* early on post-cessation of stimulation of 3D chondrocyte pellets, i.e., detected at T0.5- or T4-hours. This agrees with the literature with reported ~10-fold increase in *fos* and ~3-fold increase in *jun* mRNA observed immediately after load cessation in embryonic mouse costal chondrocytes (embedded in agarose gels) subjected to 20 kPa dynamic compressive strain for 30 minutes (Bougault et al. 2012). An ~11-fold increase in *FOSB* mRNA, 4-fold

increase in *FOS* mRNA and 1.8-fold increase in *JUND* mRNA were also observed at T=0 hours, following the exposure of human knee chondrocytes (seeded in collagen scaffolds) to 25% dynamic compressive strain (1 Hz, 3 hours) (Scholtes et al. 2018). Other studies also corroborate the findings in this chapter in the early and significant induction of *c-fos* and *c-jun* following force application. Human chondrocytic cell lines (HCS-2/8) subjected to 30 MPa static hydrostatic pressure for 3-, 6- and 12-hours demonstrated a 9.9-, 9.8- and 6.6-fold upregulation of *C-JUN* mRNA respectively, at T=0 hours (Sironen et al. 2002). Moreover, following application of 7.5% cyclical tensile strain (1Hz, 30 minutes), skeletally immature bovine chondrocytes exhibited significantly elevated mRNA levels of *c-fos* (1.65-fold) and *c-jun* (1.5-fold) 4 hours post-load cessation (Thomas et al. 2011). However, there are differences in the magnitudes of upregulation (fold changes) for *c-fos* and *c-jun* mRNA transcripts between this chapter and the above-mentioned previous publications which might be due to the divergent types, magnitudes and durations of loads applied to cells as well as interspecies variations and cell immortalisation (cell-lines).

### 3.4.4. A 770xg centrifugal force mediated the late induction of mechano-responsive catabolic genes in a 3D chondrocyte pellet model

To further aid in the identification of a centrifugal force capable of inducing anticipated mechano-signalling events detectable at the transcriptional level within a 24-hour period following 15 minutes of centrifugation (either 200-, 770- or 1000xg forces), this chapter also selected a panel of well-known mechano-sensitive catabolic genes that are representative of late responses (*adamts-4*, *adamts-5* and *mmp-3*) entirely based on previous literature revealing their late mechano-regulation in cartilage or chondrocytes (Lee et al. 2005b; Monfort et al. 2006; Patwari et al. 2003). In essence, mechanical load-induced AP-1 activation as discussed in section 3.4.3 is known to control the transcription of metalloproteinase family members (i.e., MMPs and ADAMTSs), which are involved in cartilage catabolism (De Croos et al. 2008; Malfait et al. 2002; Tortorella et al. 1999; Vincenti and Brinckerhoff 2002;). Taken together, this study also revealed stronger induction of late response mechano-sensitive catabolic genes following application of 770xg centrifugal force as compared to the 200- and 1000-xg forces. Specifically, this chapter demonstrated significant increases in the expression of *adamts-4*, *adamts-5* and *mmp-3* genes following cessation of 770xg force, with maximal amounts observed particularly at T8 hours before the signals returned to baseline levels or demonstrated

subtle reductions at T24 hours hence confirming that their activation is downstream of AP-1 induction as evidenced by mechano-regulation of AP-1 members *c-fos* and *c-jun* at either T0.5- or T4-hours. The findings in this chapter showing significantly increased *adamts-4*, *adamts-5* and *mmp-3* mRNA levels following application of 15 minutes of 770xg centrifugal force also corroborates the results of previous studies. Immature bovine cartilage explants subjected to injurious static compressive load (average peak stress of ~20MPa, 1 Hz) demonstrated an ~250-fold increase in *mmp-3* mRNA at T12 hours before dropping to ~50-fold at T24 hours (Lee et al. 2005b). Moreover, an ~2-3-fold increase in *adamts-4* mRNA was also reported within a 24-hour period following the exposure of bovine cartilage explants to compressive load. An ~40-fold increase in *adamts-5* transcription was observed 12 hours post-load cessation which remained elevated at ~10-fold at T24 hours (Lee et al. 2005b). Furthermore, significant induction of *mmp-3* following application of 15 minutes of 770xg centrifugal force in this chapter also agrees with the findings of previous publications. Upregulated *mmp-3* mRNA levels were observed in immature bovine cartilage explants subjected to injurious compressive load (Patwari et al. 2003). The mechano-sensitive nature of *mmp-3* was also reported by Monfort et al. (2006) who demonstrated reduced *MMP-3* transcription in human femoral head cartilage with prior exposure to mechanical load *in vivo* (Monfort et al. 2006).

### 3.4.5. Increasing duration of 770xg force application influences mechano-signalling in 3D chondrocytes pellets with and without PCM

Since 15 minutes of 770xg force was demonstrated to induce robust mechano-signalling events in the initial regimen optimisation experiments, other experiments were designed to determine whether increasing the load duration would induce elevated changes in mechano-sensitive gene levels in 3D chondrocyte pellets with or without PCM hence further optimising a more physiologically relevant centrifugal regimen and suitable model system. In summary, this chapter demonstrated that application of 60 minutes of 770xg force to 3D chondrocyte pellets induced more pronounced *c-fos* transcription, but no apparent differences in *c-jun* mRNA levels when compared to the 15 minutes regimen; this suggests a possible divergent regulation of these early mechano-responsive genes as stronger responses were observed in *c-fos* induction while unaffected *c-jun* mRNA levels were observed following an increase in load duration. Moreover, significant downregulation of the mechano-responsive catabolic gene *mmp-3* following increased load duration

suggests that this longer duration of load suppressed the transcription of this gene in pellets with no PCM. Increasing the duration of 770xg load from 15- to 60-minutes resulted in significant increases in *adamts-4* mRNA levels and unaltered *adamts-5* transcripts suggesting differential regulation of these late mechano-responsive catabolic genes in the employed 3D model (no PCM) with stronger induction of *adamts-4* and no effects on *adamts-5*. Moreover, the work in chapter 3 discovered novel findings in the enhanced mechano-induction of the early response gene *c-fos*, and quicker regulation of the early (*c-jun*) and late (*adamts-4*) response genes in 3D pellets with PCM following application of 60 minutes of 770xg force as compared to 15 minutes of force application within a 24-hour window. Overall, chapter 3 provided novel data indicating the quicker and/or stronger induction of early mechano-responsive and late mechano-responsive catabolic genes following the employment of a longer centrifugal duration in both the 3D chondrocyte pellets with and without PCM hence suggesting the suitability of 60 minutes of 770xg force for use in future mechanobiology experiments. However, no independent repeat experiments were conducted to validate the reproducibility of these novel findings thus repeating the experiments would need to be performed to confirm the data findings.

### 3.4.6. Increasing load duration appeared to maintain the chondrocyte phenotype in 3D chondrocyte pellets with no PCM but reduced mechano-sensitivity of *sox9* in pellets with PCM

Previous studies have mimicked mechanical loading of chondrocytes using centrifugal forces without assessing the influence of increased load duration and PCM deposition on cell behaviours. These studies also demonstrated huge differences in time points of analysing transcripts/components of cartilage ECM as compared to the experimental protocols adopted in this chapter. Although transcription does not necessarily equate to biosynthesis, the observation of no significant changes in sGAG concentration within a 24-hour window in this chapter (both, with and without PCM) agrees with the finding of a previous study in which aggrecan core protein mRNA transcripts remained unaltered at 1-, 2- and 4-weeks following application of 15 minutes of 771xg force either once or three times a day over a 4-week period in bovine chondrocyte pellets (Prittinen et al. 2019). Moreover, Prittinen et al. (2019) also demonstrated no changes in *sox9* expression at 1-, 2- and 4-weeks following application of centrifugal force (Prittinen et al. 2019); however, this chapter revealed significant increases in *sox9* mRNAs following application of 60 minutes of 770xg force to 3D chondrocyte pellets with responses appearing to be stronger at earlier time points and persisting for most time points within a 24-hour window of

investigation hence disagreeing with the findings of Prittinen et al. (2019). This disparity could clearly be attributed to divergent time points of transcript examination since this chapter analysed *sox9* mRNA levels within a 24-hour window following load application, whilst Prittinen et al. (2019) examined mRNA transcripts 1-4 weeks following daily application of centrifugal force. Differing frequencies of application of centrifugal force between this chapter findings and those reported by Prittinen et al. (2019) might also account for the observed disagreement in chondrocyte behaviours between the two studies as this chapter only used a single episode of 770xg force for 15 minutes whereas the other study utilised a daily repeated 771xg force regimen. Since PCM has an important role in mechanotransduction, differences in PCM content between pellet cultures utilised in this PhD study and Prittinen et al. (2019) might explain the inconsistency of the observed findings between the two studies, as this study used either 3D pellets cultured up to 3- or 10-days whilst Prittinen et al. (2019) used pellets cultured for up to 4 weeks. The lack of effects on sGAG amounts following application of either 15- or 60-minutes of 770xg force observed in this chapter contradicts the results of Inoue et al. (1990) who demonstrated significant increases in proteoglycan synthesis (indicated by elevated [$^{35}$S] sulphate incorporation into proteoglycans) in rabbit articular chondrocytes subjected to 3xg centrifugal force for either 12-, 18-, 24- or 32-hours (Inoue et al. 1990). However, the discrepancy might be attributed to differing sensitivities of the employed analysis methods as the DMMB assay utilised in the current study is less sensitive than sGAG radioactive labelling. Also consistent with the findings of this chapter was the observation of unaltered aggrecan mRNA levels in rabbit articular chondrocyte pellet cultures subjected to 6.9 MPa centrifugal pressure for 15 minutes every 24 hours (Maeda et al. 2005).

Furthermore, this chapter demonstrated significant reductions in mRNA levels for the chondrocyte phenotype marker *sox9* following application of 60 minutes of 770xg force to pellets with PCM suggesting that increasing the load duration might be disruptive to the chondrocyte phenotype when applied to 3D pellets with PCM. Cell responses observed in this chapter (sections 3.3.3.3.1 - 3.3.3.3.6) might be attributed to PCM deposition in chondrocyte pellets as previous studies have revealed the crucial role of this matrix region in facilitating the transduction of both biomechanical and biochemical signals to chondrocytes following exposure of cartilage to mechanical loads (Alexopoulos et al. 2005; Guilak et al. 2006; Haider et al. 2006; Khoshgoftar et al. 2018; Knight et al. 1998) therefore corroborating the findings of this chapter. Other studies have demonstrated the importance of components of the PCM including type VI collagen, decorin (DCN) and perlecan in the

transduction of mechanical cues to resident chondrocytes. Type VI collagen (*COL6A1*$^{+/-}$) knockdown resulted in reductions in the expression of genes encoding *ACAN*, biglycan (*BGN*), *DCN* and *SOX9* during chondrogenesis; whilst DCN (*DCN*$^{+/-}$) knockdown induced significant increases in the expression of genes encoding *ACAN*, *BGN* and *SOX9* but not *COL6A1* in human mesenchymal stem cells (hMSCs) (Twomey et al. 2014). Moreover, *col6a1*$^{+/-}$ and type VI collagen knockout (*col6a1*$^{-/-}$) in mice resulted in significant reductions in mechanical properties of the PCM (Alexopoulos et al. 2009). Thus, the inclusion of PCM deposition in the 3D chondrocyte model utilised in this chapter is likely to contribute to the enhanced induction of mechano-signalling responses observed here. However, no independent repeat experiments were conducted to validate the reproducibility of the novel findings unveiled in this chapter thus repeating the experiments would need to be performed to confirm the data findings. Overall, the early and late mechano-responsive gene data in this chapter suggest the suitability of this longer load duration (60 minutes of 770xg force) for utilisation in mechanobiology experiments described in chapter 4 which investigates the influence of PCM (and the absence of PCM) in mediating mechanical signals and their effect on chondrocyte clocks and the regulation of cartilage metabolism though it appears to reduce the mechano-response of a chondrocyte phenotype gene marker in the presence of PCM. Additionally, the ability of increased load duration to induce stronger regulation of early and late mechano-responsive genes as well as sustaining increased transcription of a chondrogenic phenotype gene in pellets with no PCM as compared to pellets with PCM which demonstrated quicker regulation of most mechano-responsive genes concomitant with reduced mechano-sensitivity of a chondrogenic phenotype gene suggests the suitability of 3D pellets with no PCM for employment in further ‘‘*mechanobiology meets chronobiology*” experiments in chapters 4 and 5. However, to be more stringent in the selection of a more suitable 3D model for chapter 5 experiments (assessing the influence of Dex treatment, once daily 770xg load for 3-days, twice daily 770xg load for 1- and 2-days on disrupted circadian rhythms in an *in vitro* 3D inflammatory OA model), both the pellets with and without PCM were utilised in chapter 4 investigations aimed at determining the influence of a single episode of 770xg force for 60 minutes on chondrocyte circadian clocks before selecting pellets with no PCM for employment in chapter 5 investigations as described in section 4.3.5.

### 3.4.7. Summary

- Two *in vitro* 3D model systems comprising either pellets with or without PCM were developed using skeletally immature bovine chondrocytes and characterised for studying chondrocyte mechanobiology. Cell viability was validated by live/dead staining only in 3D pellets with no PCM, whereas biosynthesis was confirmed using the DMMB assay showing sGAG accumulation in culture media, while minimal/no NO release was confirmed using the Griess assay in both the 3D pellets with and without PCM
- *hprt* and *18s* were identified as the most suitable reference genes for qPCR normalisation unaltered following load, and 770xg centrifugal force was revealed to induce robust regulation of early mechano-responsive (*c-fos* and *c-jun*) and late mechano-responsive catabolic genes (*adamts-4*, *adamts-5* and *mmp-3*) as compared to 200- and 1000-xg forces within a 24-hour window in pellets with no PCM
- Increasing the duration of 770xg force application from 15- to 60-minutes induced stronger and/or quicker regulation of the early mechano-responsive gene *c-fos* and *c-jun*, and the late mechano-responsive catabolic gene *adamts-4* within a 24-hour window of investigation in both the pellets with and without PCM
- In pellets with no PCM, increasing the duration of 770xg force application from 15- to 60-minutes sustained the expression of a gene marker for the chondrocyte phenotype *sox9* at most time points, but suppressed its transcription in pellets with PCM within a 24-hour window
- Both the pellets with and without PCM will be utilised in chapter 4 to compare the responses of chondrocyte circadian clocks to a single episode of 770xg force (60 minutes) between the two models within a 72-hour period; thus, assessing whether an established PCM will enhance clock responses to load

# Chapter 4

## Characterisation of chondrocyte circadian clocks and evaluating the influence of centrifugal loading on circadian rhythm in 3D chondrocyte pellets

## 4.1. Introduction

### 4.1.1. Mechanical loading and the circadian clock

To date, very few publications have reported the influence of mechanical loading on cartilage circadian clocks (Dudek et al. 2023; Heywood et al. 2022; Kanbe et al. 2006). Newborn mice rib chondrocytes in a 3D sponge model revealed significantly downregulated *clock* mRNAs following application of 5% cyclical tensile strain over a 4-day period (1 Hz, 15 minutes/hour), thus identifying clock as a mechano-sensitive gene (Kanbe et al. 2006). Primary bovine articular chondrocytes subjected to daily 12-hour bouts of 10% cyclic biaxial tensile strain (0.33 Hz) exhibited circadian periodicity in the expression of the molecular clock protein, bmal1, aligning with diurnal mechanical stimulation (Heywood et al. 2022). Furthermore, the introduction of a 6-hour phase shift in the loading protocol induced an equivalent shift of the circadian clockwork indicative of *in vitro* synchronised chondrocyte circadian clocks in response to repeated daily mechanical loading (Heywood et al. 2022). Daily treadmill running (45 minutes at 15m/min speed) was revealed to induce an ~8-hour phase shift of the circadian clocks in femoral head cartilage and IVD tissues but not the SCN in an *in vivo* per2::luc reporter mice model (Dudek et al. 2023). In an *ex vivo* per2::luc tissue explant culture model, cyclical compressive load (0.5 MPa, 1 Hz for 1 hour, using the FlexCell compression system) was demonstrated to substantially increase the amplitude of circadian rhythm in mice femoral head cartilage and IVD tissues (Dudek et al. 2023). The application of cyclical compressive load at the peak of per2::luc induced a significant increase in the amplitude of circadian rhythm, with a minimal phase shift whilst a phase delay or advance was observed when compression was applied at other per2::luc phases. Additionally, circadian rhythm was disrupted when cyclical compressive load was applied at the trough of per2::luc oscillation. This is indicative of the significance of the phase of a rhythm in modulating the circadian clock response to mechanical loading (Dudek et al. 2023). Mechanistically, the above-mentioned clock responses to mechanical loading were revealed to be mediated through the PLD2-mTORC2-AKT-GSK3β pathway by RNAseq and biochemical analysis suggested mechanical loading as a potent tissue specific zeitgeber to synchronise musculoskeletal circadian rhythms (Dudek et al. 2023).

The scarcity of publications demonstrating the mechano-regulation of circadian clocks in cartilage clearly warrants further investigation of the influence of mechanical loading on circadian rhythm. The model system developed and characterised in chapter 3 was used

to investigate the effects of mechanical load (induced by centrifugation) on circadian rhythm in 3D chondrocyte pellet cultures.

### 4.1.2. Aims

The aim of the work presented in chapter 4 is to comprehensively characterise circadian clocks in control 3D chondrocyte pellets with no PCM (i.e., the first 3D model system characterised in chapter 3) and assess whether the expression of gene markers for the chondrocyte phenotype and/or ECM anabolism and OA phenotype (i.e., ECM catabolism) exhibit circadian rhythmicity in this characterised 3D model. Furthermore, chapter 4 also aims to investigate the response of primary chondrocytes in the two characterised 3D models (pellets with and without PCM) to stimulation with a single episode of centrifugal force (60 minutes of 770xg force as established in chapter 3) to determine how mechanical load influences (i) the cartilage clock within 3 LD cycles, and (ii) cartilage metabolism.

#### 4.1.2.1. Specific chapter objectives

- To characterise the expression of clock genes (*bmal1*, *clock*, *cry1*, *npas2*, *nr1d1*, *nr1d2*, *per1* and *per2*), gene marker of the chondrocyte phenotype (*sox9*) and ECM catabolism markers (*adamts-4*, *adamts-5*, *mmp-3* and *mmp-13*) in control 3D chondrocyte pellets with no PCM within 3 LD cycles
- To characterise the expression of clock genes in 3D chondrocyte pellets either with no PCM (*bmal1*, *clock* and *cry1*) or established PCM (*bmal1*, *cry1*, *dbp* and *per2*) within 3 LD cycles following their respective exposure to a single episode of centrifugal force (60 minutes of 770xg force)
- To characterise the expression of gene markers of ECM anabolism (*acan* and *col2a1*) and catabolism (*adamts-4*) within a 24-hour period in 3D chondrocyte pellets, with and without PCM, following their respective exposure to a single episode of 770xg centrifugal force (60 minutes)

## 4.2. Experimental protocols

### 4.2.1. Characterisation of the baseline expression of mRNA transcripts for clock genes, and gene markers for the chondrocyte phenotype and ECM catabolism in 3D chondrocyte pellets with no PCM

To determine whether skeletally immature chondrocytes possess self-sustained circadian clocks, 3D chondrocyte pellet cultures were established (as described in 2.1.2) and characterised in chapter 3. Following equilibration, quadruple technical replicates of control 3D pellets (i.e., n = 4 per time point) were harvested within a 72-hour period at 4-hour intervals, by adding 1 ml of TRIzol$^{TM}$ reagent and immediately storing at -80$^{o}$C, until further processing of mRNAs and analysis of gene expression as described in sections 2.2 - 2.7. At each 4-hour interval culture media was collected and stored at -20$^{o}$C until further processing (section 2.9). All experiments commenced at 10:00am with the first collection of samples designated as ZT0 hours; culture media was changed an hour before ZT0 hours and every 24 hours thereafter until the cessation of the experiment to replenish essential nutrients and eliminate waste metabolites. To assess the reproducibility of findings, a repeat experiment was set up using an independent chondrocyte preparation (i.e., N = 2).

### 4.2.2. Investigating chondrocyte responses to stimulation with a single episode of centrifugal force in 3D chondrocyte pellets with and without PCM

The two 3D pellet models characterised in chapter 3 (i.e., pellets with or without PCM) were utilised to determine the influence of centrifugal force on circadian clocks and the expression of gene markers for cartilage ECM metabolism in the presence of differing amounts of PCM. Following the equilibration of 3D chondrocyte pellets with no PCM, quadruple technical replicates (i.e., n = 4 per time point) were subjected to a single episode of 770xg force (60 minutes) at 10:00am (ZT0 hours) and harvested within a 72-hour period at 4-hour intervals by adding 1 ml of TRIzol$^{TM}$ reagent [Fig. 4.1] and immediately storing at -80$^{o}$C until further processing of mRNAs and analysis of gene expression as described in sections 2.2 - 2.7. At each 4-hour interval culture media was collected and stored at -20$^{o}$C until further processing (section 2.9). In an independent experiment, 3D pellets with PCM were also loaded at an equivalent centrifugal force, harvested, stored and processed as described above to determine the influence of PCM

on chondrocyte responses to a single episode of load. Additionally, control cultures were also harvested at similar time points as their loaded counterparts (for both 3D pellets with and without PCM) and treated under identical conditions except for centrifugal force exposure [Fig. 4.1]. In both the control and 770xg loaded pellet cultures, culture medium was replenished daily (1 ml removal and replenishment with standard culture media as described in section 2.1.2.). Furthermore, to assess the influence of a single episode of mechanical load (60 minutes of 770xg force) on anabolic and catabolic markers, fold changes in *acan, col2a1* and *adamts-4* mRNA transcripts were quantified by sampling only at T24 hours to demonstrate chondrocyte behaviours. Mechanical loading was always performed at the same time of day (i.e., 10:00 am) for both experiment (3D pellets with and without PCM).

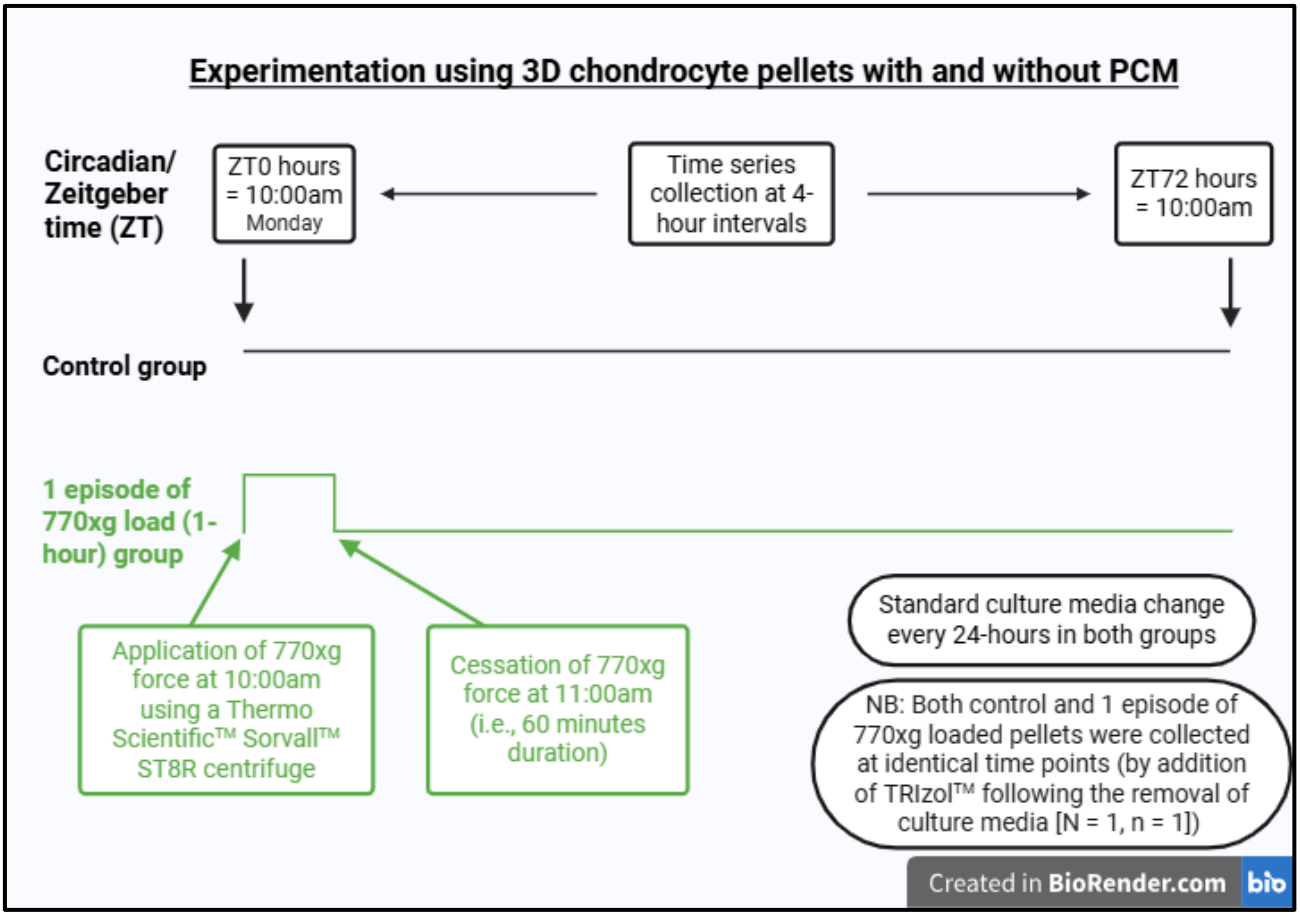


**Figure 4.1. Schematic illustration of an experimental set-up used to assess the influence of a single episode of 770xg force for 60 minutes on chondrocyte circadian clocks in 3D pellets with and without PCM**. The diagram indicates control 3D pellets with or without PCM as well as those subjected to a single episode of 770xg centrifugal force (60 minutes) which were collected at 4-hour intervals (with ZT0 hours selected as 10:00am on Monday representing the time of commencing force application) by adding 1 ml TriZol™ reagent and storage at -80°C within a 72-hour period prior to further processing (N = 1, n = 4) (Created in BioRender).

## 4.3. Results

### 4.3.1. Bovine circadian clock gene primer optimisation

Bovine clock gene primers (*bhlhe40, bhlhe41, bmal1, clock, cry1*, *dbp, nfil3, npas2, nr1d1, nr1d2*, *per1, per2, rorα* and *rorγ*) were designed, optimised and validated as shown in Appendices 3 - 6.

This PhD demonstrated circadian rhythmicity in the expression of most of the above-mentioned clock genes (Appendices 7 - 11) as well as expression profiles for ECM anabolic genes (*acan*, *col2a1*) and a chondrocyte phenotype marker gene (*sox9*) (Appendix 12) in 2D chondrocyte cultures.

### 4.3.2. Baseline chondrocyte behaviours within a 72-hour period in 3D chondrocyte pellets with no PCM

#### 4.3.2.1. Significant increases in sGAG concentration were observed at 24-hour intervals in control 3D pellet cultures

Control 3D pellets with no PCM exhibited significantly increased sGAG concentration between T0- and T24-hours (T0 vs 24 hours: 0.448±0.31 µg/ml, 33.3±1.06 µg/ml [p = 0.03038]) [Fig. 4.2]; T24- and T48-hours (T24 vs 48 hours: 33.3±1.06 µg/ml, 36.2±1.80 µg/ml [p = 0.0421]) [Fig. 4.2]; and T48- and T72-hours (T48 vs 72 hours: 36.2±1.80 µg/ml, 46.1±1.61 µg/ml [p = 0.03038]) [Fig. 4.2]. Data was validated in independent repeat experiments.

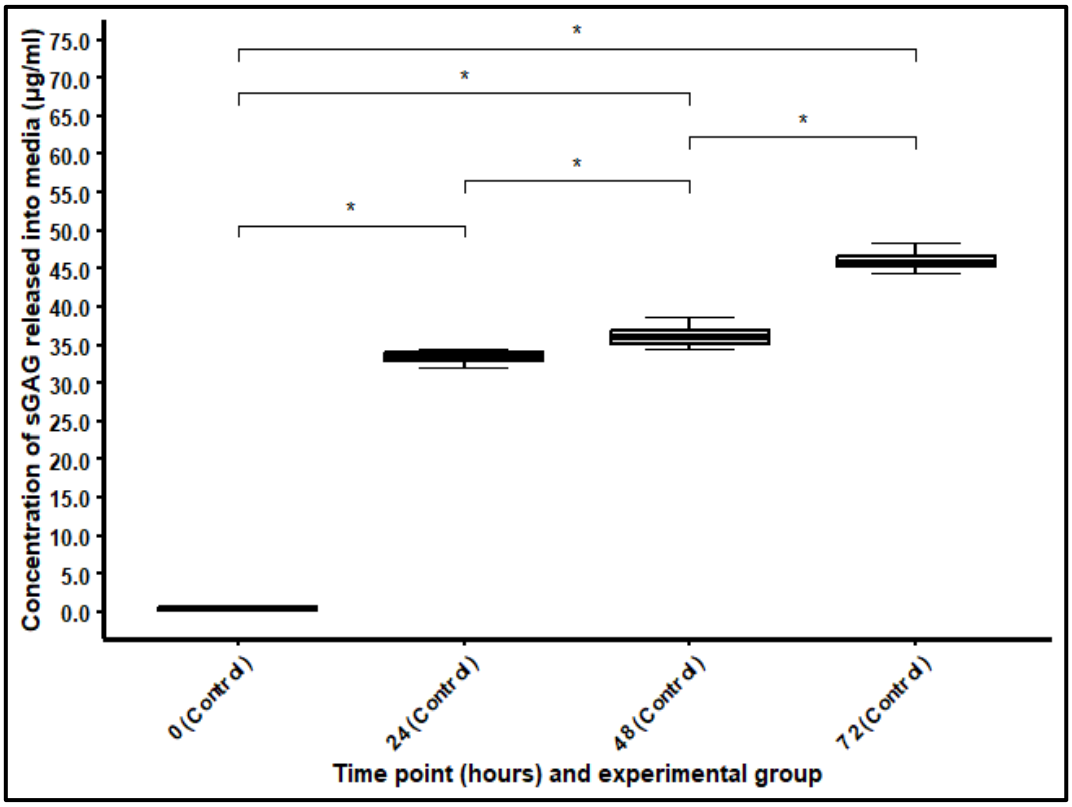


**Figure 4.2. Baseline sGAG concentration at 24-hour intervals within a 72-hour window in a 3D model.** The graph illustrates box and whisker plots representing the concentration of sulphated GAG in media samples collected from control 3D pellets with no PCM at T0-, T24-, T48- and T72-hours. Statistically significant differences between two time points were determined by a Wilcoxon rank sum test in the R software and graphically annotated using the ggpubr package; statistical significance is indicated by * $p<0.05$. Data is representative of the average total concentration of sGAG ± SD (n = 4, N = 2).

### 4.3.2.2. Nitrite/NO concentration was unaffected in control 3D pellet cultures within 72-hours

Control 3D pellets with no PCM exhibited no significant differences in nitrite/NO concentration within a 72-hour period with minimal NO detected (T0: 1.38±0.23 µM; T24: 1.11±0.16 µM, T48: 1.02±0.23 µM, T72: 1.19±0.16 µM, data not shown). Data was validated in independent repeat experiments.

#### 4.3.2.3. RefFinder identified *hprt* and *18s* to be the most stable HKGs

A similar methodology described previously (sections 2.6.4 and 3.3.1.4) was utilised and ultimately *hprt* and *18s* were identified as the two most suitable HKGs for qPCR normalisation of target gene expression in control 3D pellets with no PCM as they did not change within 3 LD cycles [Appendix 13].

#### 4.3.2.4. Assessment of baseline circadian rhythmicity of clock gene mRNAs in 3D chondrocyte pellets with no PCM

##### 4.3.2.4.1. 3D pellet cultures exhibited a reproducible rhythmic expression of *bmal1* and *clock* mRNA transcripts in at least one LD cycle

***bmal1*** 3D chondrocyte pellets with no PCM demonstrated a circadian rhythm of *bmal1* mRNA transcripts ($r^2$ = 0.824, p = 0.0001) throughout the 72-hour timeframe. This circadian rhythm was characterised by an amplitude of 0.596, a period of 20.9 hours and a peak at ZT14 hours [Fig. 4.3A]. The independent repeat confirmed rhythmicity of *bmal1* mRNA ($r^2$ = 0.800, p = 0.0001) as characterised by an amplitude of 0.553, a 22.3-hour period and a peak at ZT12 hours [Fig. 4.3A]. Although there were subtle differences in the rhythm features between the repeats, these were not statistically different (i.e., amplitude [p = 0.6615]; period [p = 0.9999]; and phase [p = 0.6694]).

***clock*** Control 3D pellets with no PCM demonstrated rhythmic oscillations of *clock* mRNA transcripts in the first LD cycle only ($r^2$ = 0.999, p = 0.0001), as characterised by an amplitude of 0.721, a period of 20 hours and a peak at ZT12 hours [Fig. 4.3B]. However, in the independent repeat dataset, *clock* transcripts were rhythmically expressed within 3 LD cycles ($r^2$ = 0.846, p = 0.0001) with an amplitude of 0.354, a period of 22.9 hours and peaking at ZT12 hours [Fig. 4.3B]. No statistical analyses were performed to determine differences in the amplitude, period and phase in circadian rhythm of *clock* transcription between the two-control 3D repeat experiments. This was due to insufficient rhythm characteristics data from individual LD cycles as only one out of three LD cycles met circadian rhythmicity criteria for these genes (i.e., insufficient number of rhythm features data [n] within a 72-hour period for statistical analysis; of which at least an n of 2 is required).

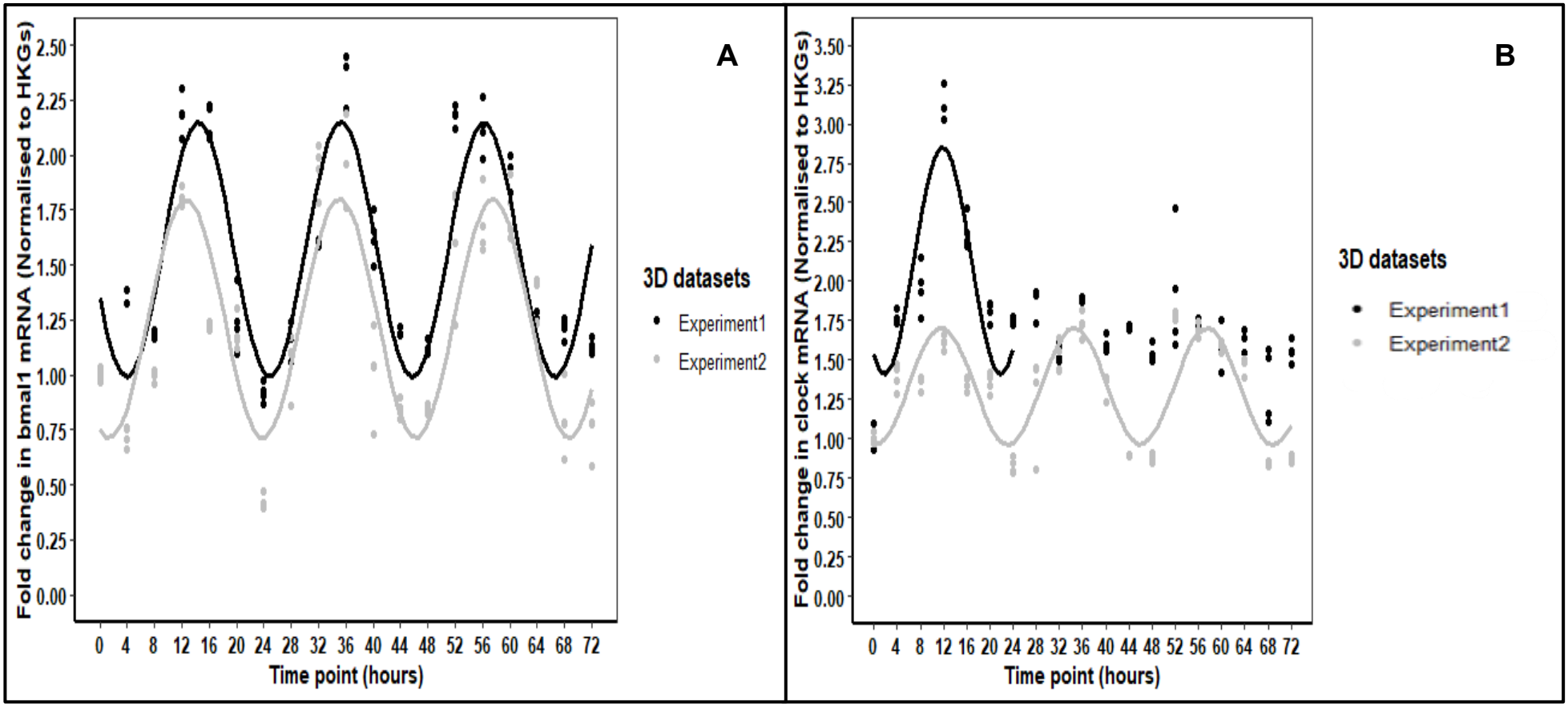


**Figure 4.3. Reproducible 3D chondrocyte cultures' baseline circadian rhythmicity for *bmal1* and *clock* mRNA transcripts in at least 1 LD cycle in two independent repeats.** The graphs illustrate data points representing fold changes in mRNA transcripts (normalised to *18s* and *hprt*) plotted against time of collection (4-hour interval) of control 3D chondrocyte pellets with no PCM before qPCR quantification of the following clock genes within a 72-hour period: **A**) *bmal1* [rhythmic within 3 LD cyles] and **B**) *clock* [*clock* mRNA rhythmicity was lost after the first 24 hours of culture in experiment 1 samples]. Black dots and curves represent experiment 1 datasets; Grey dots and curves represent experiment 2 datasets. The fitted cosinusoidal waves indicate rhythmic oscillations of mRNA transcripts for a specific gene determined by the CircWaveBatch software ($R^2 > 0.8$, $p < 0.05$) and graphically plotted in the R software using the ggplot2 package. The absence of a cosinusoidal wave in plot indicates arrhythmic expression patterns for specific genes determined by the CircWaveBatch software ($R^2 < 0.8$, or $p > 0.05$). Data is representative of the fold changes in mRNA transcripts ($n = 4$, $N = 2$).

#### 4.3.2.4.2. Rhythmic oscillations of *npas2, nr1d1, per1* and *per2* mRNA transcripts within 3 LD cycles in control 3D pellets with no PCM

***npas2*** Control chondrocyte pellet cultures exhibited circadian rhythmicity of *npas2* mRNA transcripts across the 72-hour period of investigation ($r^2$ = 0.812, p = 0.0001); this rhythm was characterised by an amplitude of 0.211, a period of 21.7 hours and a peak around ZT16 hours [Fig. 4.4A].

***nr1d1*** *nr1d1* mRNA transcripts also exhibited rhythmic oscillations across the 3 LD cycles ($r^2$ = 0.917, p = 0.0001), as characterised by an amplitude of 0.115, a 19.1-hour period and a peak around ZT2 hours [Fig. 4.4B].

***per1*** Control 3D chondrocyte pellets revealed rhythmic expression of *per1* mRNA within 3 LD cycles ($r^2$ = 0.901, p = 0.0001), with its rhythm showing an amplitude of 0.411, period of 28 hours and a peak at ZT0 hours [Fig. 4.4C].

***per2*** Likewise, *per2* mRNA was also rhythmic within the 72-hour timeframe ($r^2$ = 0.836, p = 0.0037) as characterised by an amplitude of 0.973, period of 22.7 hours and a peak around ZT8 hours [Fig. 4.4D].

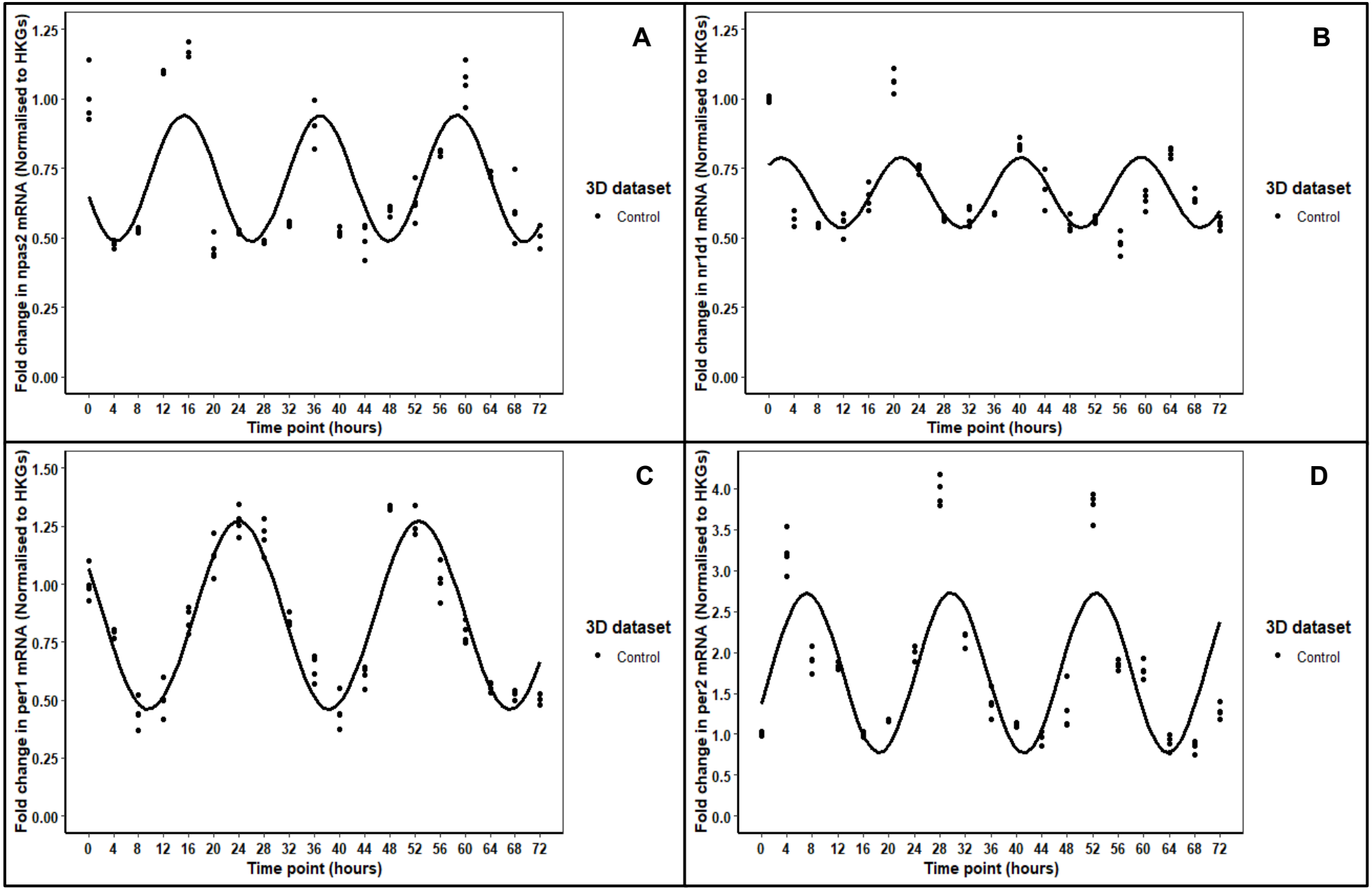
A
Fold change in npas2 mRNA (Normalised to HKGs)
Time point (hours)
3D dataset
Control
B
Fold change in nr1d1 mRNA (Normalised to HKGs)
Time point (hours)
3D dataset
Control
C
Fold change in per1 mRNA (Normalised to HKGs)
Time point (hours)
3D dataset
Control
D
Fold change in per2 mRNA (Normalised to HKGs)
Time point (hours)
3D dataset
Control

**Figure 4.4. Baseline circadian rhythmicity for *npas2*, *nr1d1*, *per1* and *per2* mRNA transcripts in 3D chondrocyte cultures within 3 LD cycles.** The graphs illustrate data points (black dots) representing fold changes in mRNA transcripts (normalised to *18s* and *hprt*) plotted against time of collection (4-hour interval) of 3D control chondrocyte pellets with no PCM before qPCR quantification of the following clock genes within a 72-hour period: **A**) *npas2*, **B**) *nr1d1*, **C**) *per1* and **D**) *per2*. The fitted cosinusoidal waves (black curves) indicate rhythmic oscillations of mRNA transcripts for a specific gene determined by the CircWaveBatch software ($R^2 > 0.8$, $p < 0.05$) and graphically plotted in the R software using the ggplot2 package. Data points represent fold changes in mRNA transcripts (n = 4, N = 1).

#### 4.3.2.4.3. No circadian expression of *cry1* and *nr1d2* mRNA transcripts within 3 LD cycles in control 3D pellets with no PCM

Control 3D chondrocyte pellets exhibited no rhythmic expression of *cry1* ($r^2 = 0.285$, $p = 0.0001$) [Fig. 4.5A] and *nr1d2* ($r^2 = 0.461$, $p = 0.0001$) mRNA transcripts [Fig. 4.5B] within a 72-hour window of investigation.

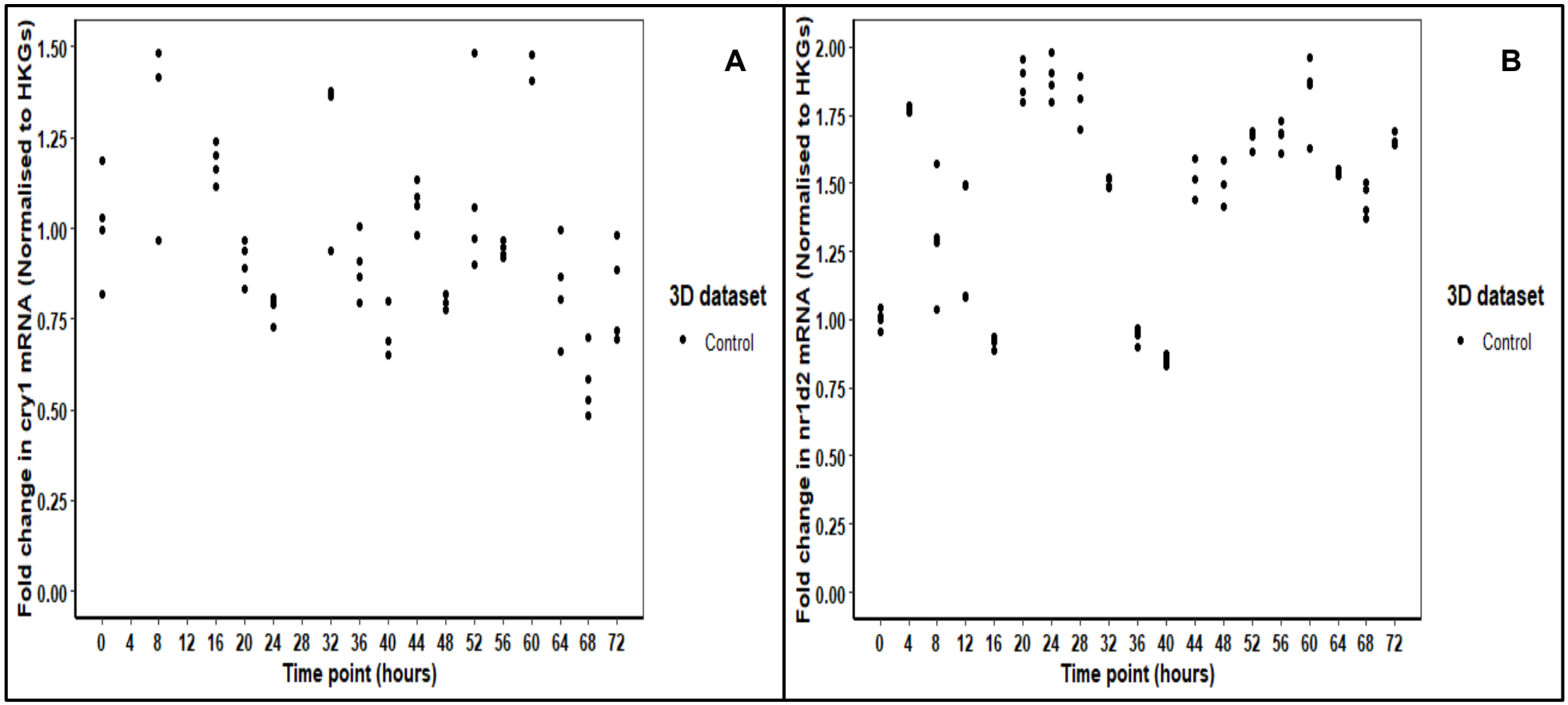


**Figure 4.5. Baseline expression profiles for *cry1* and *nr1d2* mRNA transcripts in 3D chondrocyte cultures within 3 LD cycles.** The graphs illustrate data points (black dots) representing fold changes in mRNA transcripts (normalised to *18s* and *hprt*) plotted against time of collection (4-hour interval) of control 3D chondrocyte pellets with no PCM before qPCR quantification of the following clock genes within a 72-hour period: **A**) *cry1* and **B**) *nr1d2*. The absence of a cosinusoidal wave in plots indicate arrhythmic expression of these genes determined by the CircWaveBatch software ($R^2 < 0.8$, or $p > 0.05$). Data points represent fold changes in mRNA transcripts (n = 4, N = 1).

#### 4.3.2.5. Characterisation of the baseline expression of gene markers of chondrocyte remodelling in a 3D chondrocyte model

##### 4.3.2.5.1. No circadian oscillations in so9 mRNA levels in control 3D cultures within 3 LD cycles

Control 3D chondrocyte pellets with no PCM exhibited no circadian rhythm of *sox9* transcription within a 72-hour period ($r^2$ = 0.202, p = 0.0003) [Fig. 4.6].

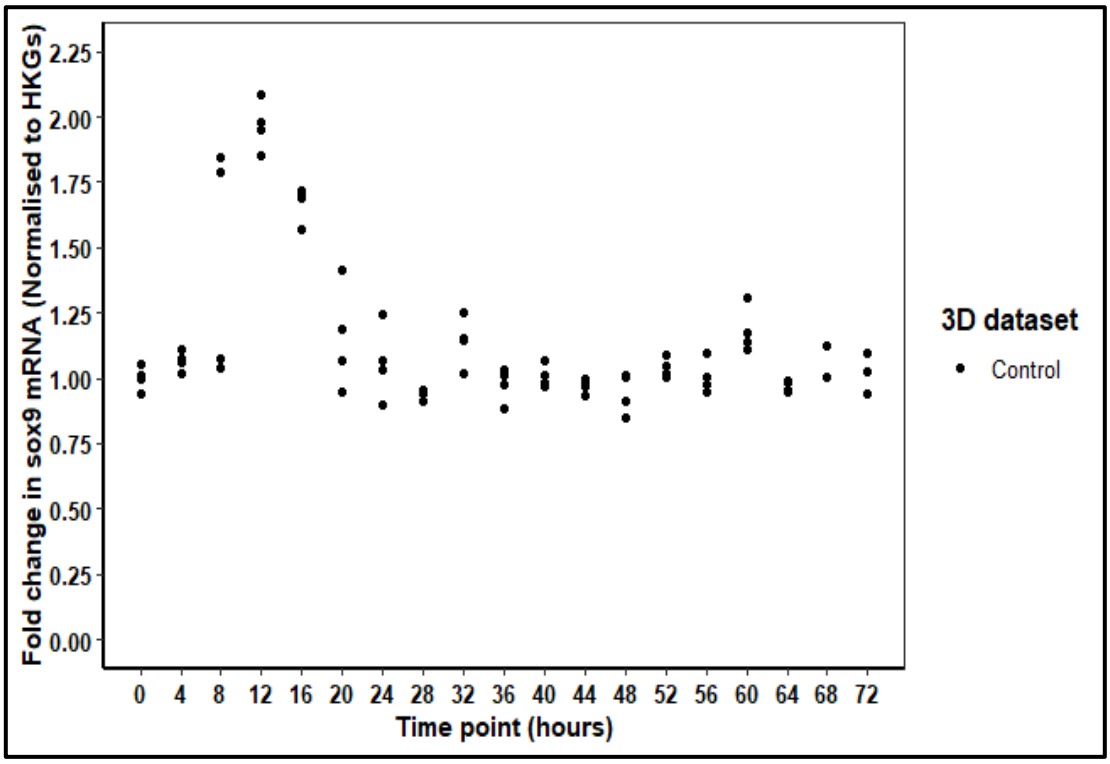


**Figure 4.6. Baseline mRNA expression profile for *sox9* in 3D chondrocyte cultures within a 72-hour period.** The graphs illustrate data points (black dots) representing fold changes in *sox9* mRNA transcripts (normalised to *18s* and *hprt*) plotted against time of collection (4-hour interval) of control 3D chondrocyte pellets with no PCM. The absence of a cosinusoidal wave indicates arrhythmic *sox9* mRNA expression within 3 LD cycles determined by the CircWaveBatch software ($R^2$ < 0.8 and p < 0.05). Data points represent fold changes in mRNA transcripts (n = 4, N = 1).

#### 4.3.2.5.2. Arrhythmic expression of *mmp-3, mmp-13*, *adamts-4* and *adamts-5* mRNA transcripts within a 72-hour period in control 3D pellets with no PCM

Control 3D cultures demonstrated no circadian rhythm of *mmp-3* ($r^2 = 0.479$, $p = 0.0001$ [Fig. 4.7A]) or *mmp-13* transcription within a 72-hour period ($r^2 = 0.101$, $p = 0.0207$) [Fig. 4.7B]. Likewise, control 3D cultures exhibited arrhythmic expression of *adamts-4* ($r^2 = 0.322$, $p = 0.0001$) [Fig. 4.7C] and *adamts-5* ($r^2 = 0.485$, $p = 0.0223$) [Fig. 4.7D] mRNA within a 72-hour period of investigation.

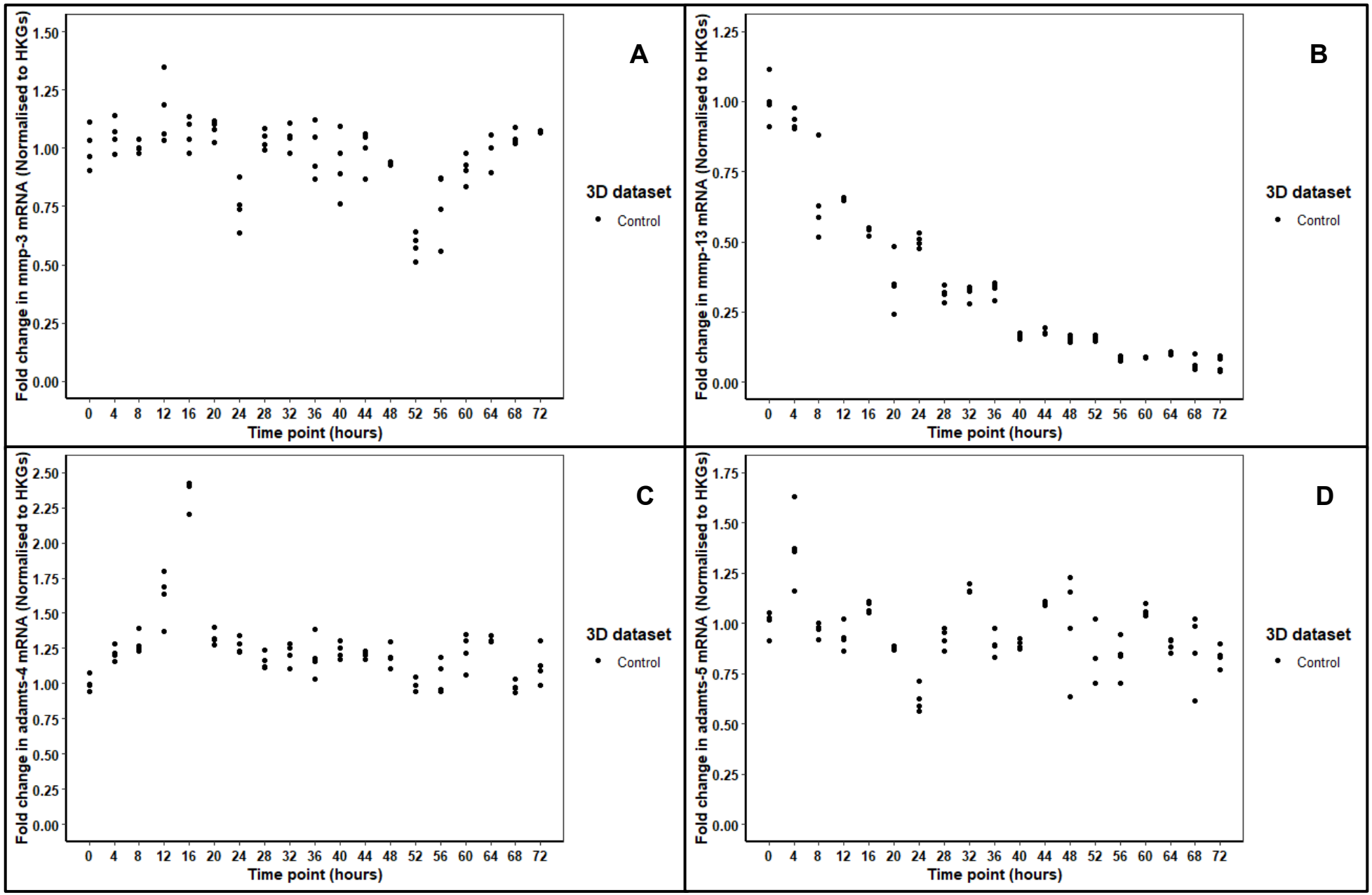
A
Fold change in mmp-3 mRNA (Normalised to HKGs)
1.50
1.25
1.00
0.75
0.50
0.25
0.00
0 4 8 12 16 20 24 28 32 36 40 44 48 52 56 60 64 68 72
Time point (hours)
3D dataset
Control
B
Fold change in mmp-13 mRNA (Normalised to HKGs)
1.25
1.00
0.75
0.50
0.25
0.00
0 4 8 12 16 20 24 28 32 36 40 44 48 52 56 60 64 68 72
Time point (hours)
3D dataset
Control
C
Fold change in adamts-4 mRNA (Normalised to HKGs)
2.50
2.25
2.00
1.75
1.50
1.25
1.00
0.75
0.50
0.25
0.00
0 4 8 12 16 20 24 28 32 36 40 44 48 52 56 60 64 68 72
Time point (hours)
3D dataset
Control
D
Fold change in adamts-5 mRNA (Normalised to HKGs)
1.75
1.50
1.25
1.00
0.75
0.50
0.25
0.00
0 4 8 12 16 20 24 28 32 36 40 44 48 52 56 60 64 68 72
Time point (hours)
3D dataset
Control

**Figure 4.7. Baseline mRNA expression profiles for *mmp-3*, *mmp-13, adamts-4* and *adamts-5* in 3D chondrocyte pellets within a 72-hour period.** The graphs illustrate data points (black dots) representing fold changes in mRNA transcripts (normalised to *18s* and *hprt*) plotted against time of collection (4-hour interval) of control 3D chondrocyte pellets with no PCM before qPCR quantification of the following catabolic enzyme genes within 3 LD cycles: **A)** *mmp-3*, **B)** *mmp-13*, **C)** *adamts-4* and **D)** *adamts-5*. The absence of a cosinusoidal wave in the plot indicates arrhythmic expression of a specific gene determined by the CircWaveBatch software ($R^2 < 0.8$, or $p > 0.05$). Data points represent fold changes in mRNA transcripts (n = 4, N = 1).

### 4.3.3. Responses of 3D chondrocyte pellets with and without PCM to a single episode of mechanical loading (simulated by 60 minutes of 770xg force)

#### 4.3.3.1. Application of a single episode of 770xg force (60-minutes) had no effect on sulphated GAG release in 3D pellets with and without PCM within a 72-hour window

Control 3D pellets with no PCM exhibited significant increases in sGAG concentration within the 72-hour culture increasing from 5.9±0.32 µg/ml (T0 hours) to 15.5±1.73 µg/ml (T72 hours) [p = 0.02843] (data not shown). Likewise, 3D pellets with no PCM subjected to a single episode of 770xg force for 60 minutes demonstrated significantly increased sGAG concentration between T0- (5.9±0.32 µg/ml), and T72-hours (13.6±0.75 µg/ml) [p = 0.0294] (data not shown). However, no significant differences were observed between controls and 770xg loaded pellets at 24-hour intervals within a 72-hour window of investigation (T24 hours [p = 0.8852]; T48 hours [p = 0.1102]; T72 hours [p = 0.1102]). Data is comparable to that reported in section 3.3.2.1 using the same 3D model.

In control 3D pellets with PCM, significant increases in sGAG levels were observed within the 72-hour culture period increasing from 11.1±0.50 µg/ml (T0 hours) to 23.6±2.10 µg/ml (T72 hours) [p = 0.0294] (data not shown). Likewise, 3D pellets with PCM subjected to a single episode of 770xg force for 60 minutes demonstrated similar increases in sGAG concentration within the same timeframe (data not shown). However, no significant differences were observed between controls and 770xg loaded pellets at 24-hour intervals within this 72-hour window (T24 hours [p = 0.0999]; T48 hours [p = 0.4705]; T72 hours [p = 0.8852]). Pellet cultures in this experimental set-up exhibited divergent cell responses as compared to those described in section 3.3.2.1, where an overall reduction in sGAG concentration was observed between T24- and T72-hours in both control 3D pellets with PCM and those subjected to one episode of 770xg force for 60 minutes.

#### 4.3.3.2. Undetectable nitrite/NO was observed in 3D pellets with and without PCM within a 72-hour window

No nitrite/NO was detectable at 24-hour interval within a 72-hour window of investigation in both the control 3D pellets with and without PCM and those subjected to a single episode of 770xg force for 60 minutes (data not shown). Data is comparable to that reported in section 3.3.2.2 using the same 3D models.

### 4.3.3.3. Circadian clock dynamics in 3D chondrocyte pellets with and without PCM in response to a single episode of 770xg centrifugal force (60 minutes)

#### 4.3.3.3.1. Application of a single episode of 770xg force for 60 minutes induced no significant changes in circadian rhythm of *bmal1* transcription within a 72-hour period in 3D pellets with and without PCM

No circadian regulation of *bmal1* mRNA levels was observed in control ($r^2 = 0.698$, $p < 0.0001$) and 770xg loaded ($r^2 = 0.403$, $p = 0.0016$) 3D pellets with no PCM in the first LD cycle suggesting a transient lack of rhythmicity in both groups within the first 24-hours [Fig. 4.8A]. However, control 3D pellets with no PCM exhibited rhythmic expression of *bmal1* mRNA in the second and third LD cycles ($r^2 = 0.821$, $p = 0.0001$), characterised by an amplitude of 0.641, a period of 23.3 hours and a peak at ZT10 hours [Fig. 4.8A]. Likewise, 3D pellets with no PCM exposed to a single episode of 770xg force for 60 minutes demonstrated circadian oscillations of *bmal1* mRNA in the second and third LD cycles ($r^2 = 0.893$, $p = 0.0001$), with a rhythm showing the following features: amplitude; 0.505, period; 23 hours and a peak at ZT10 hours [Fig. 4.8A]. No significant differences were observed in the amplitude ($p = 0.6391$), period ($p = 0.4415$), and phase ($p = 0.1024$) of *bmal1* mRNA rhythm between the control and loaded pellet cultures with no PCM (data not shown).

Control 3D pellets with PCM revealed rhythmicity of *bmal1* mRNA transcripts throughout the 72-hour period of investigation ($r^2 = 0.833$, $p = 0.0001$), as characterised by: amplitude; 0.572, period; 22.5 hours, and a peak at ZT12 hours [Fig. 4.8B]. Likewise, rhythmic oscillations of *bmal1* mRNA transcripts were also observed within a 72-hour window in 3D pellets with PCM subjected to a single episode of 770xg force for 60 minutes ($r^2 = 0.828$, $p = 0.0001$), with a rhythm demonstrating: amplitude; 0.709, period; 20.8 hours, and a peak at ZT14 hours [Fig. 4.8B]. However, the observed differences in the amplitude, period, and

phase of *bmal1* mRNA rhythm between individual LD cycles of control pellets with PCM and those exposed to a single episode of 770xg force (60 minutes) were not significant [amplitude; ($p = 0.3393$), period ($p = 0.1635$), phase; ($p = 0.9713$)] (data not shown).

This indicates that one episode of 770xg force regimen had no effect on the rhythmicity of this gene forming the positive arm of the transcriptional/translation feedback loop of the mammalian core circadian clock mechanism in pellets with and without PCM.

#### 4.3.3.3.2. Application of one episode of 770xg force for 60 minutes did not alter the circadian regulation of *cry1* transcription in pellets with no PCM, whilst no circadian regulation of *cry1* transcription was observed within a 72-hour in 3D pellets with PCM (in the absence and presence of load)

Control 3D pellets with no PCM exhibited circadian rhythm of *cry1* mRNA levels in the first two LD cycles within a 72-hour window of investigation ($r^2 = 0.815$, $p = 0.0001$), as characterised by an amplitude of 0.414, a 20-hour period and a peak at ZT12 hours [Fig. 4.8C]. Likewise, 3D pellets with no PCM subjected to one episode of 770xg force for 60 minutes revealed rhythmic expression of *cry1* mRNA transcripts in the first two LD cycles ($r^2 = 0.800$, $p = 0.0001$), with a rhythm displaying an amplitude of 0.436, period of 20 hours, and peaking at ZT12 hours [Fig. 4.8C]. However, no statistical analyses were performed for differences in amplitude, period, and phase of *cry1* mRNA circadian rhythm between the control and 770xg loaded cultures due to inconsistent rhythmicity profiles of *cry1* mRNA in individual LD cycle, i.e., one LD cycle failed to meet the circadian rhythmicity determination requirements ($r^2 > 0.8$ and $p < 0.05$) (data not shown) though it appeared rhythmic when assessed in conjunction with the other LD cycle.

Control pellets with PCM demonstrated a lack of rhythmicity of *cry1* mRNA throughout the 72-hour period of investigation ($r^2 = 0.165$, $p = 0.0014$) [Fig. 4.8D]. Likewise, following application of a single episode of 770xg force (60 minutes) to pellets with PCM, no rhythmic oscillations of *cry1* mRNA levels were observed within 3 LD cycles ($r^2 = 0.275$, $p = 0.0001$) [Fig. 4.8D].

This indicates that an episode of 770xg load (60 minutes) had no influence on the circadian rhythm of this gene forming the negative arm of the transcriptional/translation feedback loop of the mammalian core circadian clock mechanism in pellets with no PCM

and that the circadian control of this gene was lost in pellets cultured for an extended period and loading did not reset its lost circadian rhythm.

**Pellets with no PCM** **Pellets with PCM**

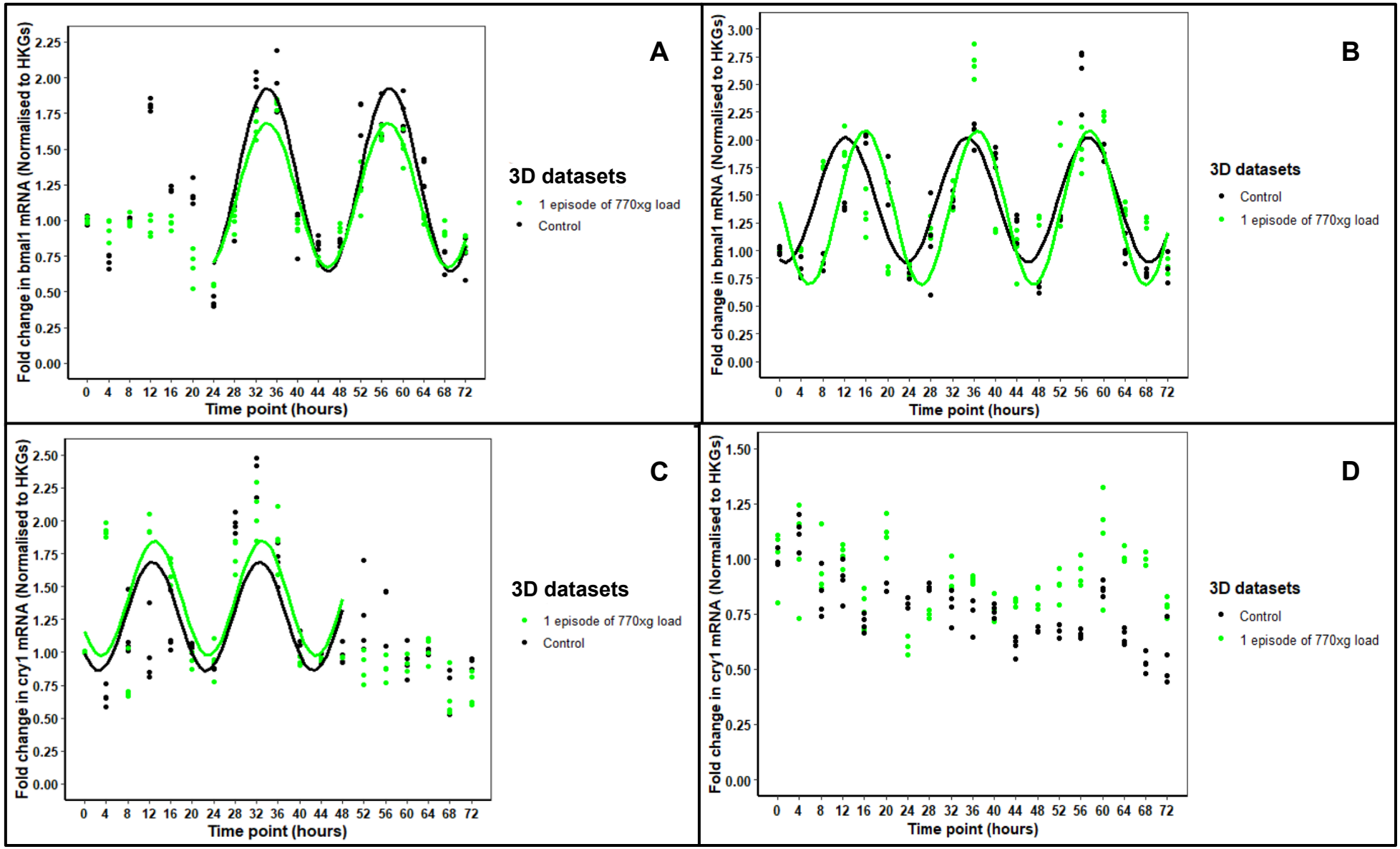

**Figure 4.8. Effect of a single episode of 770xg force (60 minutes) on *bmal1* and *cry1* transcription in 3D pellets with and without PCM within 3 LD cycles**. Fold change in mRNA transcripts (normalised to *18s* and *hprt*) plotted against time of collection (4-hour interval) of control 3D pellets (black dots) and those subjected to an episode of 770xg force for 60 minutes (green dots) either in the absence or presence of PCM (n = 4, N = 1) before qPCR quantification of the following genes within a 72-hour period: **A**) *bmal1* in pellets with no PCM [control and 770xg loaded cultures exhibited no rhythmicity in the first LD cycle, recovered afterwards with comparable parameters], **B**) *bmal1* in pellets with PCM [no significant changes in rhythmicity following load], **C**) *cry1* in pellets with no PCM [rhythmicity appeared to be unaffected by load] and **D**) *cry1* in pellets with PCM [no circadian rhythm in both the control and loaded pellets]. The fitted cosinusoidal waves (black and green curves) indicate rhythmic oscillations of mRNA transcripts for a specific gene determined by the CircWaveBatch software ($R^2 > 0.8$, $p < 0.05$) and graphically plotted in the R software using the ggplot2 package. The absence of a cosinusoidal wave in a plot indicates an arrhythmic expression pattern of a specific gene determined by the CircWaveBatch software ($R^2 < 0.8$, $p > 0.05$).

#### 4.3.3.3.3. Transient disruption of *clock* mRNA circadian rhythm in the first LD cycle following application of a single episode of 770xg force, unaltered in the second and third LD cycles in pellets with no PCM

Control 3D pellets with no PCM exhibited rhythmic expression of *clock* mRNA transcripts within three LD cycles ($r^2 = 0.846$, $p = 0.0001$) characterised by the following: amplitude; 0.354, period; 22.9 hours, and a peak at ZT12 hours [Fig. 4.9]. However, no rhythmic oscillations of *clock* mRNA levels were observed in the first LD cycle in 3D pellets with no PCM exposed to one episode of 770xg force for 60 minutes ($r^2 = 0.264$, $p = 0.0217$) [Fig. 4.9], yet these cultures exhibited circadian rhythm of *clock* mRNA in the second and third LD cycles ($r^2 = 0.812$, $p = 0.0001$) [Fig. 4.9] as characterised by a 0.401 amplitude, a 21.8-hour period, and a peak around ZT9 hours [Fig. 4.9]. Although there were subtle differences in the rhythm features between control and 770xg loaded cultures with no PCM, these were not statistically different when analysed per individual LD cycle across a 72-hour period (amplitude; $p = 0.5523$, period; $p = 0.4462$, phase; $p = 0.3028$) (data not shown).

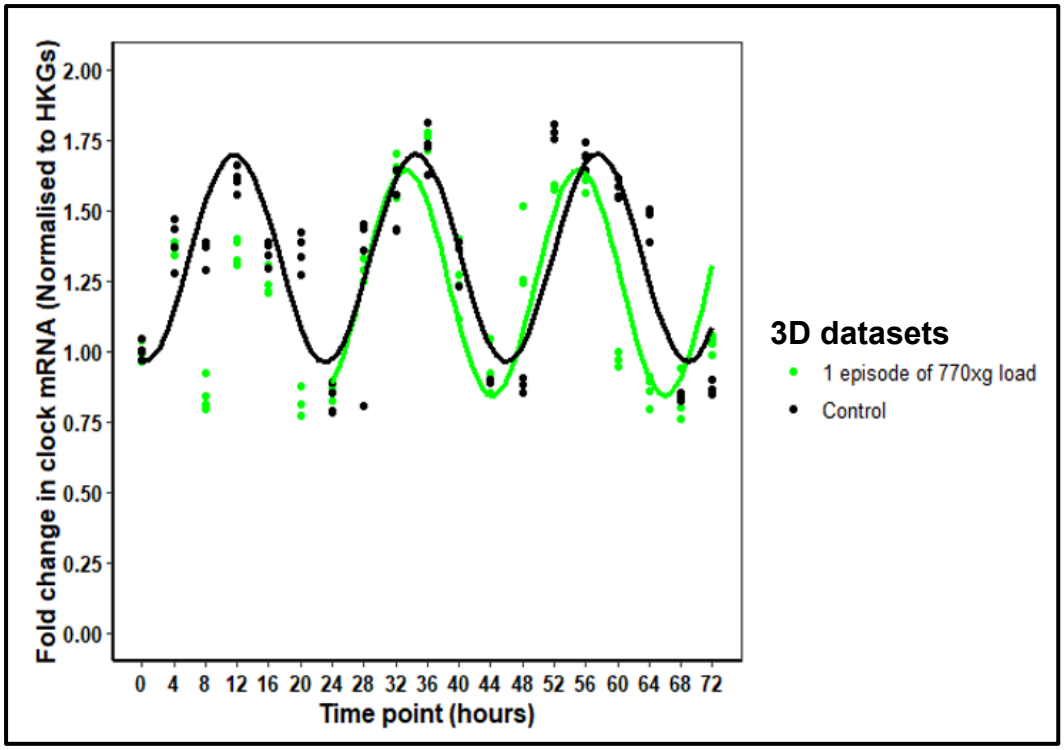


**Figure 4.9. Effect of a single episode of 770xg force (60 minutes) on *clock* transcription in 3D pellets with no PCM within 3 LD cycles**. Fold change in *clock* mRNA transcripts (normalised to *18s* and *hprt*) plotted against time of collection (4-hour interval) of control 3D pellets with no PCM (black dots) and those subjected to an episode of 770xg force for 60 minutes (green dots) (n = 4, N = 1) quantified by qPCR within a 72-hour period. The absence of a cosinusoidal wave in first LD cycle of the loaded dataset suggests a transient disruption of *clock* mRNA rhythmicity following load application. The fitted cosinusoidal waves (black curves: baseline circadian oscillations within a 72-hour period, green curves: recovery of circadian rhythmicity in the second and third LD cycles following load application) indicate rhythmic oscillations of *clock* mRNA transcripts determined by the CircWaveBatch software ($R^2 > 0.8$, $p < 0.05$) and graphically plotted in the R software using the ggplot2 package.

#### 4.3.3.3.4. No apparent differences in circadian regulation of *dbp* transcription following application of one episode of 770xg force for 60 minutes in pellets with PCM

In control pellets with PCM, *dbp* mRNA levels were expressed in a rhythmic manner in the second and third LD cycle ($r^2 = 0.848$, $p = 0.0131$), with an amplitude of 0.157, a period of 20 hours, and a peak around ZT18 hours [Fig. 4.10A]. In contrast, following application of a single episode of 770xg force (60 minutes) to pellets with PCM, circadian regulation of *dbp* transcription was observed in the first two LD cycles ($r^2 = 0.800$, $p = 0.0002$), characterised by an amplitude of 0.172, a 20-hour period, and a peak at ZT20 hours [Fig. 4.10A]. However, no statistical analyses were performed to investigate differences in amplitude, period, and phase of *cry1* mRNA circadian rhythm between the control and 770xg loaded (1 episode for 60 minutes) cultures with PCM due to inconsistent rhythmicity profiles of *dbp* mRNA in individual LD cycle, i.e., one LD cycle failed to meet the circadian rhythmicity determination criteria ($r^2 > 0.8$ and $p < 0.05$) (data not shown), although it appeared rhythmic when assessed in conjunction with the other LD cycle. However, data implies that an episode of 770xg load (60 minutes) has no impact on the circadian rhythm of this gene forming the positive arm of an auxiliary feedback loop in the mammalian core circadian clock mechanism in pellets with PCM.

#### 4.3.3.3.5. Persistence of circadian regulation of *per2* transcription following application of one episode of 770xg force for 60 minutes in pellets with PCM

*per2* mRNA transcripts were rhythmic in the first and second LD cycles in control 3D pellets with PCM ($r^2 = 0.875$, $p = 0.0001$), as characterised by an amplitude of 0.685, a 20-hour period and a peak at ZT4 hours [Fig. 4.10B]. Likewise, following application of one episode of 770xg force (60 minutes) to pellets with PCM, circadian rhythmicity of *per2* mRNA transcripts was also observed in the first and second LD cycles ($r^2 = 0.840$, $p = 0.0001$) with: 0.503 amplitude, 20-hours period, and a peak at ZT2 hours [Fig. 4.10B]. No differences were observed in the amplitude ($p = 0.4637$), period ($p = NA$ since the period was identical across the two LD cycles), and phase ($p = 0.3522$) of *per2* mRNA rhythm between control 3D pellets with PCM and those exposed to a single episode of 770xg force (60 minutes) (data not shown). This indicates that an episode of 770xg load (60 minutes) had no effect on the rhythmicity of this gene forming the negative arm of the transcriptional/translation feedback loop of the mammalian core circadian clock mechanism in pellets with PCM.

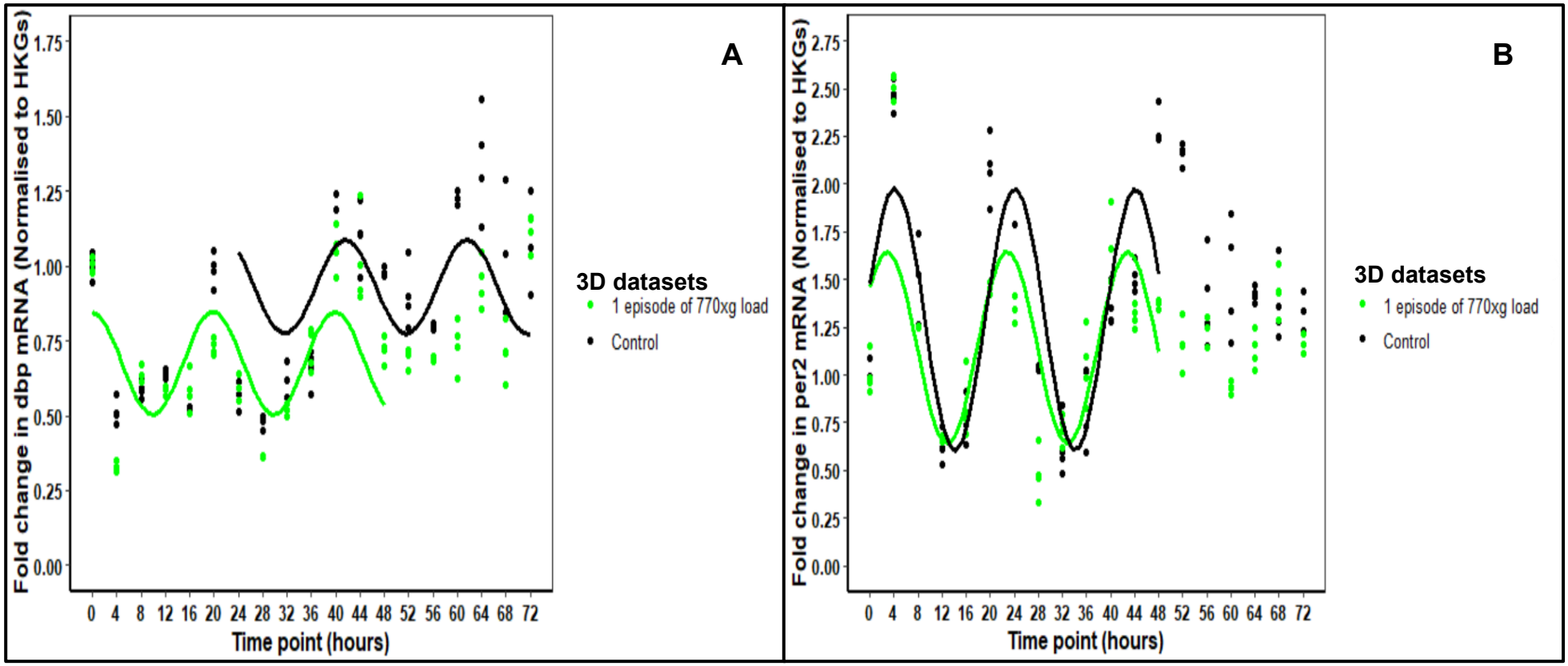


**Figure 4.10. Effect of a single episode of 770xg force (60 minutes) on *dbp* and *per2* transcription in 3D pellets with PCM within 3 LD cycles.** Fold change in mRNA transcripts (normalised to *18s* and *hprt*) plotted against time of collection (4-hour interval) of control 3D pellets with PCM (black dots) and those subjected to an episode of 770xg force for 60 minutes (green dots) (n = 4, N = 1) before qPCR quantification of the following genes within a 72-hour period: **A**) *dbp* [rhythmicity appeared to be unaffected by load] and **B**) *per2* [no significant changes in rhythmicity following load application]. The fitted cosinusoidal waves (black and green curves) indicate rhythmic oscillations of mRNA transcripts for a specific gene determined by the CircWaveBatch software ($R^2 > 0.8$, $p < 0.05$) and graphically plotted in the R software using the ggplot2 package. The absence of a cosinusoidal wave in specific LD cycles indicates transient arrhythmic gene expression patterns determined by the CircWaveBatch software ($R^2 < 0.8$, $p > 0.05$).

#### 4.3.3.4. Determination of expression patterns of gene markers for ECM anabolism and catabolism in 3D chondrocyte pellets with and without PCM in response to a single episode of mechanical load (60 minutes of 770xg force)

##### 4.3.3.4.1. No circadian regulation of *acan* transcription within a 24-hour window following application of one episode of 770xg force for 60 minutes, with mRNA levels unaltered at T24 hours in pellets with no PCM, but upregulated at T24 hours in pellets with PCM

Control 3D pellets with no PCM demonstrated no circadian rhythm of a gene marker of anabolism *acan* in the first LD cycle ($r^2 = 0.226$, $p = 0.0408$) [Fig. 4.11A]. Following application of a single episode of mechanical load, (i.e., 60 minutes of 770xg force), 3D pellets with no PCM also exhibited no rhythmic expression of *acan* mRNA ($r^2 = 0.259$, $p = 0.0235$) [Fig. 4.11A] therefore mirroring the behaviours of control pellet cultures. However, application of one episode of 770xg force (60 minutes) induced no significant changes in *acan* mRNA transcripts at T24 hours in pellets with no PCM [Fig. 4.11B].

Likewise, no circadian rhythm of *acan* transcription was observed in control 3D chondrocyte pellets with PCM in the first LD cycle ($r^2 = 0.175$, $p = 0.0899$) [Fig. 4.11C]. Following application of one episode of 770xg force for 60 minutes, 3D pellets with PCM still exhibited no rhythmic expression of *acan* mRNA in the first LD cycle ($r^2 = 0.205$, $p = 0.0571$) [Fig. 4.11C]. Analysis of *acan* mRNA levels 24 hours following cessation of a single episode of 770xg load (60 minutes) revealed a significant 1.53-fold increase relative to control 3D pellets with PCM ($p = 0.0294$) [Fig. 4.11D].

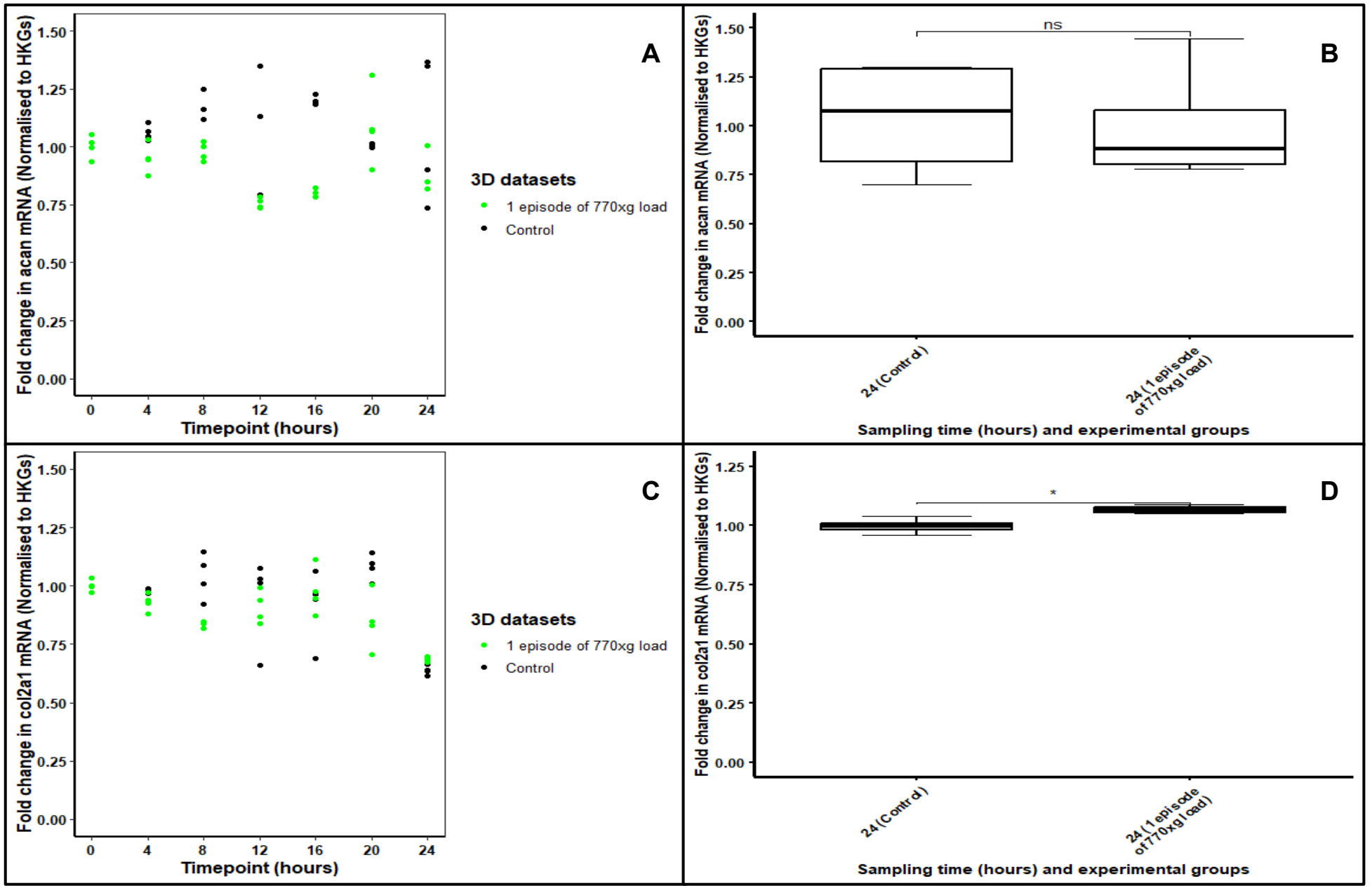
A
Fold change in acan mRNA (Normalised to HKGs)
1.50
1.25
1.00
0.75
0.50
0.25
0.00
0
4
8
12
16
20
24
Timepoint (hours)
3D datasets
1 episode of 770xg load
Control
B
ns
Fold change in acan mRNA (Normalised to HKGs)
24 (Contrd)
24 (1episode of770xgload)
Sampling time (hours) and experimental groups
C
Fold change in col2a1 mRNA (Normalised to HKGs)
Timepoint (hours)
3D datasets
1 episode of 770xg load
Control
D
*
Fold change in col2a1 mRNA (Normalised to HKGs)
24 (Contrd)
24 (1episode of770xgload)
Sampling time (hours) and experimental groups

**Figure 4.11. Effect of a single episode of 770xg force (60 minutes) on *acan* transcription in 3D chondrocyte pellets with and without PCM within one LD cycle.** Data illustrates fold changes in *acan* mRNA transcripts (normalised to *18s* and *hprt*) (n = 4, N = 1) plotted against either time of collection (4-hour interval) of control 3D pellets and those exposed to one episode of 770xg force for 60 minutes or measurements only at T24 hours in the absence or presence of PCM. The illustration shows the following: **A)** circadian time series quantification of *acan* mRNA transcripts in pellets with no PCM within a 24-hour period, **B)** *acan* mRNA transcripts measured at T24 hours in pellets with no PCM, **C)** circadian time series quantification of *acan* mRNA transcripts in pellets with PCM and **D)** *acan* mRNA transcripts measured at T24 hours in pellets with PCM. Black dots; control datasets, green dots; 1 episode of 770xg load datasets. The absence of cosinusoidal waves indicates arrhythmic expression of this anabolism marker gene determined by the CircWaveBatch software ($R^2 < 0.8$, $p>0.5$). Box and whisker plots represent average fold changes in *acan* mRNA levels ± SD (n = 4, N = 1); statistical significance was assessed between control and 770xg loaded cultures within a 24-hour period using a Wilcoxon rank sum test (* $p<0.05$, ns = no significance).

#### 4.3.3.4.2. No circadian regulation of *col2a1* transcription within a 24-hour window following application of one episode of 770xg force for 60 minutes, with mRNA levels upregulated at T24 hours in pellets with and without PCM

Control 3D pellets with no PCM demonstrated no circadian rhythm of the anabolism marker *col2a1* in the first LD cycle ($r^2 = 0.191$, $p = 0.0707$) [Fig. 4.12A]. Following application of one episode of 770xg force (60 minutes), 3D pellets with no PCM still exhibited no rhythmic expression of *col2a1* mRNA in the first LD cycle ($r^2 = 0.095$, $p = 0.2884$) [Fig. 4.12A]. Analysis of *col2a1* mRNA levels 24 hours following cessation of one episode of 770xg force for 60 minutes revealed subtle increases relative to control 3D pellets with no PCM (1.07-fold, $p = 0.01672$) [Fig. 4.12B].

Likewise, no circadian expression of *col2a1* was observed in control 3D chondrocyte pellets with PCM in the first LD cycle ($r^2 = 0.260$, $p = 0.0232$) [Fig. 4.12C]. No circadian rhythm of *col2a1* transcription was also observed following exposure of 3D pellets with PCM to a single episode of 770xg force (60 minutes) ($r^2 = 0.277$, $p = 0.0174$) [Fig. 4.12C]. However, a single episode of 770xg force (60 minutes) induced a significant 1.55-fold increase in *col2a1* mRNA transcripts at T24-hours when compared to control pellets with PCM ($p = 0.0294$) [Fig. 4.12D].

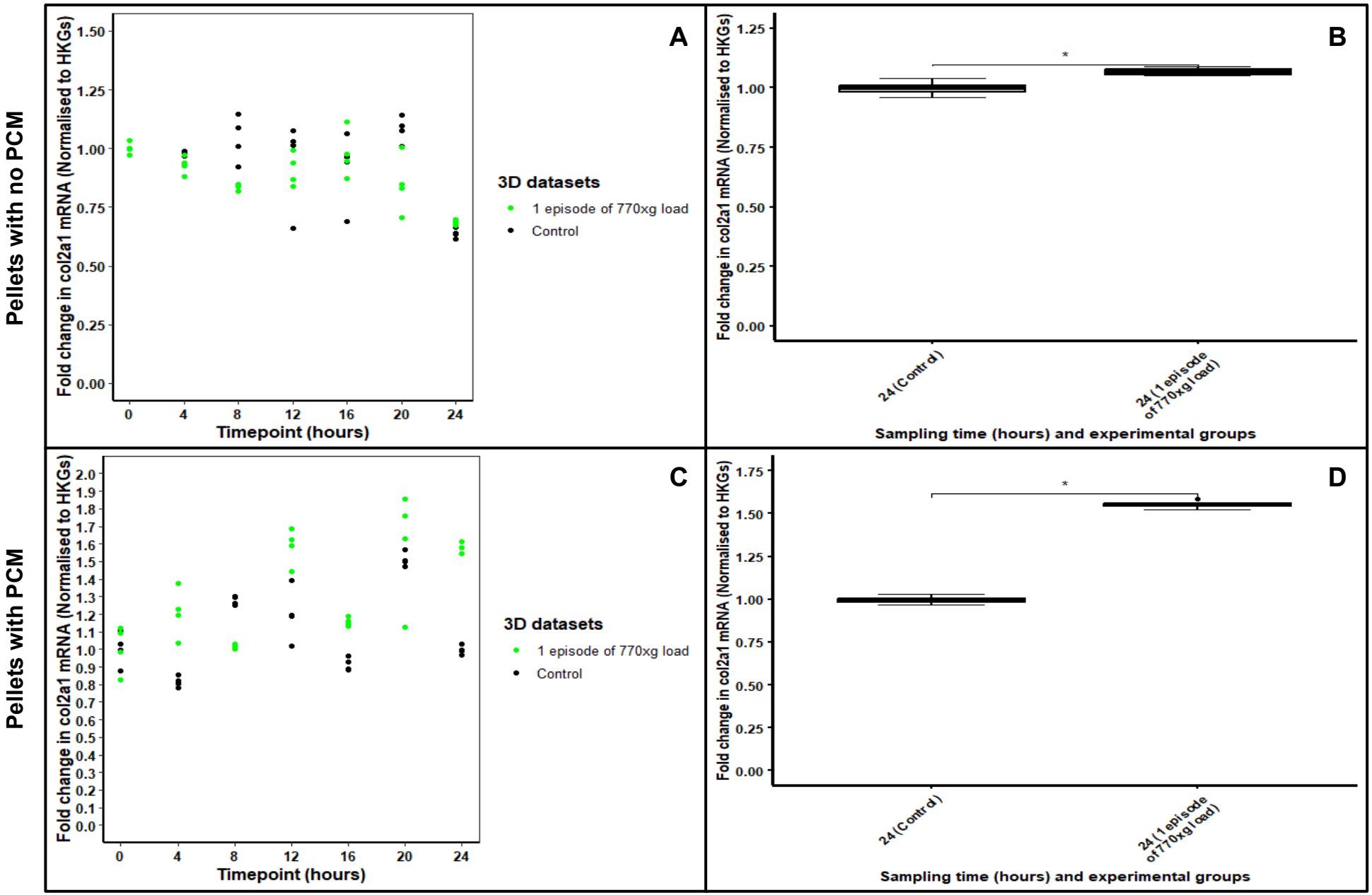
Pellets with no PCM
Pellets with PCM
A
B
C
D
Fold change in col2a1 mRNA (Normalised to HKGs)
Timepoint (hours)
3D datasets
1 episode of 770xg load
Control
Sampling time (hours) and experimental groups
24 (Contrd)
24 (1 episode of 770xg load)
*

**Figure 4.12. Effect of a single episode of 770xg force (60 minutes) on *col2a1* transcription in 3D chondrocyte pellets with and without PCM within one LD cycle.** Data illustrates fold changes in *col2a1* mRNA transcripts (normalised to *18s* and *hprt*) (n = 4, N = 1) plotted against either time of collection (4-hour interval) of control 3D pellets and those exposed to one episode of 770xg force for 60 minutes or measurements only at T24 hours in the absence or presence of PCM. The illustration shows the following: **A)** circadian time series quantification of *col2a1* mRNA transcripts in pellets with no PCM within a 24-hour period, **B)** *col2a1* mRNA transcripts measured at T24 hours in pellets with no PCM, **C)** circadian time series quantification of *col2a1* mRNA transcripts in pellets with PCM and **D)** *col2a1* mRNA transcripts measured at T24 hours in pellets with PCM. Black dots; control datasets, green dots; 1 episode of 770xg load datasets. The absence of cosinusoidal waves indicates arrhythmic expression of this anabolism marker gene determined by the CircWaveBatch software ($R^2 < 0.8$, or $p>0.5$). Box and whisker plots represent average fold changes in *col2a1* mRNA levels ± SD (n = 4, N = 1); statistical significance was assessed between control and 770xg loaded cultures within a 24-hour period using a Wilcoxon rank sum test (* $p<0.05$, ns = no significance).

#### 4.3.3.4.3. Application of one episode of 770xg force for 60 minutes had no effect circadian rhythm of *adamts-4* transcription, with mRNA levels unaltered at T24 hours in pellets with no PCM, but upregulated at T24 hours in pellets with PCM

Control chondrocyte pellets with no PCM revealed circadian rhythm of the catabolism marker *adamts-4* in the first LD cycle ($r^2 = 0.802$, $p = 0.0001$), as characterised by an amplitude of 0.434, a 25-hour period and a peak around ZT6 hours [Fig. 4.13A]. Following application of a single episode of mechanical load (60 minutes of 770xg force) to pellets with no PCM, rhythmic expression of *adamts-4* mRNA was maintained ($r^2 = 0.883$, $p = 0.0001$) as characterised by the following: amplitude; 0.350, period; 24 hours, and peak around ZT7 hours [Fig. 4.13A]. However, no statistical analyses were performed for differences in amplitude, period, and phase of *adamts-4* mRNA circadian rhythm between the control and loaded (1 episode of 770xg load) cultures as there were insufficient datasets to analyse (N = 1). Analysis of *adamts-4* mRNA levels 24 hours following cessation of a single episode of 770xg force (60 minutes) revealed no significant changes relative to control 3D pellets with no PCM [Fig. 4.13B].

However, no circadian pattern in the expression of *adamts-4* mRNA was observed in control 3D pellets with PCM ($r^2 = 0.349$, $p = 0.0047$) [Fig. 4.13C] and those subjected to an episode of 770xg force for 60 minutes within a 24-hour period ($r^2 = 0.389$, $p = 0.0021$) [Fig. 4.13C]. However, analyses of *adamts-4* mRNA transcripts at T24 hours revealed a significant 2.39-fold increase following application of a single episode of 770xg force (60 minutes) to pellets with PCM ($p = 0.0294$) [Fig. 4.13D].

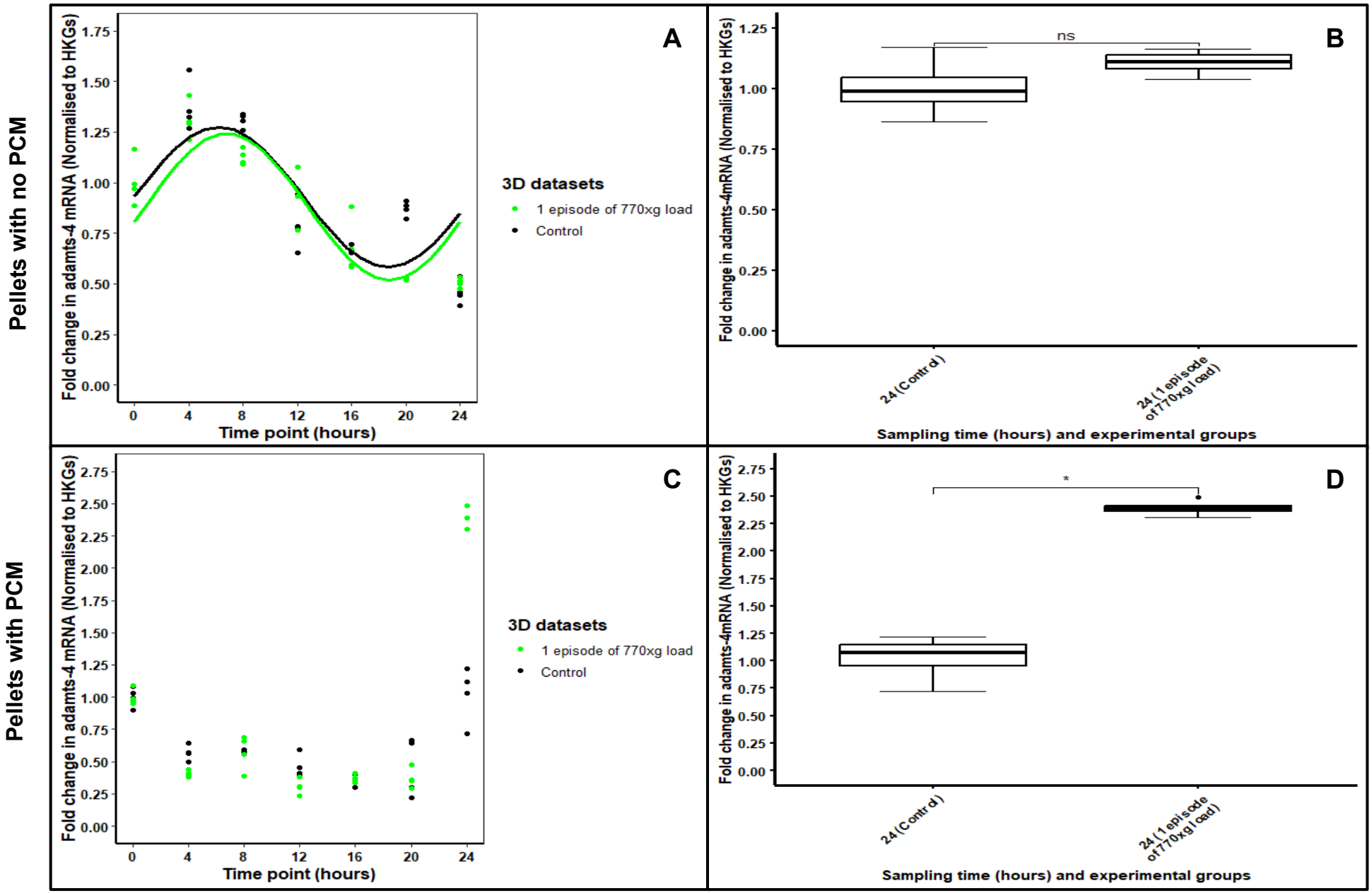
Pellets with no PCM
Pellets with PCM
A
B
C
D
Fold change in adamts-4 mRNA (Normalised to HKGs)
Time point (hours)
3D datasets
1 episode of 770xg load
Control
ns
*
24 (Contrd)
24 (1 episode of 770xg load)
Sampling time (hours) and experimental groups

**Figure 4.13. Effect of a single episode of 770xg force (60 minutes) on *adamts-4* transcription in 3D chondrocyte pellets with and without PCM within one LD cycle.** Data illustrates fold changes in *adamts-4* mRNA transcripts (normalised to *18s* and *hprt*) (n = 4, N = 1) plotted against either time of collection (4-hour interval) of control 3D pellets [black dots] and those exposed to one episode of 770xg force for 60 minutes [green dots] or measurements only at T24 hours in the absence or presence of PCM. The illustration shows the following: **A)** circadian time series quantification of *adamts-4* mRNA transcripts in pellets with no PCM within a 24-hour period, **B)** *adamts-4* mRNA transcripts measured at T24 hours in pellets with no PCM, **C)** circadian time series quantification of *adamts-4* mRNA transcripts in pellets with PCM and **D)** *adamts-4* mRNA transcripts measured at T24 hours in pellets with PCM. The fitted cosinusoidal waves (black and green curves, represent control and 1 episode of 770xg load datasets, respectively) indicate rhythmic oscillations of *adamts-4* mRNA transcripts in pellets with no PCM determined by the CircWaveBatch software ($R^2 > 0.8$, $p < 0.05$) and graphically plotted in the R software using the ggplot2 package (n = 4, N = 1). The absence of cosinusoidal waves indicates arrhythmic expression of this anabolism marker gene in pellets with no PCM determined by the CircWaveBatch software ($R^2 < 0.8$, or $p>0.5$). Box and whisker plots represent average fold changes in *adamts-4* mRNA levels ± SD (n = 4, N = 1); statistical significance was assessed between control and 770xg loaded cultures within a 24-hour period using a Wilcoxon rank sum test (* $p<0.05$, ns = no significance).

#### 4.3.3.5. The presence of PCM had no discernible effect on the mechano-regulation of chondrocyte circadian clocks following application of a single episode of mechanical load

In general, chapter 4 data demonstrates no effect of a single episode of 770xg force on circadian rhythms of clock gene transcription in both the 3D pellets without [Figs. 4.8A and C; Fig. 4.9] and with PCM [Figs. 4.8B and D; Figs. 4.10A and B] as only a transient disruption of *clock* rhythmic transcription was observed following application of mechanical load to pellets with no PCM [Fig. 4.9]. This suggests a potential short-lived mechano-regulation of circadian clocks in the absence of PCM, while other data suggests that the presence of PCM in pellets did not enhance the mechano-regulation of circadian clocks in chondrocytes; this is unexpected since previous studies have demonstrated the importance of PCM in the transduction of mechanical force to cells. Taken together, data informed the decision to select only the pellets with no PCM for utilisation in chapter 5 investigations aimed at determining whether application of 770xg force (60 minutes) either once daily for 3-days, twice daily for 1-day or twice daily for 2-days will reset disrupted circadian rhythms of clock genes in a 3D *in vitro* inflammatory OA model induced through 24-hour exposure of 3D pellets to the proinflammatory cytokine IL-1 in combination with OSM.

## 4.4. Discussion

The work in this chapter has characterised bovine circadian clocks at a transcriptional level (using qPCR) in control 3D chondrocyte pellet cultures derived from cartilage harvested from skeletally immature calves' legs. Analysis of sGAG release using the DMMB assay demonstrated significant increases at 24-hour intervals within a 72-hour period in both the control 3D chondrocyte pellet cultures with and without PCM. Control 3D chondrocyte pellets with and without PCM also demonstrated either undetectable levels or maintained low concentrations of nitrite/NO (~1 μM) within a 72-hour window suggestive of no inflammation. Circadian expression of clock genes (*bmal1*, *clock*, *cry1, npas2*, *nr1d1*, *per1* and *per2*) as well as a gene marker of ECM catabolism (*adamts-4* but not *adamts-5*, *mmp-3* and *mmp-13*) but not ECM anabolic genes (*acan* and *col2a1*) was observed in at least one LD cycle within a 72-hour period in control 3D chondrocyte pellets whilst control pellets with PCM demonstrated rhythmic expression of *bmal1*, *dbp* and *per2* but not *cry1* mRNAs in at least two LD cycles within a 72-hour window Using the 3D models characterised in chapter 3 (absence or presence of PCM), application of a single episode of mechanical load (60 minutes of 770xg force) induced no significant alterations, when compared to control cells in: (i) sGAG release at 24-hour intervals within a 72-hour window, (ii) nitrite/NO release at 24-hour intervals within a 72-hour window or (iii) chondrocyte circadian clocks within a 72-hour window. In pellets with no PCM, mechanical loading appeared to transiently disrupt *clock* mRNA circadian oscillations only in the first LD cycle before recovery in the second and third LD cycles with rhythm parameters comparable to those of control cultures with no PCM. Moreover, rhythmic expression of *adamts-4* but not *acan* and *col2a1* mRNAs were observed within a 24-hour period following exposure of 3D pellets with no PCM to a single episode of 770xg force; it suggests this loading regime does not impact rhythmicity of an ECM catabolism marker *adamts-4* and that ECM anabolism gene markers *acan* and *col2a1* are not under circadian control in pellets with no PCM in the absence or presence of a single loading episode.

In 3D pellets with PCM, a single episode of 770xg force (60 minutes) did not change circadian rhythmicity of *bmal1* and *per2* transcription within a 72-hour period, suggesting this loading regimen does not impact chondrocyte circadian clocks; thus, corroborating the findings of the 3D model in which pellets had no PCM. Additionally, no circadian expression of ECM anabolism gene markers (*acan* and *col2a1* hence corroborating the findings of the 3D model in which pellets had no PCM) and a catabolism marker (*adamts-4*) was observed within a 24-hour period in both the control pellets with PCM and those subjected to a single episode of 770xg force (60 minutes) indicating that these genes are arrhythmic following extended *ex vivo* culture and that this centrifugal loading regime is incapable of inducing their rhythmic expression. Taken together, data also suggests that *adamts-4* mRNA rhythmicity had most likely been lost during the PCM deposition period (9 days of *ex vivo* culture) since analysis of *adamts-4* mRNA within a 24-hour period revealed circadian rhythmicity of this ECM catabolism marker in pellets with no PCM (section 4.3.3.4.3). Moreover, this chapter showed that a single episode of 770xg force (60 minutes) is incapable of inducing a resurgence (reset) in the circadian expression of this catabolism marker following its potential dampening.

### 4.4.1. Immature bovine chondrocytes possess self-sustained circadian clocks eliciting rhythmic expression of clock genes

Control 3D chondrocyte cultures demonstrated reproducible baseline circadian rhythmicity for mRNA transcripts of *bmal1* and *clock,* in two independent experiments as well as *npas2*, *nr1d1*, *per1* and *per2* in one independent experiment suggesting the existence of *in vitro* functional circadian clocks in control immature bovine primary chondrocytes (without PCM) which regulates the rhythmicity of these clock genes. Moreover, circadian regulation of clock genes' transcription was observed for *bmal1*, *dbp* and *per2* in control 3D chondrocytes pellets with PCM in at least 2 LD cycles within a 72-hour window, indicative of functionality of bovine circadian clocks following an extended *ex vivo* culture (up to day 12).

The baseline circadian pattern in clock gene expression observed in this thesis might be attributed to the use of insulin-containing standard culture media (insulin transferrin selenium (ITS)); previous studies revealed that insulin can reset circadian clocks by altering the amplitude and phase of circadian rhythms through the induction of period proteins (i.e., translational regulation) in *in vitro* cultured per2::luc murine primary

fibroblasts, *ex vivo* cultured organotypic liver, kidney slices and intestinal organoids derived from adult per2::luc mice and *in vivo* following the injection of insulin into per2::luc mice (Crosby et al. 2019). However, no significant changes in per2::luc activity was observed in organotypic SCN slices following insulin application suggesting that this model of feeding-fasting rhythm effectively decouples peripheral clocks from the SCN clock (Crosby et al. 2019). Mechanistically, the introduction of insulin to mimic feeding-induced insulin increase triggers enhanced signalling through phosphatidylinositol 3,4,5-trisphosphate ($PIP_3$), mechanistic target of rapamycin complex 1 (mTORC1) pathway and microRNA (miRNA) downregulation resulting in the rapid induction of per translation which is also sustained through increased *per* mRNA transcripts (Crosby et al. 2019). Likewise, insulin was demonstrated to increase *PER2* mRNA and protein levels in human stem cell–derived adipocytes, mouse 3T3-L1 cells, and adipose tissue explants from per2::luc mice resulting in a phase shift of circadian oscillations suggestive of the insulin-induced regulation of circadian clocks both *in vitro* and *ex vivo* (Tuvia et al. 2021). In a human *in vitro* study, phase shifting and increases in the amplitude of oscillations in *PER2-LUC* activity was observed in scalp root hair cell cultures following the introduction of insulin into cultures (Kajimoto et al. 2018). These clock responses were reproduced in an *in vitro* murine study in which insulin was introduced to whisker follicle cells of per2::luc mice (Kajimoto et al. 2018). Collectively, this data demonstrated the potency of insulin in resetting human and murine circadian clocks. Moreover, using microfluidic technology in an *in vitro* study, exposure of per2::luc mice fibroblasts to insulin at differing time windows reset their circadian clocks indicative of the ability of feeding-induced insulin increase to entrain murine peripheral clocks (Gagliano et al. 2021). Importantly, previous studies have demonstrated the circadian nature in the secretion of insulin by human (Boden et al. 1996; Saini et al. 2016) and rat (La Fleur et al. 1999) pancreatic islet cells; thus, insulin signalling might be another way in which various peripheral clocks are entrained (Chan et al. 2022).The baseline circadian rhythmicity of clock gene transcription observed in this chapter agree with the findings from Gossan et al. (2013) who demonstrated the existence of molecular circadian clocks in healthy (i.e., untreated and non-osteoarthritic) human chondrocyte cell line and mouse cartilage which regulated rhythmic circadian oscillations in *bmal1*, *cry1*, *dbp*, *nfil3*, *npas2*, *nr1d1/2*, *per2* and *rorα* mRNA expression within a 48-hour period (Gossan et al. 2013). Moreover, the circadian rhythmicity of *cry1* and *per2* mRNA transcripts observed in this chapter are also consistent with the findings reported by Guo et al. (2015) who evidenced robust circadian fluctuation in *cry1*-luc and per2::luc expression in *ex vivo* cultured cartilage explants obtained from untreated/non-osteoarthritic

femoral heads and xiphoid processes of transgenic clock reporter mice (Guo et al. 2015). Furthermore, baseline circadian rhythm of *per2* transcription observed in this chapter corroborates the findings of Dudek et al. (2016) who demonstrated circadian rhythmicity in per2::luc bioluminescence recordings in healthy femoral head wild-type mouse knee cartilage as compared to their *col2a1 bmal1*$^{-/-}$ littermates hence evidencing the *ex vivo* functionality of circadian clocks in healthy murine cartilage. Dudek et al. (2016) further demonstrated that the bmal1/clock complex controls endogenous circadian rhythms in murine and human chondrocytes hence regulating cartilage homeostasis and integrity (Dudek et al. 2016).

Additionally, circadian rhythm of *bmal1* and *nr1d1* transcription findings observed in control chondrocyte pellets in this chapter also agrees with the outcomes reported in a study where mRNA levels for *BMAL1* and *NR1D1* were observed to be rhythmically expressed in healthy (i.e., untreated and non-osteoarthritic) human chondrocytes within a 48-hour period indicative of the *ex vivo* functionality of circadian clocks in human cartilage (Akagi et al. 2017). The observation of reproducible baseline circadian oscillations in *cry1* mRNA transcripts in this chapter corroborates the findings of Bekki et al. (2020) who demonstrated circadian rhythmicity of *CRY-1* and *CRY-2* mRNA transcripts in healthy (non-osteoarthritic) human femoral head chondrocytes within a 46-hour period therefore verifying the existence of autonomous circadian clocks in human cartilage (Bekki et al. 2020). The revelation of circadian rhythm in *per2* transcription by this chapter also corroborates the findings from a study in which circadian rhythm of per2::luc activity was observed in control mouse femoral head cartilage explants hence confirming the existence of *ex vivo* functional circadian clocks in murine cartilage (Pferdehirt et al. 2022). The *per2* rhythmicity data in this chapter also agrees with the observation of a circadian pattern in *per2* expression in porcine knee primary articular chondrocytes (embedded in agarose) transduced with a per2-luciferase lentivirus indicative of the existence of self-sustained circadian clocks in porcine cartilage cultured *ex vivo* (Pferdehirt et al. 2022). Furthermore, this chapter data is also consistent with the findings of a human study in which circadian expression of clock genes including *BMAL1*, *CLOCK*, *CRY1*, *CRY2*, *PER1* and *PER2* was observed within a 24-hour period in healthy unstimulated (control) tibial plateau chondrocytes hence verifying the presence of self-sustained circadian clocks in human cartilage (Snelling et al. 2016).

### 4.4.2. Immature bovine chondrocytes exhibited differential regulation in the transcription of gene markers for cartilage ECM metabolism

The work in this chapter demonstrated no circadian rhythm in the transcription of ECM anabolism markers *acan* and *col2a1* within a 24-hour period, and ECM catabolism markers, *adamts-5*, *mmp-3* and *mmp-13* within 3 LD cycles in control 3D pellets with no PCM suggesting that chondrocyte circadian clocks have no control on the expression of these cartilage ECM genes in this 3D model. Likewise, no circadian expression of *acan*, *col2a1* and *adamts-4* mRNAs was observed in control 3D pellets with PCM. The observed lack of *acan* mRNA circadian rhythm in this chapter (in both the absence and presence of PCM) contradicts the findings of a study in which *ACAN* transcription was demonstrated to exhibit circadian rhythmicity within a 24-hour period in healthy human knee chondrocyte monolayer cultures (Snelling et al. 2016). However, the lack of *col2a1* circadian rhythm observed in this study corroborates the findings of Snelling et al. (2016) who revealed a lack of circadian rhythm of *COL2A1* transcription in healthy human knee chondrocyte monolayer cultures (Snelling et al. 2016). However, both the arrhythmic expression of *acan* and *col2a1* mRNA observed in this chapter disagrees with the findings of a previous study in which circadian rhythm of *acan* and *col2a1* transcription were observed (shown to oscillate at the same phase as they both peaked at ZT2 under both the LD and dark-dark (DD) conditions) in rat growth plate cartilage, hence suggesting that these gene markers for ECM anabolic activities are under circadian regulation (Honda et al. 2013). Moreover, this experimental chapter demonstrated no circadian expression of *sox9* transcription within a 72-hour period suggesting that this chondrocyte phenotype gene marker is not under the control of circadian clocks. This is inconsistent with the findings of Honda et al. (2013) who reported circadian expression of *sox9* mRNA expression in unstimulated (control) rat rib growth plate cartilage within a 24-hour period peaking at ZT2 under the LD condition and at ZT6 under the DD condition indicative of a phase shift in *sox9* transcription following changes between the LD and DD conditions (Honda et al. 2013).

Nonetheless, interspecies variation (bovine vs murine vs human) and differing types and anatomical locations of utilised cartilage which clearly experience divergent biomechanical conditions *in vivo* (i.e., metacarpophalangeal articular cartilage vs rib growth plate cartilage vs knee articular cartilage, respectively) might account for some of the discrepancies observed between this chapter findings and those reported by Honda et al. (2013) and Snelling et al. (2016). Additionally, the use of 2D versus 3D pellets with and without PCM might explain the inconsistency of findings between Snelling et al. (2016) and this thesis.

The work in this chapter also revealed no circadian rhythm of *adamts-4* transcription in control 3D pellets within a 72-hour window of investigation, yet circadian oscillations in mRNA transcripts of this catabolic gene but not *acan* and *col2a1* were observed within a 24-hour period in both the control and mechanically loaded (single episode of 770xg force [60 minutes]) 3D chondrocyte pellets with no PCM in an independent experiment; this is suggestive that chondrocyte circadian clocks regulate *adamts-4* expression, but that a single episode of 770xg load does not influence the rhythmicity of these other genes in bovine cartilage. However, *adamts-4* data reported here was obtained from two independent experiment with unequal timeframes of analyses (72- versus 24-hours) indicative of divergent cell responses and the lack of reproducibility of *adamts-4* rhythmicity data in this chapter. Circadian expression of *adamts-4* within a 24-hour period in this chapter corroborate the findings of a previous study in which circadian expression of *adamts-4* mRNA amongst other catabolism markers (not assessed in this chapter) was observed in control mouse xiphoid and growth plate cartilage indicative of the circadian regulation of this cartilage ECM catabolism marker (Gossan et al. 2013).

However, the lack of circadian rhythm in *adamts-4* transcription in control 3D pellets with no PCM within a 72-hour period and its' lack of rhythmicity within a 24-hour period in control pellets with PCM disagrees with the finding of Gossan et al. (2013); this disparity might clearly be attributed to differing timeframes of transcripts analysis as this chapter assessed rhythmicity either within a 72-hour period or in 3D chondrocyte pellets cultured for up to 10 days whilst Gossan et al. (2013) analysed transcripts within a 40-hour period. Furthermore, the utilisation of differing model systems namely, 3D chondrocyte pellets versus cartilage explants might also account for the disagreement between this chapter and the other study. Nonetheless, the loss of *adamts-4* rhythmicity in pellets with PCM might suggest the dampening of circadian rhythm of this gene marker of catabolic activities following extended *ex vivo* culture as previous data in this thesis demonstrated the circadian regulation of this gene in 3D chondrocyte pellets with no PCM cultured over a shorter timeframe, i.e., up to ~4 days (sections 4.3.3.4.3). The loss of *adamts-4* rhythmicity in control 3D cultures following extended *ex vivo* cultivation is possibly a consequence of the lack of entrainment cues in an *in vitro* microenvironment resulting in a gradual dampening of oscillations until complete loss of circadian control of this catabolic clock-controlled gene. Additionally, data also suggests the insufficiency of a single episode of 770xg force to synchronise circadian clocks and reset *adamts-4*'s lost circadian rhythm following its potential dampening during extended *ex vivo* culture. Moreover, the utilised loading regime did not induce circadian expression of *acan* and *col2a1* mRNAs in both the

pellets with and without PCM suggesting its lack of clock synchronisation. With this, it could be hypothesised that the utilised mechanical loading regime does not synchronise dampened circadian rhythmicity of a catabolism marker gene (*adamts-4*); therefore, cells might have eventually lost temporal regulation of cartilage remodelling which may subsequently promote cartilage degeneration in which catabolic pathways dominate over biosynthesis hence potentially leading to OA development.

### 4.4.3. A single episode of 770xg force on 3D chondrocyte pellets with no PCM did not impact circadian rhythm of *bmal1* and *cry1* mRNA, but transiently disrupted *clock* mRNA rhythms in the first LD cycle only, whilst no discernible effects were observed in circadian rhythm of *bmal1* and *per2* in pellets with PCM

In this chapter, control 3D pellets with no PCM demonstrated circadian regulation of clock gene transcription including: *bmal1*, *clock*, *cry1*, *npas2*, *nr1d1*, *nr1d2*, *per1* and *per2* indicative of the presence of autonomous circadian clocks in immature bovine articular chondrocytes. Furthermore, application of a single episode of 770xg force (60 minutes) to this model system had no effect on circadian rhythm of *bmal1* and *clock* transcription in two consecutive LD cycles (between T24- and T72-hours), suggesting no impact of this loading regime on circadian clocks. Nevertheless, possibly a novel finding, a trend implying an initial loss of *clock* circadian rhythms (i.e. only in the first LD cycle) was observed suggesting that a single episode of mechanical loading (60 minutes of 770xg force) might have disrupted circadian clocks in the employed 3D model; specifically targeting this component of the positive arm of the core clock feedback loop (transcriptional activator), the rhythm of *bmal1* (a heterodimeric partner of *clock* was arrhythmic in both the controls and loaded pellets in the first LD cycle) and *cry1* mRNA expression (transcriptional repressor which was rhythmic between T0- and T48-hours) was unaffected in an equivalent timeframe. Nonetheless, repeat experiments are necessary to validate the observed cell behaviours. Likewise, 3D chondrocyte pellets with PCM exhibited circadian expression of *bmal1* and *per2* mRNAs in control cultures and following application of a single episode of 770xg force (60 minutes) with no significant alterations in amplitude, period and phase. However, circadian rhythmicity of *dbp* transcription following application of load appeared to mirror that for controls although no statistical analyses were performed to confirm that its rhythm was not significantly altered. Overall, this data suggests that this 770xg centrifugal regimen had no discernible effect on chondrocyte circadian clocks in these pellets with a predicted substantial PCM deposition. This informed the decision to select 3D pellets with no PCM for employment in chapter 5

investigations aimed at assessing the impact of applying 770xg force for 60 minutes either once daily for 3-days, twice daily for 1-day or twice daily for 2-days on disrupted circadian rhythms (induced through exposure to the proinflammatory cytokine IL-1α in combination with OSM) in an inflammatory OA model.

Unaltered circadian rhythmicity in the transcription of the above-mentioned clock genes as observed in both pellets with and without PCM contradicts the findings of a previous study in which an ~8 phase advancement was observed in mice femoral head cartilage and intervertebral disc explants (but not SCN tissue) following mechanical loading, hence indicating the alteration of circadian rhythm post physiological loading and the capability of physical exercise to decouple the skeletal clocks and the central SCN clock (Dudek et al. 2023). Furthermore, they demonstrated that 0.5 MPa cyclical compressive force (1 hour, 1Hz) induced a significant increase in the amplitude of per2::luc circadian rhythm which persisted for three or more days in an *ex vivo* per2::luc tissue explant culture model (Dudek et al. 2023) hence further disagreeing with the findings of this chapter. Moreover, Dudek et al. (2023) also reported the disruption of circadian rhythm when compressive forces were applied at the trough of *per2* rhythm, whereas loading at the start of mice's active phases induced the most robust clock responses, hence emphasising that circadian phase is vital in the modulation of clock response to load (Dudek et al. 2023). Mechanistically, a transcriptome-wide analysis revealed that the *in vivo* load-induced clock changes involve the PLD2-mTORC2-AKT-GSK3β pathway (Dudek et al. 2023). The outcomes of this chapter (no changes in rhythms of circadian clock genes) also disagrees with the findings of Heywood et al. (2022) who revealed that daily 12-hour bouts of 10% cyclic biaxial tensile strain (0.33 Hz, 3 days period) synchronised bovine chondrocyte (metacarpophalangeal cartilage; 18-24 months old) circadian rhythmicity of bmal1 protein expression aligning it to diurnal mechanical stimulation, and that a 6-hour phase shift in daily 12-hour bouts of 10% cyclic biaxial tensile strain resulted in an equivalent shift of the chondrocyte circadian clockwork (Heywood et al. 2022). Taken together, data from this chapter and the findings of Heywood et al. (2022) indicates circadian regulation of the core clock gene, *bmal1* at both the mRNA and protein levels in bovine cartilage. Also inconsistent with the findings of this chapter was the downregulation of *clock* mRNA transcripts following application of 5% cyclical tensile strain to newborn mice rib chondrocytes in a 3D sponge model within a 4-day period (1 Hz, 15 minutes/hour) (Kanbe et al. 2006). The discrepancies between the finding of this chapter and those of previous publications might be attributed to differing types of mechanical loads exposed to the

respective models as well as variations in the mode (constant compression, shear forces and hydrostatic pressure versus cyclical tensile strain) and durations of loading. Moreover, interspecies variation might also account for discrepancies between the findings of this chapter and those for Dudek et al. (2023) and Kanbe et al. (2006); whereas cartilage maturation might account for disagreement with the findings of Heywood et al. (2022) who utilised skeletally mature bovine chondrocytes as compared to the use of skeletally immature bovine chondrocytes in this PhD project. Furthermore, the disagreement between the findings of this chapter and those from previous publications might be attributed to the differing times of stimulus application within the circadian cycle since Dudek et al. (2023) demonstrated divergent clock responses depending on whether mechanical load was applied at the peak or trough of *per2* expression. Moreover, the use of *in vitro* versus *in vivo* models, and cartilage explants versus 3D pellet model (with or without PCM) might also account for the disagreement between this chapter findings and those of other studies. Additionally, Dudek et al. (2023) measured circadian clock dynamics by real-time recording of per2::luc reporter activity which is more sensitive than 4-hour circadian time series qPCR quantification of clock gene mRNAs employed in this thesis which might explain the inconsistencies in load-induced circadian clock responses between the two studies.

The inadequacy of a single episode of 770xg force (60 minutes) to affect chondrocyte circadian clocks in 3D pellets in this chapter might suggest that this centrifugation regimen was not within a physiological range (defined in chapter 1 for each type of mechanical force, i.e., sections 1.2.1.1 [~10-20% dynamic compressive stress, 0.5 hours or more], 1.2.1.2 [3-10% cyclical tensile strain, 0.17 -0.5 Hz, 2 -12 hours], 1.2.1.3 [~5-10 MPa dynamic hydrostatic/osmotic pressure, 2 hours - 2 weeks], and 1.2.1.4 [1-3% dynamic shear stress, 0.01 - 1 Hz]), or either the centrifugal force magnitude or duration were insufficient to trigger clock responses. Although the reproducibility of some of the findings of this chapter were not validated in repeat experiments, the disagreement with previous literature clearly warrants further optimisation of a physiological centrifugal loading regimen intertwining an optimal magnitude, frequency and duration of centrifugation to elicit anabolic and clock responses in cartilage chondrocytes. Notwithstanding, it is imperative to repeat experiments entailing the application of a single episode of 770xg force (60 minutes) to 3D pellet cultures (either with or without PCM) before time series quantification of clock gene expression to assess the reproducibility of novel findings established in this chapter prior to the evaluation of consistency or disagreement with

results from previous studies. Also inconsistent with the observation of no effects of a single episode of 770xg force (60 minutes) on the amplitude, period and phase of clock gene circadian expression in 3D chondrocyte cultures in this chapter are the findings of previous studies which reported the mechano-regulation of circadian clocks in various musculoskeletal cells/tissues including bone (Bouchard et al. 2022), intervertebral disc (Ding et al. 2021), muscle (Bae et al. 2006; Saracino et al. 2019; Sasaki et al. 2016; Vanmunster et al. 2022; Wang et al. 2021; Wolff & Esser 2012; Yamanaka et al. 2008), and periodontal ligament (Qin et al. 2019) [reviewed in Dintwa et al. 2023].

### 4.4.4. Summary

- Application of a single episode of 770xg force (60 minutes) to 3D pellets with or without PCM induced no significant changes in sGAG and nitrite/NO release when compared to controls within a 72-hour period
- *hprt* and *18s* were identified as the two most suitable reference genes for qPCR normalisation as they were not altered within a 72-hour period, and immature articular chondrocytes were shown to possess autonomous circadian clocks evidenced by rhythmic expression of clock genes (*bmal1*, *clock, npas2*, *nr1d1*, *per1* and *per2*) in control 3D chondrocyte pellets, either with or without PCM, within 3 LD cycles
- *clock* mRNAs were not expressed in a rhythmic manner between T0- and T24-hours following load application to 3D pellets with no PCM suggestive of a transient impact of one episode of mechanical load on this transcriptional activator. However, circadian expression of *bmal1* and *clock* genes was not affected between T24- and T72-hours as both control and loaded cultures revealed comparable circadian rhythmicity, suggesting no impact of this loading regime on circadian clocks in pellets with no PCM
- A single episode of mechanical load (770xg force, 60 minutes) did not alter circadian rhythms of *bmal1* and *per2* transcription in 3D pellet cultures with PCM within a 72-hour window suggesting its lack of impact on circadian clocks in pellets with PCM
- 3D pellets with no PCM were selected for utilisation in chapter 5 investigation since the presence of PCM did not induce discernible clock responses to one episode of 770xg force (60 minutes)

# Chapter 5

## Characterisation of the responses of a 3D pellet culture system to proinflammatory cytokine stimulation and evaluation of the responses of a 3D inflammatory OA model system to differing mechanical loading regimens (simulated through centrifugation)

## 5.1 Introduction

### 5.1.1. Catabolic cytokines disrupt circadian clocks in cartilage

Following the discovery of self-sustained circadian clocks in cartilage tissues or *in vitro* cultured chondrocytes (section 1.3.2), previous studies further demonstrated the capacity of catabolic cytokines to disrupt these clocks resulting in the loss of circadian rhythm. Abolished *cry1*-luc activity was observed in mice xiphoid cartilage explants subjected to 5 ng/ml interleukin-1 beta (IL-1β), indicative of the disruption of intrinsic circadian clocks in resident chondrocytes (Guo et al. 2015). In addition to the dampening of *cry1*-luc circadian oscillations, IL-1β dysregulated the expression of endogenous clock genes such as *dbp*, *nfil3*, *nr1d1*, *per1* and *per2*, as well as clock-controlled catabolic pathways including *adamts-4*, *mmp-13* and *mmp-14*, as well as an inhibitor of metalloproteinases *timp4*. Mechanistically, the IL-1β mediated cartilage clock responses implicate the involvement of the NFκB signalling pathway, partly through its interference with the transcriptional activation role of the CLOCK/BMAL1 complex (Guo et al. 2015). The involvement of NFκB signalling in IL-1β mediated disruption of circadian rhythms was verified in primary human knee chondrocytes exposed to 10 ng/ml IL-1β which resulted in increased phosphorylation of the NF-κB p65 subunit (Alhilali et al. 2021). Another recent study which supports these findings demonstrated that administration of either 1 ng/ml IL-1 alpha (α) or 1 ng/ml IL-1β to murine femoral head cartilage explants disrupted *per2* rhythmicity (Pferdehirt et al. 2022). IL-1β-treated (1 ng/ml) cartilage tissue engineered from murine induced pluripotent stem cells (miPSCs) resulted in the lengthening of the period of *per2* circadian oscillations, whilst treatment with 1 ng/ml IL-1α resulted in a rapid loss in *per2* circadian rhythm and a reduction in bioluminescence amplitude (Pferdehirt et al. 2022); this suggests that inflammatory cytokines can disrupt circadian clocks in native and tissue engineered cartilage. More importantly, 5 ng/ml IL-1α in combination with 10ng/ml oncostatin M (OSM) have previously been reported to act synergistically to induce an inflammatory OA phenotype in primary bovine chondrocytes (Barksby et al. 2006) therefore informing the decision to select these two cytokines for utilisation in this PhD project.

### 5.1.2. External cues synchronise peripheral clocks in various tissues including cartilage

Peripheral circadian clocks in differing mammalian tissues are normally synchronised *in vitro* using external cues such as serum shock, temperature fluctuation, application of

forskolin and Dex exposure before circadian time series analysis of rhythmicity based on the rationale of designed experiments (Balsalobre et al. 1998; Buhr et al. 2010; Gossan et al. 2013; Guo et al. 2015; Perelis et al. 2015; Powell et al. 2022; Woo et al. 2010). Rat-1 fibroblasts and H35 hepatoma cells supplemented with 5% FBS in their standard culture media were exposed to 50% horse serum for 2 hours (serum shock) resulting in the synchronisation of circadian clock as evidenced by circadian expression of *per1*, *per2*, *dbp* and *tef* mRNAs within a 72-hour period (Balsalobre et al. 1998). Likewise, introduction of a 1-hour pulse of 50% FBS to primary human airway epithelial cells (AECs) induced circadian expression of *ARNTL*, *NR1D1* and *NR1D2* mRNA within a 48-hour period (Powell et al. 2022); this corroborates the clock synchronisation capacity of serum shock *in vitro*. Moreover, circadian oscillations in mRNA transcripts for *ARNTL*, *CRY1*, *CRY2*, *NR1D1*, *NR1D2*, *PER1* and *PER2* were observed within a 48-hour period in human AECs subjected to temperature cycling for 6 days (12 hours at 37°C, 12 hours at 34°C) (Powell et al. 2022). In another *ex vivo* study, pituitary and lung but not SCN tissue explants from per2::luc mice demonstrated circadian oscillations in per:2:luc bioluminescence activity within a 24-hour period following exposure to 12hr:12hr 36°C:38.5°C temperature cycles indicative of the potential of temperature fluctuations to synchronise peripheral circadian clocks in diverse tissues but not the master clock (SCN) (Buhr et al. 2010). Furthermore, a 1-hour pulse of 10 μM forskolin (FSK) (a known clock-synchronizing agent) induced circadian oscillations in per2::luc activity in an *in vitro* model employing murine pancreatic islet cells (Perelis et al. 2015). Likewise, circadian oscillations in *cry1*-luc activity in murine xiphoid cartilage explants was observed following application of 10 μM FSK; however, FSK failed to synchronise IL-1β-induced disruption of *cry1*-luc oscillations (Guo et al. 2015). Additionally, other studies have demonstrated the chondroprotective effects as well as the circadian clock synchronisation potential of Dex in extended *ex vivo* culture dampened/disrupted rhythms using inflammatory OA and post-traumatic OA models, thus making it the most widely used synthetic glucocorticoid (GC) in chronobiology studies (Gossan et al. 2013; Guo et al. 2015; Bajpayee et al. 2016). Dexamethasone (100 nM) was demonstrated to re-synchronise the dampened circadian rhythm of per2::luc mice in xiphoid and femoral head cartilages following extended *in vitro* culture (Gossan et al. 2013). Furthermore, the application of 100 nM Dex to IL-1β (5 ng/ml) treated mouse cartilage reversed their disrupted circadian rhythm resulting in the restoration of the overall level and oscillatory amplitude of the *cry1*-luc circadian rhythm (Guo et al. 2015). Moreover, 1–2-week-old bovine cartilage explants exposed to a single dose of Dex using the AVIDIN conjugation delivery system (AVIDIN-Dex conjugates, resembling targeted

intra-cartilage drug delivery) resulted in the suppression of IL-1α induced sGAG loss over a three-week period, and revealed the restoration of sGAG release with no induction of cytotoxicity (Bajpayee et al. 2016). Taken together, data demonstrates both the capacity of Dex to counteract the catabolic effects of cytokines in cartilage and its ability to synchronise circadian rhythms following cytokine-induced disruption therefore suggesting its suitability for utilisation in this PhD project. Mechanistically, GCs such as Dex exert their action on cell metabolism (e.g., chondrocyte) through glucocorticoid receptor (GR) signalling (Dickmeis and Foulkes 2011; Kassel and Herrlich 2007). GR is a member of the nuclear receptor subfamily residing in the cytoplasm existing as part of a chaperone-containing multiprotein complex in the absence of GC ligands. Upon GC binding, GR translocates to the nucleus where it acts as a transcription factor by homodimerising and binding to glucocorticoid response elements (GREs) in the promoters of target genes such as clock, ECM catabolic and anabolic genes and others (Dickmeis and Foulkes 2011; Kassel and Herrlich 2007). Other glucocorticoid signalling events have also been reported in which ligand-bound GRs interact with other transcription factors that do not involve the binding to GREs before inducing transcription of target genes (Dickmeis and Foulkes 2011; Schoneveld et al. 2004).

### 5.1.3. Mechanical loading and cytokine-induced inflammatory OA

Over the past few decades, various studies have separately characterised the influence of mechanical loading on cartilage turnover (sections 1.2.1 - 1.2.3), the presence of self-sustained circadian clocks in cartilage and its resident cells, chondrocytes (section 1.3.2), and the circadian clock disruption potential of catabolic cytokines (section 5.1.1). Surprisingly, no publications have been identified which demonstrates the resetting of disrupted circadian rhythm through mechanical stimulation in cartilage, a musculoskeletal tissue revealed to exhibit time of day dependent alterations in physiology (section 1.3) and a tissue in which mechanical loading is imperative for function (section 1.2). This prompted the conduction of *ex vivo* 3D pellet culture experiments in efforts to determine whether application of centrifugal force once daily for 3-days, twice daily for 1-day or twice daily for 2-days can reset circadian clocks in chondrocyte cultures exhibiting an inflammatory OA phenotype; in particular because mechanical loading has recently been identified as an authentic time cue in bovine cartilage (Heywood et al. 2022) and murine cartilage and intervertebral disc (IVD) tissues (Dudek et al. 2023).

### 5.1.4. Aims and objectives

The aim of the work presented in this chapter is to develop and characterise an *in vitro* 3D inflammatory OA model system through exposure of 3D chondrocyte pellets to the proinflammatory cytokine IL-1 in combination with OSM before investigating the influence of mechanical loading (mimicked by 60 minutes of 770xg force predicted to expose cells to compression, shear forces, and hydrostatic pressure) on altered circadian rhythm in this model. Initially, this chapter aims to investigate the responses of 3D-primary chondrocyte pellet cultures to stimulation with 5 ng/ml IL-1α in combination with 10 ng/ml OSM within 3 LD cycles to determine (i) how these proinflammatory cytokines influence the cartilage clock, and (ii) whether markers of ECM metabolism are affected (and whether they possess and/or lose rhythmicity following cytokine stimulation). Furthermore, the work of this chapter also sets out to assess the responses of the characterised 3D inflammatory OA model to application of either: (1) dexamethasone in the presence of 5ng/ml IL-1β and 10ng/ml OSM [constantly], (2) 770xg force [60 minutes] once daily for 3-days in the presence of 5ng/ml IL-1β and 10ng/ml OSM, or (3) 770xg force [60 minutes] twice daily for 1- or 2-days following 24-hour exposure to 5 ng/ml IL-1α in combination with 10 ng/ml OSM; to determine (i) whether dexamethasone reverses the inflammatory state and synchronises chondrocyte circadian clocks, (ii) whether differing mechanical loading regimens alters chondrocyte circadian rhythm, and (iii) whether markers of ECM metabolism are affected.

#### 5.1.4.1. Specific chapter objectives

- To evaluate the effect of 5 ng/ml IL-1α in combination with 10 ng/ml OSM on sGAG and NO release, the activity of catabolic enzymes, adamts-4 and mmp-13 (as a measure of activated catabolic pathways), the stability of housekeeping genes, the expression of a chondrocyte phenotype gene marker (*sox9*), gene markers of ECM catabolism (*adamts-4, adamts-5*, *mmp-3* and *mmp-13*), and clock genes (*bmal1*, *nr1d1*, *nr1d2* and *per2*) within a 72-hour period in the 3D model
- To determine the influence of 100 nM dexamethasone on sGAG and nitrite/NO release, the stability of housekeeping genes, the expression of a gene marker of ECM anabolism (*acan*), gene marker of ECM catabolism (*mmp-3*), and clock genes (*bmal1* and *per2*) within a 48-hour period in a 3D inflammatory OA model (induced

by 24-hour exposure to 5ng/ml IL-1β in combination with 10ng/ml OSM kept in culture throughout the experiment)

- To evaluate the effect of applying 770xg force (60 minutes) once daily for 3-days on sGAG and nitrite/NO release, the expression of a gene marker of ECM anabolism (*acan*), a gene marker of ECM catabolism (*mmp-3*), and clock genes (*bmal1* and *per2*) within a 48-hour period in a 3D inflammatory OA model
- To evaluate the effect of applying 770xg force (60 minutes) either twice daily for 1-day or twice daily for 2-days on sGAG and nitrite/NO release, the expression of a gene marker of ECM anabolism (*acan*), gene marker of ECM catabolism (*adamts-4*), and clock genes (*bmal1*, *npas2*, *nr1d1*, *per1* and *per2*) in individual LD cycles within a 48-hour period in a 3D inflammatory OA model (induced by 24-hour exposure to 5ng/ml IL-1α in combination with 10ng/ml OSM only)

## 5.2. Experimental protocols

### 5.2.1. Investigating the effect of catabolic cytokines on circadian clocks and the expression of gene markers of anabolism and catabolism in 3D chondrocyte pellets

To determine whether proinflammatory cytokines can disrupt circadian clocks and induce an inflammatory OA phenotype in a 3D model, bovine chondrocyte pellets were constantly exposed to IL-1α in combination with OSM (Peprotech, London, UK) for 72 hours. Following equilibration of 3D cultures with no PCM, quadruple technical replicates (i.e., n = 4 per time point) were exposed to 5 ng/ml IL-1α in combination with 10 ng/ml OSM at 10:00am (ZT0 hours) and harvested at 4-hour intervals starting from ZT0 hours by adding 1 ml of TRIzol$^{TM}$ reagent and immediately storing at -80$^{o}$C within a 72-hour period until further processing of mRNAs and analysis of gene expression as previously described (sections 2.2 - 2.7). At each 4-hour interval, culture media was collected and stored at -20$^{o}$C until further processing (sections 2.9 and 2.10). Additionally, control cultures were also harvested at equivalent time points as their cytokine-stimulated counterparts and treated under identical conditions except for proinflammatory cytokine exposure. In both the control and cytokine stimulated pellet cultures, culture medium was replenished daily (0.5 ml removal and replenishment with standard culture media as described in section 2.1.2) with appropriate replenishment of cytokines where relevant.

### 5.2.2. Investigating whether application of 770xg load once daily for 3-days or constant dexamethasone application can reset altered circadian rhythm in a 3D *in vitro* model of inflammatory OA

To determine whether application of 770xg load once daily for 3-days is capable of resetting circadian clocks within 2 LD cycles in 3D chondrocyte pellets following cytokine-induced rhythm disruption, inflammatory OA pellets were exposed to 770xg force (60 minutes) once daily for 3-days. Following equilibration of 3D cultures with no PCM, quadruple technical replicates (i.e., n = 4 per time point) were exposed to 5 ng/ml IL-1β in combination with 10 ng/ml OSM at 10:00am (ZT0 hours) and incubated for 24 hours before applying 60 minutes of 770xg force, once per day for a period of three days (cytokines were kept in culture throughout) [Fig. 5.1]. Culture media and pellets were harvested in a circadian time series manner and processed (as previously described in section 5.2.1) from ZT0 hours which was 24 hours after the application of 770xg force for

60 minutes (at 10:00 am) [Fig. 5.1]. To serve as circadian rhythm rescue positive controls, pellet cultures initially exposed to proinflammatory cytokines for 24-hours were treated with 100 nM dexamethasone throughout the culture period (co-applied with cytokines) prior to serial collection and processing at similar time points as the 770xg force group [Fig. 5.1]. Moreover, a negative control group of chondrocyte pellets were set up with no prior exposure to cytokines, not subjected to centrifugal force nor exposed to Dex, harvested and processed at similar time points [Fig. 5.1]. To serve as circadian rhythm disruption positive controls, another group of pellet cultures were constantly exposed to 5 ng/ml IL-1β in combination with 10 ng/ml OSM throughout the 72-hour period of investigation, harvested and processed at equivalent time points as the above-mentioned groups [Fig. 5.1]. In each group, culture media was changed daily (0.5ml removal and replenishment with standard culture media) with appropriate replenishment of specific stimuli being utilised, e.g., Dex and/or cytokines where relevant. In the loaded group, mechanical loading was performed at the same time as previous studies (i.e., 10:00 am) and cytokines were always introduced at the same time to induce an inflammatory OA phenotype or disrupt circadian clocks (i.e., 10:00 am).

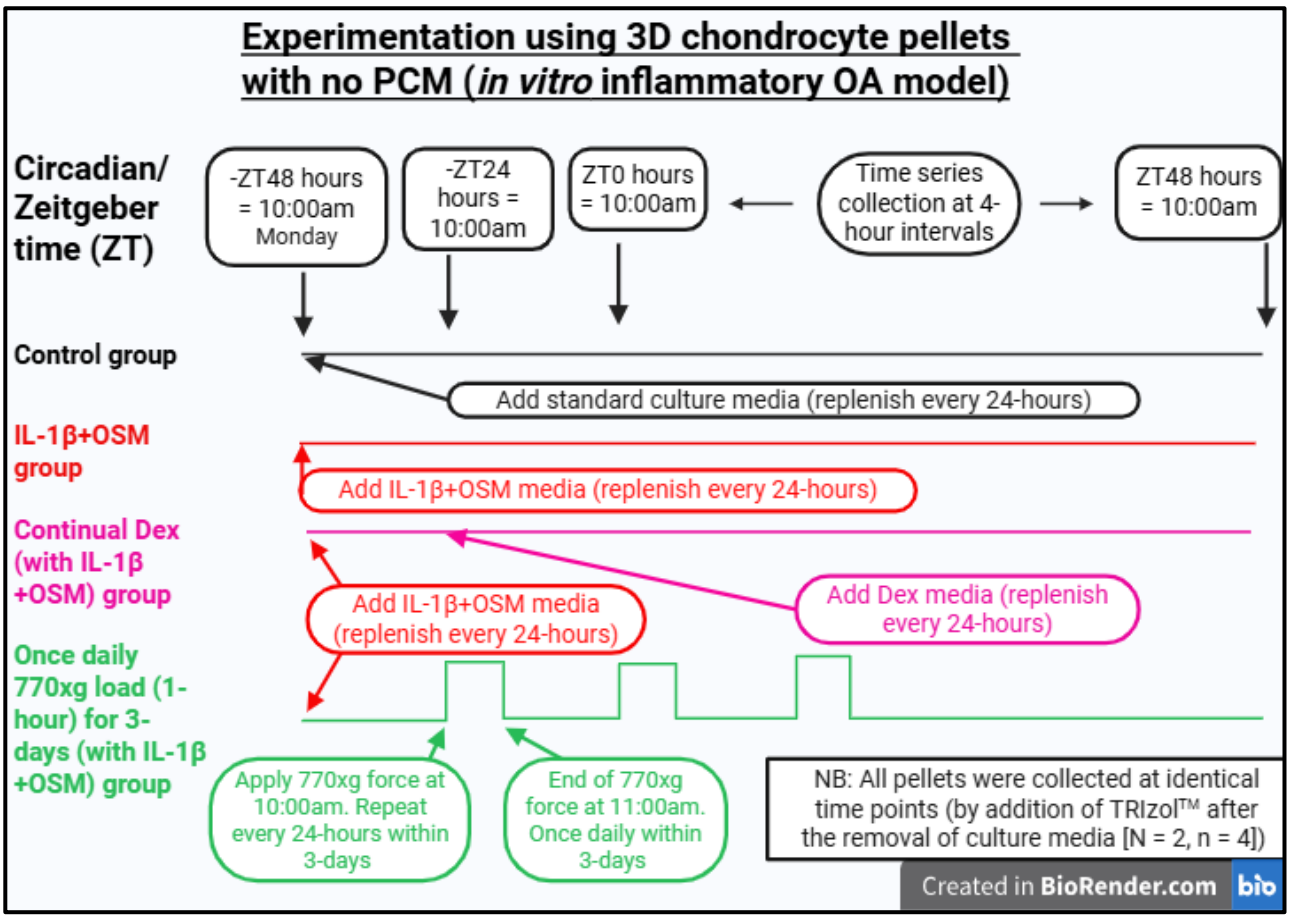


**Figure 5.1. Schematic illustration of an experimental set-up used to assess the influence of once daily application of 770xg force (60 minutes) for 3-days and continuous Dex exposure on chondrocyte circadian clocks in 3D inflammatory OA pellets with no PCM**. The diagram shows control 3D chondrocyte pellet cultures as well as 3D inflammatory OA pellets (induced through application of 5 ng/ml IL-1β in combination with 10 ng/ml OSM) subjected to either once daily 770xg load (60 minutes) for 3-days or 100 nM Dex treatment continuously [as well as the cytokine (IL-1β+OSM) group] which were collected at 4-hour intervals (with ZT0 hours selected as 10:00am on Wednesday representing a time point 24 hours post the initiation of 770xg force or Dex application) by adding 1 ml TriZol™ reagent and storage at -80°C within a 48-hour period prior to further processing (N = 2, n = 4) (Created in BioRender).

### 5.2.3. Assessing whether application of mechanical load twice daily can reset disrupted circadian rhythm in a 3D *in vitro* inflammatory OA model

To determine whether disrupted circadian rhythms in clock gene expression can be reset by application of mechanical load twice daily for 1-or 2-days in a 3D inflammatory OA model, 3D chondrocyte pellets with no PCM which had had exposure to the proinflammatory cytokines for 24 hours were subjected to twice daily episodes of 60 minutes of 770xg force in a single day or 2 consecutive days. Following 24-hour exposure of equilibrated 3D cultures to 5 ng/ml IL-1α in combination with 10 ng/ml OSM, triplicate technical replicates (i.e., n = 3 per time point) were subjected to either (a) load of 770xg centrifugal force for 1 hour in the morning (AM centrifugation at 10:00 hours) and for 1 hour in the afternoon (PM centrifugation at 16:00 hours) herein termed twice daily load for 1-day [Fig. 5.2], or (b) AM and PM load of 770xg force (1-hour each) within a 48-hour period herein termed twice daily load for 2-days [Fig. 5.2]. For the twice daily load for 1-day group, ZT0 hours was taken 24 hours after the initiation of the AM centrifugal regimen, culture media and pellets were harvested and processed at 4-hour intervals within a 24-hour period as previously described in section 5.2.1 [Fig. 5.2]. However, in the twice daily load for 2-days group, ZT0 hours was taken 48 hours after the initiation of the first AM centrifugal regimen before culture media and pellets were harvested and processed as previously described in section 5.2.1 [Fig. 5.2]. Hence, pellets for the twice daily load for 1- and 2-days groups were collected in different LD cycles, but both were collected within a 24-hour period. Corresponding control pellets were also set-up and cultured under identical conditions but devoid of experimental treatment, harvesting and processing was carried out at 4-hour intervals at time points described above for the twice daily load for 1- and 2-days groups [5.2]. An independent set of pellets was exposed to proinflammatory cytokines (5 ng/ml IL-1α and 10 ng/ml OSM) for 24-hours before stimulus removal; pellets were subsequently kept in culture with no further stimulation for the same length of time as the control group described above, harvested and processed at identical time points described above (named the cytokine (IL-1α+OSM) group) [Fig. 5.2]. For all the groups described, culture media was changed daily (~1.4ml removal and replenishment with standard culture media). As stated in section 5.2.2, the first mechanical load was performed at the same time as previous loading experiments and cytokines were introduced at the same time as previous inflammatory OA induction experiments.

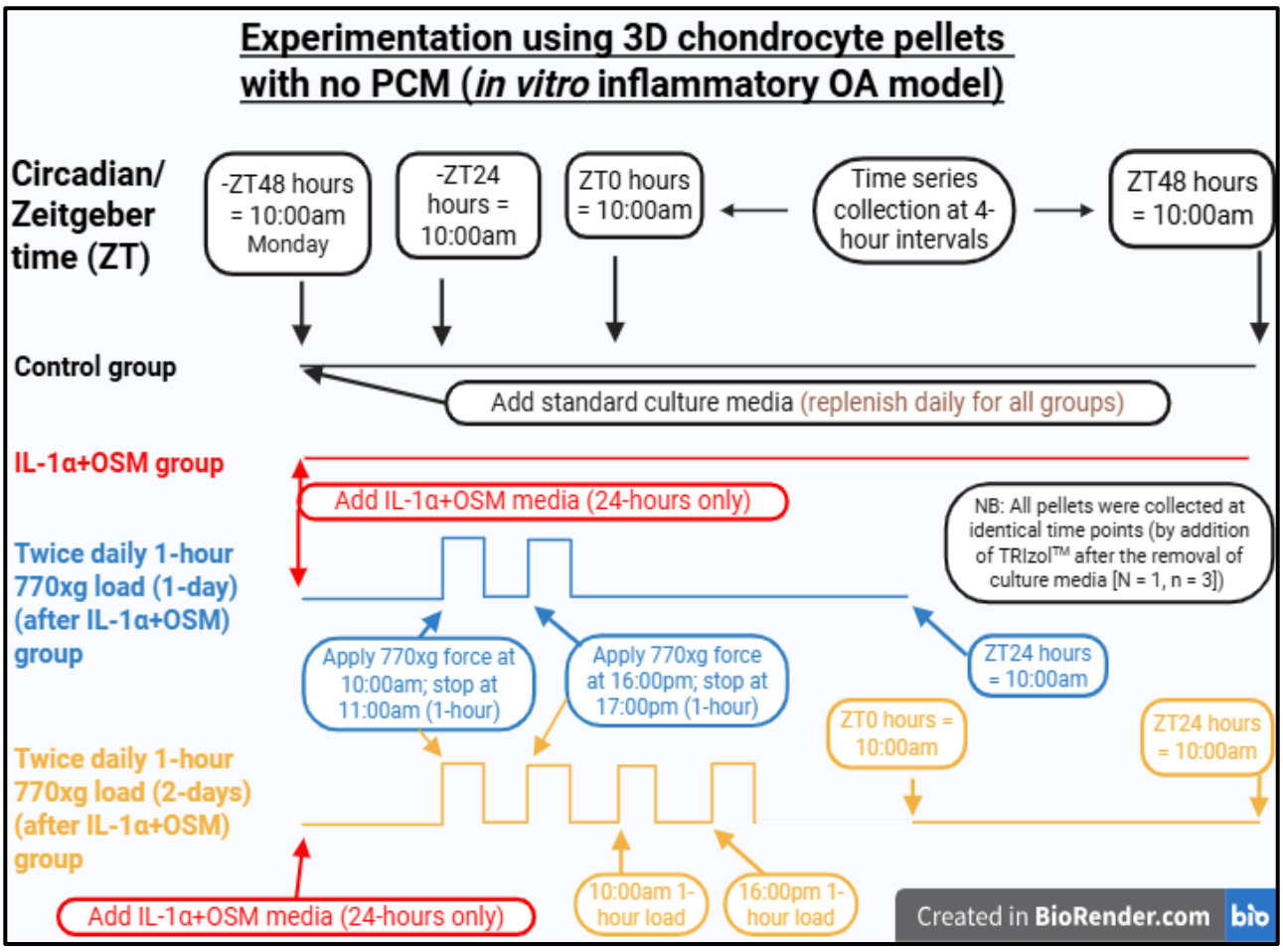


**Figure 5.2. Schematic illustration of an experimental set-up used to assess the influence of twice daily application of 770xg force (60 minutes) either for 1- or 2-days on chondrocyte circadian clocks in 3D inflammatory OA pellets with no PCM**. The diagram indicates control 3D chondrocyte pellet cultures as well as those subjected to either load of 770xg centrifugal force for 1 hour in the morning (10:00am) and for 1 hour in the afternoon (16:00pm) herein termed twice daily load for 1-day or AM and PM load of 770xg force (1-hour each) within a 48-hour period herein termed twice daily load for 2-days (following their exposure to a combination of 5 ng/ml IL-1α and 10 ng/ml OSM for 24 hours) [as well as the cytokine (IL-1α+OSM) group] which were collected at 4-hour intervals (in the twice daily load for 1-day group and its corresponding controls, ZT0 hours was selected as 10:00am on Wednesday representing a time point 24 hours post the initiation of an AM load, whereas ZT0 hours for the twice daily load for 2-days group was selected as 10:00am on Thursday representing a time point 48 hours post the initiation of the first AM load) by adding 1 ml TriZol™ reagent and storage at -80$^{o}$C within a 24-hour period in two independent LD cycles prior to further processing (N = 1, n = 3) (Created in BioRender).

## 5.3. Results

### 5.3.1. Effect of proinflammatory cytokine stimulation on chondrocyte behaviours in a 3D pellet model

#### 5.3.1.1. The influence of cytokine treatment on sGAG release

The DMMB assay was employed to quantify the total amount of sGAG at 24-hour intervals within a 72-hour period in culture media samples harvested from control and cytokine-treated (5 ng/ml IL-1α and 10 ng/ml OSM) chondrocyte pellets with no PCM.

##### 5.3.1.1.1. Significant increase in sGAG concentration within a 72-hour period in control chondrocyte pellets with no PCM

As expected, media samples harvested from control pellet cultures exhibited significantly increased concentrations of sGAG at 24-hour intervals as detected between T0- and T24-hours (T0 vs 24 hours: 0.448±0.307 μg/ml, 33.3±1.06 μg/ml; $p = 0.03038$); between T24- and T48-hours (T24 vs 48 hours: 33.3±1.06 μg/ml, 36.2±1.80 μg/ml; $p = 0.04207$), as well as between T48- and T72-hours (T48 vs 72 hours: 36.2±1.80 μg/ml, 46.1±1.61 μg/ml; $p = 0.03038$) [Fig. 5.3].

##### 5.3.1.1.2. Cytokine treatment significantly decreased sGAG release within a 72-hour period in pellets with no PCM

Although sGAG were detected in the media samples harvested from cytokine-stimulated chondrocytes, as expected, levels were significantly lower than amounts produced by control chondrocytes. Cytokine stimulation significantly reduced the amount of sGAG detected at T24- (58.9%, $p = 0.03038$), T48- (59.1%, $p = 0.03038$) and T72-hours (74.2%, $p = 0.03038$) when compared to time-matched control pellet cultures [Fig. 5.3].

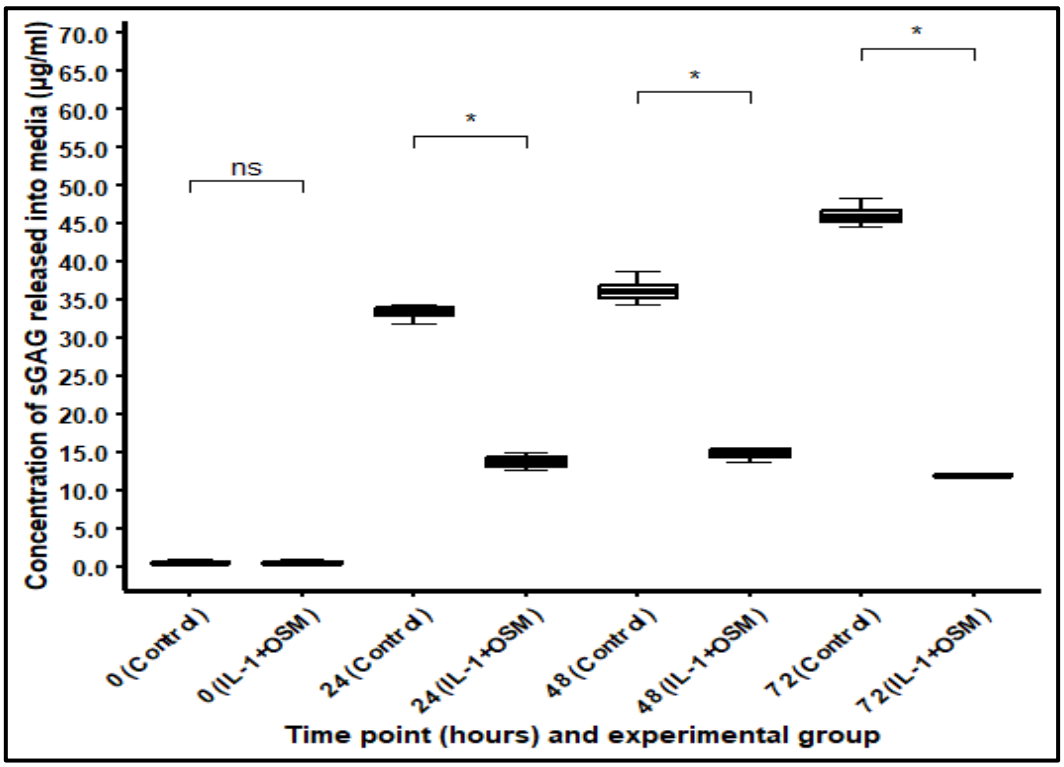


**Figure 5.3. Influence of 5 ng/ml IL-1α in combination with 10 ng/ml OSM on sulphated GAG release in a 3D pellet model.** The graph illustrates box and whisker plots representing the total concentration of sGAG ± SD in culture media collected at T0-, 24-, 48- and 72-hours from control and cytokine-treated (IL-1α+OSM) pellets with no PCM. Statistically significant differences in sGAG concentrations between control and cytokine-treated pellets at the same time point were determined by a Wilcoxon rank sum test in the R software and graphically annotated using the ggpubr package; statistical significance is indicated by * $p<0.05$; ‘‘ns’’ not significant (n = 4, N = 1).

#### 5.3.1.2. The influences of cytokine stimulation on nitrite/NO release in 3D pellets with no PCM

The Griess assay was employed to quantify the total amount of nitrite (indicative of NO production) at 24-hour intervals within a 72-hour period in culture media samples harvested from control and cytokine-treated chondrocyte pellets with no PCM as a marker of an inflammatory phenotype.

##### 5.3.1.2.1. Cytokine treatment significantly induced nitrite/NO release in chondrocyte pellets with no PCM within a 72-hour period

As anticipated, barely detectable levels of nitrite were released from control chondrocyte pellets within a 72-hour period. In contrast, chondrocytes stimulated with 5 ng/ml IL-1α in combination with 10 ng/ml OSM significantly induced nitrite/NO production, increasing from 1.38±0.230 μM to 14.2±0.464 μM within a 72-hour timeframe [Fig. 5.4]; relative to control chondrocyte pellets, cytokines resulted in a 6-fold (T24, $p = 0.0294$), 14.6-fold (T48 hours, $p = 0.03038$) and 11.9-fold increase (T72 hours, $p = 0.03038$) in nitrite/NO production [Fig. 5.4].

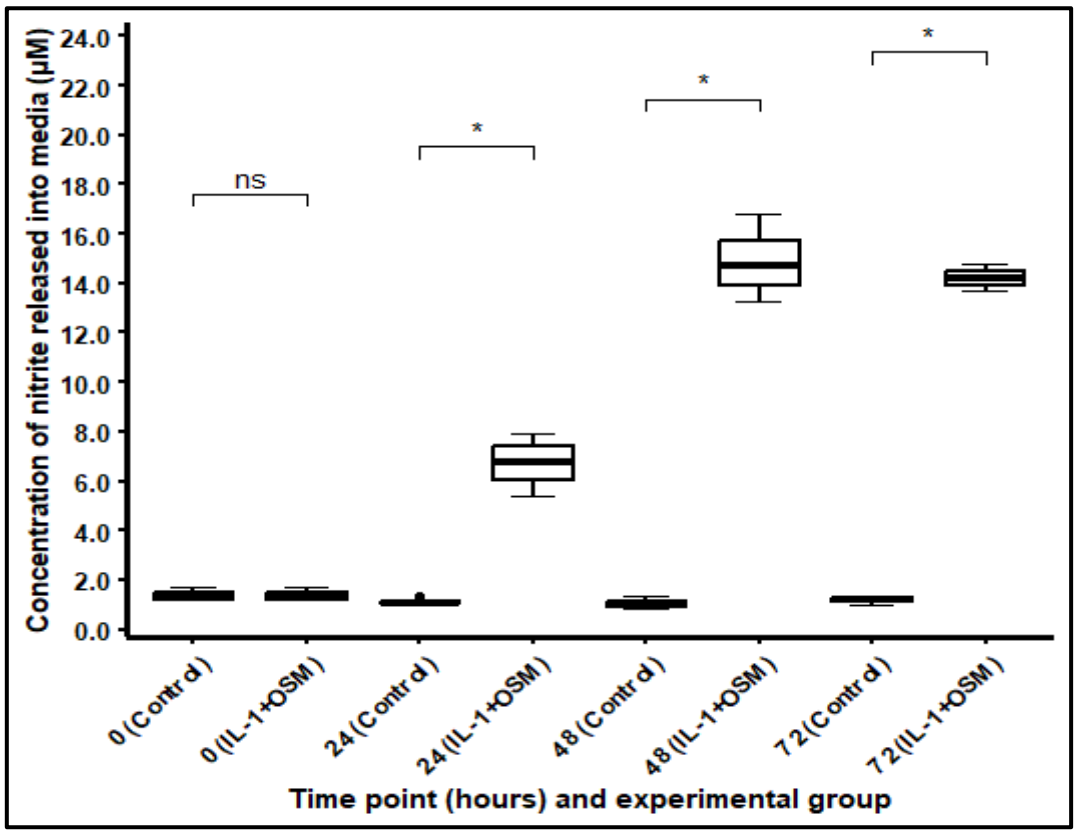


**Figure 5.4. Influence of 5 ng/ml IL-1α in combination with 10 ng/ml OSM on nitrite/NO release in a 3D pellet model.** The graph illustrates box and whisker plots representing the total concentration of nitrite/NO ± SD (n = 4, N = 1) in culture media collected at T0-, 24-, 48- and 72-hours from control and cytokine-treated (IL-1α+OSM) samples. Statistically significant differences in nitrite/NO concentration between control and cytokine-treated chondrocyte pellets within the same time point were determined by a Wilcoxon rank sum test in the R software and graphically annotated using the ggpubr package; statistical significance is indicated by * $p<0.05$; ‘‘ns’’ not significant.

#### 5.3.1.3. The impact of cytokine stimulation on catabolic enzyme activity in 3D pellets with no PCM

To determine the activation status of catabolic enzymes following cytokine stimulation of chondrocyte pellets, SensoLyte® 520 aggrecanase-1 fluorimetric assay and SensoLyte® 520 generic MMP fluorimetric assay were employed to detect aggrecanase-1 (adamts-4) and mmp-13 activity, respectively; enzyme activity is measured as 5-FAM (nM) reflecting cleavage of the FRET substrate. Media samples were collected at 24-hour intervals within a 72-hour period following exposure of 3D chondrocyte pellets to 5 ng/ml IL-1α in combination with 10 ng/ml OSM; unstimulated pellet cultures served as controls.

##### 5.3.1.3.1. Cytokine treatment significantly increased the activity of aggrecanase-1 within a 72-hour period

Minimal aggrecanase-1 activity was observed in control chondrocyte pellets with no PCM within the culture period; in contrast, a 2.79-fold increase in 5-FAM was measured after 24 hours of cytokine stimulation compared to control cultures ($p = 1.1e-06$) [Fig. 5.5A]. The FRET signal remained significantly elevated at T48 hours (2.93-fold, $p = 0.00025$) and T72 hours (1.65-fold, $p = 0.0032$) relative to control cultures [Fig. 5.5A].

##### 5.3.1.3.2. Cytokine treatment significantly increased the activity of mmp-13 within a 72-hour period

A significant decrease in 5-FAM concentration was observed between T24 and T48 hours in control 3D pellets with no PCM (T24 vs 48 hours: 1513±142 nM, 796±304 nM; $p = 0.011$), with activity levels remaining low at T72 hours (T24 vs T72, $p = 3.8e-05$) [Fig. 5.5B]. When compared to cytokine-treated cultures, the 5-FAM concentration in cytokine-stimulated cultures exceeded that of control cultures by 1.85-fold at T48 hours ($p = 0.0150$) and 3.94-fold at T72 hours ($p = 0.00270$) [Fig. 5.5B].

These data [Figs. 5.3 - 5.5] demonstrate the expected chondrocyte responses to proinflammatory cytokine stimuli and confirmed cell behaviours prior to analysing the influence of cytokine treatment on circadian rhythm and ECM metabolism at a transcriptional level.

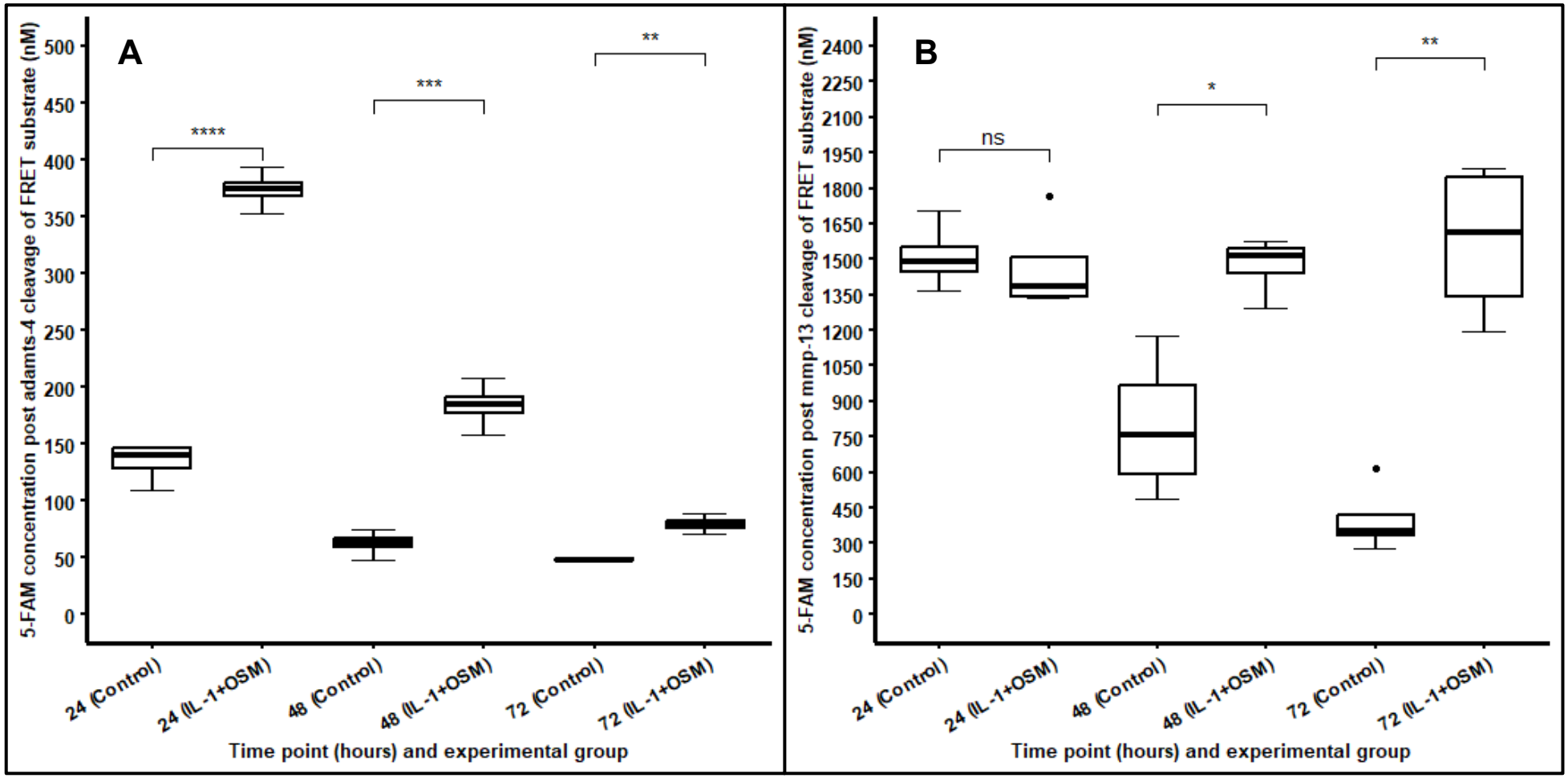


**Figure 5.5. Effect of 5 ng/ml IL-1α in combination with 10 ng/ml OSM on adamts-4 and mmp-13 enzyme activity in a 3D chondrocyte pellet model.** Box and whisker plots represents the concentration of 5-FAM in media samples collected at T24-, 48- and 72-hours from control and cytokine-treated (IL-1α+OSM) 3D pellets with no PCM following the cleavage of FRET peptides by activated enzymes: **A**) adamts-4, and **B**) mmp-13. Black dots represent outliers in datasets. Statistical significances of differences in 5-FAM concentration between control and cytokine-treated datasets at a given time point or two time points within the same experimental group were determined by a Welch Two Sample t-test in the R software and graphically annotated using the ggpubr package; statistical significance is indicated by * for $p<0.05$, ** for $p<0.01$, *** for $p<0.001$, **** for $p<0.0001$; ‘‘ns’’ indicates no statistical significance. Data represent the total concentration of 5-FAM ± SD (n = 4, N = 1).

#### 5.3.1.4. The impact of cytokine stimulation on gene expression

##### 5.3.1.4.1. RefFinder identified *hprt* and *18s* to be the most stable HKGs

A similar methodology described previously (sections 2.6.4 and 3.3.1.4) was utilised and *hprt* and *18s* were identified as the two most stable HKGs for qPCR normalisation of target gene expression in cytokine stimulated 3D cultures as their expression did not change within the 3 days of investigation [Appendix 14].

##### 5.3.1.4.2. A gene marker for the chondrocyte phenotype

To further verify the anti-anabolic effect of proinflammatory cytokines in 3D chondrocyte pellets with no PCM, *sox9* mRNA expression was measured at T24 hours.

###### 5.3.1.4.2.1. Cytokine stimulation significantly downregulated *sox9* transcription at T24 hours

A significant reduction in *sox9* transcript levels was observed at T24 hours following cytokine treatment of chondrocyte pellets with no PCM (1.66-fold, $p = 0.0012$) [Fig. 5.6].

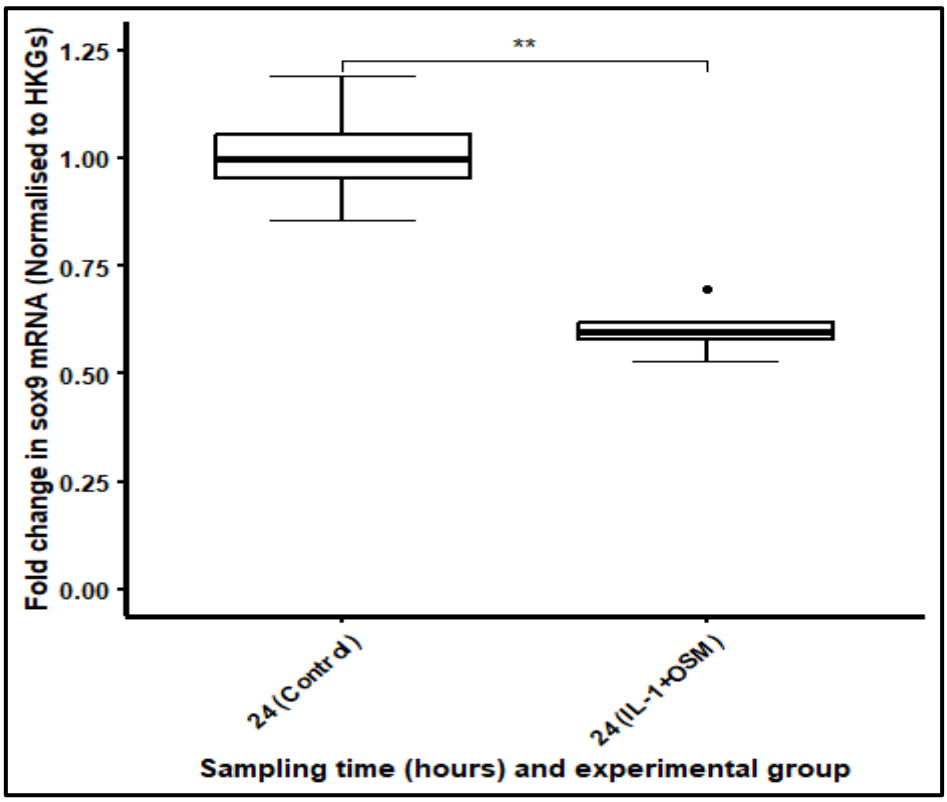


**Figure 5.6. Effect of 5 ng/ml IL-1α in combination with 10 ng/ml OSM on the expression of *sox9* mRNA at T24 hours in a 3D chondrocyte pellet model.** The graph illustrates box and whisker plots representing the fold change in *sox9* mRNA transcripts (normalised to *18s* and *hprt*) plotted against time point of collection (T24 hours) of control 3D chondrocyte pellets with no PCM and those exposed to 5 ng/ml IL-1α in combination with 10 ng/ml OSM. A black dot represents an outlier in the cytokine (IL-1α+OSM) dataset. Statistically significant differences between the control and cytokine-treated cultures at T24 hours were determined by a Welch Two Sample t-test in the R software and graphically annotated using the ggpubr package; statistical significance is indicated by ** for $p<0.01$. Data represent average fold changes in *sox9* mRNA transcripts ± SD (n = 4, N = 1).

#### 5.3.1.4.3. Gene markers of ECM catabolism

To further verify the catabolic effect of proinflammatory cytokines in 3D chondrocyte pellets with no PCM, gene expression levels for several markers of ECM catabolism were assessed including *mmp-3, mmp-13, adamts-4* and *adamts-5* mRNA transcripts at T24 hours.

##### 5.3.1.4.3.1. Cytokine-stimulation upregulated the expression of *mmp-3* and *mmp-13* mRNA transcripts at T24 hours

As expected, cytokine-treated chondrocyte pellets with no PCM significantly increased expression of *mmp-3* and *mmp-13* mRNAs at T24 hours (*mmp-3*: 13.90-fold, p = 0.0294 [Fig. 5.7A], *mmp-13*: 2.48-fold, p = 0.03038 [Fig. 5.7B]). Moreover, a similar trend evidencing cytokine induced *mmp-3* and *mmp-13* upregulation was observed at successive time points within a 72-hour period of investigation (data not shown). However, this did not translate into increased mmp-13 enzyme activity as no significant differences were observed between control and cytokine-treated cultures at T24 hours [Fig. 5.5B].

##### 5.3.1.4.3.2. Cytokine-treatment significantly increased the expression of *adamts-4* and *adamts-5* mRNA transcripts at T24 hours

As expected, cytokine stimulation of pellets with no PCM induced a significant 74.90-fold increase in *adamts-4* (p = 0.03038 [Fig. 5.8A] and 78.60-fold increase in *adamts-5* mRNA transcripts at T24 hours (p = 0.03038 [Fig. 5.8B]). Furthermore, a similar trend evidencing cytokine induced *adamts-4* and *adamts-5* mRNA upregulation was observed at successive time points within the 72-hour period of investigation (data not shown). In corroboration, equivalent responses were observed in adamts-4 enzyme activity as a significant 2.79-fold increase in 5-FAM was observed between control and cytokine-treated cultures at T24 hours [Fig. 5.5B].

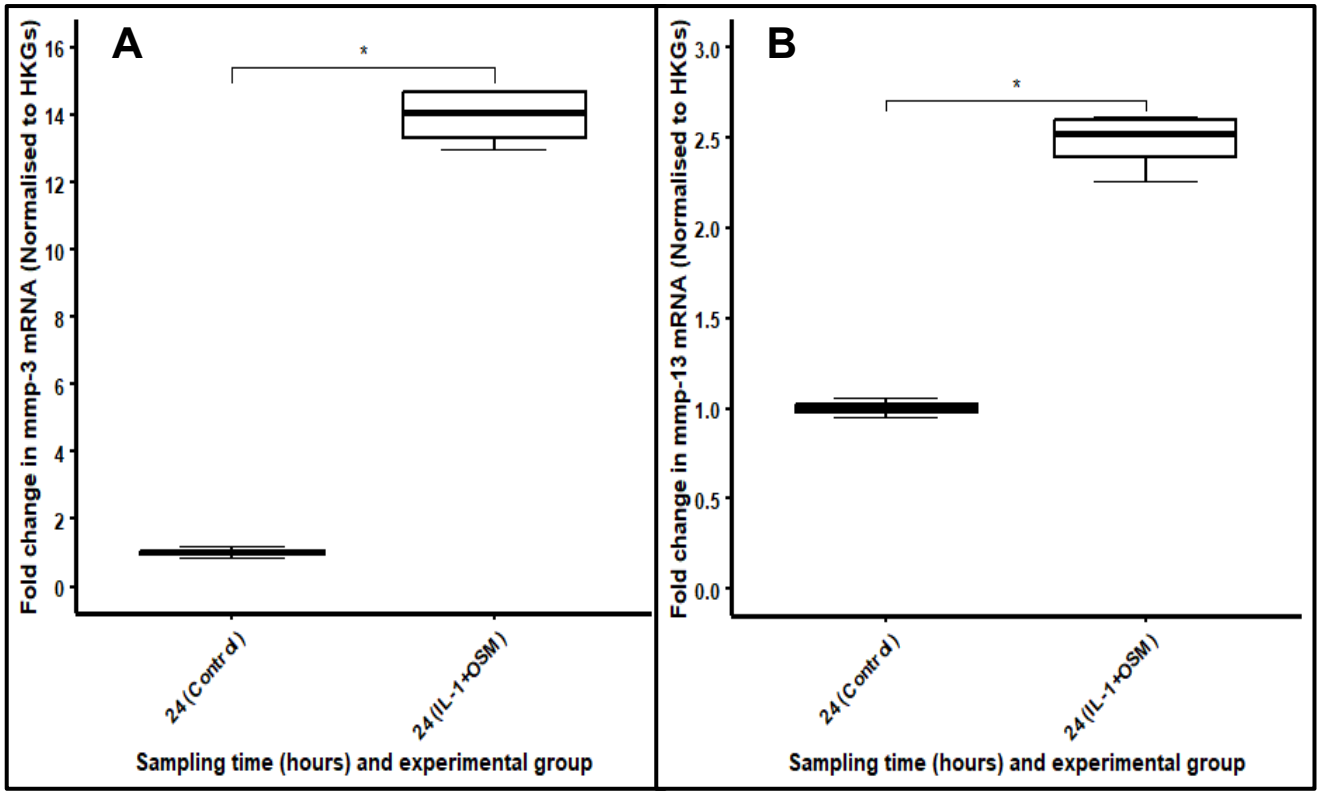


**Figure 5.7. Effect of 5 ng/ml IL-1α in combination with 10 ng/ml OSM on the expression of *mmp-3* and *mmp-13* mRNA at T24 hours in a 3D model.** The graphs illustrate box and whisker plots representing the fold changes in mRNA transcripts (normalised to *18s* and *hprt*) plotted against time point of collection (T24 hours) of control 3D chondrocyte pellets with no PCM and those exposed to 5 ng/ml IL-1α in combination with 10 ng/ml OSM. qPCR quantification of mRNA levels for the following catabolic genes were performed: **A**) *mmp-3* and **B**) *mmp-13*. Statistically significant differences between the control and cytokine-treated (IL-1α+OSM) cultures at T24 hours were determined by a Wilcoxon rank sum test in the R software and graphically annotated using the ggpubr package; statistical significance is indicated by * $p<0.05$. Data represent average fold changes in mRNA transcripts ± SD (n = 4, N = 1).

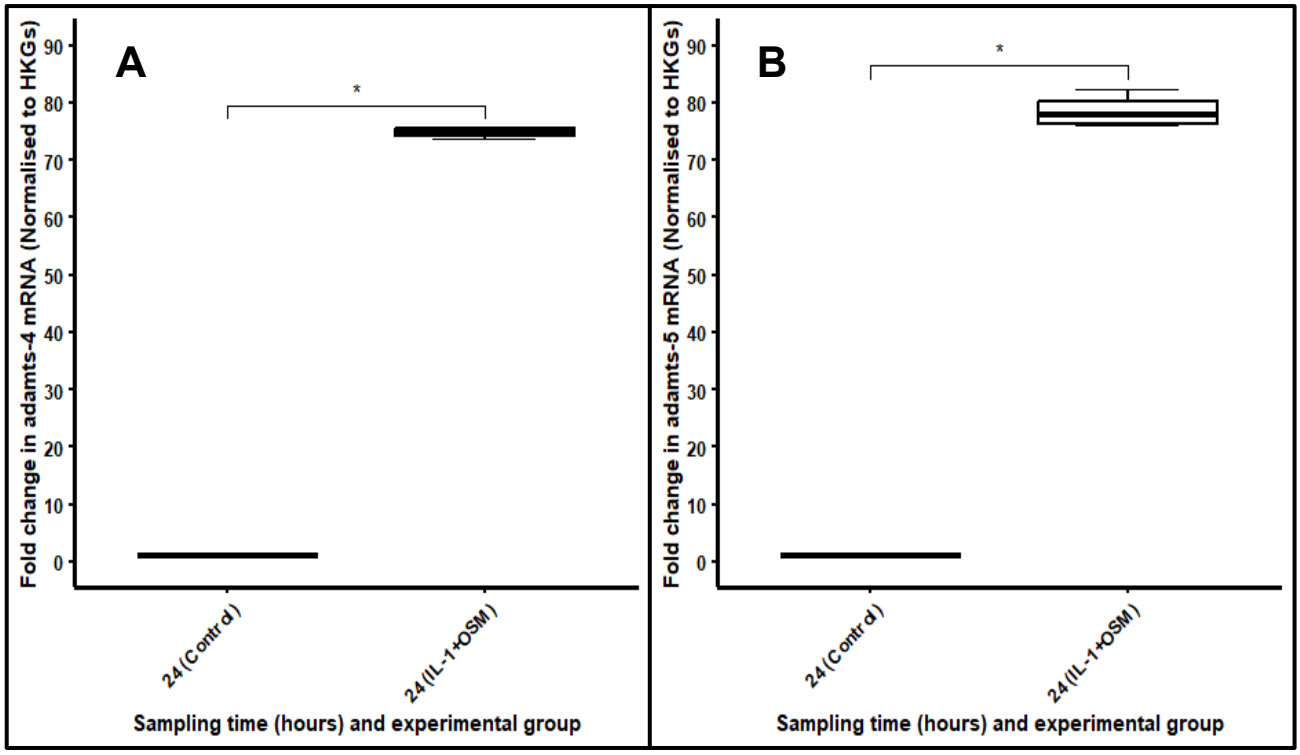


**Figure 5.8. Effect of 5 ng/ml IL-1α in combination with 10 ng/ml OSM on the expression of *adamts-4* and *adamts-5* mRNAs at T24 hours in a 3D model.** The graphs illustrate box and whisker plots representing the fold changes in mRNA transcripts (normalised to *18s* and *hprt*) plotted against time point of collection (T24 hours) of control 3D chondrocyte cultures and those exposed to 5 ng/ml IL-1α in combination with 10 ng/ml OSM. qPCR quantification of mRNA levels for the following catabolic genes were performed: **A**) *adamts-4* and **B**) *adamts-5*. Statistically significant differences between the control and cytokine-treated (IL-1α+OSM) cultures at T24 hours were determined by a Wilcoxon rank sum test in the R software and graphically annotated using the ggpubr package; statistical significance is indicated by * $p<0.05$. Data represent average fold change in mRNA transcripts ± SD (n = 4, N = 1).

#### 5.3.1.4.4. Circadian clock genes

mRNA transcripts for circadian clock genes were selected for analyses as described in section 5.2.1 which are representative of the positive arm (*bmal1*) and negative arm (*per2*) of the core clock transcriptional/translational feedback loop as well as repressors of an auxiliary feedback loop (*nr1d1*, *nr1d2*).

##### 5.3.1.4.4.1. Circadian regulation of *bmal1*, *nr1d1* and *per2* mRNA transcripts, but not *nr1d2* mRNA, abolished following cytokine stimulation within a 72-hour period

***bmal1*** Control chondrocyte pellets with no PCM revealed circadian rhythm of *bmal1* ($r^2$ = 0.824, p = 0.0001) within 3 LD cycles as characterised by an amplitude of 0.596, a period of 20.9 hours and a peak at ZT14 hours [Fig. 5.9A]. Following cytokine treatment, this regulation was lost ($r^2$ = 0.030, p = 0.3292) [Fig. 5.9A].

***nr1d1*** Rhythmic oscillations of *nr1d1* transcripts were observed within a 72-hour period in control pellets with no PCM ($r^2$ = 0.917, p = 0.0001) characterised by an amplitude of 0.115, a 19.1-hour period and a peak around ZT2 hours [Fig. 5.9B]. Cytokine treatment abolished circadian regulation of this gene ($r^2$ = 0.457, p = 0.0002) [Fig. 5.9B].

***per2*** Control 3D chondrocyte pellets with no PCM demonstrated rhythmic oscillation of *per2* mRNA ($r^2$ = 0.836, p = 0. 0037) in three successive LD cycles [Fig. 5.9C]. *per2* mRNA rhythm exhibited an amplitude of 0.973, period of 22.7 hours and a peak around ZT8 hours [Fig. 5.9C]; *per2* rhythmicity was lost following cytokine stimulation ($r^2$ = 0.113, p = 0.0125) [Fig. 5.9C].

***nr1d2*** No circadian expression of *nr1d2* mRNA transcripts was observed in control 3D chondrocyte pellets with no PCM within the 72-hour timeframe ($r^2$ = 0.461, p = 0.0001) [Fig. 5.9D]. Likewise, cytokine-treated 3D pellet cultures exhibited no circadian rhythm of this gene within the same timeframe ($r^2$ = 0.032, p = 0.3045) [Fig. 5.9D].

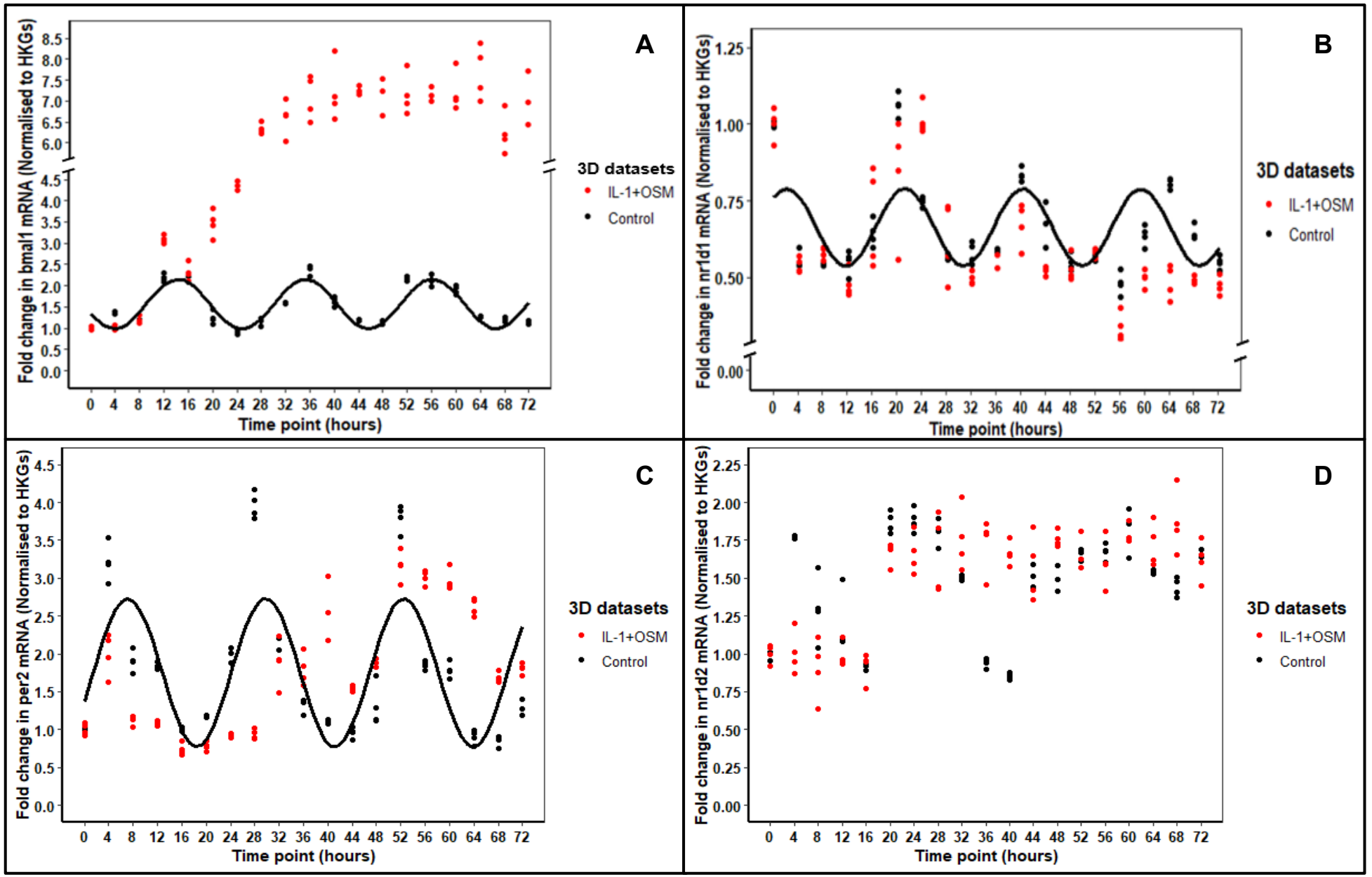
A
Fold change in bmal1 mRNA (Normalised to HKGs)
Time point (hours)
3D datasets
IL-1+OSM
Control
B
Fold change in nr1d1 mRNA (Normalised to HKGs)
Time point (hours)
3D datasets
IL-1+OSM
Control
C
Fold change in per2 mRNA (Normalised to HKGs)
Time point (hours)
3D datasets
IL-1+OSM
Control
D
Fold change in nr1d2 mRNA (Normalised to HKGs)
Time point (hours)
3D datasets
IL-1+OSM
Control

**Figure 5.9. Influence of 5 ng/ml IL-1α in combination with 10 ng/ml OSM on *bmal1*, *nr1d1, per2* and *nr1d2* transcription within 3 LD cycles in a 3D model.** The graphs illustrate fold change in mRNA transcripts (normalised to *18s* and *hprt*) plotted against time of collection (at 4-hour intervals) of control 3D chondrocyte cultures and those exposed to 5 ng/ml IL-1α in combination with 10 ng/ml OSM. Samples were collected at 4-hour intervals within a 72-hour period followed by qPCR quantification of mRNA levels for: **A)** *bmal1* (representing a transcriptional activator of the core clock), **B)** *nr1d1* (representing a transcriptional repressor of an auxiliary feedback loop), **C)** *per2* (representing a transcriptional repressor of the core clock) and **D)** *nr1d2* (representing a transcriptional repressor of an auxiliary feedback loop). Black dots represent control datasets; red dots represent cytokine-stimulated (IL-1α+OSM) datasets. The fitted cosinusoidal waves (Black curves) indicate rhythmic oscillations of mRNA transcripts for a specific gene determined by the CircWaveBatch software ($R^2 > 0.8$, $p < 0.05$) and graphically plotted in the R software using the ggplot2 package. The absence of a cosinusoidal wave in the plot (red dots and black dots for *nr1d2* only) indicates arrhythmic expression of a specific gene following cytokine stimulation determined by the CircWaveBatch software ($R^2 < 0.8$, or $p > 0.05$). Data points represent average fold change in mRNA transcripts ($n = 4$, $N = 1$).

#### 5.3.1.4.4.5. Determination of circadian rhythm for a chondrocyte phenotype marker gene in the presence and absence (control) of proinflammatory cytokines in 3D chondrocyte pellets with no PCM

mRNA expression of a chondrocyte phenotype gene marker *sox9* was analysed (section 5.2.1) to determine whether 3D chondrocyte pellets with no PCM exhibit circadian rhythmicity of this gene in the presence and absence of 5 ng/ml IL-1α in combination with 10 ng/ml OSM.

##### 5.3.1.4.4.5.1. Control and cytokine-treated 3D pellet cultures demonstrated no rhythmicity of *sox9* mRNA within 3 LD cycles

Control 3D pellets with no PCM exhibited no rhythmic expression of *sox9* transcripts within a 72-hour timeframe ($r^2 = 0.202$, $p = 0.0003$) [Fig. 5.10]. This lack of circadian rhythmicity was also observed following cytokine stimulation ($r^2 = 0.096$, $p = 0.0251$) [Fig. 5.10].

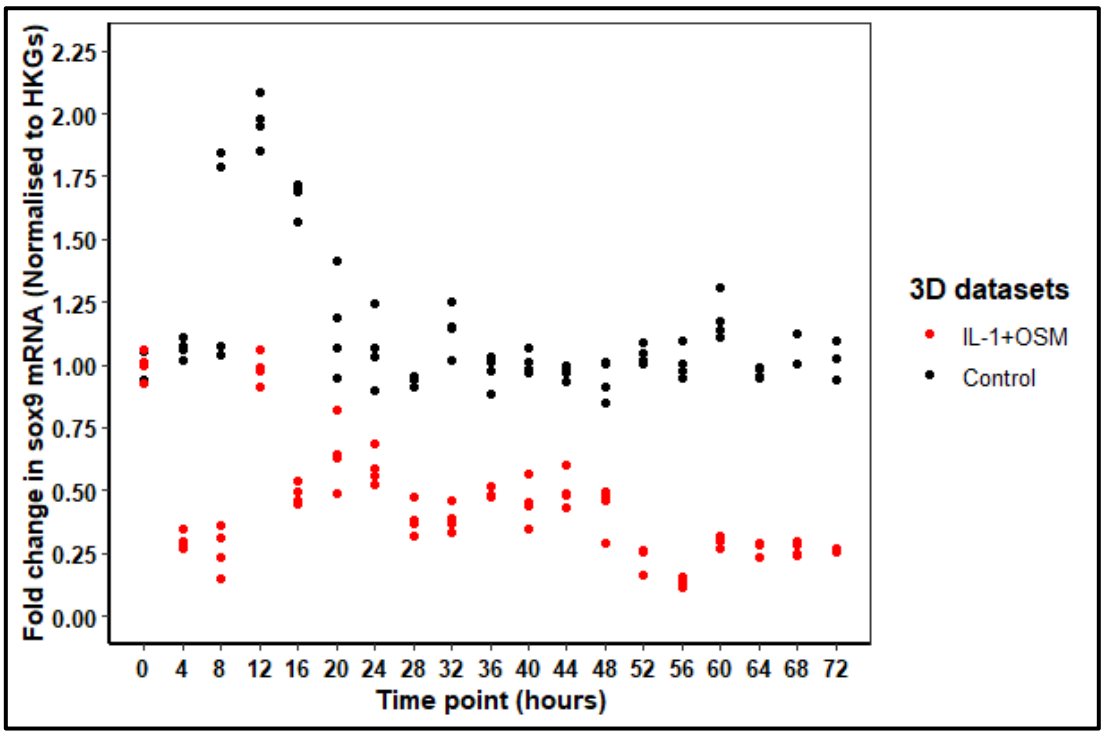


**Figure 5.10. Influence of IL-1α and OSM on *sox9* mRNA transcripts in 3D chondrocyte pellets within a 72-hour period.** The graph illustrates fold change in *sox9* mRNA transcripts (normalised to *18s* and *hprt*) plotted against time of collection (at 4-hour intervals) of control 3D chondrocyte pellets with no PCM and those exposed to 5 ng/ml IL-1α in combination with 10 ng/ml OSM (kept throughout culture period). Samples were collected at 4-hour intervals within a 72-hour period followed by qPCR quantification of *sox9* mRNA levels. Black dots represent control datasets; red dots represent cytokine-stimulated (IL-1α+OSM) datasets. The absence of cosinusoidal waves in plots indicates arrhythmic expression of *sox9* mRNA in control pellets and following cytokine stimulation determined by the CircWaveBatch software ($R^2 < 0.8$, or $p > 0.05$) and graphically plotted in the R software using the ggplot2 package. Data points represent fold change in mRNA transcripts (n = 4, N = 1).

#### 5.3.1.4.4.6. Assessment of circadian rhythm for cartilage ECM catabolic genes in the presence and absence of proinflammatory cytokines in 3D pellets with no PCM

mRNA transcripts for cartilage ECM catabolic genes, *adamts-4, adamts-5, mmp-3* and *mmp-13* were analysed (as described in section 5.2.1) to determine whether 3D chondrocyte pellets with no PCM exhibit circadian rhythmicity of these genes in the presence and absence of 5 ng/ml IL-1α in combination with 10 ng/ml OSM.

##### 5.3.1.4.4.6.1. Control pellet cultures exhibited no circadian rhythm of *mmp-3*, *mmp-13*, and *adamts-5* mRNAs within 3 LD cycles, persisting following cytokine exposure

Analysis of gene expression within a 72-hour period in control chondrocyte pellets with no PCM confirmed the lack of a circadian rhythm of mRNA transcripts for *mmp-3* ($r^2$ = 0.479, p = 0.0001) [Fig. 5.11A], *mmp-13* ($r^2$ = 0.101, p = 0.0207) [Fig. 5.11B], *adamts-4* ($r^2$ = 0.322, p = 0.0001) [Fig. 5.11C] and *adamts-5* ($r^2$ = 0.485, p = 0.0223) [Fig. 5.11D]. This lack of rhythmicity persisted in the cytokine-treated chondrocyte pellets with no PCM [Fig. 5.11A – D].

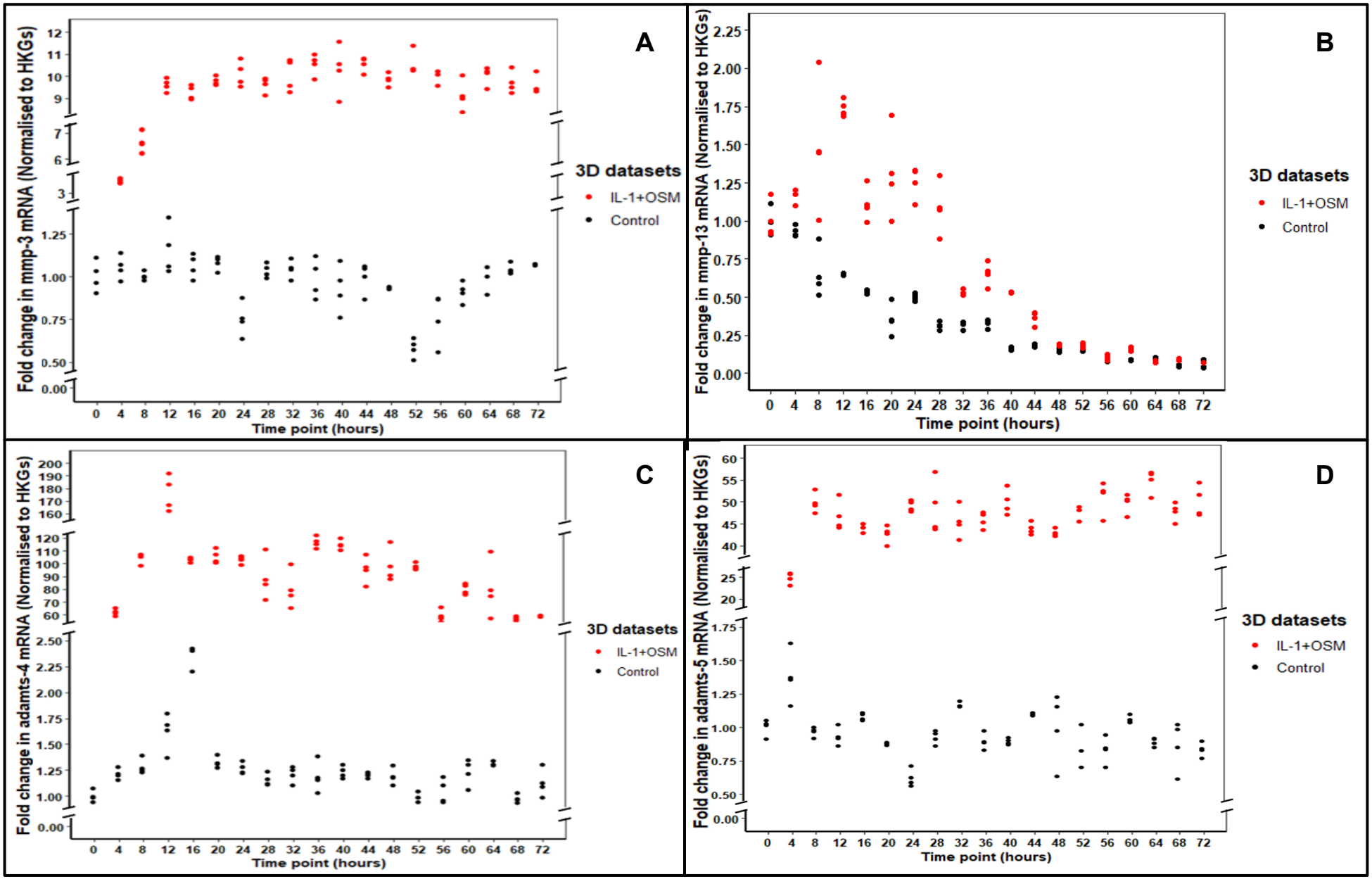
A
Fold change in mmp-3 mRNA (Normalised to HKGs)
Time point (hours)
3D datasets
IL-1+OSM
Control
B
Fold change in mmp-13 mRNA (Normalised to HKGs)
Time point (hours)
3D datasets
IL-1+OSM
Control
C
Fold change in adamts-4 mRNA (Normalised to HKGs)
Time point (hours)
3D datasets
IL-1+OSM
Control
D
Fold change in adamts-5 mRNA (Normalised to HKGs)
Time point (hours)
3D datasets
IL-1+OSM
Control

**Figure 5.11. Influence of IL-1α in combination with OSM on *mmp*-3, *mmp-13*, adamts-*4* and *adamts-5* transcription within 3 LD cycles in 3D pellets with no PCM.** Fold change in mRNA transcripts (normalised to *18s* and *hprt*) plotted against time of collection (at 4-hour intervals) of control 3D chondrocyte cultures and those exposed to 5 ng/ml IL-1α in combination with 10 ng/ml OSM. Samples were collected at 4-hour intervals within a 72-hour period followed by qPCR quantification of mRNA levels for: **A**) *mmp-3*, **B**) *mmp-13*, **C**) *adamts-4* and **D**) *adamts-5*. Black dots represent control datasets; red dots represent cytokine-stimulated (IL-1α+OSM) datasets. The absence of a cosinusoidal wave in plots indicates arrhythmic expression of a specific gene in control 3D cultures and following cytokine stimulation determined by the CircWaveBatch software ($R^2 < 0.8$, or $p > 0.05$). Data points represent fold change in mRNA transcripts (n = 4, N = 1).

### 5.3.2. Responses of 3D chondrocyte cultures to mechanical loading once daily for 3-days or constant dexamethasone exposure in an *in vitro* inflammatory OA model

Having established in chapter 4 and 5 that control 3D chondrocyte pellets with no PCM exhibited circadian rhythm for clock genes (*bmal1*, *clock*, *cry1, npas2*, *nr1d1, nr1d2*, *per1* and *per2*), and the cartilage ECM catabolic gene (*adamts-4*), and that proinflammatory cytokines disrupt circadian rhythms of the above-mentioned genes, experiments were carried out (described in section 5.2.2) to establish if mechanical loading (mimicked through single daily exposure to 60 minutes of 770xg centrifugal force for 3-days) or Dex exposure had any influence on disrupted circadian rhythms (i.e. can it synchronise circadian rhythm of *bmal1* and *per2* transcription following cytokine-induced rhythm disruption?), inflammation (sGAG and NO levels, catabolic enzyme activities [aggrecanase-1/adamts-4] and mmp-13) and transcription of gene markers of ECM anabolism and catabolism (*acan* and *mmp-3*, respectively) are either restorative or disruptive in a 3D inflammatory OA model.

#### 5.3.2.1. Application of cytokines, separately or in combination with either Dex or once daily 770xg force, had no effect on sulphated GAG release in 3D pellets with no PCM

sGAG levels did not change in control pellets with no PCM assessed at 24-hour intervals within a 48-hour window with levels ranging from 2.21±0.44 µg/ml at T0 hours, 1.91±0.35 µg/ml at T24 hours, and 2.21±0.31 µg/ml at T48 hours. Similar sGAG concentrations were observed in 3D pellets subjected either to constant cytokine stimulation (5 ng/ml IL-1β in combination with 10 ng/ml OSM), continual Dex treatment in the presence of cytokines, or once daily episode of 770xg force (60 minutes) for 3-days in the presence of cytokines (data not shown). Surprisingly, no significant differences were observed when comparing sGAG levels between control cultures and those subjected to the above-mentioned stimuli at each time point (i.e., T0 hours: control vs cytokines [p = 0.1832], control vs Dex+cytokines [p = 0.8817], control vs 770xg force+cytokines [p = 0.05451]; T24 hours: control vs cytokines [p = 0.2975], control vs Dex+cytokines [p = 0.1416], control vs 770xg force+cytokines [p = 0.2308]; T48 hours: control vs cytokines [p = 0.08143], control vs Dex+cytokines [p = 0.3719], control vs 770xg force+cytokines [p = 0.766]) (data not shown).

#### 5.3.2.2. Application of cytokines, separately or in combination with Dex or once daily 770xg force had no effect on nitrite/NO release in 3D pellets with no PCM

Nitrite levels were below the limit of detection at T0-, T24- and T48-hours in control pellets with no PCM and those initially exposed to proinflammatory cytokines (5 ng/ml IL-1β in combination with 10 ng/ml OSM) before either application of Dex (constant exposure in the presence of cytokines) or once daily episode of 60 minutes of 770xg force for 3-days (in the presence of cytokines) (data not shown).

#### 5.3.2.3. RefFinder identified *hprt* and *18s* to be the most stable HKGs

Using the methodology described previously (sections 2.6.4 and 3.3.1.4), *hprt* and *18s* were identified as the two most stable HKGs for qPCR normalisation of target gene expression in cytokine-stimulated 3D pellets with no PCM either subjected to a single episode of 770xg force (60 minutes) for 3-days [in the presence of cytokines] or continual Dex exposure in the presence of cytokines, as these genes did not change within a 48-hour period of investigation [Appendix 15].

#### 5.3.2.4. The effect of applying 770xg force once daily for 3-days or constant Dex exposure on *acan* and *mmp-3* transcription in cytokine-stimulated pellets with no PCM

To verify the: (i) anti-anabolic and catabolic effects of proinflammatory cytokines, and (ii) the anti-inflammatory properties of Dex, as well as (iii) determining whether once daily 770xg force exposure for 3-days has anti-inflammatory actions on cytokine-stimulated 3D chondrocyte pellets, fold changes in *acan* and *mmp-3* transcript levels at T24 hours were used as an example to demonstrate chondrocyte responses.

##### 5.3.2.4.1. Downregulation of *acan* mRNA and upregulation of *mmp-3* mRNA at T24 hours following cytokine stimulation

***acan*** Following cytokine stimulation, a significant 2.75-fold reduction in *acan* mRNA transcripts was observed at T24 hours in 3D pellets with no PCM ($p = 0.03038$) [Fig. 5.12A]; this was validated in a repeat experiment.

***mmp-3*** A significant 2.19-fold increase in *mmp-3* mRNA transcripts was observed in cytokine-stimulated 3D pellets with no PCM at T24 hours (p = 0.03038 [Fig. 5.12B]; this was validated in a repeat experiment.

#### 5.3.2.4.2. Significant increase in *acan* transcription and reduction in *mmp-3* transcription at T24 hours in cytokine-stimulated cultures following Dex treatment

***acan*** Co-application of Dex with cytokines in 3D chondrocyte pellets with no PCM previously exposed to proinflammatory cytokines resulted in significant increases in *acan* mRNA transcripts relative to the cytokine group at T24 hours (p = 0.03038) [Fig. 5.12A]. This indicates that Dex returned *acan* transcription to control levels [Fig. 5.12A].

***mmp-3*** Introduction of Dex to cytokine-stimulated pellets with no PCM significantly reduced *mmp-3* transcription relative to the cytokine group at T24 hours (p = 0.03038) [Fig. 5.12B], with mRNA levels comparable to the control group [Fig. 5.12B].

#### 5.3.2.4.3. Once daily application of 770xg force (60 minutes) for 3-days in the presence of cytokines had no effect on *acan* transcription at T24 hours

At T24 hours, once daily application of 770xg force for 3-days did not modulate the significant cytokine-induced 2.16-fold reduction in *acan* mRNA transcripts relative to control levels (p = 0.03038) [Fig. 5.12A]. However, a marginal increase in *acan* transcription was observed relative to the cytokine group (p = 0.03038); this was validated in a repeat experiment.

#### 5.3.2.4.4. Once daily application of 770xg force (60 minutes) for 3-days in the presence of cytokines had no effect on *mmp-3* transcription at T24 hours

At T24 hours, the significantly elevated *mmp-3* mRNA levels persisted following once daily application of 770xg force for 3-days to cytokine-stimulated 3D pellets with no PCM (2.29-fold, p = 0.03038) [Fig. 5.12B]; this was validated in a repeat experiment.

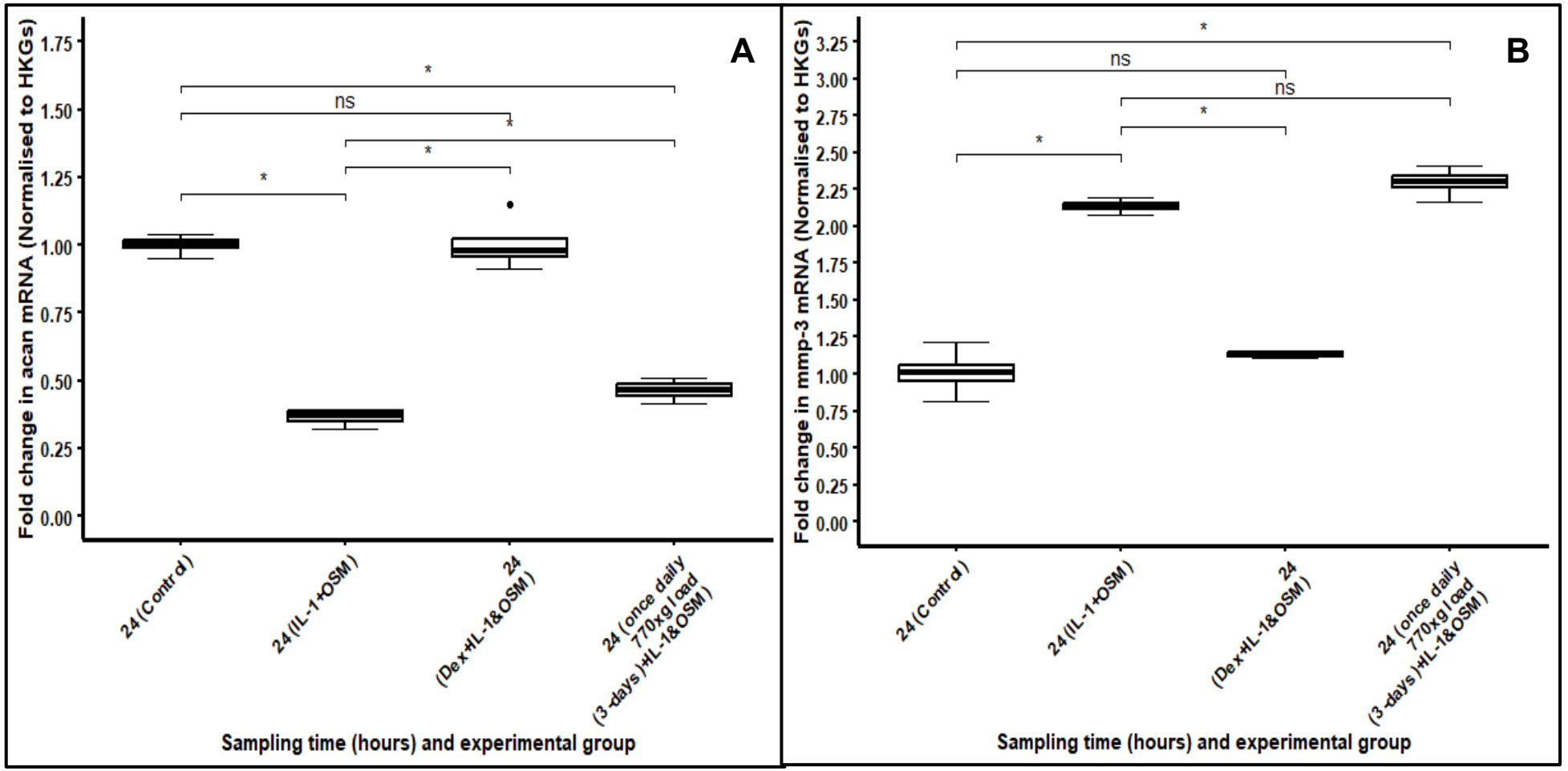


**Figure 5.12. mRNA levels for *acan* and *mmp-3* at T24 hours in response to application of 770xg force once daily for 3-days or continual Dex exposure in a 3D inflammatory OA model.** Fold change in mRNA transcripts (normalised to *18s* and *hprt*) plotted against sampling time point (T24 hours) for control 3D chondrocyte cultures and those subjected either to constant Dex exposure or 770xg force (60 minutes) once daily for 3-days after being exposed to 5 ng/ml IL-1α in combination with 10 ng/ml OSM for 24-hour (as well as the cytokine group) before qPCR quantification of the following matrix genes: **A**) *acan*, and **B**) *mmp-3*. A black dot represents an outlier in the Dex+cytokines dataset. Box and whisker plots are representative of average fold change in mRNA transcripts ± SD (n = 4, N = 2); statistical significance was assessed between control and relevant treatments at T24 hours using a Wilcoxon rank sum test in the R software and graphically annotated using the ggpubr package (* $p<0.05$, ns = no significance).

#### 5.3.2.5. Chondrocyte circadian clock responses to once daily application of 770xg force (60 minutes) for 3-days or constant Dex exposure in a 3D inflammatory OA model

##### 5.3.2.5.1. Circadian regulation of *bmal1* and *per2* transcription disrupted following cytokine stimulation within 2 LD cycles

***bmal1*** Control 3D chondrocyte pellets with no PCM exhibited rhythmic expression of *bmal1* mRNA throughout the 48-hour period of investigation ($r^2 = 0.820$, $p = 0.0001$), characterised by an amplitude of 0.265, a period of 21.4 hours, and a peak around ZT15 hours [Fig. 5.13A]. Following application of proinflammatory cytokines, this regulation was lost ($r^2 = 0.575$, $p = 0.0221$) [Fig. 5.13A]. *bmal1* mRNA rhythmicity was validated in the repeat experiment, with proinflammatory cytokines disrupting this circadian rhythm (data not shown).

***per2*** A circadian pattern of *per2* gene transcription was observed in control 3D pellets with no PCM within a 48-hour timeframe ($r^2 = 0.835$, $p = 0.0001$) [Fig. 5.13B], displaying an amplitude of 0.290, a 20-hour period, and a peak around ZT6 hours. Application of proinflammatory cytokines abolished this circadian rhythm ($r^2 = 0.272$, $p = 0.0004$) [Fig. 5.13B]. Circadian regulation of *per2* transcription was validated in a repeat experiment which was lost following cytokine stimulation (data not shown).

##### 5.3.2.5.2. Induction of *bmal1* and *per2* mRNA rhythmicity in cytokine-stimulated 3D cultures following continual application of dexamethasone in the presence of cytokines

***bmal1*** As anticipated, cytokine-stimulated pellets with no PCM exposed to 100 nM Dex (co-applied with cytokines) demonstrated circadian expression of *bmal1* mRNA transcripts within a 48-hour period ($r^2 = 0.841$, $p = 0.0001$) [Fig. 5.13A], as characterised by an amplitude of 0.258, a period of 21.4 hours, and a peak around ZT13 hours. However, the observed differences in the amplitude, period and phase angle of *bmal1* mRNA rhythm between individual LD cycles of control and Dex+cytokine-treated 3D pellet cultures were not statistically different (amplitude; $p = 0.1044$, period; $p = 0.4532$, phase; $p = 0.6149$ (data not shown)).

***per2*** As expected, subjecting cytokine-stimulated 3D pellets with no PCM to Dex in the presence of cytokines resulted in the resurgence of circadian regulation of *per2* transcription in throughout the 48-hour period of investigation ($r^2$ = 0.852, p = 0.0001) [Fig. 5.13B], characterised by an amplitude of 0.396, period of 20 hours, and a peak at ZT12 hours hence demonstrating an ~6 hour phase shift relative to controls.

#### 5.3.2.5.3. Once daily application of 770xg force for 3-days (in the presence of cytokines) did not reset circadian rhythmicity of *bmal1* and *per2* transcription in cytokine-stimulated 3D pellets with no PCM

***bmal1*** Interestingly, cytokine-stimulated 3D pellets subjected to once daily exposure to 770xg force (60 minutes) for 3-days exhibited arrhythmic expression of *bmal1* mRNA within 2 LD cycles ($r^2$ = 0.175, p = 0.0089) [Fig. 5.13A], which was validated in a repeat experiment.

***per2*** Likewise, the lack of rhythmicity of *per2* transcription within 2 LD cycles in cytokine-stimulated 3D pellet cultures persisted following once daily application of 770xg force (60 minutes) for 3-days ($r^2$ = 0.1036, p = 0.0686) [Fig. 5.13B], an outcome that was validated in a repeat experiment.

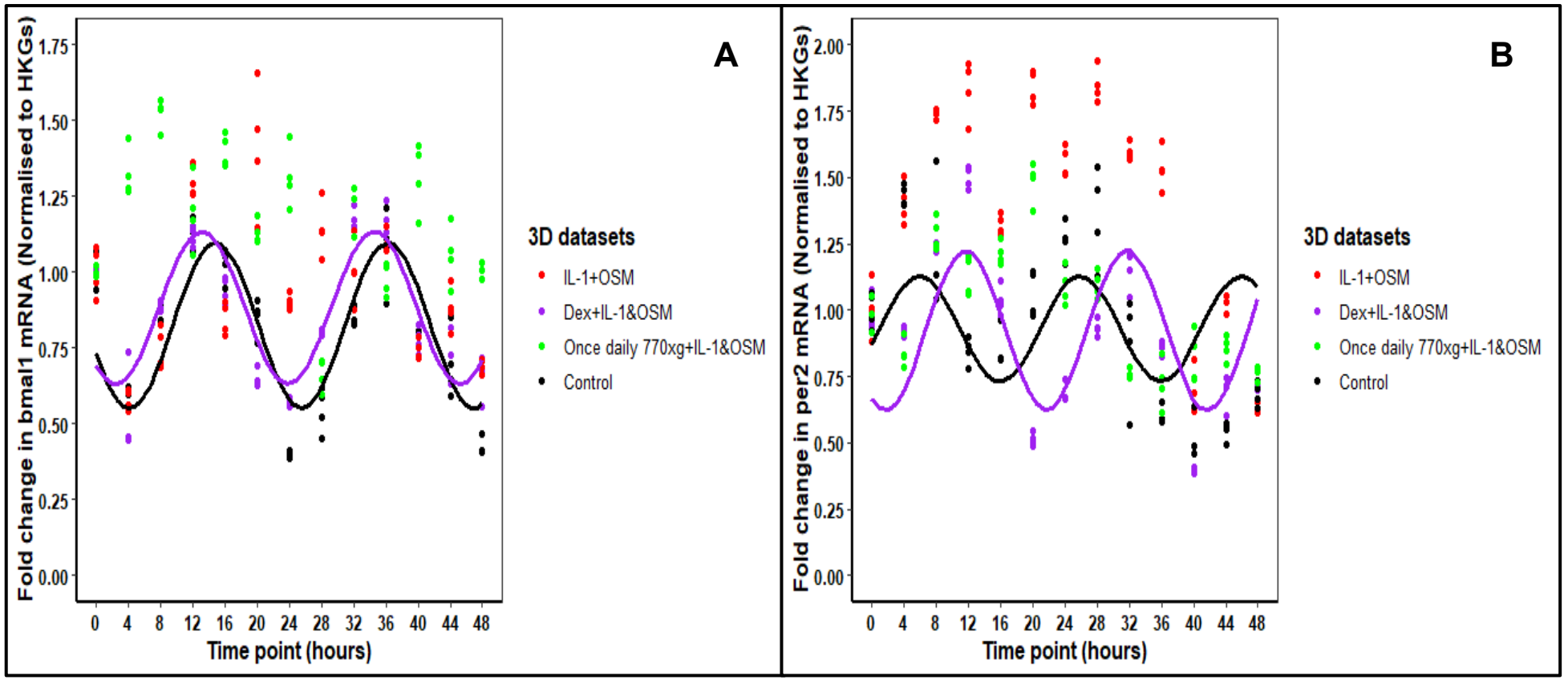


**Figure 5.13. Effect of applying 770xg force once daily for 3-days or continual Dex exposure on *bmal1* and *per2* transcription in a 3D inflammatory OA model.** Fold change in mRNA transcripts (normalised to *18s* and *hprt*) plotted against time of collection (4-hour interval) of control 3D chondrocyte pellet cultures and those exposed to once daily 770xg force (60 minutes) for 3-days in the presence of cytokines (after they were exposed to 5 ng/ml IL-1β in combination with 10 ng/ml OSM for 24 hours) or continual Dex in the presence of cytokines (including the cytokine only group) before qPCR quantification of the following genes within a 48-hour period: **A**) *bmal1*, and **B**) *per2*. Black dots; control datasets, green dots; once daily 770xg force for 3-days datasets, purple dots; Dex plus cytokine datasets, red dots; cytokine (IL-1α+OSM) datasets. The fitted cosinusoidal waves (black or purple curves) indicate rhythmic oscillations of mRNA transcripts in controls and following co-application of Dex and cytokines determined by the CircWaveBatch software ($R^2 > 0.8$, $p < 0.05$) and graphically plotted in the R software using the ggplot2 package. The absence of a cosinusoidal wave in a plot indicates an arrhythmic expression of a gene determined by the CircWaveBatch software ($R^2 < 0.8$, or $p > 0.05$). Data is representative of the fold change in mRNA levels ($n = 4$, $N = 2$).

### 5.3.2.6. Investigating the influence of once daily application of 770xg force for 3-days or continual Dex exposure on *acan* and *mmp-3* expression (and determining their rhythmicity status) in inflammatory OA pellets with no PCM

Following the determination of clock gene responses to once daily 770xg force application for 3-days or constant Dex treatment in an *in vitro* inflammatory OA model, analyses were carried out to assess similar parameters for a cartilage ECM anabolic gene *acan* and catabolic gene *mmp-3* using the same 3D model.

#### 5.3.2.6.1. Lack of circadian regulation of *acan* and *mmp-3* transcription persisted following cytokine stimulation

***acan*** Control 3D pellets with no PCM exhibited arrhythmic expression of *acan* mRNA ($r^2$ = 0.158, p = 0.1173) within a 24-hour period [Fig. 5.14A]. No rhythmic oscillations of *acan* mRNA were observed following cytokine stimulation either ($r^2$ = 0.185, p = 0.0777) in the first LD cycle [Fig. 5.14A]; responses were validated in a repeat experiment.

***mmp-3*** *mmp-3* mRNA was not rhythmic in control 3D pellets with no PCM ($r^2$ = 0.049, p = 0.2938) within a 48-hour period [Fig. 5.14B]. Following exposure to proinflammatory cytokines, 3D chondrocyte pellets continued to exhibit a lack of circadian regulation of *mmp-3* transcription ($r^2$ = 0.350, p = 0.0001) within a 48-hour period [Fig. 5.14B]; all responses were validated in a repeat experiment.

#### 5.3.2.6.2. Lack of circadian control of *acan* and *mmp-3* transcription persisted in cytokine-treated 3D pellets with no PCM following continual exposure to dexamethasone

Following application of Dex and cytokines, 3D pellet cultures with prior exposure to cytokines still exhibited no circadian expression of ***acan*** within a 24-hour period ($r^2$ = 0.014, p = 0.8416) [Fig. 5.14A], or ***mmp-3*** mRNA within two LD cycles ($r^2$ = 0.209, p = 0.0032) [Fig. 5.14B].

#### 5.3.2.6.3. Lack of circadian regulation of *acan* and *mmp-3* transcription in cytokine-treated cultures persisted following once daily application of 770xg force for 3-days

Cytokine-treated 3D pellets with no PCM subjected to once daily episodes of 770xg force (60 minutes) for 3-days (in the presence of cytokines) exhibited no rhythmic oscillations of ***acan*** mRNA within a 24-hour period ($r^2$ = 0.230, p = 0.0384) [Fig. 5.14A] or ***mmp-3*** mRNA

levels within two LD cycles ($r^2$ = 0.134, p = 0.0298) [Fig. 5.14B]; data findings were validated in a repeat experiment.

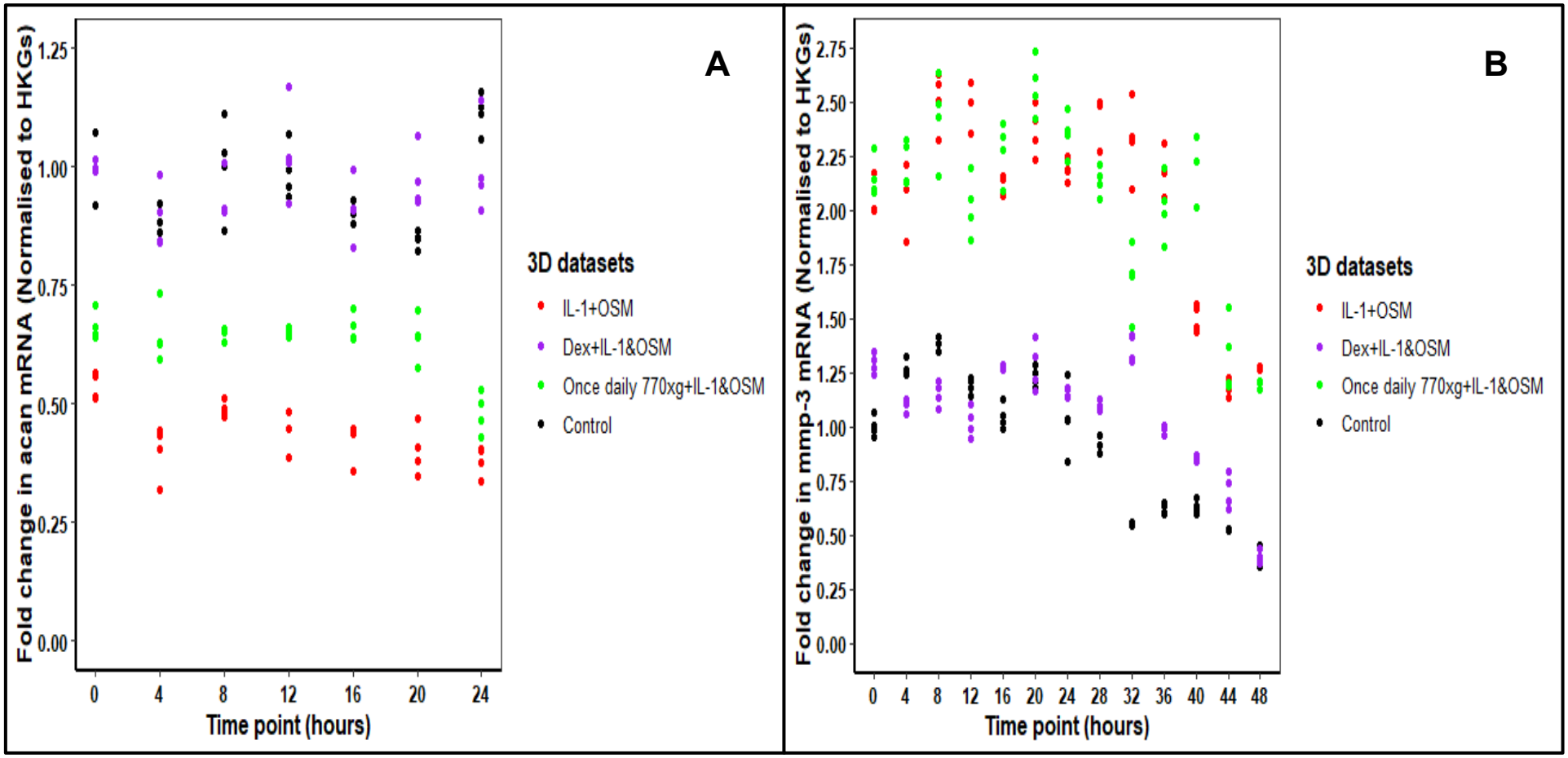


**Figure 5.14. Effect of applying 770xg force once daily for 3-days or continual Dex exposure on *acan* and *mmp-3* transcription within a 48-hour timeframe in a 3D inflammatory OA model.** Fold change in mRNA transcripts (normalised to *18s* and *hprt*) plotted against time of collection (4-hour interval) of control 3D chondrocyte pellets with no PCM and those exposed to 770xg centrifugal force (60 minutes) once daily for 3 days in the presence of cytokines (after they were exposed to a combination of 5 ng/ml IL-1β and 10 ng/ml OSM for 24-hours) or constant Dex in the presence of cytokines (including the cytokine [IL-1α+OSM] only group) before qPCR quantification of the following genes either within a 24 or 48-hour period: **A**) *acan* [1 LD cycle], and **B**) *mmp-3* [2 LD cycles]. Black dots; control datasets, green dots; once daily 770xg force for 3-days+cytokine datasets, purple dots; Dex+cytokine datasets, red dots; cytokine (IL-1α+OSM) datasets. The absence of a cosinusoidal wave in a plot indicates an arrhythmic expression of these genes determined by the CircWaveBatch software ($R^2 < 0.8$, or $p > 0.05$). Data is representative of the fold change in mRNA transcripts (n = 4, N = 2).

### 5.3.3. Response of 3D chondrocyte cultures to application of 770xg force twice daily for 1- or 2-days in an *in vitro* inflammatory OA model

Having established the inability of once daily application of 770xg force (60 minutes) for 3-days to (i) reset chondrocyte circadian clocks (no induction of *bmal1* and *per2* mRNAs circadian rhythm following cytokine exposure) nor (ii) reverse the anti-anabolic and catabolic effects of proinflammatory cytokines (persistence of downregulated *acan* mRNA and upregulated *mmp-3* mRNA following cytokine exposure) in a 3D inflammatory OA model, experiments were carried out (described in section 5.2.3) to establish if application of 770xg force (60 minutes) twice daily for 1- or 2-days will be sufficient to reset the disrupted circadian rhythm of clock genes (*bmal1*, *npas2*, *nr1d1*, *per1* and *per2*) and reverse the anti-anabolic effects (*acan* transcription) and catabolic effects (*adamts-4* transcription) of proinflammatory cytokines in 3D inflammatory OA pellets with no PCM.

#### 5.3.3.1. Application of 770xg force (60 minutes) twice daily for 1- or 2-days had no effect on reduced sGAG release in 3D inflammatory OA pellets with no PCM

Significant increases in sGAG concentration were observed in control pellets with no PCM relative to T0 hours with levels increasing from 9.83±0.231 µg/ml at T0 hours, 16.8±1.06 µg/ml at T24 hours [p= 0.002], and at T48 hours where 15.4±0.23 µg/ml was detected [p = 4.018e-05] [Fig. 5.15A]. In cytokine-treated 3D pellets, sGAG concentration remained unaltered at 24-hour intervals within a 48-hour window relative to T0 hours (8.36±1.06 µg/ml) with: T24 = 9.69±0.462 µg/ml [p = 0.1544], and T48 hours = 9.83±0.611 µg/ml [p = 0.131] [Fig. 5.15B].

Surprisingly, cytokine stimulation had no effect on sGAG levels relative to controls at T0 hours, i.e., in the first LD cycle of investigation (p = 0.1397) [Fig. 5.16A]; however, a significant reduction in sGAG concentration was observed between control and cytokine-treated cultures at T24 hours (p = 0.0004447) [Fig. 5.16A]. Likewise, significant reductions in sGAG concentration were observed at T24 hours in the second LD cycles in cytokine-treated 3D pellets (corresponding to the twice daily load for 2 days timeframe) (p = 0.004454) [Fig. 5.16B].

Significantly reduced sGAG concentrations were observed at T0- (p = 0.007085) and T24-hours (p = 0.00145) between control and cytokine-treated cultures subjected to 770xg

force (60 minutes) twice daily for 1-day [Fig. 5.16A]. However, similar sGAG levels were observed between cytokine-treated and twice daily for 1-day 770xg force stimulated cultures (following cytokine stimulation) at T0- ($p = 0.9488$), and T24-hours ($p = 0.2772$) [Fig. 5.16A].

Cytokine-treated pellet cultures subjected to 770xg force (60 minutes) twice daily for 2-days had significantly reduced sGAG levels at T0- ($p = 0.0143$) and T24-hours ($p = 0.03112$) when compared to corresponding controls [Fig. 5.16B]. Cytokine-treated and twice daily for 1-day 770xg force stimulated cultures (following cytokine stimulation) had comparable sGAG concentrations at T0- ($p = 0.9582$) and T24-hours ($p = 0.935$) to the cytokine with twice daily load for 2-days regimen [Fig. 5.16B].

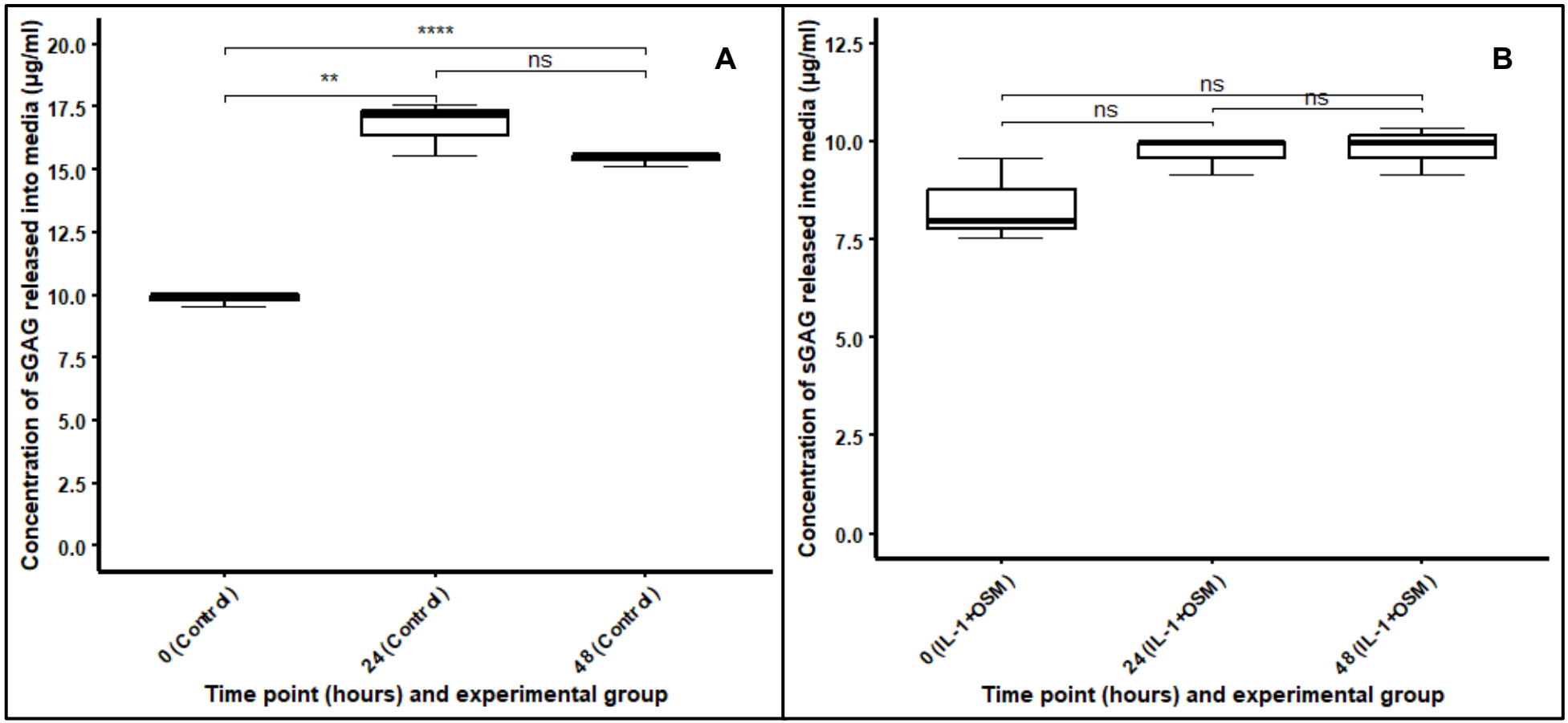


**Figure 5.15. Baseline sGAG concentrations and the influence of proinflammatory cytokines on sGAG release within a 48-hour window in a 3D model.** The graph illustrates box and whisker plots representing the total concentration of sGAG ± SD in culture media collected at T0-, 24- and 48-hours from: **A**) control cultures, and **B**) cytokine-treated cultures (5 ng/ml IL-1α in combination with 10 ng/ml OSM for 24-hours). Statistically significant differences in sGAG concentration between two time points within the same experimental group were determined by a Welch Two Sample t-test in the R software and graphically annotated using the ggpubr package (** $p<0.01$, **** $p<0.0001$, ns = no significance) (n = 4, N = 1).

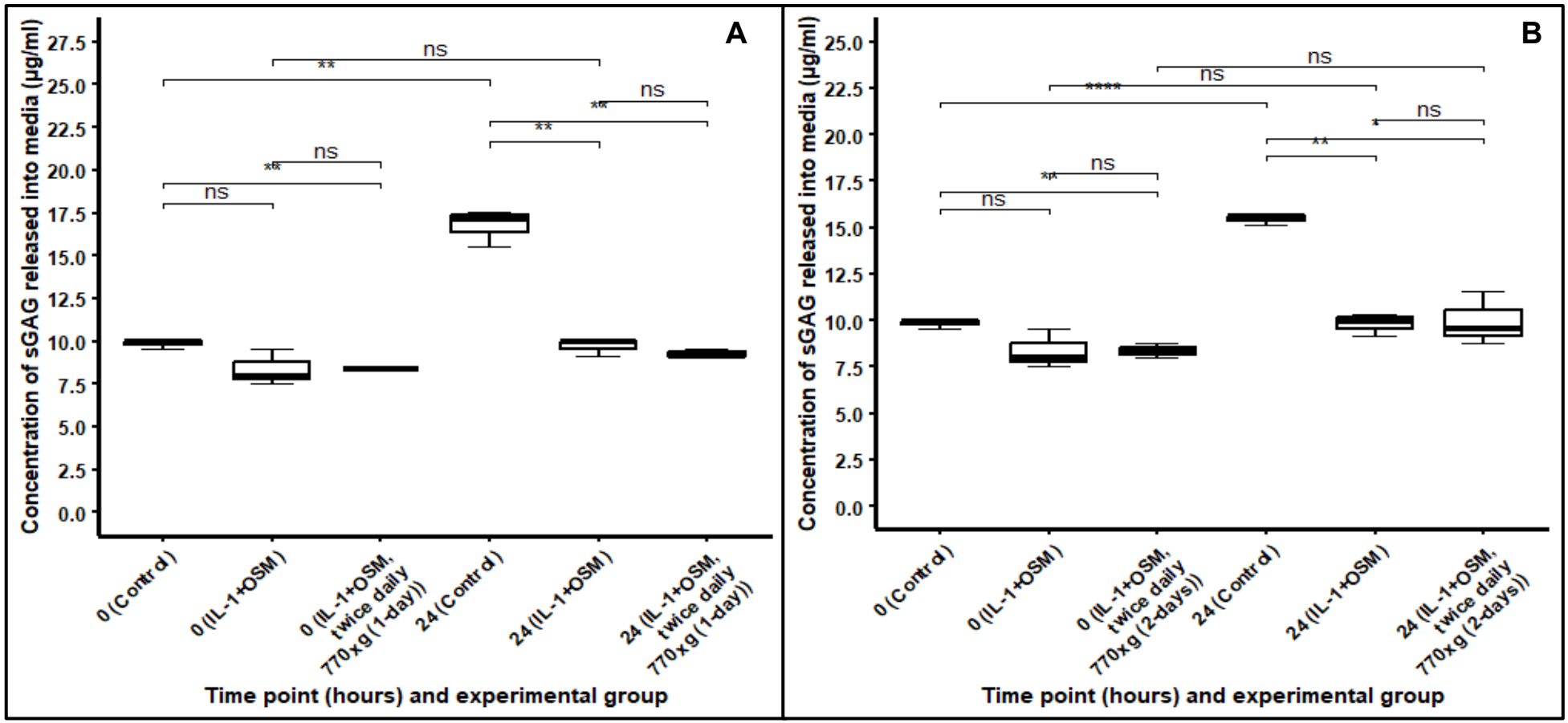


**Figure 5.16. Influence of applying 770xg force (60 minutes) either twice daily for 1- or 2-days on sulphated GAG release within 2 consecutive LD cycles in 3D inflammatory OA pellets with no PCM.** The graph illustrates box and whisker plots representing the total concentration of sGAG ± SD in culture media collected from the following experimental groups at the following time points: **A**) control, IL-1α plus OSM and twice daily load for 1-day (following IL-1α plus OSM stimulation); T0- and T24-hours, and **B**) control, IL-1α plus OSM and twice daily load for 2-days (following IL-1α plus OSM stimulation); T0- and T24-hours (technically T24 and 48-hours relative to the initial T0 hours as described in Fig. 5.2). Statistically significant differences in sGAG concentration between two experimental groups or time points within the same group were determined by a Welch Two Sample t-test in the R software and graphically annotated using the ggpubr package (* $p<0.05$, ** $p<0.01$, **** $p<0.0001$, ns = no significance) (n = 4, N = 1).

### 5.3.3.2. Application of 770xg force (60 minutes) twice daily for 1- or 2-days had no effect on cytokine-induced nitrite/NO release in 3D inflammatory OA pellets with no PCM

In control pellet cultures, the concentration of nitrite/NO was barely detectable within a 48-hour window and was not significantly altered between T0 hours (1.44±0.24 μM), T24 hours (1.36±0.14 μM) and T48 hours (1.6±0.14 μM) [Fig. 5.17A]. In contrast, nitrite/NO concentration was significantly elevated in cytokine-treated pellet cultures at 24-hour intervals within a 48-hour window relative to T0 hours (1.56±0.37 μM) with levels increasing to 3.27±0.12 μM at T24 hours ($p = 0.0092$), and at T48 hours where 2.54±0.12 μM was detected ($p = 0.0018$) [Fig. 5.17B]. Surprisingly, no significant differences in nitrite/NO production were observed following cytokine stimulation when compared to controls at T0 hours, i.e., in the first LD cycle of investigation ($p = 0.6949$) [Fig. 5.18A]; however, significantly increased nitrite/NO production was observed between control and cytokine-treated cultures at T24 hours ($p = 0.00558$) [Fig. 5.18A]. Likewise, significantly elevated nitrite/NO production was detected at T24 hours in the second LD cycle in cytokine-treated 3D pellets (corresponding to the twice daily load for 2-days timeframe) ($p = 0.04032$) [Fig. 5.18B].

No differences in nitrite/NO concentration were detected in cytokine-treated pellet cultures with application of twice daily load for 1-day relative to controls at T0 hours ($p = 0.889$) [Fig. 5.18A]. However, a significant increase was observed following cytokine stimulation at T24 hours ($p = 0.000223$) [Fig. 5.18A], but, similar nitrite/NO levels were also observed when comparing cytokine-treated against twice daily load for 1-day stimulated cultures (following cytokine stimulation) at T0- ($p = 0.9322$) and T24-hours ($p = 0.0872$) [Fig. 5.18A].

As with the twice daily load for 1-day regimen, cytokine-treated pellet cultures subjected to twice daily load for 2-days stimulation also showed no significant differences in nitrite/NO concentration at T0 hours when compared to controls ($p = 0.2901$) [Fig. 5.18B]. At T24 hours, significantly increased nitrite/NO concentration was observed following cytokine stimulation relative to controls ($p = 0.00801$) [Fig. 5.18B], but these cytokine-induced nitrite/NO levels were comparable to the twice daily load for 2-days stimulated cultures (following cytokine stimulation) at T0- ($p = 0.399$) and T24-hours ($p = 0.8051$) [Fig. 5.18B].

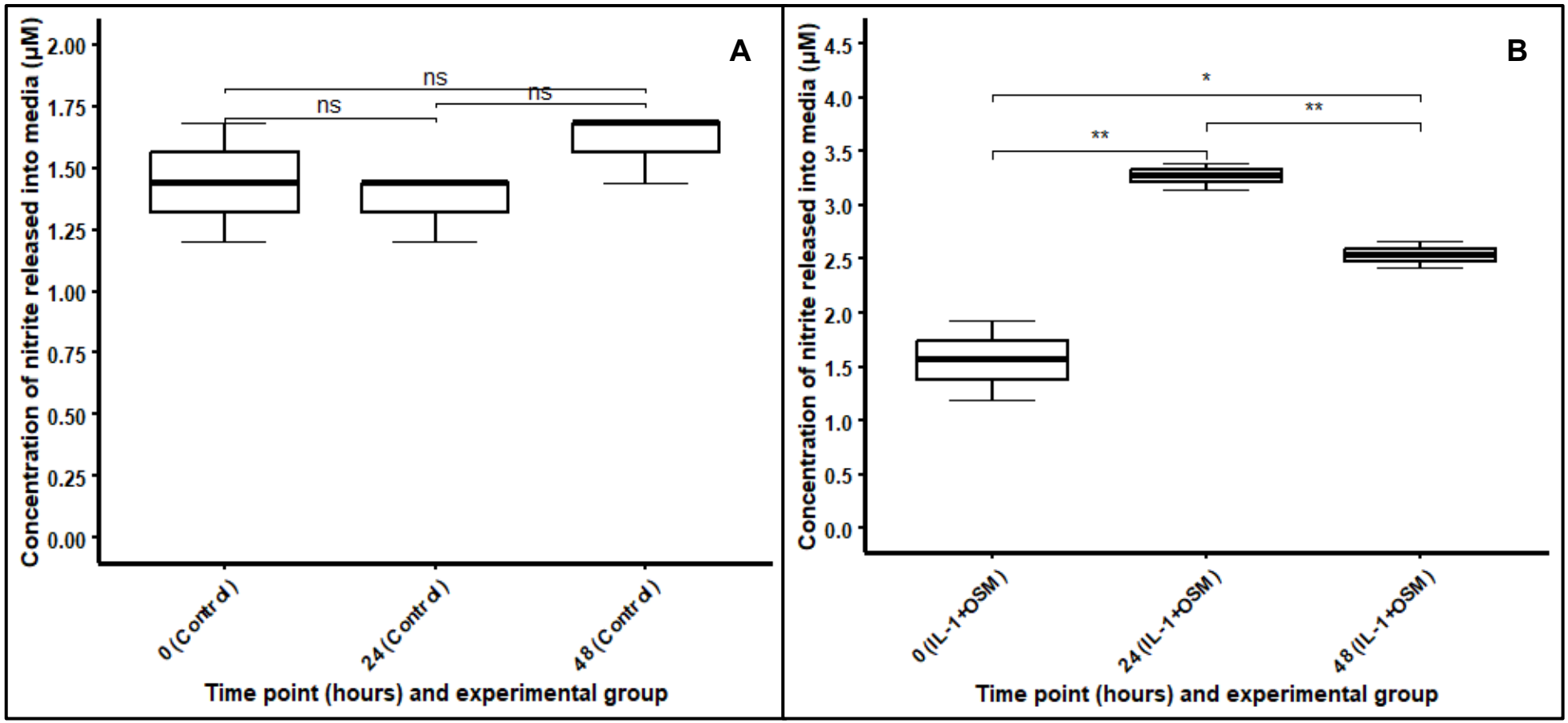


**Figure 5.17. The influence of proinflammatory cytokines on nitrite/NO release within a 48-hour window in a 3D chondrocyte pellets with no PCM.** The graph illustrates box and whisker plots representing the total concentration of nitrite/NO ± SD in culture media collected at T0-, 24- and 48-hours from: **A**) control cultures, and **B**) cytokine-treated cultures (5 ng/ml IL-1α in combination with 10 ng/ml OSM). Statistically significant differences in nitrite/NO concentrations between two time points within the same experimental group were determined by a Welch Two Sample t-test in the R software and graphically annotated using the ggpubr package (* $p<0.05$, ** $p<0.01$, ns = no significance) (n = 4, N = 1).

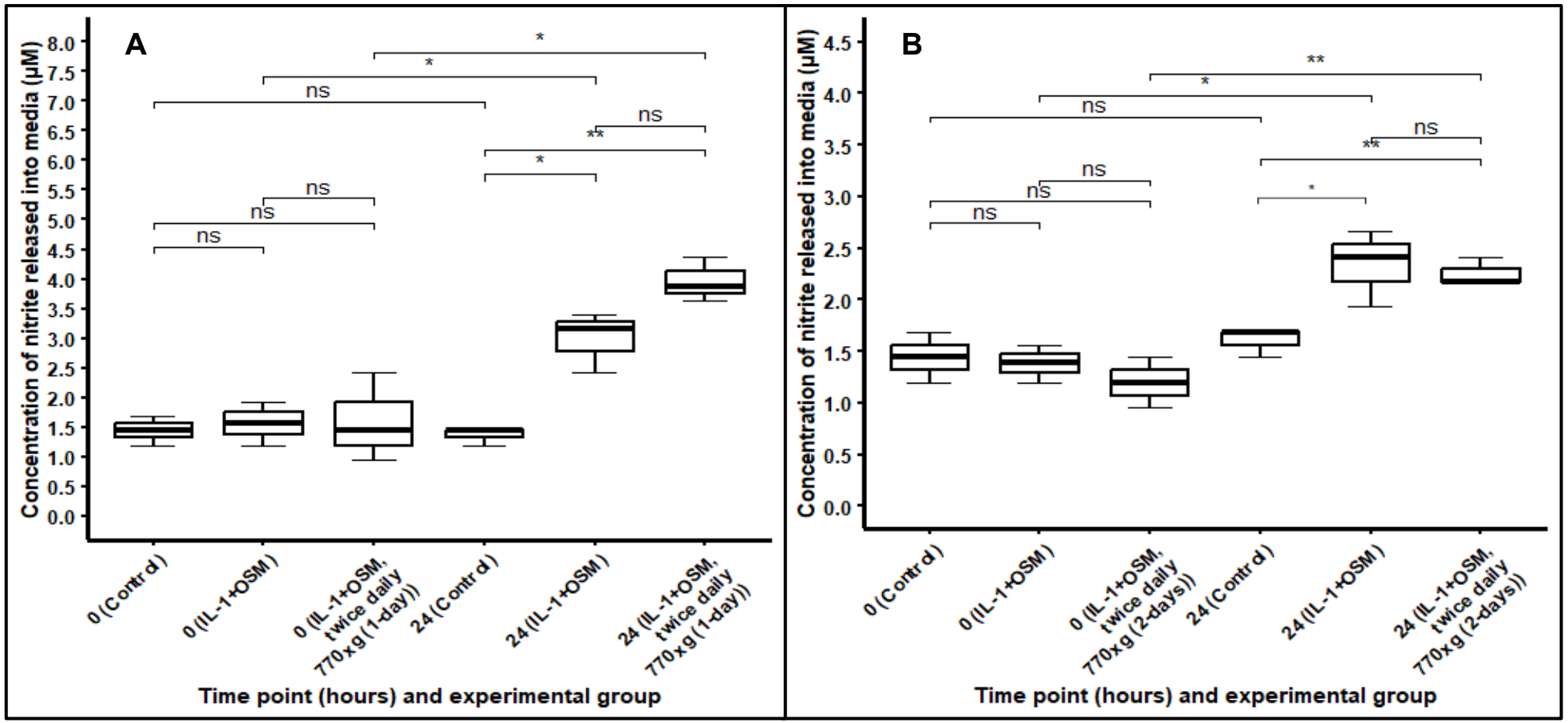


**Figure 5.18. Influence of applying 770xg force (60 minutes) either twice daily for 1- or 2-days on nitrite/NO release within 2 consecutive LD cycles in 3D inflammatory OA pellets with no PCM.** The graph illustrates box and whisker plots representing the total concentration of nitrite/NO ± SD in culture media collected from the following experimental groups at the following time points: A) control, IL-1α plus OSM and twice daily load for 1-day (following IL-1α plus OSM stimulation); T0- and T24-hours, and **B**) control, IL-1α plus OSM and twice daily load for 2-days (following IL-1α plus OSM stimulation); T0- and T24-hours (technically T24 and 48-hours relative to the initial T0 hours as described in Fig. 5.2). Statistically significant differences in nitrite/NO concentrations between two experimental groups or time points within the same group were determined by a Welch Two Sample t-test in the R software and graphically annotated using the ggpubr package (* $p<0.05$, ** $p<0.01$, ns = no significance) (n = 4, N = 1).

#### 5.3.3.3. The effect of applying 770xg force (60 minutes) either twice daily for 1- or 2-days on *acan* and *adamts-4* transcription in cytokine-stimulated pellets with no PCM

To confirm the anti-anabolic and catabolic effects of proinflammatory cytokines as well as determining whether applying 770xg force (60 minutes) either twice daily for 1- or 2-days has anti-inflammatory actions on cytokine-stimulated chondrocytes, changes in *acan* and *adamts-4* mRNA transcripts at T24- and T48-hours were used as examples to demonstrate chondrocyte responses.

##### 5.3.3.3.1. Downregulation of *acan* mRNA and upregulation of *adamts-4* mRNA at T24- and 48-hours following cytokine stimulation

***acan*** A significant 7.75-fold reduction in *acan* transcription, a marker of ECM anabolism, was observed at T24 hours in cytokine-stimulated 3D pellets with no PCM ($p = 2.3e-05$) [Fig. 5.19A]. Furthermore, a 1.71-fold decrease in *acan* mRNA was observed 48 hours post-stimulation ($p = 0.01768$) [Fig. 5.19B].

***adamts-4*** Application of proinflammatory cytokines to 3D pellets with no PCM resulted in a 3.46-fold upregulation of the ECM catabolism marker *adamts-4* mRNA, 24-hours post-stimulation ($p = 0.005785$) [Fig. 5.20A]. Again, a 2.96-fold upregulation of *adamts-4* mRNA was observed at T48 hours following cytokine stimulation ($p = 0.00132$) [Fig. 5.20A].

##### 5.3.3.3.2. Persistent downregulation of *acan* mRNA and upregulation of *adamts-4* mRNA at T24- and 48-hours in cytokine-stimulated 3D pellets with no PCM following application of 770xg force twice daily for 1- and 2-days

***acan*** Significantly reduced *acan* mRNA levels were observed at T24 hours in cytokine-treated 3D pellets following twice daily 770xg load for 1-day (6.58-fold, $p = 0.000592$) [Fig. 5.19A]. A reduction in *acan* mRNA levels at T24 hours (i.e., at T48 hours relative to the twice daily 770xg load for 1-day timeframe) persisted following twice daily 770xg load for 2-days of cytokine-treated 3D pellet cultures (1.61-fold, $p = 0.0147$) [Fig. 5.19B].

***adamts-4*** Following twice daily 770xg load for 1-day, cytokine-treated 3D pellets still revealed a 2.24-fold upregulation in *adamts-4* mRNA transcripts at T24 hours ($p = 5.084e-06$) [Fig. 5.20A]. Similarly, cytokine-treated 3D pellet cultures also continued to demonstrate significantly increased mRNA transcripts for *adamts-4* 24-hours post twice

daily 770xg load for 2-days (i.e., at T48 hours relative to the twice daily 770xg load for 1-day timeframe) (2.55-fold, p = 0.003074) [Fig. 5.20A].

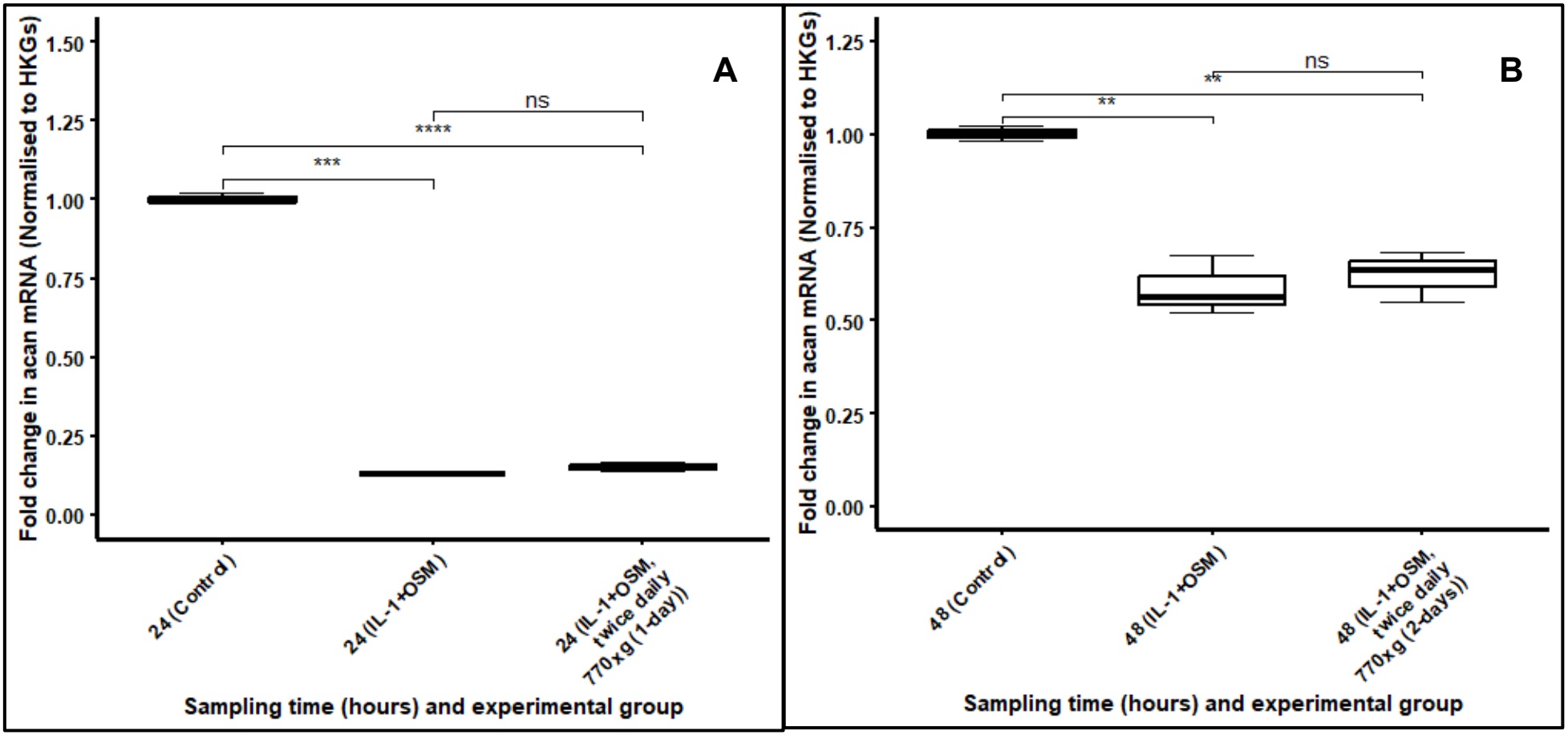


**Figure 5.19. *acan* mRNA levels at T24- and T48-hours in 3D inflammatory OA pellets with no PCM in response to application of 770xg force either twice daily for 1- or 2-days.** Box and whisker plots represent average fold change in *acan* mRNA transcripts (normalised to *18s* and *hprt*) ± SD (n = 3, N = 1) plotted against either T24- or T48-hours for control 3D chondrocyte pellets with no PCM and those subjected to 770xg force either twice daily for 1- or 2-days after being exposed to 5 ng/ml IL-1α in combination with 10 ng/ml OSM for 24-hour (as well as the cytokine [IL-1α+OSM] group) before qPCR quantification at specific time points: **A**) T24 hours for the control, cytokine and twice daily load for 1-day groups, and **B**) T48 hours for the control, cytokine and twice daily load for 2-days groups (this is actually T24 hour for the loaded group only because T0 hours was taken 48 hours after the initiation of the first AM centrifugation as described in section 5.2.3 and Fig. 5.2). Statistical significance was assessed between control and relevant treatments using a Welch Two Sample t-test in the R software and graphically annotated using the ggpubr package (** $p<0.01$, *** $p<0.001$, **** $p<0.0001$, ns = no significance).

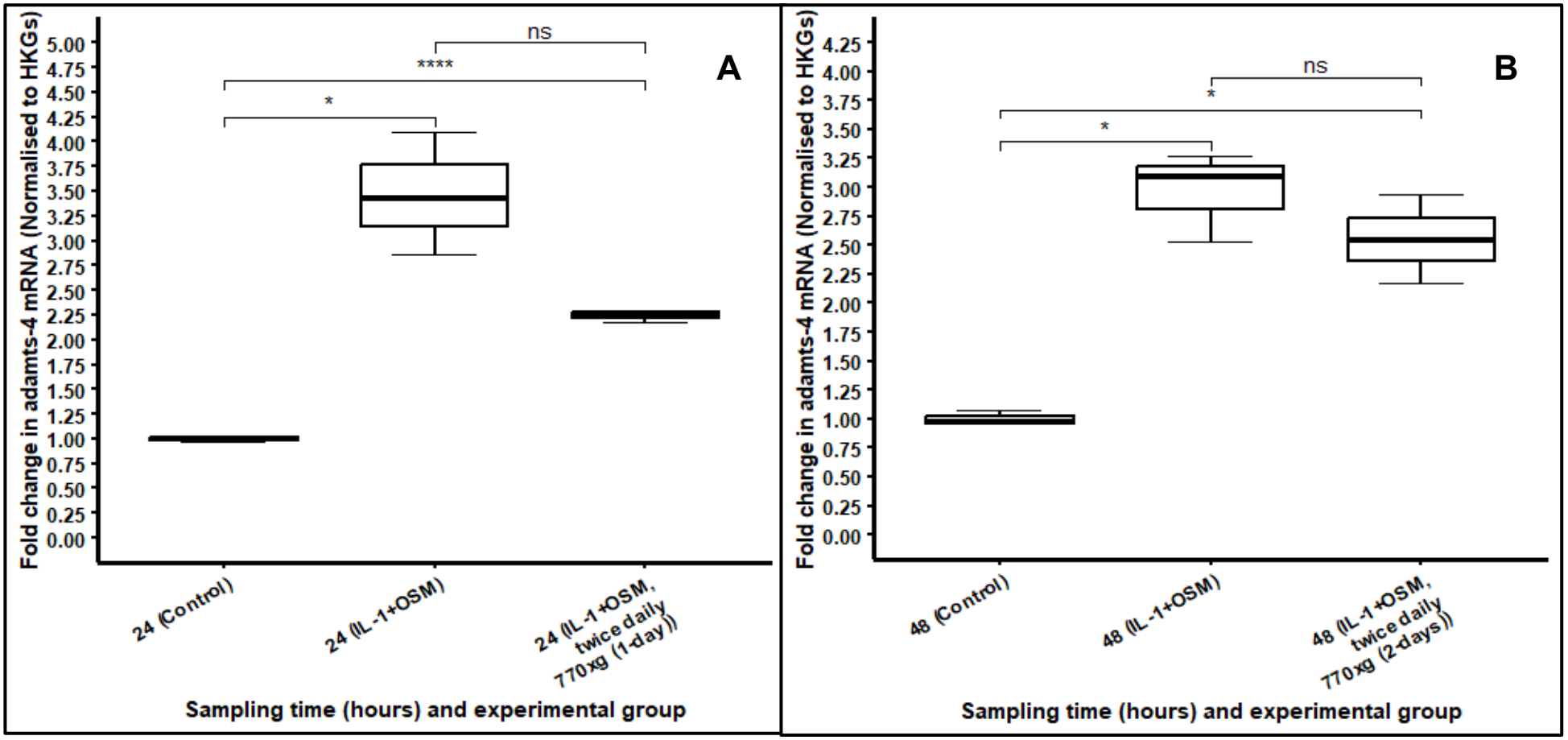


**Figure 5.20. *adamts-4* mRNA levels at T24- and T48-hours in 3D inflammatory OA pellets with no PCM in response to application of 770xg force either twice daily for 1- or 2-days.** Box and whisker plots represent average fold change in *adamts-4* mRNA transcripts (normalised to *18s* and *hprt*) ± SD (n = 3, N = 1) plotted against either T24- or T48-hours for control 3D chondrocyte pellets with no PCM and those subjected to 770xg force either twice daily for 1- or 2-days after being exposed to 5 ng/ml IL-1α in combination with 10 ng/ml OSM for 24-hour (as well as the cytokine [IL-1α+OSM] group) before qPCR quantification at specific time points: **A**) T24 hours for the control, cytokine and twice daily load for 1- day groups, and **B**) T48 hours for the control, cytokine and twice daily load for 2-days groups (this is actually T24 hour for the loaded group only because T0 hours was taken 48 hours after the initiation of the first AM centrifugation as described in section 5.2.3 and Fig. 5.2). Statistical significance was assessed between control and relevant treatments using a Welch Two Sample t-test in the R software and graphically annotated using the ggpubr package (* $p<0.05$, **** $p<0.0001$, ns = no significance).

### 5.3.3.4 Circadian clock gene transcription dynamics following cytokine stimulation and application of 770xg force (60 minutes) either twice daily for 1- or 2-days in 3D chondrocyte pellets with no PCM

Following determination of differing chondrocyte responses (Figs 5.15 – 5.20) to confirm expected cell behaviours to cytokine-treatment as well as the impact of applying 770xg force either twice daily for 1- or 2-days on inflammatory OA pellet cultures, analyses were carried out to assess circadian clock responses to load (i.e., transcriptional analysis of *bmal1*, *npas2*, *nr1d1*, *per1* and *per2*) at 4-hour intervals in two consecutive LD cycles in experimental samples (described in section 5.2.3 - control, 24-hour cytokine stimulation, twice daily 770xg load for 1-day following 24-hour cytokine stimulation, and twice daily 770xg load for 2-days following 24-hour cytokine stimulation [Fig. 5.2]).

#### 5.3.3.4.1. Circadian regulation of *npas2* transcription in control 3D pellets, abolished following cytokine treatment

Circadian regulation of *npas2* transcription was observed within 2 LD cycles in control 3D pellets with no PCM ($r^2$ = 0.946, p = 0.0001), with an amplitude of 0.840, a period of 20 hours, and a peak around ZT16 hours [Fig. 5.21]. Circadian rhythmicity was abolished following treatment with proinflammatory cytokines ($r^2$ = 0.075, p = 0.245) [Fig. 5.21].

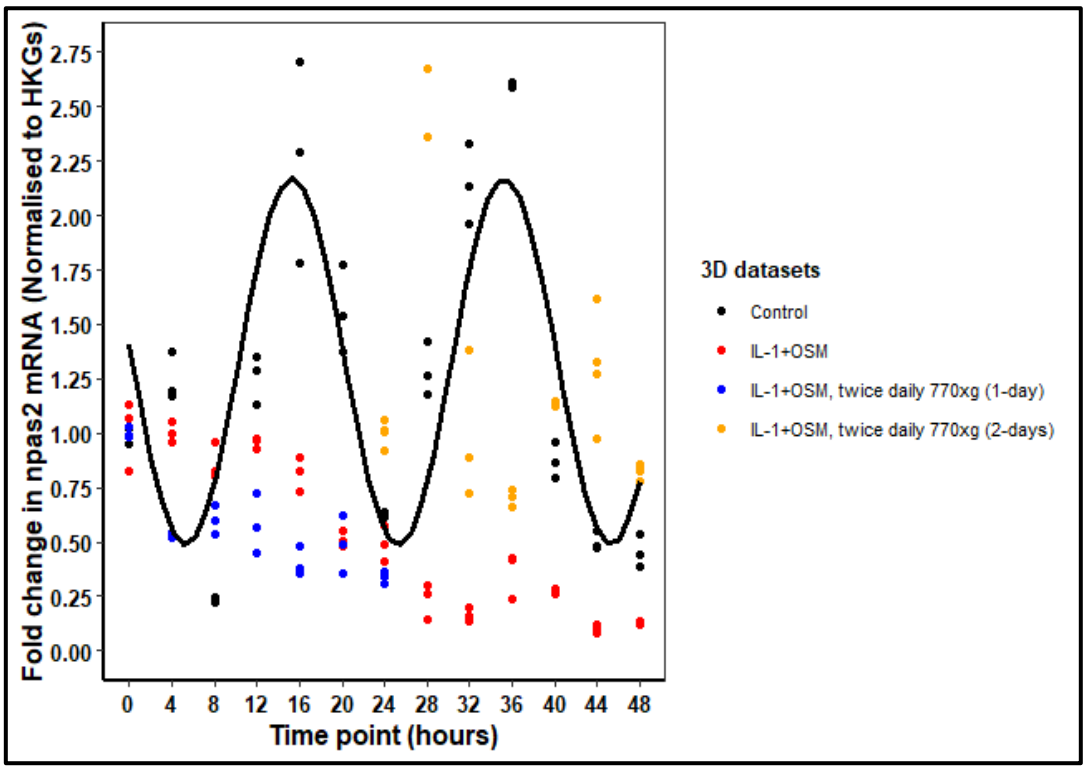


**Figure 5.21. Influence of applying 770xg force either twice daily for 1- or 2-days on *npas2* transcription in 3D inflammatory OA pellets with no PCM (induced through stimulation using IL-1α in combination with OSM).** Fold change in mRNA transcripts (normalised to *18s* and *hprt*) plotted against time of collection (at 4-hour intervals) of control 3D chondrocyte pellets with no PCM and those subjected to 770xg force (60 minutes) either twice daily for 1- or 2-days following 24-hour exposure to 5 ng/ml IL-1α in combination with 10 ng/ml OSM (as well as the cytokine [IL-1α+OSM] group) before qPCR quantification of *npas2* mRNA transcripts in two consecutive LD cycles. Black dots; control datasets, red dots; cytokine (i.e., IL-1α plus OSM) datasets, blue dots; twice daily 770xg force (60 minutes) for 1-day after IL-1α plus OSM exposure datasets, orange dots; twice daily 770xg force (60 minutes) for 2-days after IL-1α plus OSM exposure datasets. The fitted cosinusoidal waves (black curves) indicate rhythmic oscillations of *npas2* mRNA transcripts determined by the CircWaveBatch software ($R^2 > 0.8$, $p < 0.05$) and graphically plotted in the R software using the ggplot2 package. The absence of a cosinusoidal wave in a plot indicates an arrhythmic expression of *npas2* gene determined by the CircWaveBatch software ($R^2 < 0.8$, or $p > 0.05$). Data points represent fold change in mRNA transcripts (n = 3, N = 1).

#### 5.3.3.4.2. Control 3D pellets with no PCM demonstrated no circadian expression of *bmal1*, *nr1d1*, *per1* and *per2* mRNA transcripts, persisting following cytokine stimulation

Control 3D pellets with no PCM exhibited no circadian rhythm of *bmal1* ($r^2$ = 0.398, p = 0.0001 [Fig. 5.22A]), *nr1d1* ($r^2$ = 0.518, p = 0.001) [Fig. 5.22B], *per1* ($r^2$ = 0.295, p = 0.0018) [Fig. 5.22C] and *per2* ($r^2$ = 0.580, p = 0.0099) [Fig. 5.22D] transcription within a 48-hour period. Likewise, arrhythmic expression of these genes was also observed following cytokine treatment: *bmal1* ($r^2$ = 0.227, p = 0.0098) [Fig. 5.22A], *nr1d1* ($r^2$ = 0.371, p = 0.015) [Fig. 5.22B], *per1* ($r^2$ = 0.314, p = 0.0011) [Fig. 5.22C] and *per2* ($r^2$ = 0.178, p = 0.0297) [Fig. 5.22D].

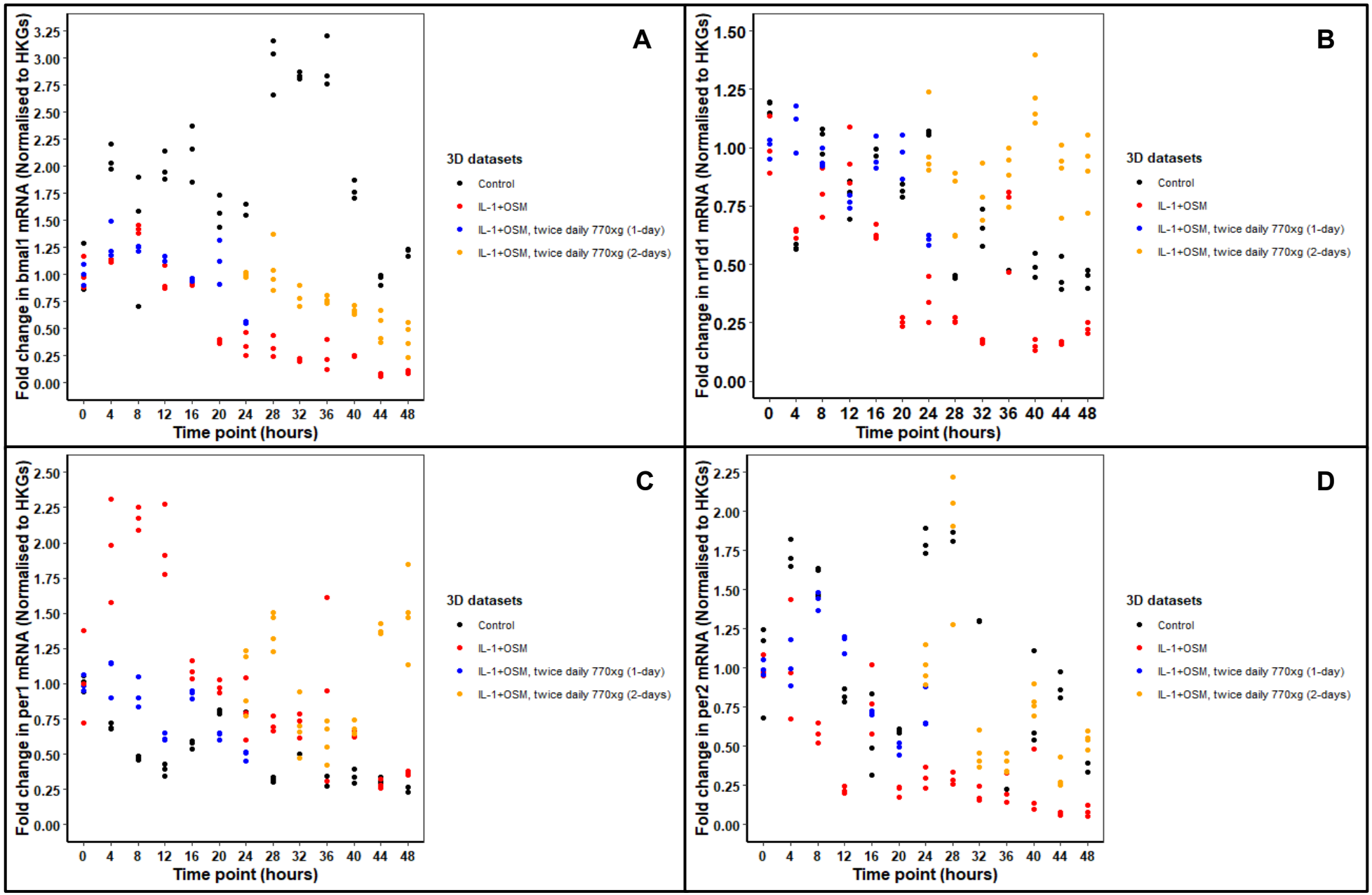
A
Fold change in bmal1 mRNA (Normalised to HKGs)
Time point (hours)
3D datasets
Control
IL-1+OSM
IL-1+OSM, twice daily 770xg (1-day)
IL-1+OSM, twice daily 770xg (2-days)
B
Fold change in nr1d1 mRNA (Normalised to HKGs)
Time point (hours)
3D datasets
Control
IL-1+OSM
IL-1+OSM, twice daily 770xg (1-day)
IL-1+OSM, twice daily 770xg (2-days)
C
Fold change in per1 mRNA (Normalised to HKGs)
Time point (hours)
3D datasets
Control
IL-1+OSM
IL-1+OSM, twice daily 770xg (1-day)
IL-1+OSM, twice daily 770xg (2-days)
D
Fold change in per2 mRNA (Normalised to HKGs)
Time point (hours)
3D datasets
Control
IL-1+OSM
IL-1+OSM, twice daily 770xg (1-day)
IL-1+OSM, twice daily 770xg (2-days)

**Figure 5.22. Influence of applying 770xg force either twice daily for 1- or 2-days on *bmal1*, *nr1d1, per1* and *per2* transcription in 3D inflammatory OA pellets with no PCM (induced through stimulation using IL-1α in combination with OSM).** Fold change in mRNA transcripts (normalised to *18s* and *hprt*) plotted against time of collection (at 4-hour intervals) of control 3D chondrocyte pellets with no PCM and those subjected to 770xg force (60 minutes) either twice daily for 1- or 2-days following 24-hour exposure to 5 ng/ml IL-1α in combination with 10 ng/ml OSM (as well as the cytokine [IL-1α+OSM] group) before qPCR quantification of the following genes in two consecutive LD cycles: **A)** *bmal1*, **B)** *nr1d1*, **C)** *per1* and **D)** *per2*. Black dots; control datasets, red dots; cytokine (i.e., IL-1α plus OSM) datasets, blue dots; twice daily 770xg force (60 minutes) for 1-day after IL-1α plus OSM exposure datasets, orange dots; twice daily 770xg force (60 minutes) for 2-days after IL-1α plus OSM exposure datasets. The fitted cosinusoidal waves (black curves) indicate rhythmic oscillations of mRNA transcripts for a particular clock gene determined by the CircWaveBatch software ($R^2 > 0.8$, $p < 0.05$) and graphically plotted in the R software using the ggplot2 package. The absence of a cosinusoidal wave in plots indicate arrhythmic expression of genes determined by the CircWaveBatch software ($R^2 < 0.8$, or $p > 0.05$) and graphically plotted in the R software using the ggplot2 package. Data points represent fold change in mRNA transcripts (n = 3, N = 1).

#### 5.3.3.4.3. No circadian regulation of clock gene transcription following application of 770xg force (60 minutes) either twice daily for 1- or 2-days in cytokine-treated 3D pellets with no PCM

Following the application of 770xg force twice daily for 1-day to cytokine-stimulated 3D pellets with no PCM, no rhythmic oscillations of the following gene transcripts were observed: ***npas2*** ($r^2$ = 0.263, p = 0.064) [Fig. 5.21], ***bmal1*** ($r^2$ = 0.516, p = 0.0001) [Fig. 5.22A], ***nr1d1*** ($r^2$ = 0.614, p = 0.0002) [Fig. 5.22B], ***per1*** ($r^2$ = 0.343, p = 0.0228) [Fig. 5.22C] and ***per2*** mRNA ($r^2$ = 0.456, p = 0.0042) [Fig. 5.22D].

Likewise, cytokine-treated 3D pellets with no PCM subjected to 770xg force twice daily for 2-days exhibited no circadian regulation of these clock genes: ***npas2*** ($r^2$ = 0.222, p = 0.0437) [Fig. 5.21], ***bmal1*** ($r^2$ = 0.375, p = 0.0028) [Fig. 5.22A], ***nr1d1*** ($r^2$ = 0.425, p = 0.001) [Fig. 5.22B], ***per1*** ($r^2$ = 0.710, p = 0.0001) [Fig. 5.22C], and ***per2*** ($r^2$ = 0.318, p = 0.0083) [Fig. 5.22D].

### 5.3.3.5. Investigating whether *acan* and *adamts-4* transcription is controlled by circadian clocks and whether applying 770xg force (60 minutes) either twice daily for 1- or 2-days would influence their expression in 3D inflammatory OA pellets with no PCM

Following the determination of clock responses (Figs. 5.21 and 5.22) to application of 770xg force (60 minutes) either twice daily for 1- or 2-days within two consecutive LD cycles in an *in vitro* inflammatory OA model, analyses were carried out using the same samples to evaluate if a cartilage ECM anabolic gene marker, *acan* and catabolic gene marker, *adamts-4* exhibit circadian rhythmicity in transcription and determine the influence of applying 770xg force (60 minutes) either twice daily for 1- or 2-days on their transcription.

#### 5.3.3.5.1. *acan* transcription is not rhythmically regulated in response to cytokine and/or load stimuli

No circadian rhythm of *acan* transcription was observed in **control** 3D pellets with no PCM in individual LD cycles across the 48-hour period of investigation (first LD cycle: $r^2 = 0.518$, $p = 0.0014$; second LD cycle; $r^2 = 0.516$, $p = 0.00512$) [Fig. 5.23A]. Likewise, no circadian expression of *acan* mRNA levels was observed following **cytokine** stimulation (first LD cycle: $r^2 = 0.371$, $p = 0.0154$, second LD cycle: $r^2 = 0.344$, $p = 0.0226$) [Fig. 5.23A]. The lack of circadian rhythm of *acan* transcription was also observed following **application of 770xg force twice daily for 1-day** to cytokine-treated 3D pellets with no PCM ($r^2 = 0.522$, $p = 0.0013$) [Fig. 5.23A] and **application of 770xg force twice daily for 2-days** to cytokine-treated cultures ($r^2 = 0.213$, $p = 0.0503$) [Fig. 5.23A].

#### 5.3.3.5.2. Circadian regulation of *adamts-4* transcription is abolished following cytokine stimulation and is not rescued following application of 770xg force either twice daily for 1- or 2-days

**Control** 3D pellets with no PCM revealed circadian expression of *adamts-4* mRNA across a 48-hour period of investigation ($r^2 = 0.859$, $p = 0.0001$) [Fig. 5.23B], characterised by an amplitude of 0.498, a period of 20 hours and a peak around ZT13 hours. Similar responses were observed in previous findings as *adamts-4* mRNA was demonstrated to oscillate in a circadian manner in control and 770xg loaded pellet cultures within a 24-hour window in chapter 4 (Fig. 4.11). Circadian rhythm was not observed for *adamts-4* mRNA

levels in 2 consecutive LD cycles following **cytokine** treatment ($r^2$ = 0.166, p = 0.0383) [Fig. 5.23B]. Following **application of 770xg force (60 minutes) twice daily for 1-day** to cytokine-treated 3D pellets with no PCM, *adamts-4* mRNA rhythmicity was not observed ($r^2$ = 0.402, p = 0.0099) [Fig. 5.23B], a trend that was also observed following **application of 770xg force (60 minutes) twice daily for 2-days** in the second LD cycle ($r^2$ = 0.497, p = 0.0002) [Fig. 5.23B].

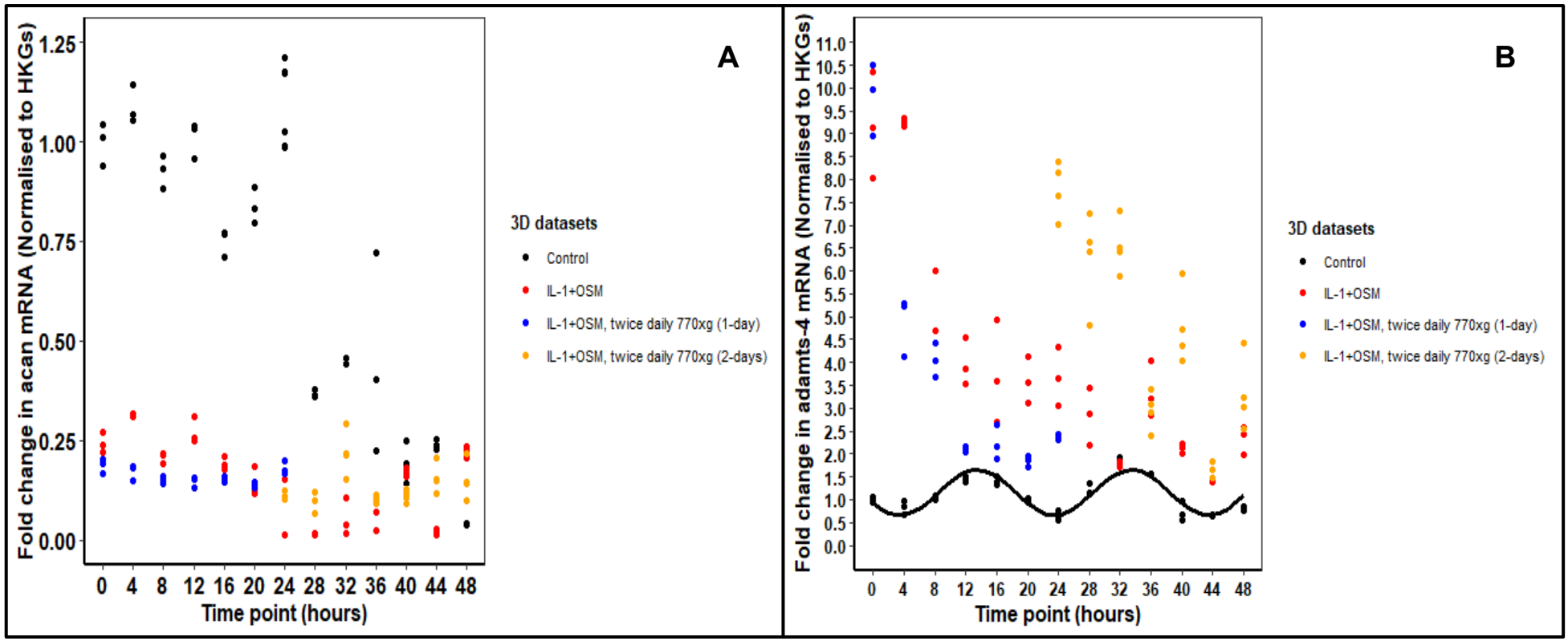


**Figure 5.23. Effect of applying 770xg force either twice daily for 1- or 2-days on *acan* and *adamts-4* transcription in 3D inflammatory OA pellets with no PCM (induced through stimulation with IL-1α in combination with OSM).** Fold change in mRNA transcripts (normalised to *18s* and *hprt*) plotted against sampling time within a 48-hour period (at 4-hour intervals) for control 3D chondrocyte pellets with no PCM and those subjected to 770xg force (60 minutes) either twice daily for 1- or 2-days following 24-hour exposure to 5 ng/ml IL-1α in combination with 10 ng/ml OSM (as well as the cytokine [IL-1α+OSM] group) before qPCR quantification of: **A**) *acan* mRNA transcripts, and **B**) *adamts-4* mRNA transcripts. Black dots; control datasets, red dots; cytokine (i.e., IL-1α plus OSM) datasets, blue dots; twice daily 770xg force (60 minutes) for 1-day after IL-1α plus OSM exposure datasets, orange dots; twice daily 770xg force (60 minutes) for 2-days after IL-1α plus OSM exposure datasets. The fitted cosinusoidal waves (black curve) indicate rhythmic oscillations of *adamts-4* mRNA transcripts in control pellet cultures across a 48-hour period, determined by the CircWaveBatch software ($R^2 > 0.8$, $p < 0.05$) and graphically plotted in the R software using the ggplot2 package. The absence of a cosinusoidal wave in a plot indicates an arrhythmic expression of a specific gene determined by the CircWaveBatch software ($R^2 < 0.8$, or $p > 0.05$). Data points represent fold changes in mRNA transcripts (n = 3, N = 1).

## 5.4. Discussion

The work in this chapter has characterised the induction of an *in vitro* 3D inflammatory OA model through exposure of 3D chondrocyte pellet cultures to the proinflammatory cytokines IL-1 and OSM. Overall, analysis of sGAG release using the DMMB assay demonstrated significant increases within a 48- or 72-hour window. Moreover, application of 5 ng/ml IL-1α in combination with 10 ng/ml OSM reduced sGAG release and downregulated *sox9* and *acan* transcription, whilst increasing the expression of *adamts-4, adamts-5*, *mmp-3* and *mmp-13* genes as well as demonstrating increased activity of adamts-4 and mmp-13 enzymes. This data indicates both the catabolic and anti-anabolic effects of proinflammatory cytokines. Surprisingly, in one experiment, application 5 ng/ml IL-1β in combination with 10 ng/ml OSM had no effect on sGAG and NO release into culture media within a 48-hour period suggesting that the cytokines might have partially lost their efficacy though they induced expected transcriptional changes. Application of 100 nM dexamethasone restored sGAG release and *acan* and *mmp-3* mRNA expression to control levels in this inflammatory OA model hence verifying the anti-inflammatory properties of this synthetic drug (Gossan et al. 2013; Guo et al. 2015; Bajpayee et al. 2016). Barely detectable levels of nitrite were produced by control 3D chondrocyte pellet cultures within the 48- or 72-hour window suggestive of no/minimal inflammation; however, application of proinflammatory cytokines significantly induced nitrite production as expected (Chowdhury et al. 2001; Chowdhury et al. 2008). As observed in chapter 4, control 3D pellet cultures demonstrated circadian expression of clock genes (*bmal1*, *npas2*, *nr1d1*, *per1* and *per2* within 3 LD cycles) and a gene marker of catabolism (*adamts-4* within a 24-hour period). As discussed (section 4.4.1), the baseline circadian rhythmicity of the above-mentioned clock genes in control 3D cultures might be attributed to the use of insulin-containing culture media as insulin has previously been shown to synchronise circadian clock in various *in vitro*, *ex vivo* and *in vivo* models (Chan et al. 2022; Crosby et al. 2019; Gagliano et al. 2021; Kajimoto et al. 2018; Tuvia et al. 2021); this suggest that chondrocyte circadian clocks in 3D pellet culture utilised in this PhD project may have been synchronised unintentionally. In chapter 5, circadian rhythm of clock genes was lost following application of proinflammatory cytokines. Dexamethasone induced resurgences of rhythmic *bmal1* and *per2* transcription in cytokine-treated pellet cultures indicative of its clock synchronisation properties. Using the 3D inflammatory OA model characterised in this chapter, mechanical load (mimicked through application of 770xg force [60 minutes] either once daily for 3-days, twice daily for 1-day or twice daily for 2-

days) had no effect on the disrupted circadian rhythm of *bmal1*, *npas2*, *nr1d1*, *nr1d2*, *per1* and *per2* mRNAs. Mechanical load was unable to rescue cytokine-induced downregulation of *acan* mRNA and upregulation of *mmp-3* and *adamts-4* mRNAs. Furthermore, application of 770xg force [60 minutes] either once daily for 3-days, twice daily for 1-day or twice daily for 2-days did not reverse the cytokine-mediated reduction in sGAG release and increased NO production observed in the 3D model indicating that these mechanical load regimens do not possess anti-inflammatory actions.

### 5.4.1. Proinflammatory cytokines suppress anabolic and induce catabolic markers of ECM homeostasis

Significant transcriptional increases in *adamts-4, adamts-5, mmp-3* and *mmp-13*, concomitant with increased activity of adamts-4 and mmp-13 enzymes following cytokine stimulation, observed in this chapter, is consistent with the findings from a previous study in which a synergistic induction of several MMPs was observed following the stimulation of primary human articular chondrocytes with IL-1α in combination with OSM (Barksby et al. 2006). Barksby et al. (2006) revealed significant increases in *MMP-3* and *MMP-13* mRNA amongst other *MMPs* following cytokine treatment. Transcriptional upregulation of markers of cartilage ECM catabolic activities including *adamts-4* and *adamts-5*, as well as *mmp-1*, *-3*, *-9* and *-13* were observed following the stimulation of mature bovine chondrocytes with 10 ng/ml IL-1α (Torzilli et al. 2011), hence agreeing with the observations of this chapter. Consistent with the significant cytokine-induced reduction in proteoglycan synthesis at 24-, 48- and 72-hours observed in this chapter was the reported increase in proteoglycan loss 1- and 2-days following exposure of mature bovine chondrocytes to IL-1α (Torzilli et al. 2011). However, a discrepancy was observed between the findings of this chapter and those reported by Torzilli et al. (2011) since the former demonstrated a significant decrease in proteoglycan release 72 hours post stimulation whilst the latter revealed no significant changes in proteoglycan loss at day 3. However, this disagreement might be attributed to the utilisation of a combination of 5 ng/ml IL-1α and 10 ng/ml OSM in this chapter which have previously been shown to act synergistically in inducing an inflammatory state in cells as opposed to the use of 10 ng/ml IL-1α only by Torzilli et al. (2011). Moreover, the observed elevations in NO release following cytokine stimulation in this chapter corroborates the findings of McNulty et al. (2013) who demonstrated that skeletally mature porcine cartilage explants exposed to 0.01-10 ng/ml of either IL-1α or IL-1β dose dependently increased NO production with maximal induction observed following 1 ng/ml

IL-1α treatment. McNulty et al. (2013) also demonstrated a significant dose dependent increase in total mmp enzyme activity following treatment with 0.01 to 10 ng/ml IL-1α or IL-1β; this agrees with the findings of this chapter which revealed significantly increased mmp-13 and adamts-4 enzyme activity within 72-hours post cytokine stimulation.

### 5.4.2. Proinflammatory cytokines disrupt circadian clocks in skeletally immature bovine 3D chondrocyte pellets

3D chondrocyte pellets exposed to IL-1α in combination with OSM demonstrated a lack of circadian rhythmicity for clock gene transcripts including *bmal1*, *clock*, *cry1*, *nr1d1*, *npas2*, *per1* and *per2*, whilst the control chondrocyte pellets exhibited transcriptional rhythmicity in at least one experiment. This indicates the capacity of proinflammatory cytokines to disrupt circadian clocks in immature bovine chondrocyte pellet cultures. These findings corroborate the outcomes reported by Guo et al. (2015) who was the first to prove that catabolic cytokines disrupt circadian clocks in cartilage. Guo et al. (2015) exposed murine cartilage explants to 5 ng/ml IL-1β and recorded the bioluminescence of the luciferase reporter protein fused to the promoters of *cry1* and *per2*, observing disruption of circadian rhythm. IL-1β was reported to disrupt chondrocytes' circadian clocks through an NFκB-dependent pathway partly involving tampering with the function of the core clock/bmal1 complex (Guo et al. 2015).

Consistent with the *bmal1* mRNA expression data in this chapter (loss of circadian rhythmicity upon cytokine exposure) was the observation of dampened *BMAL1* mRNA expression in human OA and aged mouse cartilage as previously described by Dudek et al. (2016). Furthermore, Dudek et al. (2016) demonstrated that chondrocyte-specific *bmal1*$^{-/-}$ mice cartilage showed dampened circadian rhythm and progressive cartilage degradation. Moreover, *bmal1* was reported to direct the circadian expression of genes involved in pathways such as anabolism, catabolism and apoptosis (Dudek et al. 2016). Mechanistically, *bmal1* regulates cartilage homeostasis through the TGF-β and nuclear factor of activated T cells, cytoplasmic, calcineurin dependent 2 (NFATC2) signalling pathways; *bmal1*$^{-/-}$ chondrocytes showed a reduction in phosphorylated SMAD (suppressor of mothers against decapentaplegic) 2/3 (p-SMAD2/3) and NFATC2 levels (indicative of inhibition of chondrogenic differentiation [Baugé et al. 2013]), whilst demonstrating an increase in p-SMAD1/5 levels (indicative of promoting hypertrophic differentiation [Baugé et al. 2013]). This study suggested a shift in signalling towards the catabolism of ECM

components as observed in OA and aged cartilage (Baugé et al. 2013; Dudek et al. 2016), therefore enforcing the identification of circadian rhythm disruption as a risk factor for OA development.

Moreover, the observation of cytokine disrupted circadian rhythmicity of *bmal1* and *per2* transcripts in this chapter agrees with the results of Rong et al. (2019) who revealed the abolishment of *BMAL1* and *PER2* circadian rhythm in healthy primary human chondrocytes exposed to 10 ng/ml IL-1β within a 24-hour window. The observed disruption of rhythmicity in *per2* transcription following the application of catabolic cytokines in this chapter is also consistent with Pferdehirt et al. (2022) who demonstrated the loss of circadian rhythmicity in *per2* expression (indicated by dampened PER2::luc bioluminescence activity) in murine cartilage and cartilage tissue engineered from miPSCs subsequent to their exposure to either 1 ng/ml IL-1α or 1 ng/ml IL-1β.

This chapter verified the potential of proinflammatory cytokines IL-1α or IL-1β in combination with OSM to induce an inflammatory state in 3D chondrocyte pellets as described previously in various models, suggestive of the suitability of cytokine challenge for use in mechanistic studies investigating the influence of various stimuli on chondrocytes exhibiting an inflammatory OA phenotype.

### 5.4.3. Dexamethasone reversed the inflammatory state and synchronised the circadian clocks of cytokine-stimulated 3D chondrocyte pellets

Dexamethasone was selected for use based on previous literature where it was reported to possess potent anti-inflammatory and/or clock synchronisation properties (Bajpayee et al. 2016; Guo et al. 2015; Li et al. 2015; Szapary et al. 2023). In these previous literature, 100 nM Dex was continually left in culture media before downstream analyses to assess its anti-inflammatory and/or clock synchronisation properties in cultures which had had exposure to catabolic cytokines (Bajpayee et al. 2016; Guo et al. 2015; Li et al. 2015; Szapary et al. 2023). However, other studies demonstrated the capacity of a pulse of 100 nM Dex treatment to synchronise diverse peripheral clocks (e.g., 2-hour pulse in HEK 293T and NIH 3T3 cells [Woo et al. 2010]; 1-hour pulse in murine xiphoid cartilage explants and SW-1353 cells [Gossan et al. 2013]) with no prior exposure to catabolic cytokine; thus, continual Dex exposure was utilised in this PhD project since 3D pellet cultures were initially exposed to a combination of 5ng/ml IL-1β and 10ng/ml OSM (inflammatory OA induction). Nonetheless, as described in section 5.1.2, other methods of

synchronising circadian clocks exist but they were not selected for differing reasons. For instance, forskolin (a known clock synchroniser) was not able to synchronise disrupted cry1-luc circadian rhythm in murine xiphoid cartilage explants following IL-1β application indicative of its lack of anti-inflammatory properties (Guo et al. 2015). Due to the inaccessibility of automated temperature cycling incubators, temperature fluctuations could not be used in the study. Moreover, since this PhD studies mechanobiology, frequent movement of pellets between two incubators set at different temperature is not advisable as it could potentially introduce unintentional and unquantifiable mechanical loads to pellets hence affecting cell behaviours. Furthermore, the use of serum shock to synchronise chondrocyte circadian clocks was not performed because of an increased complexity of media changes when dealing with numerous samples; in fact, frequent media changes might also introduce unintentional and unquantifiable mechanical stimulation to 3D pellets hence influencing cell responses.

As expected, a complete reversal of anti-anabolic and catabolic pathways was observed in cytokine-stimulated 3D pellets following application of 100 nM Dex in this thesis as evidenced by reproducible increases in *acan* and reduced *mmp-3* transcript levels comparable with baseline control cells' expression. Significant reductions in *mmp-3* mRNA levels (as well as *adamts-4*, *adamts-5* and *mmp-13*) were observed in cytokine-stimulated bovine articular cartilage explants following the application of dexamethasone (Li et al. 2015; Lu et al. 2011), suggesting the chondroprotective effects of dexamethasone on cartilage in these *ex vivo* models. Collectively, all these data suggest that the mechanism through which dexamethasone protects against the deterioration of cartilage ECM is by inhibiting the upregulation of matrix-degrading enzymes (e.g., MMPs and ADAMTSs) normally observed during OA development and progression. Furthermore, dexamethasone stimulation has been demonstrated to reduce the phosphorylation of JNK (c-Jun N-terminal kinase) 1 and -2 in primary human chondrocytes exposed to IL-1α, suggesting that the anti-catabolic effect of dexamethasone might also be attributed to alterations in JNK1/2 signalling (Wang et al. 2017b).

In this chapter, continual application of 100 nM dexamethasone to cytokine-stimulated 3D chondrocyte pellets induced a resurgence of rhythmic oscillations of *bmal1* and *per2* mRNA levels suggesting that Dex synchronised chondrocyte intrinsic circadian clocks in pellets exhibiting an inflammatory OA phenotype. These findings corroborate a previous study in which healthy murine cartilage explants were cultured for more than a week until their rhythmicity was lost (dampened) and the application of 100 nM dexamethasone

synchronised their resident chondrocytes' circadian clocks resulting in the re-initiation of rhythmic per2::luc oscillations (Gossan et al. 2013). Dex-induced resurgence of circadian rhythmicity in 3D pellet cultures post cytokine challenge in this chapter is consistent with the previously reported synchronisation of circadian clocks in murine cartilage by dexamethasone treatment following IL-1 stimulation hence resulting in *cry1*-luc rhythmic oscillation (Guo et al. 2015). Mechanistically, IL-1β was reported to mediate the disruption of the circadian clocks in chondrocytes through NFκB signalling (Guo et al. 2015). Since dexamethasone was demonstrated to reverse the disruptive effect of IL-1β in chondrocyte circadian clocks, the mechanism through which this anti-inflammatory agent restores disrupted circadian rhythms in cartilage explants might involve inhibition of NFκB signalling components (Guo et al. 2015). Involvement of NFκB signalling in inflammatory conditions was previously validated in a study in which the application of a 4-8% equibiaxial strain to rabbit articular chondrocytes inhibited IL-1β-induced NFκB nuclear translocation, indicating that inhibition of proinflammatory responses by mechanical forces is mediated by NFκB (Agarwal et al. 2004).

### 5.4.4. 60 minutes of 770xg force had no effect on cytokine-induced alterations in markers of ECM metabolism

The work in this chapter indicates the reproducible inability of once daily application of 770xg force (60 minutes) for 3-days in returning *acan* and *mmp-3* transcripts to basal levels, suggesting that application of this loading regime cannot influence the inflammatory pathways resulting from cytokine stimulation. These novel findings were corroborated by other analyses performed in this thesis entailing the observation of comparable sGAG concentrations between cytokine-treated cultures and those subjected to daily episodes of 770xg force (60 minutes), both of which were significantly lower than controls. Data from this chapter also demonstrated the inadequacy of once daily application of 770xg force (60 minutes) for 3-days in counteracting the inflammatory effects of catabolic cytokines as similar nitrite/NO levels were observed between cytokine-treated cultures and those subjected to 60 minutes of 770xg force per day within a 72-hour period. This disagrees with the findings of Gassner et al. (1999) who revealed significantly reduced mRNA and protein expression levels for *inos* concomitant with significant increases in proteoglycan synthesis in IL-1*β*-stimulated rabbit chondrocyte monolayers following exposure to 20% cyclical tensile strain (0.05 Hz). Findings of this chapter also contradict the results reported

by Xu et al. (2000) and Long et al. (2001) who demonstrated the suppression of cytokine-induced mRNA expression of catabolism associated proteins including *inos*, *cox-2* and *mmp-1* concomitant with increased transcription of *timps*, and the rescue of cytokine-induced inhibition of proteoglycan synthesis in rabbit chondrocyte monolayers subjected to cyclical tensile stress (6% CTS, 0.05 Hz, either 4-,8-,24- or 48-hours). Furthermore, there is disagreement between this chapter findings and those reported by Chowdhury et al. (2001) and Chowdhury et al. (2008) who demonstrated that application of 15% dynamic compression (1 Hz; 6-, 12- or 48-hours) inhibited IL-1β-induced nitrite/NO production in 3D bovine chondrocyte cultures. Moreover, unaltered nitrite/NO release data in this chapter is inconsistent with significant reductions in nitrite release in bovine chondrocyte/agarose constructs subjected to 15% dynamic compression (1 Hz, either 1.5-, 3-, 6-, 12-, 24- or 48-hours) (Chowdhury et al. 2003). Overall, the above-mentioned previous studies demonstrate the anti-inflammatory properties of differing mechanical loads. Nonetheless, agreement between gene expression, sGAG and NO release data in 3D pellets exhibiting an inflammatory OA phenotype in this chapter suggests the authenticity of the observed cell responses hence suggesting that the employed centrifugal regimen lacks anti-inflammatory effects. Further work in this chapter unveiled novel findings entailing the inability of 770xg force (60 minutes) application twice daily for 1-day or twice daily for 2-days in ameliorating the anti-anabolic and catabolic effects of proinflammatory cytokines in an inflammatory OA model; 770xg force (60 minutes) application twice daily for 1-day or twice daily for-2 days failed to rescue the response of chondrocytes to cytokine treatment hence further disagreeing with the findings of (Chowdhury et al. 2001; Chowdhury et al. 2008; Gassner et al. 1999; Long et al. 2001; Xu et al. 2000). However, the reproducibility of chondrocyte behaviours observed in this chapter needs to be validated in repeat experiments.

### 5.4.5. Exposure of chondrocytes with an inflammatory phenotype to 60 minutes of centrifugal force (770xg) had no effect on circadian clock genes

This experimental chapter demonstrated the persistence of cytokine-induced arrhythmic expression of *bma1, npas2, nr1d1*, *per1* and *per2* transcripts following application of mechanical load (770xg load [60 minutes] once daily for 3-days, twice daily for 1-day and twice daily for 2-days); this suggests the insufficiency of the utilised centrifugation regimen in synchronising disrupted circadian clocks in chondrocytes exhibiting an inflammatory OA phenotype. Nevertheless, the findings of this chapter demonstrating insufficiency of mechanical load to rescue cytokine-mediated loss of circadian rhythmicity for several clock

genes are novel since no previous publications characterising the rescue of altered circadian rhythm in chondrocytes and other musculoskeletal cells through physiological mechanical loading have been reported. It is worthwhile highlighting that the successful reversal of an inflammatory OA phenotype required constant dexamethasone treatment throughout the culture period (sections 5.3.2.4 - 5.3.2.6), whereas centrifugal force was only applied for 1-hour per regimen. It could be argued that the observed lack of synchronicity post centrifugal force exposure could potentially be attributed to inadequate exposure to centrifugal force (probably below the threshold for inducing synchronisation). This indicates the need for further optimisation of the centrifugal force regimen to dissect the appropriate duration of centrifugation for adoption in future ‘‘*mechanobiology meets chronobiology*’’ experiments.

This chapter also demonstrated that markers of ECM metabolism i.e. an ECM anabolism marker *acan* and an ECM catabolism marker *mmp-3* exhibited no circadian rhythmicity in control 3D chondrocyte pellets or following application of relevant stimuli (i.e., cytokines, dexamethasone plus cytokines, 770xg load [60 minutes] once daily for 3-days in the presence of cytokines, twice daily for 1-day and twice daily for 2-days following 24-cytokine exposure) hence suggesting that the chondrocyte clock has no control over the expression of these cartilage ECM genes. The observed lack of *acan* mRNA circadian rhythm in this chapter contradicts a study in which *ACAN* transcription was demonstrated to exhibit circadian rhythmicity within a 24-hour period in undamaged (healthy) human knee chondrocyte monolayers (Snelling et al. 2016). However, the discrepancy between results of this chapter and those reported by Snelling et al. (2016) could be attributed to interspecies variation. However, this chapter 5 data demonstrating circadian rhythm of *adamts-4* transcription only in control 3D chondrocyte pellets within a 48-hour period agrees with chapter 4 findings where circadian rhythm of *adamts-4* transcription was also observed within a 24-hour period (control 3D pellets and those subjected to a single episode of 770xg force [60 minutes]); this suggests that the expression of this catabolic gene marker is regulated by circadian clocks in immature bovine chondrocytes. Rhythmic oscillations of *adamts-4* mRNA observed in this chapter is also consistent with a previous study in which circadian expression of *adamts-4* mRNA was observed in healthy mouse xiphoid and growth plate cartilage indicative of the circadian control of this gene marker in cartilage (Gossan et al. 2013).

### 5.4.6. Summary

- Proinflammatory cytokines induced an inflammatory state in immature bovine chondrocyte pellets as demonstrated by the suppression of: (i) sGAG release, (ii) a gene marker of cartilage ECM anabolism (*acan*), and (iii) chondrocyte phenotype marker (*sox9*). Moreover, elevated expression of an inflammatory mediator (NO), increased expression of gene markers of catabolism (*adamts-4*, *mmp-3*), and activity of catabolic enzymes (adamts-4, mmp-13) were also observed
- Bovine chondrocyte circadian clocks are affected by proinflammatory cytokines as evidenced by the disruption to transcriptional expression of rhythmic clock genes (*bmal1*, *npas2*, *nr1d1*, *nr1d2*, *per1* and *per2*) within a 48- or 72-hour window
- Transcriptional analyses corroborated the capacity of dexamethasone to suppress the inflammatory effects of proinflammatory cytokines (restoration of *acan* and *mmp-3* transcripts to control levels) and synchronise chondrocyte circadian clocks (resurgence of *bmal1* and *per2* transcription) in a 3D inflammatory OA model
- 60 minutes of 770xg force had no effect on the expression of gene makers of ECM anabolism (*acan*) and catabolism (*adamts-4*, *mmp-3*) in cytokine-treated 3D pellets irrespective of centrifugation regimen (i.e., application of 770xg force [60 minutes] either once daily for 3-days, twice daily for 1-day or twice daily for 2-days)
- Cytokine-induced disruption of circadian rhythm of *bmal1* and *per2* transcription was not affected following once daily application of 770xg force (60 minutes) within a 3-day period in an inflammatory OA model
- Cytokine-induced alterations in rhythmicity of clock gene transcription (*npas2*) was not affected following application of 770xg force [60 minutes] either twice daily for 1-day or twice daily for 2-days in 3D chondrocyte pellets stimulated with proinflammatory cytokines

# Chapter 6

## General discussion

### 6.1. Importance of mechanical loading on cartilage health and disease

Articular cartilage, a highly specialised connective tissue localised in articulating surfaces of diarthrodial joints is predominantly made up of type II collagen, proteoglycans (rich in aggrecan) and water which collectively confers its biomechanical properties including the transfer of mechanical loads across the joint during articulation and ensuring a frictionless and lubricated articular surface between bones at a joint. Cartilage resident cells, chondrocytes are responsible for maintaining a turnover of cartilage ECM by balancing anabolic and catabolic events. However, environmental cues which promote a prolonged activation of catabolic pathways, e.g., upregulation of ADAMTSs and MMPs, shifts the balance towards the breakdown of matrix components which results in damage to joint tissues including cartilage hence promoting the development of OA (Arokoski et al. 2000; Mow et al. 1989). OA is the most common form of arthritis characterised by cartilage degradation, capsular fibrosis, synovitis, and osteophytes formation (March 2001). Multiple risk factors are implicated in the development of this chronic joint degenerative disease including abnormal mechanical loading, joint injury, obesity, age, genetic predisposition, gender and occupation.

Additionally, previous studies identified circadian rhythm as one of the most dysregulated pathways in human OA (Akagi et al. 2017; Snelling et al. 2016) and other studies have demonstrated disrupted circadian rhythm in OA in various models (Bekki et al. 2020; Dudek et al. 2016; Kanbe et al. 2006; Kc et al. 2015; Rong et al. 2019) therefore providing evidence on the contribution of dysregulated cartilage clocks to the OA pathology. Circadian clock disruption may occur as a result of deviations from the normal sleep-wake cycle as exemplified by night shift occupations in the modern world which leads to increased prevalence of OA in shift workers (Kc et al. 2015). Furthermore, circadian clock disruption may also occur *in vivo* due to chronic joint inflammatory conditions which subsequently contribute to OA development. *In vitro*, joint inflammation is normally mimicked by the exposure of cartilage explants or chondrocyte cultures to proinflammatory cytokines which have been demonstrated to disrupt circadian rhythm of clock genes' transcription and induce an inflammatory state characterised by increases in catabolism markers and reduction in anabolism markers hence recapitulating an OA phenotype (Alhilali et al. 2021; Guo et al. 2015; Pferdehirt et al. 2022). The ability of proinflammatory cytokines to disrupt cartilage circadian clocks was verified in this thesis through the application of 5 ng/ml IL-α/β in combination with 10 ng/ml OSM to 3D chondrocyte pellets hence generating a 3D inflammatory OA model. It is surprising that studies investigating

the link between mechanical loading and circadian rhythm in health and osteoarthritic cartilage are scarce since it is well known that mechanical loading is imperative for cartilage function (Goldring 2000; Loeser et al. 2012; Quinn et al. 1998; Wong et al. 1999) and circadian clock gene *BMAL1* controls cartilage homeostasis and integrity (Dudek et al. 2016).

With this knowledge, I hypothesised that centrifugal force, as a means of mimicking the compressive, shear and tensile stresses observed in cartilage *in vivo*, would alter chondrocytes' circadian rhythm through a change in amplitude and/or phase which could potentially influence cartilage metabolism. As proinflammatory cytokines are reported to disrupt the chondrocytes' circadian rhythm, and physiological mechanical loads have been reported to reverse the inflammatory effects of proinflammatory cytokines, I further hypothesised that centrifugal force would reset the circadian clocks in an *in vitro* model of inflammatory OA and ultimately counteract cytokine-induced catabolic pathways.

The work in this thesis has developed and characterised an *in vitro* 3D model system using chondrocytes isolated from skeletally immature bovine cartilage for employment in the study of chondrocyte mechanobiology. RefFinder software identified *hprt* and *18s* as the most stable and appropriate reference genes for qPCR normalisation of target genes following application of either centrifugal force, proinflammatory cytokines or dexamethasone. This thesis provided novel evidence revealing that application of 15 minutes of 770xg force induced early mechano-responsive genes, *c-fos* and *c-jun* and late mechano-responsive catabolic genes, *adamts-4*, *adamts-5* and *mmp-3* within a 24-hour window as compared to the 200- and 1000-xg centrifugal forces. Additionally, increasing the duration of 770xg force application from 15- to 60-minutes induced stronger mechano-regulation of the early mechano-responsive gene, *c-fos*; the mechano-responsive chondrogenic gene, *sox9* and the mechano-responsive catabolic gene, *adamts-4* in pellets with no PCM. Overall, this data indicated the suitability of 60 minutes of 770xg force for further use in investigating the influence of mechanical forces on chondrocyte circadian clocks in this PhD project.

Moreover, this PhD project characterised bovine circadian clocks at a transcriptional level in a 3D model described above providing novel evidence demonstrating circadian oscillations in the transcription of clock genes (*bmal1*, *clock*, *cry1, npas2*, *nr1d1, nr1d2*, *per1* and *per2*) and catabolic gene (*adamts-4* but not *adamts-5*, *mmp-3* and *mmp-13*) but not ECM anabolic genes (*acan* and *col2a1*) nor a gene marker of the chondrocyte

phenotype (*sox9*) in at least one LD cycle within a 72-hour period in control 3D chondrocyte pellets.

### 6.2. Importance of PCM in mechano-signalling

To determine the influence of PCM deposition on mechano-signalling, this PhD project developed and characterised two 3D *in vitro* model systems with either the absence (no PCM) or presence of PCM (termed 3D chondrocyte pellets with PCM). In pellets with no PCM, significant increases in mRNA levels for the early mechano-responsive genes *c-fos* and *c-jun* and late mechano-responsive catabolic gene *mmp-3* were observed as early as 1-hour post-cessation of 15 minutes of load, whilst comparable responses were only observed either at T4- (*c-jun* only) or T8-hours in pellets with PCM subjected to an equivalent load. This suggests the delayed regulation of these early and late response genes in the presence of PCM. However, this divergence in speed of responsiveness was not observed following a longer load application i.e., 60 minutes suggesting that PCM deposition had no additional effect on propagating a mechano-signal. Surprisingly, application of 15 minutes of load to pellets within no PCM induced significant reductions in *adamts-4* mRNA levels at T4 hours whereas a significant increase in *adamts-4* mRNA levels was observed at T8 hours in pellets with PCM. This suggests opposite and delayed regulation of this late mechano-responsive catabolic gene following loading of pellet with PCM. However, the converse was observed following a longer loading stimulus i.e., increased *adamts-4* mRNA levels 24 hours post-cessation in pellets with no PCM with comparable responses detected at T4 hours in pellets with PCM - suggestive of a quicker regulation of this late response catabolic gene following loading of pellet with PCM. Opposing behaviours were also detected for *adamts-5* and *sox9* demonstrating the complexity of influence of PCM deposition and load duration on the chondrocytes' response.

Interestingly, pellets with PCM were more liable to load-induced transcriptional increases in ECM genes i.e., *acan*, *col2a1*; clearly, an extended PCM, as observed in cartilage *in situ*, provides a biomechanical buffer and robustly transmits the signals to cells following load application (Knight et al. 1998). This corroborates reports from previous studies demonstrating the importance of the PCM in transducing mechanical signals to chondrocytes as well as the chondroprotective role of the PCM during mechanotransduction (Alexopoulos et al. 2009; Brahmachary et al. 2024; Guilak et al.

2006). Most importantly, the development of a 3D system with PCM in this PhD project improved the mechano-environment surrounding the cells, attempting to replicate that observed *in situ*, as mechanical cues are reliant on ECM molecules for relaying downstream signal transduction cascades to mediate intracellular events to effect homeostasis.

Data also revealed no circadian control of *acan* and *col2a1* transcription in both 3D chondrocyte pellets with minimal/no PCM and those with PCM suggesting that these anabolic genes are not under circadian regulation in bovine cartilage. Surprisingly, circadian expression of *adamts-4* mRNA was observed within a 24-hour period in control 3D pellets with no PCM and following their exposure to a single episode of mechanical load (60 minutes of 770xg force) but not those with PCM (both control and loaded cultures). This suggests that *adamts-4* mRNA rhythmicity had most likely been lost during the PCM deposition period and the inability of mechanical load to re-initiate circadian expression of this catabolic gene suggests that the employed load regimen does not synchronise the rhythmicity of this clock-controlled catabolic gene. With the data presented in this thesis, I believe that more work is warranted to fine-tune a more physiologically relevant centrifugal regime before future mechanobiology studies could consider utilising centrifugal force as an alternative approach to mimic mechanical stimulation of chondrocytes as it has been demonstrated to have potential in inducing transcriptional changes in mechano-responsive genes, akin to those observed in other loading models. However, this magnitude and duration of centrifugal force might still need further optimisation since some of the findings were not validated in repeat experiments, i.e., those involving an increase in the duration of centrifugation.

### 6.3. Application of a single episode of 770xg force induced a transient disruption of *clock* transcription (1st LD cycle only), yet *bmal1* and *clock* transcription were unaltered in the second and third LD cycles in pellets with no PCM whilst *bmal1* and *per2* transcription was unaffected in pellets with PCM

In 3D pellets with no PCM subjected to a single episode of mechanical load (770xg force for 60 minutes), a transient disruption of circadian rhythmicity in *clock* transcription was observed in the first LD cycle of investigation. However, no significant changes in *bmal1* and *clock* transcription were observed in the second and third LD cycles following application of a single episode of 770xg force to pellets with no PCM suggestive of no

impact of this loading regime on circadian clocks. Likewise, a single episode of 770xg force (60 minutes) did not affect circadian rhythmicity of *bmal1* and *per2* transcription in pellets with PCM; thus, verifying that a single episode of 770xg force has no effect on circadian clocks in both pellets with and without PCM. Data from both pellets with and without PCM contradicts the findings of previous studies (section 4.4.3) demonstrating that *in vivo* mechanical loading and load application to cartilage explants, 2D and 3D chondrocyte cultures induced significant alterations in circadian rhythmicity as evidenced by phase shifts in circadian oscillation in per2::luc activity (Dudek et al. 2023) and bmal1 proteins (Heywood et al. 2022), as well as significantly reduced *clock* mRNA levels (Kanbe et al. 2006). The discrepancies between the finding of this PhD and those of previous publications might be attributed to differing model systems, types of mechanical loads and variations in the modes of load application as this study modelled loading *in vitro* through constant centrifugation of 3D pellet cultures (predicted to apply compression, shear forces and hydrostatic pressure) whilst Dudek et al. (2023) used an *in vivo* physiological load and an *ex vivo* cartilage explant dynamic compression models, with Kanbe et al. (2006) and Heywood et al. (2022) utilising *in vitro* 3D and 2D models, respectively, subjected to cyclical tensile strain. Additionally, the use of a more sensitive method of measuring circadian clock dynamics such as real-time recording of per2::luc reporter activity utilised by Dudek et al. (2023) as opposed to 4-hour circadian time series qPCR quantification of mRNA transcripts for clock genes employed in this thesis might account for the inconsistencies in load-induced circadian clock responses between the two studies. Going forward, future experiments should extensively characterise a physiological centrifugal regimen with a magnitude equivalent to that of previous studies which would be applied in a dynamic manner to be as comparable as possible to *in situ* physiological loads and the above-mentioned previous studies. Another possible reason for differing effect of mechanical loads might be due to divergent durations of load between the studies as this study exposed chondrocyte pellets to load for 60 minutes while Dudek et al. (2023) utilised a 45-minute duration in the *in vivo* loading model and 30 minutes in the *ex vivo* compression model; however, Heywood et al. (2022) used 12-hour bouts of load whereas Kanbe et al. (2006) loaded chondrocyte monolayers for 15 minutes/hour therefore adopting a loading duration equivalent to these previous studies needs to be done to allow comparison of cell responses. Furthermore, cartilage maturation is another possible reason for the observation of divergent responses to the findings of Heywood et al. (2022) who utilised skeletally mature bovine chondrocyte monolayers as compared to the use of skeletally immature bovine chondrocyte 3D pellets in this PhD project. Furthermore, the

disagreement between the findings of this thesis and those from previous publications might be attributed to the differing times of stimulus application within the circadian cycle, since Dudek et al. (2023) demonstrated divergent clock responses depending on whether mechanical load was applied at the peak, trough or other phases of *per2* expression. With that, future experiments should attempt to apply mechanical load (mimicked through centrifugation) at similar circadian times as the above-mentioned studies hence making them as comparable as possible.

### 6.4. Impact of continual dexamethasone exposure and application of 770xg force either once daily for 3-days, twice daily for 1-day or twice daily for 2-days on chondrocyte circadian clocks and ECM metabolism in 3D *in vitro* inflammatory OA cultures

The work in this PhD project also characterised the induction of an *in vitro* 3D inflammatory OA model through exposure of 3D chondrocyte pellet cultures to the proinflammatory cytokine IL-1α/β in combination with OSM. Overall, significant reductions in transcript levels for an ECM anabolic marker *acan* and chondrocyte phenotype marker *sox9*, and increases in the transcription of catabolic genes *adamts-4, adamts-5*, *mmp-3* and *mmp-13* were observed in 3D chondrocyte pellets with no PCM exposed to proinflammatory cytokines concomitant with the loss of circadian rhythm of clock genes (*bmal1*, *clock*, *npas2*, *nr1d1*, *nr1d2*, *per1* and *per2*) and a gene marker of catabolism (*adamts-4*). However, application of 100 nM dexamethasone restored *acan* and *mmp-3* mRNA expression to control levels in this inflammatory OA model hence verifying the anti-inflammatory properties of this synthetic drug (Gossan et al. 2013; Guo et al. 2015; Bajpayee et al. 2016) concomitant with re-initiation of rhythmic *bmal1* and *per2* transcription in cytokine-treated pellet cultures hence confirming Dex's clock synchronisation properties. This project unveiled novel findings as application of 770xg force (60 minutes) either once daily for 3-days, twice daily for 1-day or twice daily for 2-days to cytokine-stimulated cultures had no effect on disrupted circadian rhythm of *bmal1*, *npas2*, and *per2* transcription; thus, demonstrating the insufficiency of these loading regimen on resetting disrupted circadian clocks in bovine chondrocyte cultures. Additionally, application of 770xg force (60 minutes) either once daily for 3-days, twice daily for 1-day or twice daily for 2-days to cytokine-stimulated cultures had no effect on cytokine-induced reductions in *acan* transcription and increased *mmp-3* and *adamts-4*

transcription indicating that these loading regimens lack anti-inflammatory properties as they did not return the expression of these ECM genes to baseline levels. Overall, this suggests that the utilised model system and loading regimen had no therapeutic benefits in inflammatory OA pellet cultures within a short period of investigation.

### 6.5. Limitations of the study design

Throughout this PhD project, there have been different challenges and setbacks to overcome. Following the verification of the presence of *ex vivo* functional and autonomous circadian clocks in skeletally immature bovine cartilage chondrocyte monolayers, the aim was to determine the influence of mechanical loading on circadian rhythm. The original intention was to mimic physiological mechanical load by applying cyclical tensile strain (5% strain, 1 Hz), using the Flexcell® 3000 tension system, to chondrocyte monolayers seeded in BioFlex® 6 well plates coated with pronectin. However, after the COVID-19 period, the Flexcell® 3000 tension system failed to start and was non-operational. A trawl of the literature prompted the identification of a different cell culture system which would permit the performance of robust mechanobiology experiments as well as allowing sufficient sample number for the circadian time series experiments. A 3D pellet model was selected based on previous literature (Bernstein et al. 2009; Grimm et al. 2020; Inoue et al. 1990; Maeda et al. 2005; Prittinen et al. 2019; Redlich et al. 2004; Zhang et al. 2004), however the loading regimen required optimisation; as evidenced in this thesis, although the optimised loading regimen elicited robust mechano-regulatory responses, it was not sufficient to influence the circadian clock which still requires further consideration. Most of the experiments in this PhD project employed 3D pellets with no PCM; however, experiments performed on chondrocyte pellets with a PCM revealed potentially different behaviours reinforcing the importance of cell-matrix interactions for mechano-signalling, but the presence of PCM had no discernible effects on circadian clocks following load. Therefore, future work should consider utilising 3D pellets with no PCM.

Another limitation of the study design is the lack of validation of clock gene expression data as this PhD project only evaluated circadian clock dynamics at the gene level; it would be highly informative to evaluate the expression of clock proteins using tools such as mass spectrometry (Dudek et al. 2021), enzyme-linked immunosorbent assays (ELISA) (Goding 1996; Liddell 1991) or western blotting (Dudek et al. 2021). Although this PhD project assessed the activity of adamts-4 and mmp-13 enzymes in culture media, these

findings could be further verified by Western blotting using monoclonal antibodies which recognise protease-generated neoepitopes to assess cartilage proteoglycan degradation as described by Caterson et al. (1985) and Hughes et al. (1992). Alternatively, metabolic radiolabelling using [$^{35}$S]-sulphate and [$^{3}$H]-proline to assess *de novo* synthesis and degradation of proteoglycans and collagens as described by Blain et al. (2006) could also be performed to investigate whether the optimised loading regimen favours anabolic or catabolic outcomes. Due to the time taken to develop the loading regimen, several of the experiments were not performed on independent repeats; only some experiments had two repeats whilst other investigations comprised one experiment hence the reproducibility of most findings in this thesis were not confirmed. This PhD project has a limitation of using chondrocytes derived from skeletally immature bovine cartilage, therefore it is unknown whether skeletal maturation would affect the observed cell responses hence suggesting the necessity of future studies to use a source of skeletally mature cartilage chondrocytes for comparison with immature tissues. In conjunction, it would have been informative to assess the influence of chondrocyte health on circadian responses; therefore, future work could involve the isolation of chondrocytes from macroscopically abnormal (osteoarthritic) cartilage to compare cellular mechano-responses with healthy cartilage chondrocytes in relation to circadian rhythmicity.

### 6.6. Future directions

Even though this study revealed valuable information and novel data on the responses of circadian clocks to differing centrifugal force regimens in 3D pellets with differing extents of PCM deposition (including an *in vitro* inflammatory OA model), other aspects could be explored further to gain more insight into the influence of physiological loading on circadian rhythm in normal and osteoarthritic cartilage chondrocytes.

It would be interesting to perform a study comparable to my investigation of the influence of centrifugal force on circadian clocks in healthy and OA human cartilage chondrocytes to determine whether the observed responses translate to humans. However, characterisation of circadian clocks in human cartilage is less well-defined (as compared to that in mice) due to the difficulty of obtaining normal human tissue and the logistical complexities of sampling a circadian time series collection of human tissue. To circumvent this obstacle, one study has reported chondrogenic differentiation of human embryonic stem cells (hESCs) as an alternative model to human cartilage (Naven et al. 2022). During

chondrogenic differentiation, activation of circadian clocks was observed between day 11 and day 21 which coincides with the end of the 2D stage and 10 days after 3D differentiation, respectively (Naven et al. 2022). Future studies should perform lentiviral transduction of human clock gene luciferase reporters into differentiated hESCs before exposing the engineered 3D cartilage constructs to dynamic compressive load (0.5 MPa, 1 hour, 1 Hz) followed by the monitoring of clock gene dynamics in real-time by bioluminescence recording.

Since this PhD project utilised bovine chondrocytes, future investigation might consider performing *ex vivo* loading experiments using cartilage explants obtained from a different animal species, e.g., mice with circadian clock fusion reporters, e.g., per2::Luc (Dudek et al. 2016; Dudek et al. 2023; Gossan et al. 2013; Guo et al. 2015) and per2-venus (Smyllie et al. 2016) protein level reporters; a *cry1*-luc transcriptional reporter (Guo et al. 2015) with clock gene dynamics monitored by bioluminescence photon counting in real-time, or the utilisation of a venus::bmal1 fluorescent fusion protein reporter allowing confocal imaging of the dynamics of *bmal1* gene in real-time (live imaging) in cartilage explants and cells (Yang et al. 2020). Using the abovementioned clock reporter models, future studies could utilise previously validated physiological loading regimens as simulated by widely utilised dynamic mechanical loading apparatuses such as Flexcell® compression or tension systems to apply either cyclical compressive strain to cartilage explants or constructs within a physiological range, e.g., dynamic compression of 0.5 MPa at a frequency of 1 Hz (Blain et al. 2001; 3 hours loading durations, Dudek et al. 2023; 1 hour loading durations) or cyclical tensile strain to monolayer cultured chondrocytes, e.g., 5% dynamic elongation/stretch of chondrocytes in specially designed BioFlex® 6 well culture plates at a frequency of 1 Hz for 2 hours (recommended by Bleuel et al. 2015), respectively, to assess their potential influence on circadian rhythm; this could be performed following load application at differing circadian times within a day/night cycle since it has previously been demonstrated that loading at the peak of *per2* expression induces divergent responses in comparison to loading at the trough or other phases of *per2* expression (Dudek et al. 2023).

Future studies could also utilise mice with circadian clock protein reporters e.g., per2::luc to determine what influence physiological loading has on circadian rhythm *in vivo*; a comparison with an experimental OA model could also be performed to assess responses (surgical destabilisation of the medial meniscus (DMM) or non-surgical load-induced PTOA in mice are widely used *in vivo* experimental OA models (Bateman et al. 2013, Gilbert et

al. 2018)). It would be really interesting to then harvest OA cartilage from these mice, culture them *ex vivo* and subject them to 0.5 MPa compression (1 Hz, 1 hour) before bioluminescence recording of per2::luc activity within a few days to evaluate the effect of mechanical loading on circadian clocks in cartilage exhibiting an OA-like phenotype. This would address the currently unknown question of whether physiological forces are capable of resetting or synchronising disrupted chondrocyte circadian clocks as a potential mechanism for targeting OA therapeutics.

Future studies should also be directed to compare circadian rhythmicity dynamics obtained from differing experimental set-ups using programs such as circacompare equipped with an analytic tool for explicitly estimating circadian rhythm characteristics (amplitude, phase, MESOR) and simultaneously determining statistical significance of differences between two or more experimental datasets (Parsons et al. 2020); this would allow more definitive conclusions to be reached across experimental systems with statistical power as to the influence of relevant stimuli on specific molecular pathways as well as inter-experimental comparisons.

Considering that this PhD project used Dex (a glucocorticoid know to possess anti-inflammatory properties) to synchronise circadian clocks in 3D chondrocyte pellets following cytokine-induced rhythm disruption, it would be interesting to perform alternative experiments to help disentangle the clock synchronisation effect of Dex from its anti-inflammatory effect such as investigating whether temperature cycling, forskolin or serum shock could reset disrupted circadian clocks; thus, potentially identifying other techniques with no known anti-inflammatory actions to corroborate circadian clock synchronisation for use as positive controls in circadian rhythm rescue experiments in various OA models.

### 6.7. Conclusion

In conclusion, this study confirms the capacity of centrifugal force to simulate mechanical loading with robust regulation of known early and late mechano-responsive genes. Increasing the duration of force induced stronger responses, particularly in 3D pellets with no PCM while quicker responses were observed in pellets with PCM when compared to their controls. This study is the first to demonstrate the existence of autonomous circadian clocks functional at a gene level in articular chondrocytes obtained from skeletally immature bovine calves cultured *in vitro* as 3D pellets, and that the optimised loading

regimen was unable to influence the natural circadian clock or synchronise i.e., ‘reset’ the circadian clocks of 3D pellets exhibiting an inflammatory OA phenotype. However, these findings provide valuable information in our understanding of circadian rhythm in cartilage mechanobiology and that this is only the dawn of future studies focused on shedding some light into the influence of physiological loading on disrupted circadian rhythm as relevant to night shift occupations, ageing and OA pathology. Additionally, this knowledge may aid in the refinement of future studies aimed at exploring mechano-regulation of the cartilage clock to identify potential therapeutic mechanical loading regimens and optimal time of day for exercise or physiotherapy which might be beneficial to OA patients.

# Bibliography

Acharyaa, C., Yika, J.H.N., Kishorea, A., Dinha, V.V., Di Cesareb, P.E. and Haudenschild, D.R. 2014. Cartilage oligomeric matrix protein and its binding partners in the cartilage extracellular matrix: Interaction, regulation, and role in chondrogenesis. *Matrix Biology* 37(1), pp. 102-111. doi: 10.1016/j.matbio.2014.06.001.

Agarwal, S., Deschner, J., Long, P., Verma, A., Hofman, C., Evans, C.H., and Piesco, N. 2004. Role of NF-kappaB transcription factors in antiinflammatory and proinflammatory actions of mechanical signals. *Arthritis Rheum*. 50(11), pp. 3541-8. doi: 10.1002/art.20601.

Ahmed, T.A.E. and Hincke, M.T. 2010. Strategies for Articular Cartilage Lesion Repair and Functional Restoration*. Tissue Engineering: Part B,* 16(3), pp. 305-329. doi: 10.1089/ten.TEB.2009.0590.

Akagi, R., et al. 2017. Dysregulated circadian rhythm pathway in human osteoarthritis: NR1D1 and BMAL1 suppression alters TGF-β signaling in chondrocytes. *Osteoarthritis Cartilage* 25(6), pp. 943-951. doi: 10.1016/j.joca.2016.11.007.

Akanji, O.O., Sakthithasan, P., Salter, D.M., and Chowdhury, T.T. 2010. Dynamic compression alters NFkappaB activation and IkappaB-alpha expression in IL-1beta-stimulated chondrocyte/agarose constructs. *Inflamm Res*. 59(1), pp. 41-52. doi: 10.1007/s00011-009-0068-9.

Akizuki, S., Mow, V.C., Muller, F., Pita, J.C., Howell, D.S. and Manicourt, D.H. 1986. Tensile properties of human knee joint cartilage. I. Influence of ionic concentrations, weight bearing, and fibrillation on the tensile modulus. J*. Orthop. Res.* 4(4), pp. 379-392. doi: 10.1002/jor.1100040401.

Alexopoulos, L.G., Setton, L.A., and Guilak, F. 2005. The biomechanical role of the chondrocyte pericellular matrix in articular cartilage. *Acta Biomater*. 1(3), pp. 317-25. doi: 10.1016/j.actbio.2005.02.001.

Alexopoulos, L.G., Youn, I., Bonaldo, P., and Guilak, F. 2009. Developmental and osteoarthritic changes in Col6a1-knockout mice: biomechanics of type VI collagen in the cartilage pericellular matrix. *Arthritis Rheum*. 60(3), pp. 771-9. doi: 10.1002/art.24293.

Alhilali, M., et al. 2021. IL-1β induces changes in expression of core circadian clock components PER2 and BMAL1 in primary human chondrocytes through the NMDA receptor/CREB and NF-κB signalling pathways. *Cell Signal*. 87, pp. 110143. doi: 10.1016/j.cellsig.2021.110143.

Al-Sabah, A., Stadnik, P., Gilbert, S.J., Duance, V.C., and Blain, E.J. 2016. Importance of reference gene selection for articular cartilage mechanobiology studies. *Osteoarthritis Cartilage* 24(4), pp. 719-30. doi: 10.1016/j.joca.2015.11.007.

Andersen, C.L., Jensen, J.L. and Orntoft, T.F. 2004. Normalization of real-time quantitative reverse transcription-PCR data: a model-based variance estimation approach to identify genes suited for normalization, applied to bladder and colon cancer data sets. *Cancer research* 64(15), pp. 5245-5250. doi: 10.1158/0008-5472.CAN-04-0496.
Anderson, D.E., and Johnstone, B. 2017. Dynamic Mechanical Compression of Chondrocytes for Tissue Engineering: A Critical Review. *Front Bioeng Biotechnol*. 11(5), pp. 76. doi: 10.3389/fbioe.2017.00076.
Anstaett, O.L., Brownlie, J., Collins, M.E., and Thomas, C.J. 2010. Validation of endogenous reference genes for RT-qPCR normalisation in bovine lymphoid cells (BL-3) infected with Bovine Viral Diarrhoea Virus (BVDV). *Vet Immunol Immunopathol*. 137(3-4), pp. 201-7. doi: 10.1016/j.vetimm.2010.05.006.
Arner, E.C. 2002. Aggrecanase-mediated cartilage degradation. *Curr Opin Pharmacol*. 2(3), pp. 322-9. doi: 10.1016/s1471-4892(02)00148-0.
Arokoski, J., Kiviranta, I., Jurvelin, J., Tammi, M., and Helminen, H.J. 1993. Long-distance running causes site-dependent decrease of cartilage glycosaminoglycan content in the knee joints of beagle dogs. *Arthritis Rheum*. 36(10), pp. 1451-9. doi: 10.1002/art.1780361018.
Arokoski, J.P., Jurvelin, J.S., Väätäinen, U., and Helminen, H.J. 2000. Normal and pathological adaptations of articular cartilage to joint loading. *Scand J Med Sci Sports* 10(4), pp. 186-198. doi: 10.1034/j.1600-0838.2000.010004186.x.
Bačenková, D., Trebuňová, M., Demeterová, J., and Živčák, J. 2023. Human Chondrocytes, Metabolism of Articular Cartilage, and Strategies for Application to Tissue Engineering. *Int J Mol Sci*. 24(23), pp. 17096. doi: 10.3390/ijms242317096.
Bader, D.L., Salter, D.M., and Chowdhury, T.T. 2011. Biomechanical influence of cartilage homeostasis in health and disease. *Arthritis* 2011, pp. 979032. doi: 10.1155/2011/979032.
Bae, K., Lee, K., Seo, Y., Lee, H., Kim, D., and Choi, I. 2006. Differential effects of two period genes on the physiology and proteomic profiles of mouse anterior tibialis muscles. *Mol Cells*. 22(3), pp. 275-84.
Bajpayee, A.G., Quadir, M.A., Hammond, P.T., and Grodzinsky, A.J. 2016. Charge based intra-cartilage delivery of single dose dexamethasone using Avidin nano-carriers suppresses cytokine-induced catabolism long term. *Osteoarthritis Cartilage* 24(1), pp. 71-81. doi: 10.1016/j.joca.2015.07.010.
Ballock, R.T., Heydemann, A., Wakefield, L.M., Flanders, K.C., Roberts, A.B., and Sporn, M.B. 1993. TGF-beta 1 prevents hypertrophy of epiphyseal chondrocytes: regulation of

gene expression for cartilage matrix proteins and metalloproteases. *Dev Biol*. 158(2), pp. 414-29. doi: 10.1006/dbio.1993.1200.
Balsalobre, A., Damiola, F. and Schibler, U. 1998. A serum shock induces circadian gene expression in mammalian tissue culture cells. *Cell* 93(6):929-37. doi: 10.1016/s0092-8674(00)81199-x.
Barksby, H.E. et al. 2006. Matrix metalloproteinase 10 promotion of collagenolysis via procollagenase activation: implications for cartilage degradation in arthritis. *Arthritis Rheum*. 54(10), pp. 3244-53. doi: 10.1002/art.22167.
Barksby, H.E., et al. 2006. Interleukin-1 in combination with oncostatin M up-regulates multiple genes in chondrocytes: Implications for cartilage destruction and repair. *Arthritis & Rheumatism* 54(2), pp. 540-550. doi: 10.1002/art.21574.
Bateman, J.F., Rowley, L., Belluoccio, D., Chan, B., Bell, K., Fosang, A.J., and Little, C.B. 2013. Transcriptomics of wild-type mice and mice lacking ADAMTS-5 activity identifies genes involved in osteoarthritis initiation and cartilage destruction. *Arthritis Rheum*. 65(6), pp. 1547-60. doi: 10.1002/art.37900.
Baugé, C., Girard, N., Lhuissier, E., Bazille, C., and Boumediene, K. 2013. Regulation and Role of TGFβ Signaling Pathway in Aging and Osteoarthritis Joints. *Aging Dis*. 5(6), pp. 394-405. doi: 10.14336/AD.2014.0500394.
Bekki, H., et al. 2020. Suppression of circadian clock protein cryptochrome 2 promotes osteoarthritis. *Osteoarthritis Cartilage* 28(7), pp. 966-976. doi: 10.1016/j.joca.2020.04.004.
Bernardo, B.C., Belluoccio, D., Rowley, L., Little, C.B., Hansen, U., and Bateman, J.F. 2011. Cartilage intermediate layer protein 2 (CILP-2) is expressed in articular and meniscal cartilage and down-regulated in experimental osteoarthritis. *J Biol Chem* 286(43), pp. 37758-37767. doi: 10.1074/jbc.M111.248039.
Bernstein, P., Dong, M., Corbeil, D., Gelinsky, M., Günther, K.P., and Fickert, S. 2009. Pellet culture elicits superior chondrogenic redifferentiation than alginate-based systems. *Biotechnol Prog* 25(4), pp. 1146-52. doi: 10.1002/btpr.186.
Blain, E.J. 2011. Involvement of the cytoskeletal elements in articular cartilage mechanotransduction. Kamkin, A. and Kiseleva, I., eds. *Mechanosensitivity and Mechanotransduction*, Springer, pp. 77-106.
Blain, E.J., Ali, A.Y., and Duance, V.C. 2010. Boswellia frereana (frankincense) suppresses cytokine-induced matrix metalloproteinase expression and production of pro-inflammatory molecules in articular cartilage. *Phytotherapy Research* 24(6), pp. 905-912. doi: 10.1002/ptr.3055.

Blain, E.J., Gilbert, S.J., Hayes, A.J., and Duance, V.C. 2006. Disassembly of the vimentin cytoskeleton disrupts articular cartilage chondrocyte homeostasis. *Matrix Biology* 25(7), pp. 398-408. doi: 10.1016/j.matbio.2006.06.002.
Blain, E.J., Mason, D.J. and Duance, V.C. 2001. Up-regulation of MMP expression and activation following cyclical compressive loading of articular cartilage in vitro. *Arch. Biochem. Biophys.* 396(1), pp. 49-55. doi: 10.1006/abbi.2001.2575.
Bland, Y.S., and Ashhurst, D.E. 2001. The hip joint: the fibrillar collagens associated with development and ageing in the rabbit. *J Anat.* 198(Pt 1), pp. 17-27. doi: 10.1046/j.1469-7580.2001.19810017.x.
Blaschke, U.K., Eikenberry, E.F., Hulmes, D.J.S., Galla, H.J. and Bruckner, P. 2000. Collagen XI nucleates self-assembly and limits lateral growth of cartilage fibrils. *J Biol Chem*. 275(14), pp. 10370-10378. doi: 10.1074/jbc.275.14.10370.
Bleuel, J., Zaucke, F., Brüggemann, G.P., and Niehoff, A. 2015. Effects of cyclic tensile strain on chondrocyte metabolism: a systematic review. *PLoS One* 10(3), pp. e0119816. doi: 10.1371/journal.pone.0119816.
Boden, G., Ruiz, J., Urbain, J.L. and Chen, X. 1996. Evidence for a circadian rhythm of insulin secretion. *Am J Physiol*. 271(2 Pt 1):E246-52. doi: 10.1152/ajpendo.1996.271.2.E246.
Bouchard, A.L., Dsouza, C., Julien, C., Rummler, M., Gaumond, M.H., Cermakian, N., and Willie, B.M. 2022. Bone adaptation to mechanical loading in mice is affected by circadian rhythms. *Bone* 154, pp. 116218. doi: 10.1016/j.bone.2021.116218.
Bougault, C., et al. 2012. Dynamic compression of chondrocyte-agarose constructs reveals new candidate mechanosensitive genes. *PLoS One* 7(5), pp. e36964. doi: 10.1371/journal.pone.0036964.
Brahmachary, P., Erdogan, E., Myers, E., and June, R.K. 2024. Metabolomic Profiling and Characterization of a Novel 3D Culture System for Studying Chondrocyte Mechanotransduction. *bioRxiv* [Preprint]. doi: 10.1101/2024.06.10.598340.
Buckwalter, J.A. and Mankin, H.J. 1997. Articular cartilage, part 1: tissue design and chondrocyte-matrix interaction. *J Bone Joint Surg Am*. 79(1), pp. 600-611.
Buckwalter, J.A., Mankin, H.J. and Grodzinsky, A.J. 2005. Articular cartilage and osteoarthritis. *Instr Course Lect* 54(1), pp. 465-480.
Bueno, E.M., Bilgen, B., and Barabino, G.A. 2005. Wavy-walled bioreactor supports increased cell proliferation and matrix deposition in engineered cartilage constructs. *Tissue Eng*. 11(11-12), pp. 1699-709. doi: 10.1089/ten.2005.11.1699.

Buhr, E.D., Yoo, S.H. and Takahashi, J.S. 2010. Temperature as a universal resetting cue for mammalian circadian oscillators. *Science* 330(6002):379-85. doi: 10.1126/science.1195262.
Buschmann, M.D., Kim, Y.J., Wong, M., Frank, E., Hunziker, E.B., and Grodzinsky, A.J. 1999. Stimulation of aggrecan synthesis in cartilage explants by cyclic loading is localized to regions of high interstitial fluid flow. *Arch Biochem Biophys*. 366(1), pp. 1-7. doi: 10.1006/abbi.1999.1197.
Camper, L., Heinegârd, D., and Lundgren-Akerlund, E. 1997. Integrin alpha2beta1 is a receptor for the cartilage matrix protein chondroadherin. *The Journal of cell biology 138*(5), pp. 1159-1167. doi: 10.1083/jcb.138.5.1159.
Carroll, R.G., Timmons, G.A., Cervantes-Silva, M.P., Kennedy, O.D., and Curtis, A.M. 2019. Immunometabolism around the Clock. *Trends Mol. Med* 25(7), pp. 612-625. doi: 10.1016/j.molmed.2019.04.013.
Caterson, B., Christner, J.E., Baker, J.R., and Couchman, J.R. 1985. Production and characterization of monoclonal antibodies directed against connective tissue proteoglycans. *Fed Proc*. 44(2), pp. 386-93.
Cawston, T.E., and Wilson, A.J. 2006. Understanding the role of tissue degrading enzymes and their inhibitors in development and disease. *Best Pract Res Clin Rheumatol*. 20(5), pp. 983-1002. doi: 10.1016/j.berh.2006.06.007.
Chan, K., Wong, F.S. and Pearson, J.A. 2022. Circadian rhythms and pancreas physiology: A review. *Front Endocrinol (Lausanne)*. 13:920261. doi: 10.3389/fendo.2022.920261.
Chao, P.H., West, A.C., and Hung, C.T. 2006. Chondrocyte intracellular calcium, cytoskeletal organization, and gene expression responses to dynamic osmotic loading. *Am J Physiol Cell Physiol*. 291(4), pp. C718-25. doi: 10.1152/ajpcell.00127.2005.
Choi, J.B., Youn, I., Cao, L., Leddy, H.A., Gilchrist, C.L., Setton, L.A., and Guilak, F. 2007. Zonal changes in the three-dimensional morphology of the chondron under compression: the relationship among cellular, pericellular, and extracellular deformation in articular cartilage. *J Biomech*. 40(12), pp. 2596-603. doi: 10.1016/j.jbiomech.2007.01.009.
Chowdhury, T.T., Arghandawi, S., Brand, J., Akanji, O.O., Bader, D.L., Salter, D.M., and Lee, D.A. 2008. Dynamic compression counteracts IL-1beta induced inducible nitric oxide synthase and cyclo-oxygenase-2 expression in chondrocyte/agarose constructs. *Arthritis Res Ther*. 10(2), pp. R35. doi: 10.1186/ar2389.
Chowdhury, T.T., Bader, D.L., and Lee, D.A. 2001. Dynamic compression inhibits the synthesis of nitric oxide and PGE(2) by IL-1beta-stimulated chondrocytes cultured in

agarose constructs. *Biochem Biophys Res Commun*. 285(5), pp. 1168-74. doi: 10.1006/bbrc.2001.5311.
Chowdhury, T.T., Bader, D.L., Shelton, J.C., and Lee, D.A. 2003. Temporal regulation of chondrocyte metabolism in agarose constructs subjected to dynamic compression. *Arch Biochem Biophys*. 417(1), pp.105-11. doi: 10.1016/s0003-9861(03)00340-0.
Clark, A.L., Votta, B.J., Kumar, S., Liedtke, W., and Guilak, F. 2010. Chondroprotective role of the osmotically sensitive ion channel transient receptor potential vanilloid 4: age- and sex-dependent progression of osteoarthritis in Trpv4-deficient mice. *Arthritis Rheum*. 62(10), pp. 2973-83. doi: 10.1002/art.27624.
Cohen, N.P., Foster, R. and Mow, V.C. 1998. Composition and dynamics of articular cartilage: structure, function, and maintaining healthy state. *JOSPT* 28(4), pp. 203-215. doi: 10.2519/jospt.1998.28.4.203.
Cooper, C., Snow, S., McAlindon, T.E., Kellingray, S., Stuart, B., Coggon, D., and Dieppe, P.A. 2000. Risk factors for the incidence and progression of radiographic knee osteoarthritis. *Arthritis Rheum*. 43(5), pp 995-1000. doi: 10.1002/1529-0131(200005)43:5<995::AID-ANR6>3.0.CO;2-1.
Crosby, P. et al. 2019. Insulin/IGF-1 Drives PERIOD Synthesis to Entrain Circadian Rhythms with Feeding Time. *Cell* 177(4):896-909.e20. doi: 10.1016/j.cell.2019.02.017.
Darling, E.M., and Athanasiou, K.A. 2005. Rapid phenotypic changes in passaged articular chondrocyte subpopulations. *J Orthop Res* 23(2), pp. 425-32. doi: 10.1016/j.orthres.2004.08.008.
De Croos, J.N., Pilliar, R.M., and Kandel, R.A. 2008. AP-1 DNA binding activity regulates the cartilage tissue remodeling process following cyclic compression in vitro. *Biorheology* 45(3-4), pp. 459-69.
Del Carlo, M., Schwartz, D., Erickson, E.A., and Loeser, R.F. 2007. Endogenous production of reactive oxygen species is required for stimulation of human articular chondrocyte matrix metalloproteinase production by fibronectin fragments. *Free Radic Biol Med*. 42(9), pp. 1350-8. doi: 10.1016/j.freeradbiomed.2007.01.035.
DeLise, A.M., Fischer, L., and Tuan, R.S. (2000. Cellular interactions and signaling in cartilage development. *Osteoarthritis Cartilage* 8(5), pp. 309-34. doi: 10.1053/joca.1999.0306.
Dernie, F. and Adeyoju, D. 2021. A matter of time: Circadian clocks in osteoarthritis and the potential of chronotherapy. *Experimental Gerontology* 143(1), pp. 111-163. doi: 10.1016/j.exger.2020.111163.

*Dickmeis, T. and Foulkes, N.S. 2011. Glucocorticoids and circadian clock control of cell proliferation: at the interface between three dynamic systems. Mol Cell Endocrinol. 331(1):11-22. doi: 10.1016/j.mce.2010.09.001.*

Dimicco, M.A., Kisiday, J.D., Gong, H., and Grodzinsky, A.J. 2007. Structure of pericellular matrix around agarose-embedded chondrocytes. *Osteoarthritis Cartilage* 15(10), pp.1207-16. doi: 10.1016/j.joca.2007.03.023.

Ding, S.L., et al. 2021. Excessive mechanical strain accelerates intervertebral disc degeneration by disrupting intrinsic circadian rhythm. *Exp Mol Med*. 53(12), pp. 1911-1923. doi: 10.1038/s12276-021-00716-6.

Dintwa, L., Hughes, C. E., & Blain, E. J. 2023. Importance of mechanical cues in regulating musculoskeletal circadian clock rhythmicity: Implications for articular cartilage. *Physiological Reports* 11(15), e15780. doi: 10.14814/phy2.15780.

Dreier, R., Grässel, S., Fuchs, S., Schaumburger, J., and Bruckner, P. 2004. Pro-MMP-9 is a specific macrophage product and is activated by osteoarthritic chondrocytes via MMP-3 or a MT1-MMP/MMP-13 cascade. *Exp Cell Res*. 297(2):303-12. doi: 10.1016/j.yexcr.2004.02.027. PMID: 15212936.

Du, G., et al. 2020. Roles of TRPV4 and piezo channels in stretch-evoked $Ca^{2+}$ response in chondrocytes. *Exp Biol Med (Maywood)* 245(3), pp. 180-189. doi: 10.1177/1535370219892601.

Dudek, M., et al. 2016. The chondrocyte clock gene Bmal1 controls cartilage homeostasis and integrity. *J Clin Invest*. 126(1), pp. 365-376. doi: 10.1172/JCI82755.

Dudek, M., et al. 2021. Circadian time series proteomics reveals daily dynamics in cartilage physiology. *Osteoarthritis Cartilage* 29(5), pp. 739-749. doi: 10.1016/j.joca.2021.02.008.

Dudek, M., et al. 2023. Mechanical loading and hyperosmolarity as a daily resetting cue for skeletal circadian clocks. *Nat Commun*. 14(1), pp. 7237. doi: 10.1038/s41467-023-42056-1.

Eggli, P.S., Herrmann, W., Hunziker, E.B., and Schenk, R.K. 1985. Matrix compartments in the growth place of the proximal tibia of rats. *Anat Rec*. 211(3), 246-257. doi: 10.1002/ar.1092110304.

Eyre, D.R., Weis, M.A. and Wu, J-J. 2006. Articular cartilage collagen: an irreplaceable framework? *European Cells and Materials* 12, pp.57-63. doi: 10.22203/ecm.v012a07.

Farndale, R.W. Buttle, D.J., and Barrett, A.J. 1986. Improved quantitation and discrimination of sulphated glycosaminoglycans by use of dimethylmethylene blue. *Biochimica et Biophysica Acta* 883(2), pp. 173-177. doi: 10.1016/0304-4165(86)90306-5.

Fedewa, M.M., Oegema, T.R. Jr, Schwartz, M.H., MacLeod, A., and Lewis, J.L. 1998. Chondrocytes in culture produce a mechanically functional tissue. *J Orthop Res*. 16, pp. 227-36. doi: 10.1002/jor.1100160210.
Fernandes, J.C., Martel-Pelletier, J., and Pelletier, J.P. 2002. The role of cytokines in osteoarthritis pathophysiology. *Biorheology* 39(1-2), pp. 237-46.
Ferraro, J.T., Daneshmand, M., Bizios, R., and Rizzo, V. 2004. Depletion of plasma membrane cholesterol dampens hydrostatic pressure and shear stress-induced mechanotransduction pathways in osteoblast cultures. *Am J Physiol Cell Physiol*. 286(4), pp. C831-9. doi: 10.1152/ajpcell.00224.2003.
Fitzgerald, J.B., Jin, M., Dean, D., Wood, D.J., Zheng, M.H., and Grodzinsky, A.J. 2004. Mechanical compression of cartilage explants induces multiple time-dependent gene expression patterns and involves intracellular calcium and cyclic AMP. *J Biol Chem*. 279(19), pp. 19502-11. doi: 10.1074/jbc.M400437200.
Fox, S.A.J., Bedi, A., and Rodeo, S.A. 2009. The basic science of articular cartilage: structure, composition, and function. *Sports Health* 1(6), pp. 461-8. doi: 10.1177/1941738109350438.
Frisbie, D.D. and Johnson S.A. 2019. Synovial joint biology and pathobiology. In: Auer, J.A., Stick, J.A., Kümmerle, J.M. and Prange, T. (Eds.). *Equine Surgery*. 5th ed. St. Louis, MO: Elsevier-Saunders, pp. 1326-1348.
Frye, S.R., Yee, A., Eskin, S.G., Guerra, R., Cong, X., and McIntire, L.V. 2005. cDNA microarray analysis of endothelial cells subjected to cyclic mechanical strain: importance of motion control. *Physiol Genomics* 21(1), pp. 124-30. doi: 10.1152/physiolgenomics.00029.2003.
Fukuda, K., Asada, S., Kumano, F., Saitoh, M., Otani, K., and Tanaka, S. 1997. Cyclic tensile stretch on bovine articular chondrocytes inhibits protein kinase C activity. J Lab Clin Med. 130(2), pp. 209-15. doi: 10.1016/s0022-2143(97)90098-6.
Gachon, F. (2007). Physiological function of PARbZip circadian clock-controlled transcription factors. *Ann. Med.* 39(8), pp. 562-571. doi: 10.1080/07853890701491034.
Gagliano, O. et al. 2021. Synchronization between peripheral circadian clock and feeding-fasting cycles in microfluidic device sustains oscillatory pattern of transcriptome. *Nat Commun*. 12(1):6185. doi: 10.1038/s41467-021-26294-9.
Gassner, R., et al. 1999. Cyclic tensile stress exerts anti-inflammatory actions on chondrocytes by inhibiting inducible nitric oxide synthase. *J Immunol*. 163(4), pp. 2187-92.
GBD. 2018. 2017 Disease and Injury Incidence and Prevalence Collaborators. Global, regional, and national incidence, prevalence, and years lived with disability for 354

diseases and injuries for 195 countries and territories, 1990-2017: a systematic analysis for the Global Burden of Disease Study 2017. *Lancet* 392(10159), pp. 1789-1858. doi:10.1016/S0140-6736(18)32279-7.
Gilbert, S.J. and Blain, E.J. 2018. Cartilage mechanobiology: How chondrocytes respond to mechanical load. In: Verbruggen, S.W. [Ed]. *Mechanobiology in Health and Disease*. Academic Press, pp 99-126.
Gilbert, S.J., Bonnet, C.S., and Blain, E.J. 2021. Mechanical Cues: Bidirectional Reciprocity in the Extracellular Matrix Drives Mechano-Signalling in Articular Cartilage. *Int J Mol Sci*. 22(24), pp. 13595. doi: 10.3390/ijms222413595.
Gilbert, S.J., Bonnet, C.S., Stadnik, P., Duance, V.C., Mason, D.J., and Blain, E.J. 2018. Inflammatory and degenerative phases resulting from anterior cruciate rupture in a non-invasive murine model of post-traumatic osteoarthritis. *J Orthop Res*. 36(8), pp. 2118-27. doi: 10.1002/jor.23872.
Goding, J.W., 1996. *Monoclonal antibodies: principles and practice*. Elsevier.
Goldring, M.B. 2000. The role of the chondrocyte in osteoarthritis. *Arthritis Rheum*. 43(9), pp. 1916-26. doi: 10.1002/1529-0131(200009)43:9<1916::AID-ANR2>3.0.CO;2-I.
Goldring, M.B., and Marcu, K.B. 2009. Cartilage homeostasis in health and rheumatic diseases. *Arthritis Res Ther*. 11(3):224. doi: 10.1186/ar2592.
Gooch, K.J., Kwon, J.H., Blunk, T., Langer, R., Freed, L.E., and Vunjak-Novakovic, G. 2001. Effects of mixing intensity on tissue-engineered cartilage. *Biotechnol Bioeng*. 72(4), pp. 402-7. doi: 10.1002/1097-0290(20000220)72:4<402::aid-bit1002>3.0.co;2-q.
Gossan, N., et al. 2013. The circadian clock in murine chondrocytes regulates genes controlling key aspects of cartilage homeostasis. *Arthritis Rheum*. 65(9), pp. 2334-2345. doi: 10.1002/art.38035.
Griess, P. 1879. Bemerkungen zu der abhandlung der H.H. Weselsky und Benedikt “Ueber einige azoverbindungen.” *Chem. Ber.* 12:426-8. doi: 10.1002/cber.187901201117.
Grimm, S., et al. 2020. Influence of clodronate and compressive force on IL-1ß-stimulated human periodontal ligament fibroblasts. *Clin Oral Investig*. 24(1), pp. 43-350. doi: 10.1007/s00784-019-02930-z.
Gross, S.S. and Wolin, M.S. 1995. Nitric oxide: pathophysiological mechanisms. *Annu. Rev. Physiol*. 57(no issue), pp. 737-769. doi: 10.1146/annurev.ph.57.030195.003513.
Guilak, F. 1995. Compression-induced changes in the shape and volume of the chondrocyte nucleus. *J Biomech*. 28(12), pp. 1529-41. doi: 10.1016/0021-9290(95)00100-x.

Guilak, F. and Mow, V.C. 2000. The mechanical environment of the chondrocyte: a biphasic finite element model of cell-matrix interactions in articular cartilage. *J Biomech.* 33(12), pp. 1663-1673. doi: 10.1016/S0021-9290(00)00105-6.
Guilak, F., et al. 2006. The pericellular matrix as a transducer of biomechanical and biochemical signals in articular cartilage. *Ann N Y Acad Sci.* 1068, pp. 498-512. doi: 10.1196/annals.1346.011.
Guilak, F., Meyer, B.C., Ratcliffe, A., and Mow, V.C. 1994. The effects of matrix compression on proteoglycan metabolism in articular cartilage explants. *Osteoarthritis Cartilage* 2(2), pp. 91-101. doi: 10.1016/s1063-4584(05)80059-7.
Guo, B., et al. 2015. Catabolic cytokines disrupt the circadian clock and the expression of clock-controlled genes in cartilage via an NFκB-dependent pathway. *Osteoarthritis Cartilage* 23(11), pp. 1981-1988. doi: 10.1016/j.joca.2015.02.020.
Guo, D., Ding, L., and Homandberg, G.A. 2009. Telopeptides of type II collagen upregulate proteinases and damage cartilage but are less effective than highly active fibronectin fragments. *Inflamm Res*. 58(3), pp. 161-9. doi: 10.1007/s00011-009-8090-5.
Haider, M.A., Schugart, R.C., Setton, L.A., and Guilak, F. 2006. A mechano-chemical model for the passive swelling response of an isolated chondron under osmotic loading. *Biomech Model Mechanobiol*. 5(2-3), pp. 160-71. doi: 10.1007/s10237-006-0026-1.
Hall, A.C., Urban, J.P., and Gehl, K.A. 1991. The effects of hydrostatic pressure on matrix synthesis in articular cartilage. *J Orthop Res*. 9(1), pp. 1-10. doi: 10.1002/jor.1100090102.
Harris, M.D., Anderson, A.E., Henak, C.R., Ellis, B.J., Peters, C.L., and Weiss, J.A. 2012. Finite element prediction of cartilage contact stresses in normal human hips. *J Orthop Res.* 30(7), pp. 1133-1139. doi: 10.1002/jor.22040.
Hayes, A.J., Hall, A., Brown, L., Tubo, R. and Caterson, B. 2007. Macromolecular organization and in vitro growth characteristics of scaffold-free neocartilage grafts. *Journal of Histochemistry & Cytochemistry* 55(8), pp. 853-866. doi: 10.1369/jhc.7A7210.2007.
Henrotin, Y.E., Bruckner, P., and Pujol, J.P. 2003. The role of reactive oxygen species in homeostasis and degradation of cartilage. *Osteoarthritis Cartilage* 11(10), pp. 747-55. doi: 10.1016/s1063-4584(03)00150-x.
Heywood, H.K., Gardner, L., Knight, M.M., and Lee, D.A. 2022. Oscillations of the circadian clock protein, BMAL-1, align to daily cycles of mechanical stimuli: a novel means to integrate biological time within predictive in vitro model systems. *In Vitro Model* 1(6), pp. 405-412. doi: 10.1007/s44164-022-00032-x.

Hodder, E., Guppy, F., Covill, D., and Bush, P. 2020. The effect of hydrostatic pressure on proteoglycan production in articular cartilage in vitro: a meta-analysis. *Osteoarthritis Cartilage* 28(8), pp. 1007-1019. doi: 10.1016/j.joca.2020.03.021.
Hodge, W.A., Fijan, R.S., Carlson, K.L., Burgess, R.G., Harris, W.H., and Mann, R.W. 1986. Contact pressures in the human hip joint measured in vivo. *Proc Natl Acad Sci USA* 83(9), pp. 2879-2883. doi: 10.1073/pnas.83.9.2879.
Holt, J.T., Gopal, T.V., Moulton, A.D., and Nienhuis, A.W. 1986. Inducible production of c-fos antisense RNA inhibits 3T3 cell proliferation. *Proc Natl Acad Sci USA* 83(13), pp. 4794-8. doi: 10.1073/pnas.83.13.4794.
Homandberg, G.A. 1999. Potential regulation of cartilage metabolism in osteoarthritis by fibronectin fragments. *Front Biosci*. 4, pp. D713-30. doi: 10.2741/homandberg.
Honda, K., et al. 2000. The effects of high magnitude cyclic tensile load on cartilage matrix metabolism in cultured chondrocytes. *Eur J Cell Biol*. 79(9), pp. 601-609. doi: 10.1078/0171-9335-00089.
Honda, K.K., et al. 2013. Different circadian expression of major matrix-related genes in various types of cartilage: modulation by light-dark conditions. *J Biochem*. 154(4), pp. 373-381. doi: 10.1093/jb/mvt068.
Hosseini, S.M., Wu, Y., Ito, K., and van Donkelaar, C.C. 2014. The importance of superficial collagen fibrils for the function of articular cartilage. *Biomech Model Mechanobiol*. 13, pp. 41-51. doi: 10.1007/s10237-013-0485-0.
Hosseinzadeh, A., et al. 2016. Apoptosis signaling pathways in osteoarthritis and possible protective role of melatonin. *J Pineal Res*. 61(4):411-425. doi: 10.1111/jpi.12362.
Hou, R., Tomalin, L.E. and Suárez-Fariñas, M. 2021. cosinoRmixedeffects: an R package for mixed-effects cosinor models. *BMC Bioinformatics* 22(1), pp. 553. doi: 10.1186/s12859-021-04463-3.
Hu, J.C.Y. and Athanasiou, K.A. 2003. Structure and function of articular cartilage. In: Yuehuei H. and Kylie L. Martin [Eds]. *Handbook of histology methods for bone and cartilage*. Totowa, N.J. [Great Britain]: Humana Press, pp. 73-95.
Huang, J., Ballou, L.R., and Hasty, K.A. 2007. Cyclic equibiaxial tensile strain induces both anabolic and catabolic responses in articular chondrocytes. *Gene* 404(1-2), pp. 101-9. doi: 10.1016/j.gene.2007.09.007.
Huber, M., Trattnig, S. and Lintner, F. 2000. Anatomy, biochemistry, and physiology of articular cartilage. *Invest Radiol.* 35(10), pp. 573-580. doi: 10.1097/00004424-200010000-00003.

Hughes, C.E., Caterson, B., White, R.J., Roughley, P.J., and Mort, J.S. 1992. Monoclonal antibodies recognizing protease-generated neoepitopes from cartilage proteoglycan degradation. Application to studies of human link protein cleavage by stromelysin. *J Biol Chem*. 267(23), pp. 16011-4. doi: 10.1016/S0021-9258(18)41953-9.
Hunziker, E.B. 1999. Articular cartilage repair: are the intrinsic biological constraints undermining this process insuperable? *Osteoarthritis and Cartilage* 7(1), pp. 15-28. doi: 10.1053/joca.1998.0159.
Hut, R.A., and Steijvers, L. 2007. CircWaveBatch version 3.3 software. University of Groningen, Department of Chronobiology, Netherlands. (https://clocktool.org/index.php/clock-modules/clock-tools/item/circ-wave-batch.html).
Ibidi GmbH 2015. Application Note 33. Available at: https://ibidi.com/img/cms/support/AN/AN33_Live_Dead_staining_with_FDA_and_PI.pdf.
Ikenoue, T., Trindade, M.C., Lee, M.S., Lin, E.Y., Schurman, D.J., Goodman, S.B., and Smith, R.L. 2003. Mechanoregulation of human articular chondrocyte aggrecan and type II collagen expression by intermittent hydrostatic pressure in vitro. *J Orthop Res*. 21(1), pp. 110-116. doi: 10.1016/S0736-0266(02)00091-8.
Im, H-J., et al. 2008. Basic fibroblast growth factor accelerates matrix degradation via a neuro-endocrine pathway in human adult articular chondrocytes. *J Cell Physiol*. 215(2), pp. 452-463. doi: 10.1002/jcp.21317.
Inoue, H., et al. 1990. Stimulation of Proteoglycan and DNA Syntheses in Chondrocytes by Centrifugation. *Journal of Dental Research* 69(9), pp. 1560-1563. doi: 10.1177/00220345900690090401.
Jacob, H., Curtis, A.M., and Kearney, C.J. 2020. Therapeutics on the clock: Circadian medicine in the treatment of chronic inflammatory diseases. *Biochemical Pharmacology* 182(114254), pp. 1-17. doi: 10.1016/j.bcp.2020.114254.
Jang, Y., Jung, H., Nam, Y., Rim, Y.A., Kim, J., Jeong, S.H., and Ju, J.H. 2016. Centrifugal gravity-induced BMP4 induces chondrogenic differentiation of adipose-derived stem cells via SOX9 upregulation. *Stem Cell Res Ther*. 7(1), pp. 184. doi: 10.1186/s13287-016-0445-6.
Janknecht, R., Cahill, M.A, and Nordheim, A. 1995. Signal integration at the c-fos promoter. *Carcinogenesis* 16(3), pp. 443-50. doi: 10.1093/carcin/16.3.443.
Janssen, Y.M., Heintz, N.H., and Mossman, B.T. 1995. Induction of c-fos and c-jun proto-oncogene expression by asbestos is ameliorated by N-acetyl-L-cysteine in mesothelial cells. *Cancer Res*. 55(10), pp. 2085-9.

Jin, M., Emkey, G.R., Siparsky, P., Trippel, S.B., and Grodzinsky, A.J. 2003. Combined effects of dynamic tissue shear deformation and insulin-like growth factor I on chondrocyte biosynthesis in cartilage explants. *Arch Biochem Biophys*. 414(2), pp. 223-31. doi: 10.1016/s0003-9861(03)00195-4.

Jin, M., Frank, E.H., Quinn, T.M., Hunziker, E.B., and Grodzinsky, A.J. 2001. Tissue shear deformation stimulates proteoglycan and protein biosynthesis in bovine cartilage explants. *Arch Biochem Biophys*. 395(1), pp. 41-8. doi: 10.1006/abbi.2001.2543.

Jones, A.R.C., et al. 2009. Modulation of Lubricin Biosynthesis and Tissue Surface Properties Following Cartilage Mechanical Injury. *Arthritis & Rheumatism* 60(1), pp. 133-142. doi: 10.1002/art.24143.

Jones, I.L., Klämfeldt, A., and Sandström, T. 1982. The effect of continuous mechanical pressure upon the turnover of articular cartilage proteoglycans in vitro. *Clin Orthop Relat Res*. 165, pp. 283-9.

Kajimoto, J., Matsumura, R., Node, K. and Akashi, M. 2018. Potential role of the pancreatic hormone insulin in resetting human peripheral clocks. *Genes Cells* 23(5):393-399. doi: 10.1111/gtc.12582.

Kanbe, K., Inoue, K., Xiang, C., and Chen, Q. 2006. Identification of clock as a mechanosensitive gene by large-scale DNA microarray analysis: downregulation in osteoarthritic cartilage. *Mod Rheumatol*. 16(3), pp. 131-136. doi: 10.1007/s10165-006-0469-3.

Kassel, O. and Herrlich, P. 2007. Crosstalk between the glucocorticoid receptor and other transcription factors: molecular aspects. *Mol Cell Endocrinol*. 275(1-2):13-29. doi: 10.1016/j.mce.2007.07.003.

Kato, Y., Iwamoto, M., Koike, T., Suzuki, F., and Takano, Y. 1988. Terminal differentiation and calcification in rabbit chondrocyte cultures grown in centrifuge tubes: regulation by transforming growth factor beta and serum factors. *Proc Natl Acad Sci USA* 85, pp. 9552-6. doi: 10.1073/pnas.85.24.9552.

Kc, R., et al. 2015. Environmental disruption of circadian rhythm predisposes mice to osteoarthritis-like changes in knee joint. *J Cell Physiol*. 230(9), pp. 2174-2183. doi: 10.1002/jcp.24946.

Khan, I.M., Gilbert, S.J., Singhrao, S.K., Duance, V.C. and Archer, C.W. 2008. Cartilage integration: evaluation of the reasons for failure of integration during cartilage repair. A review. *Eur Cell Mater*. 16, pp. 26-39. doi: 10.22203/ecm.v016a04.

Khoshgoftar, M., Torzilli, P.A., and Maher, S.A. 2018. Influence of the pericellular and extracellular matrix structural properties on chondrocyte mechanics. *J Orthop Res*. 36(2), pp. 721-729. doi: 10.1002/jor.23774.
Kiani, C., Chen, L., Wu, Y.J., Yee, A.J. and Yang, B.B. 2002. Structure and function of aggrecan. *Cell Research* 12(1), pp. 19-32. doi: 10.1038/sj.cr.7290106.
Kim, H.A., and Blanco, F.J. 2007. Cell death and apoptosis in osteoarthritic cartilage. *Curr Drug Targets* 8(2), pp. 333-45. doi: 10.2174/138945007779940025.
Kim, Y.J., Grodzinsky, A.J. and Plaas, A.H. 1996. Compression of cartilage results in differential effects on biosynthetic pathways for aggrecan, link protein, and hyaluronan. *Archives of biochemistry and biophysics* 328(2), pp. 331-340. doi: 10.1006/abbi.1996.0181.
Kiviranta, I., Tammi, M., Jurvelin, J., Arokoski, J., Säämänen, A.M., and Helminen, H.J. 1992. Articular cartilage thickness and glycosaminoglycan distribution in the canine knee joint after strenuous running exercise. *Clin Orthop Relat Res*. 283, pp. 302-8. doi: N/A.
Knight, M.M., Lee, D.A., and Bader, D.L. 1998. The influence of elaborated pericellular matrix on the deformation of isolated articular chondrocytes cultured in agarose. *Biochim Biophys Acta*. 1405(1-3), pp. 67-77. doi: 10.1016/s0167-4889(98)00102-5.
Kozera, B., and Rapacz, M. 2013. Reference genes in real-time PCR. *J Appl Genet.* 54(4), pp. 391-406. doi: 10.1007/s13353-013-0173-x.
Kumahashi, N., Ochi, M., Kataoka, H., Uchio, Y., Kakimaru, H., Sugawara, K., and Enomoto, K. 2004. Involvement of ATP, increase of intracellular calcium and the early expression of c-fos in the repair of rat fetal articular cartilage. *Cell Tissue Res*. 317(2), pp. 117-28. doi: 10.1007/s00441-004-0893-7.
Kurz, B., Jin, M., Patwari, P., Cheng, D.M., Lark, M.W., and Grodzinsky, A.J. 2001. Biosynthetic response and mechanical properties of articular cartilage after injurious compression. *J Orthop Res*. 19(6), pp. 1140-6. doi: 10.1016/S0736-0266(01)00033-X.
La Fleur, S.E., Kalsbeek, A., Wortel, J. and Buijs, R.M. 1999. A suprachiasmatic nucleus generated rhythm in basal glucose concentrations. *J Neuroendocrinol*. 11(8):643-52. doi: 10.1046/j.1365-2826.1999.00373.x.
Lai, W.M., Hou, J. and Mow, V.C. 1989. *Triphasic theory for articular cartilage swelling*. New York, USA: Proc. Biomech. Symp. ASME, pp. 33-36.
Lane, J.M. and Weiss, C. 1975. Review of articular cartilage collagen research. *Arthritis and Rheumatism* 18(6), pp. 553-562. doi: 10.1002/art.1780180605.

Lee, C.R., Grad, S., Maclean, J.J., Iatridis, J.C., and Alini, M. 2005. Effect of mechanical loading on mRNA levels of common endogenous controls in articular chondrocytes and intervertebral disk. *Anal Biochem*. 341(2), pp. 372-5. doi: 10.1016/j.ab.2004.10.005.
Lee, D.A., and Bader, D.L. 1997. Compressive strains at physiological frequencies influence the metabolism of chondrocytes seeded in agarose. *J Orthop Res*. 15(2), pp. 181-8. doi: 10.1002/jor.1100150205.
Lee, J.H., Fitzgerald, J.B., Dimicco, M.A., and Grodzinsky, A.J. 2005. Mechanical injury of cartilage explants causes specific time-dependent changes in chondrocyte gene expression. *Arthritis Rheum*. 52(8), pp. 2386-95. doi: 10.1002/art.21215.
Lee, W., Guilak, F., and Liedtke, W. 2017. Role of Piezo Channels in Joint Health and Injury. *Curr Top Membr*. 79, pp. 263-273. doi: 10.1016/bs.ctm.2016.10.003.
Lefebvre, V., and Smits, P. 2005. Transcriptional control of chondrocyte fate and differentiation. *Birth Defects Res C Embryo Today* 75(3), pp. 200-12. doi: 10.1002/bdrc.20048.
Leng, Y., Musiek, E.S., Hu, K., Cappuccio, F.P. and Yaffe, K. 2019. Association between circadian rhythms and neurodegenerative diseases. *Lancet Neurol*. 18(3):307-318. doi: 10.1016/S1474-4422(18)30461-7.
Li, J., et al. 2011. TRPV4-mediated calcium influx into human bronchial epithelia upon exposure to diesel exhaust particles. *Environ Health Perspect*. 119(6), pp. 784-93. doi: 10.1289/ehp.1002807.
Li, Y., Wang, Y., Chubinskaya, S., Schoeberl, B., Florine, E., Kopesky, P., and Grodzinsky, A.J. 2015. Effects of insulin-like growth factor-1 and dexamethasone on cytokine-challenged cartilage: relevance to post-traumatic osteoarthritis. *Osteoarthritis Cartilage* 23(2), pp. 266-74. doi: 10.1016/j.joca.2014.11.006.
Liddell, J., 1991. *A practical guide to monoclonal antibodies*. John Wiley and Sons, Inc.
Lin, P.M., Chen, C.T., and Torzilli, P.A. 2004. Increased stromelysin-1 (MMP-3), proteoglycan degradation (3B3- and 7D4) and collagen damage in cyclically load-injured articular cartilage. *Osteoarthritis Cartilage* 12(6), pp. 485-96. doi: 10.1016/j.joca.2004.02.012.
Livak, K.J. and Schmittgen, T.D. 2001. Analysis of relative gene expression data using real-time quantitative PCR and the 2 $^{-\Delta\Delta C_T}$ Method. *Methods* 25(4), pp. 402-408. doi: 10.1006/meth.2001.1262.
Loeser, R.F., Goldring, S.R., Scanzello, C.R., and Goldring, M.B. 2012. Osteoarthritis: a disease of the joint as an organ. *Arthritis Rheum*. 64(6), pp. 1697-707. doi: 10.1002/art.34453.

Long, P., Gassner, R., and Agarwal, S. 2001. Tumor necrosis factor alpha-dependent proinflammatory gene induction is inhibited by cyclic tensile strain in articular chondrocytes in vitro. *Arthritis Rheum*. 44(10), pp. 2311-9. doi: 10.1002/1529-0131(200110)44:10<2311::aid-art393>3.0.co;2-q.

Lowrey, P.L., and Takahashi, J.S. 2004. Mammalian circadian biology: Elucidating genome-wide levels of temporal organization. *Annu Rev Genom Hum Genet.* 5(1), pp. 407-441. doi: 10.1146/annurev.genom.5.061903.175925.

Lu, Y.C., Evans, C.H., and Grodzinsky, A.J. 2011. Effects of short-term glucocorticoid treatment on changes in cartilage matrix degradation and chondrocyte gene expression induced by mechanical injury and inflammatory cytokines. *Arthritis Res Ther*. 13(5), pp. R142. doi: 10.1186/ar3456.

Lübke, C., et al. 2005. Growth characterization of neo porcine cartilage pellets and their use in an interactive culture model. *Osteoarthritis Cartilage* 13(6), pp. 478-87. doi: 10.1016/j.joca.2004.01.009.

Madhavan, S., et al. 2006. Biomechanical signals exert sustained attenuation of proinflammatory gene induction in articular chondrocytes. *Osteoarthritis Cartilage* 14(10), pp. 1023-32. doi: 10.1016/j.joca.2006.03.016.

Maeda, S., Nishida, J., Sato, T., Inomata, Y., Shimamura, T., and Horiuchi, S. 2005. Changes in microstructure and gene expression of articular chondrocytes cultured in a tube under mechanical stress. *Osteoarthritis Cartilage* 13(2), pp. 154-61. doi: 10.1016/j.joca.2004.10.019.

Malfait, A.M., Liu, R.Q., Ijiri, K., Komiya, S., and Tortorella, M.D. 2002. Inhibition of ADAM-TS4 and ADAM-TS5 prevents aggrecan degradation in osteoarthritic cartilage. *J Biol Chem*. 277(25), pp. 22201-8. doi: 10.1074/jbc.M200431200.

Mansfield, J. C., Bell, J. S. and Winlove, C. P. 2015. The micromechanics of the superficial zone of articular cartilage. *Osteoarthritis and Cartilage* 23(10), pp. 1806-1816. doi: 10.1016/j.joca.2015.05.030.

Marcelino, J., and McDevitt, C.A., 1995. Attachment of articular cartilage chondrocytes to the tissue form of type VI collagen. *Biochimica et Biophysica Acta.* 1249(2), pp. 180-188. doi: 10.1016/0167-4838(95)00026-q.

March, L. 2001. Articular Cartilage in Health and Disease. In Sambrook P [ed.]. *The Musculoskeletal System*. New York: Churchill Livingstone, pp. 86.

Martel-Pelletier, J., Boileau, C., Pelletier, J.P., and Roughley, P.J. 2008. Cartilage in normal and osteoarthritis conditions. *Best Pract Res Clin Rheumatol*. 22(2), pp. 351-84. doi: 10.1016/j.berh.2008.02.001.

Martin, J.A, and Buckwalter, J.A. 1998. Effects of fibronectin on articular cartilage chondrocyte proteoglycan synthesis and response to insulin-like growth factor-I. *J Orthop Res*. 16(6), pp. 752-757. doi: 10.1002/jor.1100160618.

Matsukawa, M., Fukuda, K., Yamasaki, K., Yoshida, K., Munakata, H., and Hamanishi, C. 2004. Enhancement of nitric oxide and proteoglycan synthesis due to cyclic tensile strain loaded on chondrocytes attached to fibronectin. *Inflamm Res*. 53(6), pp. 239-44. doi: 10.1007/s00011-004-1254-4.

Mauck, R.L., et al. 2000. Functional tissue engineering of articular cartilage through dynamic loading of chondrocyte-seeded agarose gels. *J Biomech Eng*. 22(3), pp. 252-60. doi: 10.1115/1.429656.

McIlwraith, C.W. 2002. Diseases of joints, tendons, ligaments, and related structures. In: Stashak TS, (ed.). *Adams' Lameness in Horses*. 5th ed. Philadelphia: Williams & Wilkins, pp. 459-644.

McNulty, A.L., Rothfusz, N.E., Leddy, H.A., and Guilak, F. 2013. Synovial Fluid Concentrations and Relative Potency of Interleukin-1 Alpha and Beta in Cartilage and Meniscus Degradation. *Journal of Orthopaedic Research* 31(7), pp. 1039-1045. doi 10.1002/jor.22334.

Millward-Sadler, S.J., Wright, M.O., Lee, H., Caldwell, H., Nuki, G., and Salter, D.M. 2000. Altered electrophysiological responses to mechanical stimulation and abnormal signalling through alpha5beta1 integrin in chondrocytes from osteoarthritic cartilage. *Osteoarthritis Cartilage* 8(4), pp. 272-278. doi: 10.1053/joca.1999.0301.

Mohawk, J.A., Green, C.B. and Takahashi, J.S. 2012. Central and peripheral circadian clocks in mammals. *Annu. Rev. Neurosci*. 35(1), pp. 445-462. doi: 10.1146/annurev-neuro-060909-153128.

Monfort, J., Garcia-Giralt, N., López-Armada, M.J., Monllau, J.C., Bonilla, A., Benito, P., and Blanco, F.J. 2006. Decreased metalloproteinase production as a response to mechanical pressure in human cartilage: a mechanism for homeostatic regulation. *Arthritis Res Ther*. 8(5), pp. R149. doi: 10.1186/ar2042.

Morey, E.M. and Baylink, D.J. 1979. Inhibition of Bone Formation during Space. *Science* 201(4361), pp. 1138-41. doi: 10.1126/science.150643.

Morrell, K.C., Hodge, W.A., Krebs, D.E., and Mann, R.W. 2005. Corroboration of in vivo cartilage pressures with implications for synovial joint tribology and osteoarthritis causation. *Proc Natl Acad Sci USA* 102(41), pp. 14819-24. doi: 10.1073/pnas.0507117102.

Mow, V.C. and Guo, X.E. 2002. Mechano-electrochemical properties of articular cartilage: their inhomogeneities and anisotropies. *Annu Rev Biomed Eng*. 4(1), pp. 175-209. doi: 10.1146/annurev.bioeng.4.110701.120309.
Mow, V.C., Kuei, S.C., Lai, W.M. and Armstrong, C.G. 1980. Biphasic creep and stress relaxation of articular cartilage in compression? Theory and experiments. *J. Biomech. Eng*. 102(1), pp. 73-84. doi: 10.1115/1.3138202.
Mow, V.C., Lai, W.M. and Hou, J.S. 1990. A triphasic theory for the swelling properties of hydrated charged soft biological tissues. *Appt. Mech. Rev.* 43(part 21), pp. 134-141. doi: 10.1007/978-1-4612-3448-7_10.
Mow, V.C., Proctor, C.S., and Kelly, M.A. 1989. Biomechanics of Articular Cartilage. In: Nordin M, Frankel V, editors. *Basic Biomechanics of the Muskuloskeletal system*. 2nd ed. Philadelphia: Lea and Febiger.
Mow, V.C., Ratcliffe, A. and Poole, A.R. 1992. Cartilage and diarthrodial joints as paradigms for hierarchical materials and structures. *Biomaterials* 13(2), pp. 67-97. doi: 10.1016/0142-9612(92)90001-5.
Muir, H. 1995. The chondrocyte, the architect of cartilage: biomechanics, structure, function and molecular biology of cartilage matrix molecules. *Bioessays* 17(12), pp. 1039-1048. doi: 10.1002/bies.950171208.
Murphy, G., and Nagase, H. 2008. Reappraising metalloproteinases in rheumatoid arthritis and osteoarthritis: destruction or repair? *Nat Clin Pract Rheumatol*. 4(3), pp. 128-35. doi: 10.1038/ncprheum0727.
Murphy, M.P 1999. Nitric oxide and cell death. *Biochimica et Biophysica Acta*. 1411 (2-3), pp. 401-414. doi: 10.1016/s0005-2728(99)00029-8.
Muttigi, M. S., Han, I., Park, H. K., Park, H., & Lee, S. H. 2016. Matrilin-3 Role in Cartilage Development and Osteoarthritis. *International journal of molecular sciences* 17(4), pp. 590. doi: 10.3390/ijms17040590.
Nachar, W., Busseuil, D., Shi, Y., Mihalache-Avram, T., Mecteau, M., Rhéaume, E., and Tardif, J.C. 2014. Optimisation of reference genes for gene-expression analysis in a rabbit model of left ventricular diastolic dysfunction. *PLoS One* 9(2), pp. e89331. doi: 10.1371/journal.pone.0089331.
Nagoshi, E., Saini, C., Bauer, C., Laroche, T., Naef, F. and Schibler, U. 2004. Circadian gene expression in individual fibroblasts: cell-autonomous and self-sustained oscillators pass time to daughter cells. *Cell* 119(5):693-705. doi: 10.1016/j.cell.2004.11.015.

Nakamura, T. J., Nakamura, W., Yamazaki, S., Kudo, T., Cutler, T., Colwell, C.S. and Block, G.D. 2011. Age-related decline in circadian output. *J. Neurosci*. 31(28), pp. 10201-10205. doi: 10.1523/JNEUROSCI.0451-11.2011.

Nakazato, R., Matsuda, Y., Ijaz, F. and Ikegami, K. 2023. Circadian oscillation in primary cilium length by clock genes regulates fibroblast cell migration. *EMBO Rep*. 24(12):e56870. doi: 10.15252/embr.202356870.

Naven, et al. 2022. Development of human cartilage circadian rhythm in a stem cell-chondrogenesis model. *Theranostics* 2(8), pp. 3963-3976. doi: 10.7150/thno.70893.

Nugent, G.E., Aneloski, N.M., Schmidt, T.A., Schumacher, B.L., Voegtline, M.S., and Sah, R.L. 2006. Dynamic shear stimulation of bovine cartilage biosynthesis of proteoglycan 4. *Arthritis Rheum*. 54(6), pp. 1888-96. doi: 10.1002/art.21831.

O'Conor, C.J., Leddy, H.A., Benefield, H.C., Liedtke, W.B., and Guilak, F. 2014. TRPV4-mediated mechanotransduction regulates the metabolic response of chondrocytes to dynamic loading. *Proc Natl Acad Sci USA* 111(4), pp. 1316-21. doi: 10.1073/pnas.1319569111.

Orozco-Solis, R. and Sassone-Corsi, P. 2014. Circadian clock: linking epigenetics to aging. *Curr. Opin. Genet. Dev.* 26(1), pp. 66-72. doi: 10.1016/j.gde.2014.06.003.

Owida, H.A., Kuiper, N.L., and Yang, Y. 2021. Maintenance and Acceleration of Pericellular Matrix Formation within 3D Cartilage Cell Culture Models. *Cartilage* 13(2_suppl), pp. 847S-861S. doi:10.1177/1947603519870839.

Palmoski, M., Perricone, E. and Brandt, K.D. 1979. Development and Reversal of a Proteoglycan Aggregation Defect in Normal Canine Knee Cartilage after Immobilization. *Arthritis Rheum*. 22(5), pp. 509-517. doi: 10.1002/art.1780220511.

Park, Y., Sugimoto, M., Watrin, A., Chiquet, M., and Hunziker, E.B. 2005. BMP-2 induces the expression of chondrocyte-specific genes in bovine synovium-derived progenitor cells cultured in three-dimensional alginate hydrogel. *Osteoarthritis Cartilage* 13(6), pp. 527-36. doi: 10.1016/j.joca.2005.02.006.

Parkkinen, J.J., Ikonen, J., Lammi, M.J., Laakkonen, J., Tammi, M., and Helminen, H.J. 1993. Effects of cyclic hydrostatic pressure on proteoglycan synthesis in cultured chondrocytes and articular cartilage explants. *Arch Biochem Biophys*. 300(1), pp. 458-65. doi: 10.1006/abbi.1993.1062.

Parkkinen, J.J., Lammi, M.J., Helminen, H.J., and Tammi, M. 1992. Local stimulation of proteoglycan synthesis in articular cartilage explants by dynamic compression in vitro. *J Orthop Res*. 10(5), pp. 610-20. doi: 10.1002/jor.1100100503.

Parsons, R., Parsons, R., Garner, N., Oster, H., and Rawashdeh, O. 2020. CircaCompare: a method to estimate and statistically support differences in mesor, amplitude and phase, between circadian rhythms. *Bioinformatics* 36(4), pp. 1208-1212. doi: 10.1093/bioinformatics/btz730.

Partch, C.L., Green, C.B. and Takahashi, J.S. 2014. Molecular architecture of the mammalian circadian clock. *Trends Cell Biol*. 24(2), pp. 90-99. doi: 10.1016/j.tcb.2013.07.002.

Patwari, P., et al. 2003. Proteoglycan degradation after injurious compression of bovine and human articular cartilage in vitro: interaction with exogenous cytokines. *Arthritis Rheum*. 48(5), pp. 1292-301. doi: 10.1002/art.10892.

Peake, M.A., Cooling, L.M., Magnay, J.L., Thomas, P.B., and El Haj, A.J. 1985. Selected contribution: regulatory pathways involved in mechanical induction of c-fos gene expression in bone cells. *J Appl Physiol*. 89(6), pp. 2498-507. doi: 10.1152/jappl.2000.89.6.2498.

Perelis, M. et al. 2015. Pancreatic β cell enhancers regulate rhythmic transcription of genes controlling insulin secretion. *Science* 350(6261):aac4250. doi: 10.1126/science.aac4250.

Pfaffl, M.W., Tichopad, A., Prgomet, C. and Neuvians, T.P. 2004. Determination of stable housekeeping genes, differentially regulated target genes and sample integrity: BestKeeper--Excel-based tool using pair-wise correlations. *Biotechnology letters* 26(6), pp. 509-515. doi: 10.1023/b:bile.0000019559.84305.47.

Pferdehirt, L., Damato, A.R., Dudek, M., Meng, Q.J., Herzog, E.D., and Guilak, F. 2022. Synthetic gene circuits for preventing disruption of the circadian clock due to interleukin-1-induced inflammation. *Sci Adv*. 8(21), pp. eabj8892. doi: 10.1126/sciadv.abj8892.

Phan, M.N., et al. 2009. Functional characterization of TRPV4 as an osmotically sensitive ion channel in porcine articular chondrocytes. *Arthritis Rheum*. 60(10), pp. 3028-37. doi: 10.1002/art.24799.

Plaas, A., et al. 2007. Aggrecanolysis in human osteoarthritis: confocal localization and biochemical characterization of ADAMTS5-hyaluronan complexes in articular cartilages. *Osteoarthritis Cartilage* 15(7), pp. 719-34. doi: 10.1016/j.joca.2006.12.008.

Plaas, A.H., Neame, P.J., Nivens, C.M., and Reiss, L. 1990. Identification of the keratan sulfate attachment sites on bovine fibromodulin. *J Biol Chem*. 265(33), pp. 20634-40. doi: 10.1016/S0021-9258(17)30550-1

Poole, C.A. 1997. Articular cartilage chondrons: form, function and failure. *J Anat*. 191(Pt 1), pp. 1-13. doi: 10.1046/j.1469-7580.1997.19110001.x.

Poole, C.A., Ayad, S., and Schofield, J.R. 1988. Chondrons from articular cartilage: I. Immunolocalization of type VI collagen in the pericellular capsule of isolated canine tibial chondrons. *J Cell Sci*. 90(Pt 4), pp. 635-43. doi: 10.1242/jcs.90.4.635.
Poole, C.A., Flint, M.H., and Beaumont, B.W. 1987. Chondrons in cartilage: ultrastructural analysis of the pericellular microenvironment in adult human articular cartilages. *J Orthop Res*. 5(4), pp. 509-22. doi: 10.1002/jor.1100050406.
Powell, W.T., Rich, L.M, Vanderwall, E.R., White, M.P. and Debley, J.S. 2022. Temperature synchronisation of circadian rhythms in primary human airway epithelial cells from children. *BMJ Open Respir Res*. 9(1):e001319. doi: 10.1136/bmjresp-2022-001319.
Prittinen, J., et al. 2019. Effect of centrifugal force on the development of articular neocartilage with bovine primary chondrocytes. *Cell Tissue Res*. 375(3), pp. 629-639. doi: 10.1007/s00441-018-2938-3.
Qin, X., Li, Q., Chen, W., Bai, Y., Baban, B., and Mao, J. 2019. The circadian expression of osteogenic factors in periodontal tissue loading mechanical force: new concepts of the personalized orthodontic care. *EPMA J.* 10(1), pp. 13-20. doi: 10.1007/s13167-019-0161-2.
Quinn, T.M., Grodzinsky, A.J., Hunziker, E.B., and Sandy, J.D. 1998. Effects of injurious compression on matrix turnover around individual cells in calf articular cartilage explants. *J Orthop Res.* 16(4), pp. 490-499. doi: 10.1002/jor.1100160415.
Quinn, T.M., Hunziker, E.B., and Häuselmann, H.J. 2005. Variation of cell and matrix morphologies in articular cartilage among locations in the adult human knee. *Osteoarthritis Cartilage* 13(8), pp. 672-8. doi: 10.1016/j.joca.2005.04.011.
R Core Team 2022. R: A language and environment for statistical computing. R Foundation for Statistical Computing, Vienna, Austria.
Ragan, P.M., Badger, A.M., Cook, M., Chin, V.I., Gowen, M., Grodzinsky, A.J., and Lark, M.W. 1999. Down-regulation of chondrocyte aggrecan and type-II collagen gene expression correlates with increases in static compression magnitude and duration. *J Orthop Res*. 17(6), pp. 836-42. doi: 10.1002/jor.1100170608.
Ramage, L., Nuki, G., and Salter, D.M. 2009. Signalling cascades in mechanotransduction: cell-matrix interactions and mechanical loading. *Scand J Med Sci Sports*. 19(4), pp. 457-69. doi: 10.1111/j.1600-0838.2009.00912.x.
Ranjan, V., Waterbury, R., Xiao, Z., and Diamond, S.L. 1996. Fluid shear stress induction of the transcriptional activator c-fos in human and bovine endothelial cells, HeLa, and Chinese hamster ovary cells. *Biotechnol Bioeng*. 49(4), pp. 383-90. doi: 10.1002/(SICI)1097-0290(19960220)49:4<383::AID-BIT4>3.0.CO;2-L.

Redlich, M., et al. 2004. The effect of centrifugal force on mRNA levels of collagenase, collagen type-I, tissue inhibitors of metalloproteinases and beta-actin in cultured human periodontal ligament fibroblasts. *J Periodontal Res*. 39(1), pp. 27-32. doi: 10.1111/j.1600-0765.2004.00700.x.

Refinetti, R., Lissen, G.C., and Halberg, F. 2007. Procedures for numerical analysis of circadian rhythms. *Biol Rhythm Res*. 38(4), pp. 275-325. doi: 10.1080/09291010600903692.

Reginster, J.Y. 2002. The prevalence and burden of arthritis. *Rheumatology* 41(Supp 1), pp. 3-6.

Reid, K.J. 2019. Assessment of Circadian Rhythms. *Neurol Clin*. 37(3):505-526. doi: 10.1016/j.ncl.2019.05.001.

Rengel, Y., Ospelt, C., and Gay, S. 2007. Proteinases in the joint: clinical relevance of proteinases in joint destruction. *Arthritis Res Ther*. 9(5), pp. 221. doi: 10.1186/ar2304.

Reppert, S.M. and Weaver, D.R. 2002. Coordination of circadian timing in mammals. *Nature* 418(6901), pp. 935-941. doi: 10.1038/nature00965.

Responte, D.J., Natoli, R.M., and Athanasiou, K.A. 2007. Collagens of articular cartilage: structure, function, and importance in tissue engineering. *Crit Rev Biomed Eng*.35(5), pp. 363-411. doi: 10.1615/critrevbiomedeng.v35.i5.20.

Roenneberg, T. and Merrow, M. 2005. Circadian clocks - the fall and rise of physiology. *Nature Reviews Molecular Cell Biology* 6(12), pp. 965-971. doi: 10.1038/nrm1766.

Rong, J., Zhu, M., Munro, J., Cornish, J., McCarthy, G.M., Dalbeth, N., and Poulsen, R.C. 2019. Altered expression of the core circadian clock component PERIOD2 contributes to osteoarthritis-like changes in chondrocyte activity. *Chronobiol Int*. 36(3), pp. 319-331. doi: 10.1080/07420528.2018.1540493.

Rosenberg, L. 1978. Structure of cartilage proteoglycan. In Simon, W.H. [ed.]. *The human joint in health and disease*. Philadelphia: University of Pennsylvania Press, pp. 26-30.

Roughley, P.J., and Lee, E.R. 1994. Cartilage proteoglycans: structure and potential functions. *Microsc Res Tech*. 28(5), pp. 385-97. doi: 10.1002/jemt.1070280505.

Roughley, P.J., and White, R.J. 1989. Dermatan sulphate proteoglycans of human articular cartilage. The properties of dermatan sulphate proteoglycans I and II. *Biochem J*. 262(3), pp. 823-7. doi: 10.1042/bj2620823.

Ru-song, Z., Zhu-li, Y., Yan-xiao, D., Chong-ying, Y., Ping-ping, J., and Xiao, Y. 2012. Effect of tensile stress on type collagen and aggrecan II expression in rat condylar chondrocytes. *Chin J Tissue Eng Res*. 16(20), pp. 3649-3653. doi: 10.3969/j.issn.1673-8225.2012.20.009.

Rutkauskaite, et al. 2005. Retroviral gene transfer of an antisense construct against membrane type 1 matrix metalloproteinase reduces the invasiveness of rheumatoid arthritis synovial fibroblasts. *Arthritis Rheum*. 52(7), pp. 2010-4. doi: 10.1002/art.21156.
Sah, R.L., Doong, J.Y., Grodzinsky, A.J., Plaas, A.H., and Sandy, J.D. 1991. Effects of compression on the loss of newly synthesized proteoglycans and proteins from cartilage explants. *Arch Biochem Biophys*. 286(1), pp. 20-9. doi: 10.1016/0003-9861(91)90004-3.
Sah, R.L., Kim, Y.J., Doong, J.Y., Grodzinsky, A.J., Plaas, A.H., and Sandy, J.D. 1989. Biosynthetic response of cartilage explants to dynamic compression. *J Orthop Res*. 7(5), pp. 619-36. doi: 10.1002/jor.1100070502.
Saini, C. et al. 2016. A functional circadian clock is required for proper insulin secretion by human pancreatic islet cells. *Diabetes Obes Metab*. 18(4):355-65. doi: 10.1111/dom.12616.
Sanchez-Adams, J., Leddy, H.A., McNulty, A.L., O'Conor, C.J., and Guilak, F. 2014. The mechanobiology of articular cartilage: bearing the burden of osteoarthritis. *Curr Rheumatol Rep*. 16(10), pp. 451. doi: 10.1007/s11926-014-0451-6.
Sandy, J.D. 2006. A contentious issue finds some clarity: on the independent and complementary roles of aggrecanase activity and MMP activity in human joint aggrecanolysis. *Osteoarthritis Cartilage* 14(2), pp. 95-100. doi: 10.1016/j.joca.2005.09.004.
Saracino, P.G., Rossetti, M.L., Steiner, J.L., and Gordon, B.S. 2019. Hormonal regulation of core clock gene expression in skeletal muscle following acute aerobic exercise. *Biochem Biophys Res Commun.* 508(3), pp. 871-876. doi: 10.1016/j.bbrc.2018.12.034.
Sasaki, H., et al. 2016. Forced rather than voluntary exercise entrains peripheral clocks via a corticosterone/noradrenaline increase in PER2::LUC mice. *Sci Rep*. 8(6), pp. 27607. doi: 10.1038/srep27607.
Savarese, J.J., Erickson, H. and Scully, S.P. 1996. Articular chondrocyte tenascin-C production and assembly into *de Novo* extracellular matrix. *J. Orthop. Res*. 14(1), pp. 273-281. doi: 10.1002/jor.1100140216.
Schibler, U. 2007. The daily timing of gene expression and physiology in mammals. *Dialogues Clin Neurosci.* 9(3), pp. 257-272. doi: 10.31887/DCNS.2007.9.3/uschibler.
Schmidt, M.B., Chun, L.E., Eyre, D.R. and Mow, V.C. 1987. The relationship between collagen cross-linking and tensile properties of articular cartilage. *Trans. Orthop. Res. Sot.*12, pp. 134.
Scholtes, S., Krämer, E., Weisser, M., Roth, W., Luginbühl, R., Grossner, T., and Richter, W. 2018. Global chondrocyte gene expression after a single anabolic loading period: Time

evolution and re-inducibility of mechano-responses. *J Cell Physiol*. 233(1), pp. 699-711. doi: 10.1002/jcp.25933.
Schoneveld, O.J., Gaemers, I.C. and Lamers, W.H. 2004. Mechanisms of glucocorticoid signalling. *Biochim Biophys Acta*. 1680(2):114-28. doi: 10.1016/j.bbaexp.2004.09.004.
Schroeder, A.M., and Colwell, C.S. 2013. How to fix a broken clock. *Trends Pharmacol Sci.* 34(11), pp. 605-619. doi: 10.1016/j.tips.2013.09.002.
Sharifi, N., and Gharravi, A.M. 2019. Shear bioreactors stimulating chondrocyte regeneration, a systematic review. *Inflamm Regen*. 8(39), pp. 16. doi: 10.1186/s41232-019-0105-1.
Shelton, J.C., Bader, D.L., and Lee, D.A. 2003. Mechanical conditioning influences the metabolic response of cell-seeded constructs. *Cells Tissues Organs* 175(3), pp. 140-50. doi: 10.1159/000074630.
Shiu, Y.T., Li, S., Yuan, S., Wang, Y., Nguyen, P., and Chien, S. 2003. Shear stress-induced c-fos activation is mediated by Rho in a calcium-dependent manner. *Biochem Biophys Res Commun*. 303(2), pp. 548-55. doi: 10.1016/s0006-291x(03)00388-7.
Silver, N., Best, S., Jiang, J. and Thein, S.L. 2006. Selection of housekeeping genes for gene expression studies in human reticulocytes using real-time PCR. *BMC Molecular Biology* 7, pp. 33. doi: 10.1186/1471-2199-7-33.
Sironen, R.K., et al. 2002. cDNA array reveals mechanosensitive genes in chondrocytic cells under hydrostatic pressure. *Biochim Biophys Acta*. 1591(1-3), pp. 45-54. doi: 10.1016/s0167-4889(02)00247-1.
Smith, R.L., et al. 1996. In vitro stimulation of articular chondrocyte mRNA and extracellular matrix synthesis by hydrostatic pressure. *J Orthop Res*. 14(1), pp. 53-60. doi: 10.1002/jor.1100140110.
Smyllie, N.J., et al. 2016. Visualizing and Quantifying Intracellular Behaviour and Abundance of the Core Circadian Clock Protein PERIOD2. *Curr Biol*. 26(14), pp. 1880-6. doi: 10.1016/j.cub.2016.05.018.
Snelling, S.J., Forster, A., Mukherjee, S., Price, A.J., and Poulsen, R.C. 2016. The chondrocyte-intrinsic circadian clock is disrupted in human osteoarthritis. *Chronobiol Int*. 33(5), pp. 574-579. doi: 10.3109/07420528.2016.1158183.
Stanton, H., Ung, L., and Fosang, A.J. 2002. The 45 kDa collagen-binding fragment of fibronectin induces matrix metalloproteinase-13 synthesis by chondrocytes and aggrecan degradation by aggrecanases. *Biochem J*. 364(Pt 1), pp. 181-90. doi: 10.1042/bj3640181.

Stephens, P., et al. 2004. Crosslinking and G-protein functions of transglutaminase 2 contribute differentially to fibroblast wound healing responses. *J. Cell Sci*. 117(15), pp. 3389-3403. doi: 10.1242/jcs.01188.
Sun, H.B. 2010. Mechanical loading, cartilage degradation, and arthritis. *Ann. N.Y. Acad. Sci.* 1211(1), pp. 37-50. doi: 10.1111/j.1749-6632.2010.05808.x.
Svec, D., Tichopad, A., Novosadova, V., Pfaffl, M. W., and Kubista, M. 2015. How good is a PCR efficiency estimate: Recommendations for precise and robust qPCR efficiency assessments. *Biomolecular detection and quantification* 3(1), pp. 9-16. doi: 10.1016/j.bdq.2015.01.005.
Szapary, H.J., Flaman, L., Frank, E., Chubinskaya, S., Dwivedi, G. and Grodzinsky, A.J. 2023. Effects of dexamethasone and dynamic loading on cartilage of human osteochondral explants challenged with inflammatory cytokines. *J Biomech*. 149:111480. doi: 10.1016/j.jbiomech.2023.111480.
Szirmai, J.A. 1969. Structure of cartilage. In: Engel, A. and Larsson, T. (eds.). *Aging of Connective and Skeletal Tissue*. Stockholm, Sweden: Nordiska, pp. 163-200.
Takahashi, J.S., Hong, H-K., Ko, C.H. and McDearmon, E.L. 2008. The genetics of mammalian circadian order and disorder: implications for physiology and disease. *Nat Rev. Genet.* 9(10), pp. 764-775. doi: 10.1038/nrg2430.
Tan, K. and Lawler, J. 2009. The interaction of Thrombospondins with extracellular matrix proteins. *J. Cell Commun Signal*. 3(3-4), pp. 177-187. doi: 10.1007/s12079-009-0074-2.
Theodoropoulos, J.S., DeCroos, A.J., Petrera, M., Park, S., and Kandel, R.A. 2016. Mechanical stimulation enhances integration in an in vitro model of cartilage repair. *Knee Surg Sports Traumatol Arthrosc*. 24(6), pp. 2055-64. doi: 10.1007/s00167-014-3250-8.
Thomas, R.S., Clarke, A.R., Duance, V.C., and Blain, E.J. 2011. Effects of Wnt3A and mechanical load on cartilage chondrocyte homeostasis. *Arthritis Res Ther*. 13(6), pp. R203. doi: 10.1186/ar3536.
Tortorella, M.D., et al. 1999. Purification and cloning of aggrecanase-1: a member of the ADAMTS family of proteins. *Science* 284(5420), pp. 1664-6. doi: 10.1126/science.284.5420.1664.
Tortorella, M.D., Malfait, A.M., Deccico, C., and Arner, E. 2001. The role of ADAM-TS4 (aggrecanase-1) and ADAM-TS5 (aggrecanase-2) in a model of cartilage degradation. *Osteoarthritis Cartilage* 9(6), pp. 539-52. doi: 10.1053/joca.2001.0427.
Torzilli, P.A., Askari, E. and Jenkins, J.T. 1990. Water content and solute diffusion properties in articular cartilage. In: Ratcliffe A., Woo S.LY., Mow V.C. (eds). *Biomechanics of diarthrodial joints*. New York, NY:Springer, pp. 363-390.

Torzilli, P.A., Bhargava, M., and Chen, C.T. 2011. Mechanical Loading of Articular Cartilage Reduces IL-1-Induced Enzyme Expression. *Cartilage* 2(4), pp. 364-373. doi: 10.1177/1947603511407484.
Torzilli, P.A., Grigiene, R., Borrelli, J. Jr., and Helfet, D.L. 1999. Effect of impact load on articular cartilage: cell metabolism and viability, and matrix water content. *J Biomech Eng*. 121(5), pp. 433-41. doi: 10.1115/1.2835070.
Tucker, R.W., Pardee, A.B. and Fujiwara K. 1979. Centriole ciliation is related to quiescence and DNA synthesis in 3T3 cells. *Cell* 17(3):527-35. doi: 10.1016/0092-8674(79)90261-7.
Tuvia, N. et al. 2021. Insulin Directly Regulates the Circadian Clock in Adipose Tissue. *Diabetes* 70(9):1985-1999. doi: 10.2337/db20-0910.
Twomey, J.D., Thakore, P.I., Hartman, D.A., Myers, E.G., and Hsieh, A.H. 2014. Roles of type VI collagen and decorin in human mesenchymal stem cell biophysics during chondrogenic differentiation. *Eur Cell Mater*. 27(237-50); discussion 249-50. doi: 10.22203/ecm.v027a17.
Ueki, M., et al. 2008. The effect of mechanical loading on the metabolism of growth plate chondrocytes. *Ann Biomed Eng*. 36(5), pp. 793-800. doi: 10.1007/s10439-008-9462-7.
Urban, J.P. 1994. The chondrocyte: a cell under pressure. *Br J Rheumatol.* 33(10), pp. 901-908. doi: 10.1093/rheumatology/33.10.901.
Valhmu, W.B., Stazzone, E.J., Bachrach, N.M., Saed-Nejad, F., Fischer, S.G., Mow, V.C., and Ratcliffe, A. 1998. Load-controlled compression of articular cartilage induces a transient stimulation of aggrecan gene expression. *Arch Biochem Biophys*. 353(1), pp. 29-36. doi: 10.1006/abbi.1998.0633.
van der Kraan, P., Matta, C. and Mobasheri, A. 2017. Age-Related Alterations in Signaling Pathways in Articular Chondrocytes: Implications for the Pathogenesis and Progression of Osteoarthritis-A Mini-Review. *Gerontology* 63(1), pp. 29-35. doi: 10.1159/000448711.
Vandesompele, J., De Preter, K., Pattyn, F., Poppe, B., Van Roy, N., De Paepe, A. and Speleman, F. 2002. Accurate normalization of real-time quantitative RT-PCR data by geometric averaging of multiple internal control genes. *Genome biology* 3(7), pp. research0034.1–research0034.11. doi: 10.1186/gb-2002-3-7-research0034.
Vanmunster, M., et al. 2022. Mechanosensors control skeletal muscle mass, molecular clocks, and metabolism. *Cell Mol Life Sci*. 79(6), pp. 321. doi: 10.1007/s00018-022-04346-7.

Vaughan-Thomas, A., Young, R.D., Phillips, A.C. and Duance, V.C. 2001. Characterisation of type XI collagen-glycosaminoglycan interactions. *J. Biol. Chem*. 276(7), pp. 5303-5309. doi: 10.1074/jbc.M008764200.
Versus Arthritis (2024). The state of musculoskeletal health 2024. Available online at: https://versusarthritis.org/about-arthritis/data-and-statistics/the-state-of- musculoskeletal-health/.
Vincent, T.L., Hermansson, M.A., Hansen, U.N., Amis, A.A., and Saklatvala, J. 2004. Basic fibroblast growth factor mediates transduction of mechanical signals when articular cartilage is loaded. *Arthritis Rheum*. 50(2), pp. 526-33. doi: 10.1002/art.20047.
Vincenti, M.P., and Brinckerhoff, C.E. 2002. Transcriptional regulation of collagenase (MMP-1, MMP-13) genes in arthritis: integration of complex signaling pathways for the recruitment of gene-specific transcription factors. *Arthritis Res*. 4(3), pp. 157-64. doi: 10.1186/ar401.
Waldman, S.D., Spiteri, C.G., Grynpas, M.D., Pilliar, R.M., and Kandel, R.A. 2003. Long-term intermittent shear deformation improves the quality of cartilaginous tissue formed in vitro. *J Orthop Res*. 21(4), pp. 590-6. doi: 10.1016/S0736-0266(03)00009-3.
Wang, D., Taboas, J.M., and Tuan, R.S. 2011. PTHrP overexpression partially inhibits a mechanical strain-induced arthritic phenotype in chondrocytes. *Osteoarthritis Cartilage* 19(2), pp. 213-21. doi: 10.1016/j.joca.2010.11.003.
Wang, M., et al. 2021. Mechanical Stress Affects Circadian Rhythm in Skeletal Muscle (C2C12 Myoblasts) by Reducing Per/Cry Gene Expression and Increasing Bmal1 Gene Expression. *Med Sci Monit*. 27(e928359), pp. 1-10. doi: 10.12659/MSM.928359.
Wang, Y., Wan, S., Drago, J., White, F.M., and Grodzinsky, A.J. 2017b. Phosphoproteomics analysis of signaling changes in human chondrocytes following treatment with IL-1, IGF-1 and dexamethasone. *Osteoarthritis Cartilage* 25, pp. S165-S166. doi: 10.1016/j.joca.2017.02.282.
Watanabe, H., Yamada, Y. and Kimata, K. 1998. Roles of aggrecan, a large chondroitin sulfate proteoglycan, in cartilage structure and function. *J. Biochem.* 124(4), pp. 687-693. doi: 10.1093/oxfordjournals.jbchem.a022166.
Wiberg, C., Heinegård, D., Wenglén, C., Timpl, R., and Mörgelin, M. 2002. Biglycan organizes collagen VI into hexagonal-like networks resembling tissue structures. *J Biol Chem*. 277(51), pp. 49120-6. doi: 10.1074/jbc.M206891200.
Wickham, H 2016. *ggplot2: Elegant Graphics for Data Analysis*. Springer-Verlag New York. ISBN 978-3-319-24277-4.

Wolff, G., and Esser, K.A. 2012. Scheduled exercise phase shifts the circadian clock in skeletal muscle. *Med Sci Sports Exerc*. 44(9), pp. 1663-70. doi: 10.1249/MSS.0b013e318255cf4c.

Wong, M., Siegrist, M., and Cao, X. 1999. Cyclic compression of articular cartilage explants is associated with progressive consolidation and altered expression pattern of extracellular matrix proteins. *Matrix Biology.* 18(4), pp. 391-399. doi: 10.1016/s0945-053x(99)00029-3.

Woo, K.C., Ha, D.C., Lee, K.H., Kim, D.Y., Kim, T.D. and Kim, K.T. 2010. Circadian amplitude of cryptochrome 1 is modulated by mRNA stability regulation via cytoplasmic hnRNP D oscillation. *Mol Cell Biol*. 30(1):197-205. doi: 10.1128/MCB.01154-09.

Xie, D.L., Hui, F., Meyers, R., and Homandberg, G.A. 1994. Cartilage chondrolysis by fibronectin fragments is associated with release of several proteinases: stromelysin plays a major role in chondrolysis. *Arch Biochem Biophys*. 311(2), pp. 205-12. doi: 10.1006/abbi.1994.1228.

Xie, F., Xiao, P., Chen, D., Xu, L. and Zhang, B. 2012. miRDeepFinder: a miRNA analysis tool for deep sequencing of plant small RNAs. *Plant molecular biology* 80(1), pp. 75-84. doi: 10.1007/s11103-012-9885-2.

Xu, X., Li, Z., Leng, Y., Neu, C.P., and Calve, S. 2016. Knockdown of the pericellular matrix molecule perlecan lowers in situ cell and matrix stiffness in developing cartilage. *Dev Biol*. 418(2), pp. 242-7. doi: 10.1016/j.ydbio.2016.08.029.

Xu, Z., Buckley, M.J., Evans, C.H., and Agarwal S. 2000. Cyclic tensile strain acts as an antagonist of IL-1 beta actions in chondrocytes. *J Immunol*. 165(1), pp. 453-60. doi: 10.4049/jimmunol.165.1.453.

Yamanaka, Y., Honma, S., and Honma, K. 2008. Scheduled exposures to a novel environment with a running-wheel differentially accelerate re-entrainment of mice peripheral clocks to new light-dark cycles. *Genes Cells* 13(5), pp. 497-507. doi: 10.1111/j.1365-2443.2008.01183.x.

Yang, N. and Meng, Q-J. 2016. Circadian Clocks in Articular Cartilage and Bone: A Compass in the Sea of Matrices. *Journal of Biological Rhythms* 31(5), pp. 415-427. doi: 10.1177/0748730416662748.

Yang, N., et al. 2020. Quantitative live imaging of Venus::BMAL1 in a mouse model reveals complex dynamics of the master circadian clock regulator. *PLoS Genet*. 16(4), pp. e1008729. doi: 10.1371/journal.pgen.1008729.

Yao, Q., et al. 2023. Osteoarthritis: pathogenic signaling pathways and therapeutic targets. *Sig Transduct Target Ther*. 8(1), pp. 56. doi: 10.1038/s41392-023-01330-w.

Zhai, Z., Yao, Y., and Wang, Y. 2013. Importance of suitable reference gene selection for quantitative RT-PCR during ATDC5 cells chondrocyte differentiation. *PLoS One* 8(5):e64786. doi: 10.1371/journal.pone.0064786.
Zhang, L., Su, P., Xu, C., Yang, J., Yu, W., and Huang, D. 2010. Chondrogenic differentiation of human mesenchymal stem cells: a comparison between micromass and pellet culture systems. *Biotechnol Lett*. 32(9), pp. 1339-46. doi: 10.1007/s10529-010-0293-x.
Zhang, Z., McCaffery, J.M., Spencer, R.G., and Francomano, C.A. 2004. Hyaline cartilage engineered by chondrocytes in pellet culture: histological, immunohistochemical and ultrastructural analysis in comparison with cartilage explants. *J Anat*. 205(3), pp. 229-37. doi: 10.1111/j.0021-8782.2004.00327.x.
Zhao, Z., Li, Y., Wang, M., Zhao, S., Zhao, Z., and Fang, J. 2020. Mechanotransduction pathways in the regulation of cartilage chondrocyte homoeostasis. *J Cell Mol Med*. 24(10), pp. 5408-5419. doi: 10.1111/jcmm.15204.

# Appendices

## Appendix 1

An example of an R script for creating boxplots depicting mechano-responses of 3D pellets to mechanical load (simulated through 200-, 770- and 1000-xg centrifugal forces)

```
#Setting working directory
setwd("C:/Users/…….. ")
library(ggpubr)
# Load data into R (c-fos expression following exposure of pellets to 770xg force for 60 minutes)
FOS770<- read.csv(file="C-fos 770xg.csv")
# Basic plot
my_comparisons = list( c("0.5 (Control)", "0.5 (1 episode of 770xg load)"), c("4 (Control)", "4 (1 episode of 770xg load)"), c("8 (Control)", "8 (1 episode of 770xg load)"), c("24 (Control)", "24 (1 episode of 770xg load)"))
p <- ggboxplot(FOS770, x = "Group", y = "Relative_mRNA_expression", linetype = "solid",
          size = 0.8, bxp.errorbar = TRUE,
          xlab = "Hours post load and experimental groups", ylab = "Fold change in c-fos mRNA (Normalised to HKGs)")+
theme(
   axis.ticks = element_line(size = 1),
   axis.line = element_line(size = 1.2)
 )+
 font("xy.text", size = 10, face = "bold")+
 font("xlab", size = 11, face = "bold")+
 font("ylab", size = 11, face = "bold")
p
Plot <- p +scale_y_continuous(breaks = seq(0.0,3.0,0.25), limits = c(0.0, 3.0))
# Vertical x axis text in ggpubr
Plot + rotate_x_text(45)+
   stat_compare_means(comparisons=my_comparisons, method = "wilcox.test", aes(label=..p.signif..))
```

## Appendix 2

An example of an R script for plotting *bmal1* mRNA rhythmicity profiles within a 72-hour period.

```
Setwd () ## Set up a working directory in the computer used
Install.packages("ggplot2")
Library (ggplot2) ###Load package
###Create basic datasets
time  <- c(0,0,0,0,4,4,4,4,8,8,8,8,12,12,12,12,16,16,16,16,20,20,20,20,24,24,24,24)
Loaded024hrs <-
c(1.002,1.026,0.978,0.995,0.998,0.931,0.991,0.845,0.958,1.059,0.971,0.995,1.041,1.002,0.912,0.887,1.030,
0.985,0.925,0.981,0.665,0.524,0.733,0.805,0.544,0.556,0.539,0.539)

time1  <-
c(24,24,24,24,28,28,28,28,32,32,32,32,36,36,36,36,40,40,40,40,44,44,44,44,48,48,48,48,52,52,52,52,56,56,
56,56,60,60,60,60,64,64,64,64,68,68,68,68,72,72,72,72)
Loaded2472hrs <-
c(0.544,0.556,0.539,0.539,0.900,0.995,1.070,1.033,1.775,1.696,1.566,1.622,1.837,1.850,1.818,1.775,0.931,
0.978,1.005,0.938,0.721,0.703,0.684,0.744,0.981,0.919,0.948,0.775,1.208,1.216,1.412,1.033,1.667,1.577,1.
610,1.561,1.639,1.529,1.503,1.364,1.016,1.026,1.041,0.971,0.900,1.002,0.897,0.919,0.814,0.890,0.893,0.7
75)
time2  <-
c(0,0,0,0,4,4,4,4,8,8,8,8,12,12,12,12,16,16,16,16,20,20,20,20,24,24,24,24,28,28,28,28,32,32,32,32,36,36,36
,36,40,40,40,40,44,44,44,44,48,48,48,48,52,52,52,52,56,56,56,56,60,60,60,60,64,64,64,64,68,68,68,68,72,7
2,72,72)
Unloaded <-
c(0.966,0.990,1.010,1.035,0.660,0.707,0.758,0.750,0.997,1.014,1.021,0.959,1.860,1.790,1.809,1.765,1.244,
1.218,1.210,1.206,1.157,1.301,1.173,1.117,0.396,0.467,0.419,0.396,1.106,1.098,0.856,1.169,1.939,1.784,1.
986,2.042,1.959,1.759,1.959,2.189,1.046,1.032,0.730,1.223,0.829,0.798,0.895,0.850,0.818,0.850,0.841,0.8
71,1.597,1.809,1.821,1.227,1.676,1.892,1.597,1.569,1.659,1.625,1.912,1.784,1.235,1.409,1.244,1.434,0.78
7,0.776,0.618,1.003,0.787,0.774,0.877,0.582)

df<-data.frame(time,Loaded024hrs)
df1<-data.frame(time1,Loaded2472hrs)
df2<-data.frame(time2,Unloaded)

lmfit <- lm(Loaded2472hrs~ sin(2*pi/23.3*time1) + cos(2*pi/23.3*time1), data=df1)
pframe <- data.frame(time1 =seq(min(df1$time1),max(df1$time1),length=72))
pframe$Loaded2472hrs<- predict (lmfit, newdata=pframe)
lmfit2 <- lm(Unloaded~ sin(2*pi/22.4*time2) + cos(2*pi/22.4*time2), data=df2)
pframe2 <- data.frame(time2 =seq(min(df2$time2),max(df2$time2),length=72))
pframe2$Unloaded<- predict (lmfit2, newdata=pframe2)
ggplot(NULL, aes(x, y))+
theme_bw() + theme(panel.grid = element_blank())+
  theme( axis.line = element_line(colour = "black",
                                  size = 1, linetype = "solid"))+
  theme(axis.text.x = element_text(face="bold", color="Black",
                                   size=10),
        axis.text.y = element_text(face="bold", color="Black",
                                   size=10))+
  theme(axis.title = element_text(face="bold", size = 12))+
geom_point(data = df,aes(x = time, y = Loaded024hrs,colour="Loaded024hrs")) +
```

```
geom_point(data = df1,aes(x = time1, y = Loaded2472hrs,colour="Loaded2472hrs")) +
geom_point(data = df2,aes(x = time2, y = Unloaded,colour="Unloaded")) +
  scale_colour_manual(name = "3D datasets",
                      labels = c("1 episode of 770xg load (1-hour)"," 1 episode of 770xg load (1-hour)", "Control"),
                      values = c("Loaded024hrs"="Green","Loaded2472hrs"="Green","Unloaded"="Black"))+
  theme(legend.title=element_text(size=12, face="bold"),
        legend.text=element_text(size=10)) +
geom_line(data = pframe,aes(x = time1, y = Loaded2472hrs),colour="Green", size = 1.2) +
geom_line(data = pframe2,aes(x = time2, y = Unloaded),colour="Black", size = 1.2) +
   scale_x_continuous("Time point (hours)", breaks=seq(0,72,4) , label= c("0", "4","8", "12", "16","20", "24",
"28","32", "36","40","44", "48","52","56", "60","64","68", "72"))+
  scale_y_continuous("Fold change in bmal1 mRNA (Normalised to HKGs)", breaks=seq(0.0,3.0,0.25) ,
limits= c("0.0, 3.0))''
```

## Appendix 3

**A representative plot of $C_T$ as a function of log sample quantity used to determine the efficiency of *clock* gene primers.** The graph illustrates the slope/gradient of a regression line essential in the calculation of *clock* primer efficiency determined following qPCR amplification of appropriately diluted cDNA templates obtained from control 2D bovine chondrocyte cultures. *clock* primers demonstrated an efficiency of 107.8% (n = 3, N = 1). Similar plots were observed when analysing other clock genes (data not shown).

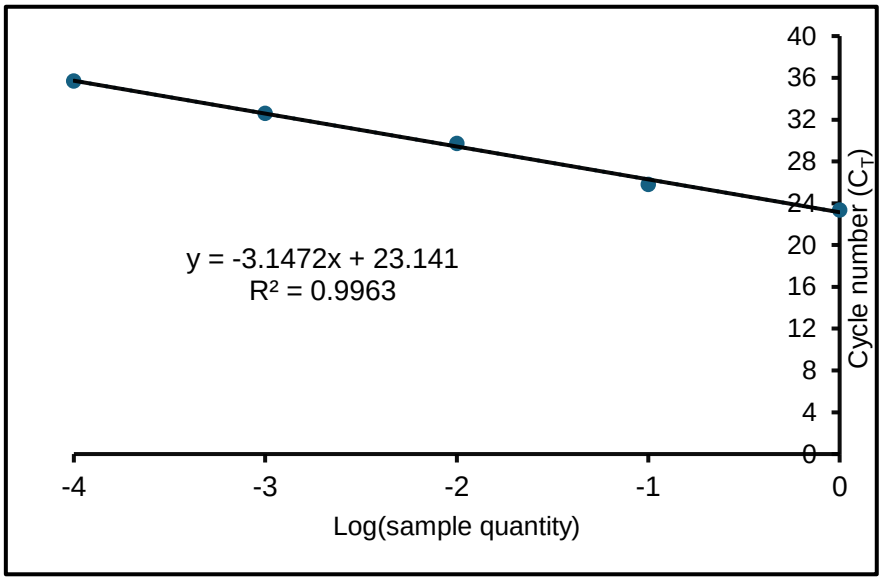

## Appendix 4

**A representative *clock* gene amplification plot obtained from the AriaMx Real-Time qPCR software indicating the accumulation of products during thermal cycling after exceeding background noise.** The graph illustrates DNA binding dye (SYBR® green) fluorescence plotted against cycle number during the amplification of specific cDNA fragments using *clock* gene primers. The three curves (grey, orange and purple) represent technical replicates (n= 3, N = 1) while a no template control (NTC) overlapping with the threshold line (light bluish line) represents no amplification (n = 1, N = 1). Similar plots were observed when analysing other clock genes (data not shown).

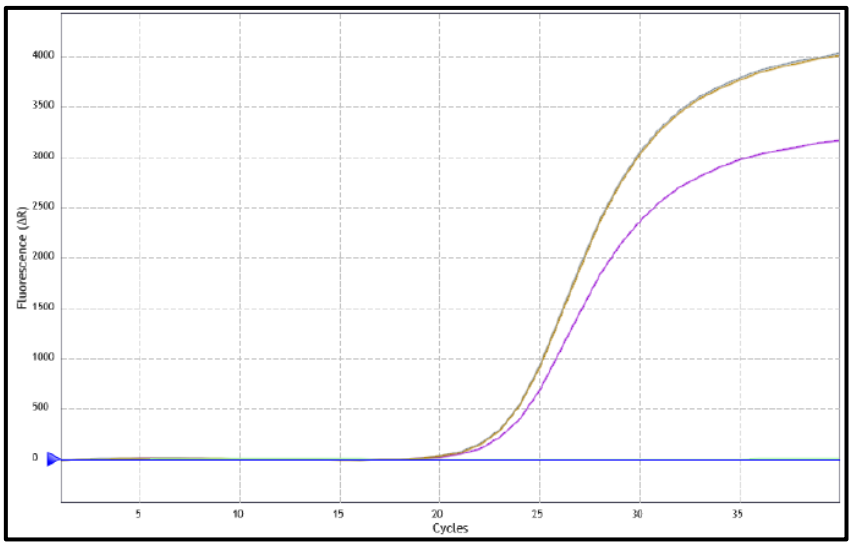

## Appendix 5

**A representative *clock* gene melting curve obtained from the AriaMx Real-Time qPCR software indicating the dissociation of one amplicon species when exposed to high temperature following 40 cycles of amplification.** The graph illustrates negative derivative of DNA binding dye (SYBR® green) fluorescence plotted against temperature following the amplification of specific cDNA fragments using *clock* primers. The three curves (blue, sky blue, and orange) represent technical replicates (n= 3, N = 1) demonstrating a single peak, while an NTC (pink) represents no peak hence no primer-dimers (n = 1, N = 1). Similar curves were observed when analysing other clock genes (data not shown).

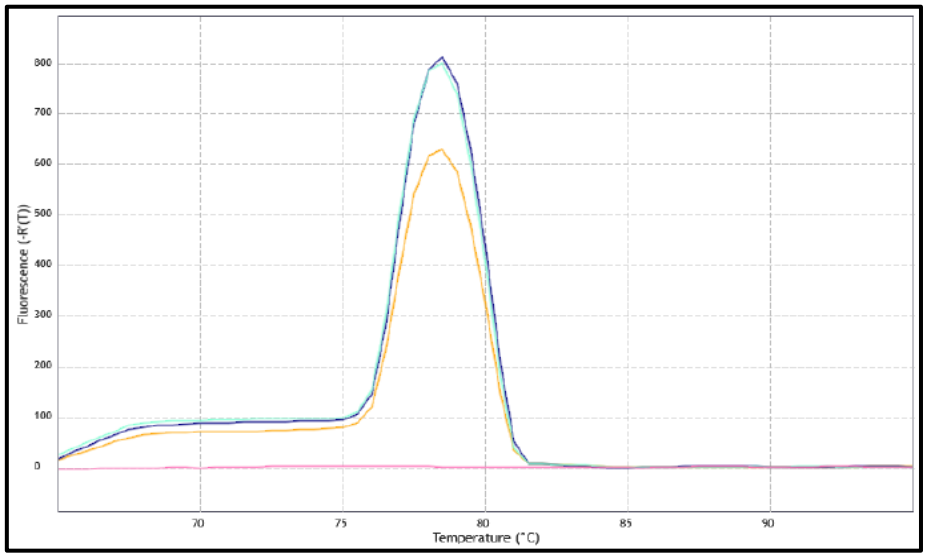

## Appendix 6

**Separation of qPCR products using agarose gel electrophoresis to validate primer specificity and amplicon sizes.** The images show white bands representing amplicons for each newly designed primer pair, as detected using UV illumination; the first lane of each gel image includes a 100bp DNA Ladder Molecular Weight Marker. Clock gene products and NTCs were ran in three independent gels in the following order: **A)** *bhlhe40, bhlhe41, bmal1, clock & cry1* (gel 1), **B)** *dbp, nfil3, npas2, nr1d1 & nr1d2* (gel 2) and **C)** *per1, per2, rorα & rorγ* (gel 3). All PCR amplicons showed one band except for *bhlhe40* which contained three bands, whilst all NTCs were clean showing no non-specific amplification.

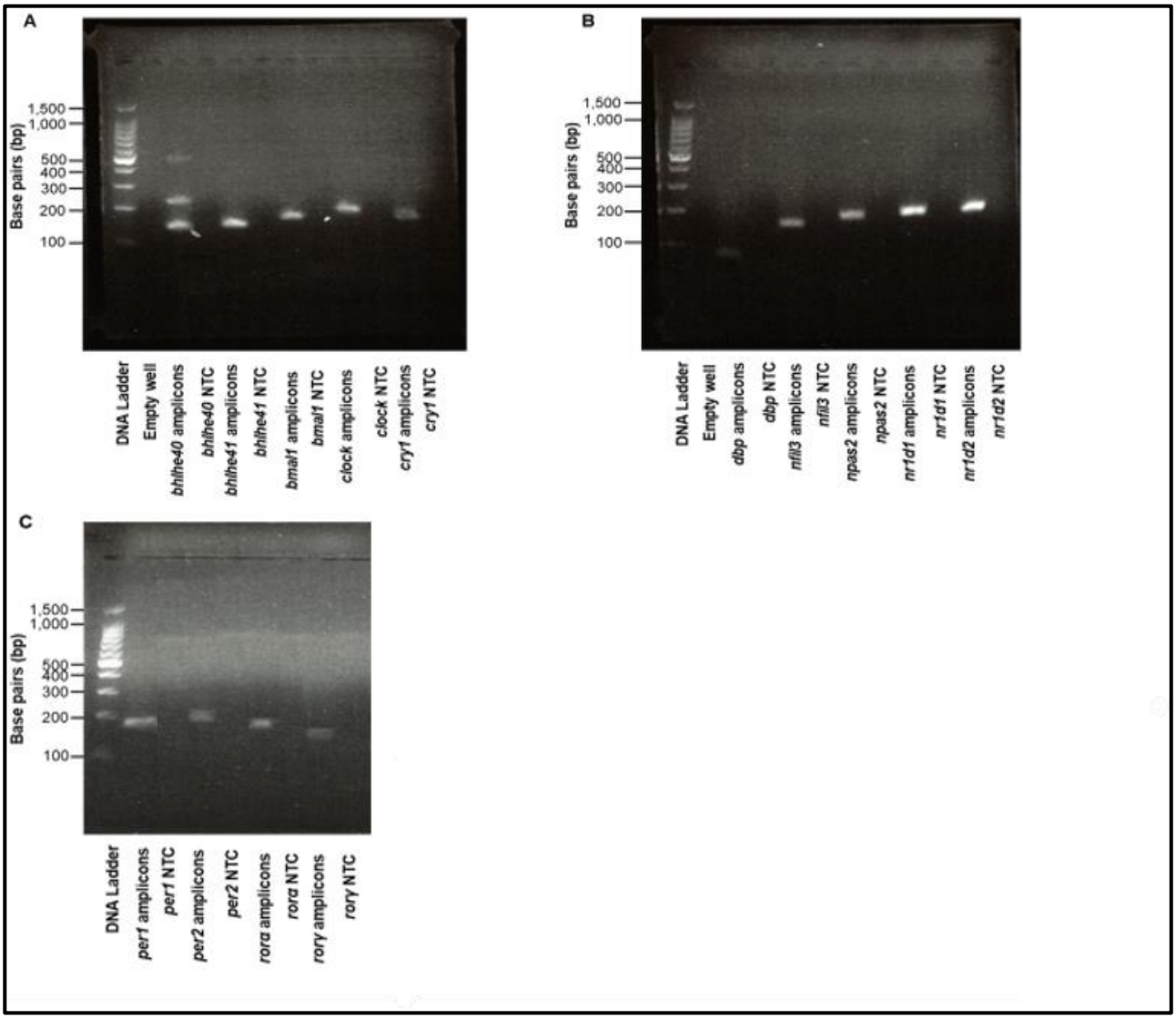

## Appendix 7

**Reproducible baseline circadian rhythmicity of *bmal1*, *npas2* and *rorα* transcription within a 72-hour period in 2D chondrocyte cultures.** Fold change in mRNA transcripts (normalised to *18s* and *hprt*) plotted against time of collection (4-hour interval) of control 2D chondrocyte cultures before qPCR quantification of the following clock genes within a 72-hour period: **A)** *bmal1*, **B)** *npas2* and **C)** *rorα*. Black dots and curves represent experiment 1 datasets; Grey dots and curves represent repeat experimental datasets. The fitted cosinusoidal waves indicate rhythmic oscillations of mRNA transcripts for a specific gene determined by the CircWaveBatch software ($R^2$> 0.8, p < 0.05) and graphically plotted in the R software using the ggplot2 package. Data points represent fold changes in mRNA transcripts (n = 4, N = 1 per repeat).

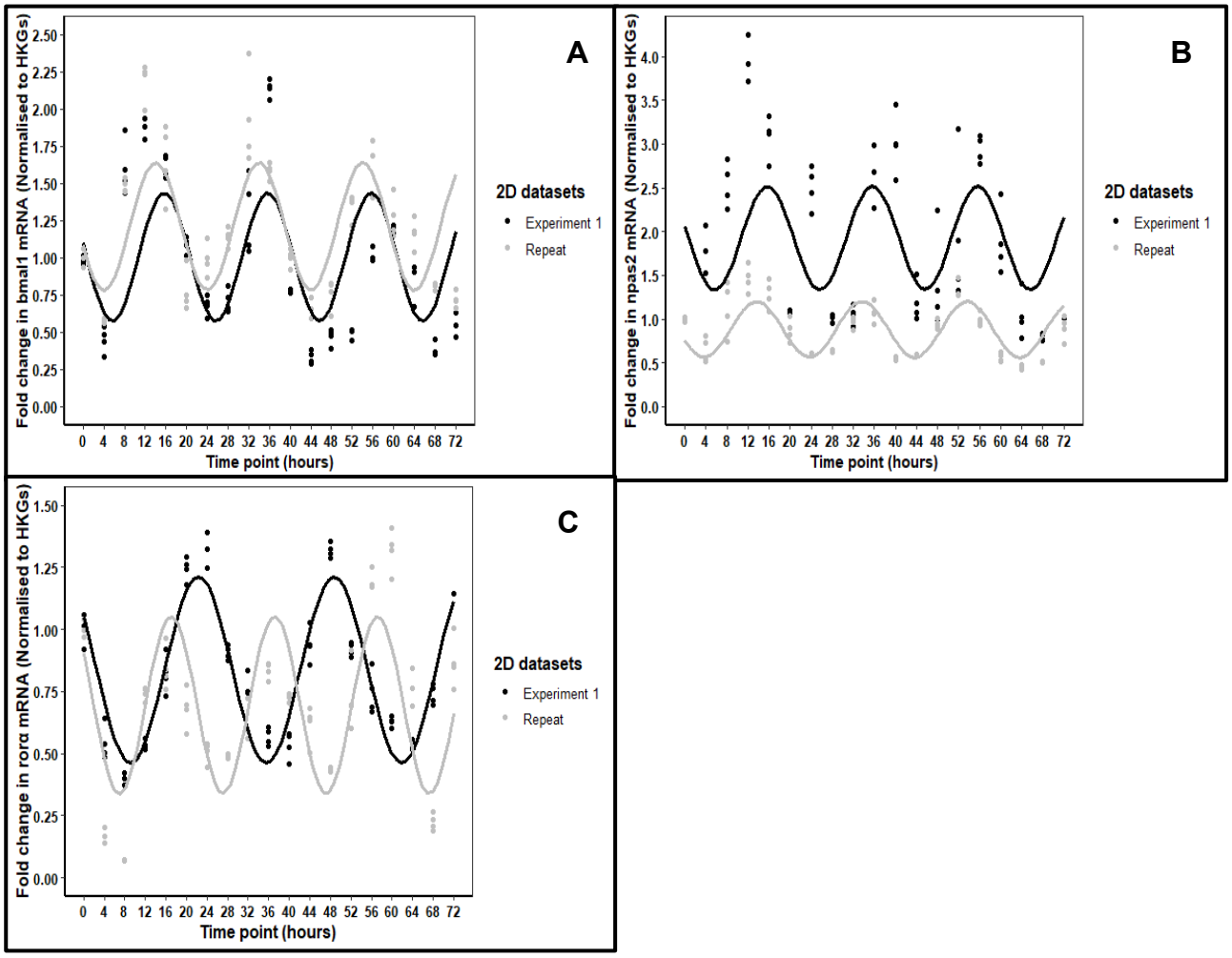

## Appendix 8

**Reproducible 2D chondrocyte cultures' baseline circadian rhythmicity for *bhlhe41*, *nr1d1* and *nr1d2* transcription in at least two LD cycles in two independent repeat experiments.** Fold changes in mRNA transcripts (normalised to *18s* and *hprt*) plotted against time of collection (4-hour interval) of control 2D chondrocyte cultures before qPCR quantification of the following clock genes within a 72-hour period; **A**) *bhlhe41*, **B**) *nr1d1* and **C**) *nr1d2.* Black dots and curves represent experiment 1 datasets; Grey dots and curves represent repeat experimental datasets. The fitted cosinusoidal waves indicate rhythmic oscillations in mRNA transcripts for a specific gene determined by the CircWaveBatch software ($R^2 > 0.8$, $p < 0.05$) and graphically plotted in the R software using the ggplot2 package. The absence of a cosinusoidal wave in a plot indicates an arrhythmic expression in a specific LD cycle determined by the CircWaveBatch software ($R^2 < 0.8$, $p > 0.05$). Data points represent fold changes in mRNA transcripts (n = 4, N = 1 per repeat).

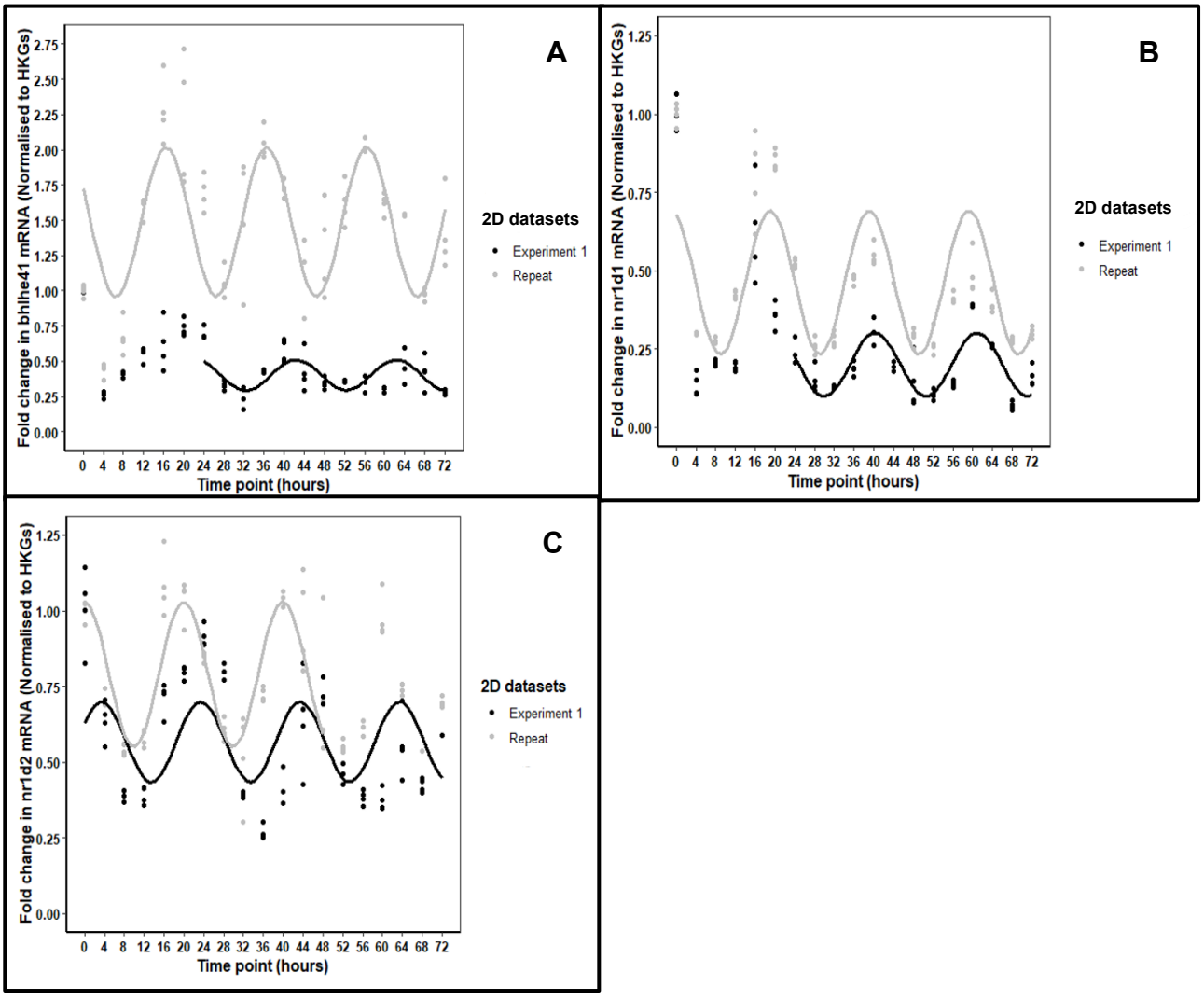

## Appendix 9

**Reproducible 2D chondrocyte cultures' baseline circadian rhythmicity for *per1* and *per2* transcription in two independent repeat experiments in at least two LD cycles.** Fold changes in mRNA transcripts (normalised to *18s* and *hprt*) plotted against time of collection (4-hour interval) of control 2D chondrocyte cultures before qPCR quantification of the following clock genes within a 72-hour period: **A**) *per1* and **B**) *per2*. Black dots and curves represent experiment 1 datasets; Grey dots and curves represent repeat experimental datasets. The fitted cosinusoidal waves indicate rhythmic oscillations in mRNA transcripts for a specific gene determined by the CircWaveBatch software ($R^2 > 0.8$, $p < 0.05$) and graphically plotted in the R software using the ggplot2 package. The absence of a cosinusoidal wave in a plot indicates an arrhythmic expression in a specific LD cycle determined by the CircWaveBatch software ($R^2 < 0.8$, $p > 0.05$). Data points represent fold changes in mRNA transcripts (n = 4, N = 1 per repeat).

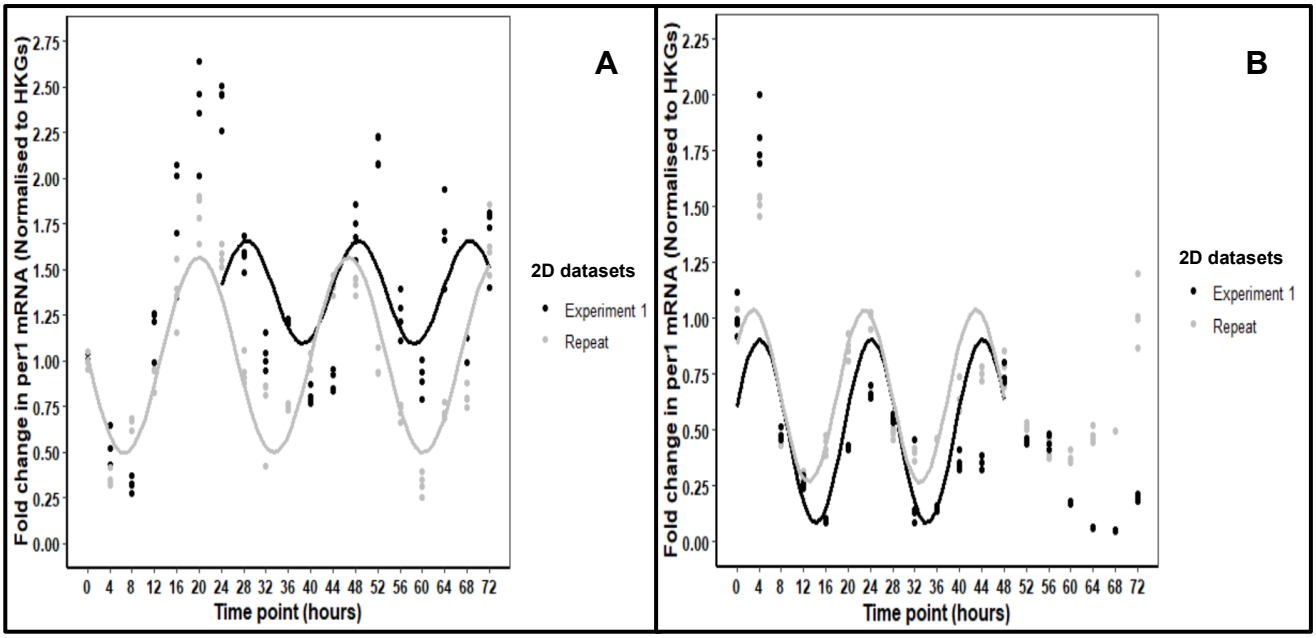

## Appendix 10

**Lack of reproducibility in 2D chondrocyte cultures' baseline circadian rhythmicity for *clock*, *nfil3* and *rorγ* transcription in two independent repeat experiments.** Fold changes in mRNA transcripts (normalised to *18s* and *hprt*) plotted against time of collection (4-hour interval) of control 2D chondrocyte cultures before qPCR quantification of the following clock genes within a 72-hour period: **A**) *clock*, **B**) *nfil3* and **C**) *rorγ*. Black dots and curves represent experiment 1 datasets; Grey dots and curves represent repeat experimental datasets. The fitted cosinusoidal waves indicate rhythmic oscillations of mRNA transcripts for a specific gene determined by the CircWaveBatch software ($R^2 > 0.8$, $p < 0.05$) and graphically plotted in the R software using the ggplot2 package. The absence of a cosinusoidal wave in a plot indicates an arrhythmic expression pattern of a specific gene determined by the CircWaveBatch software ($R^2 < 0.8$, $p > 0.05$). Data points represent fold changes in mRNA transcripts (n = 4, N = 1 per repeat).

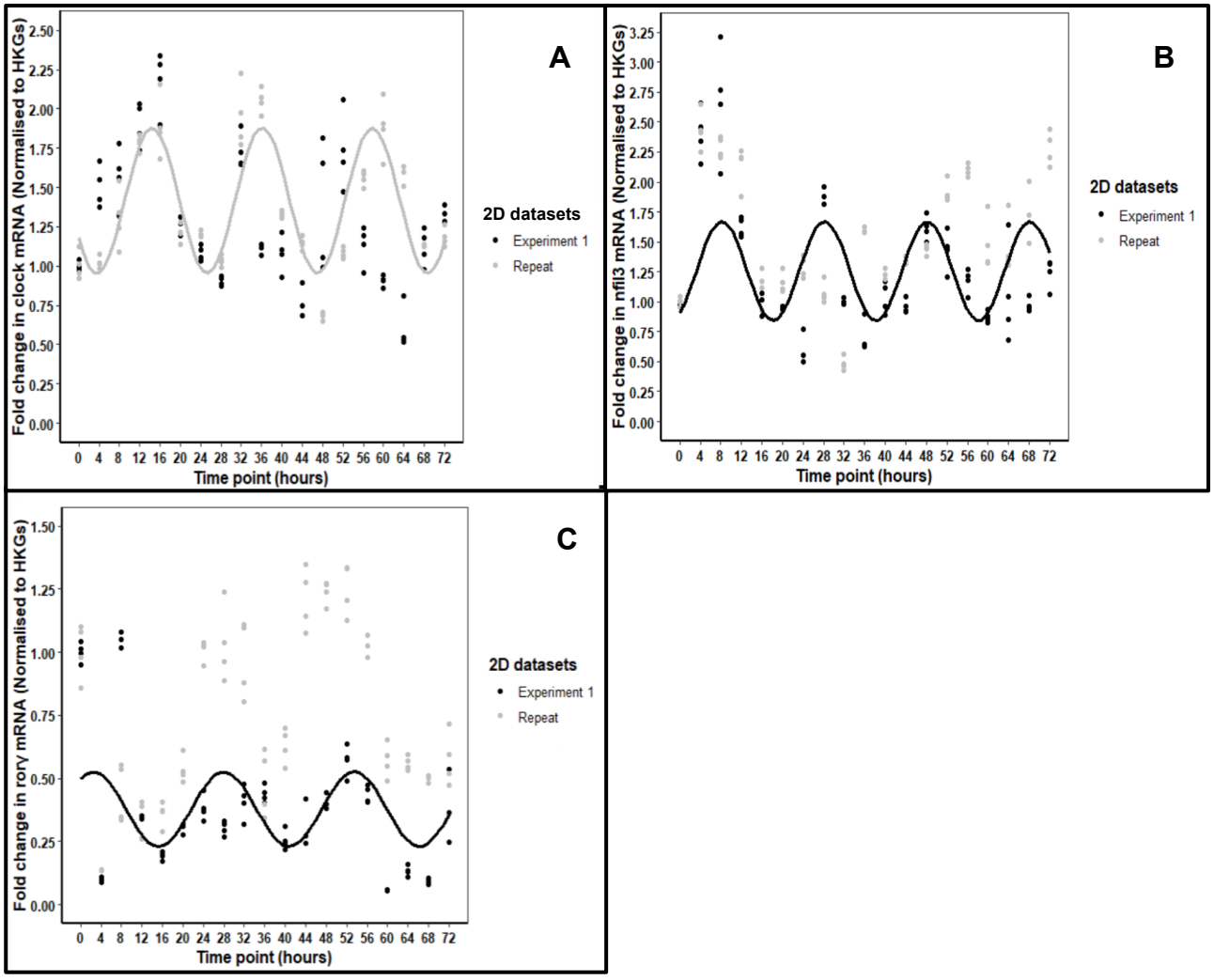

## Appendix 11

**Reproducible 2D culture baseline arrhythmic expression of *bhlhe40, cry1 and dbp* transcription in two independent repeat experiments.** Fold changes in mRNA transcripts (normalised to *18s* and *hprt*) plotted against time of collection (4-hour interval) of control 2D chondrocyte cultures before qPCR quantification of the following clock genes within a 72-hour period: **A**) *bhlhe40*, **B**) *cry1* and **C**) *dbp*. Black dots represent experiment 1 datasets; Grey dots represent repeat experimental datasets. The absence of cosinusoidal waves in the plots indicates arrhythmic expression these clock genes determined by the CircWaveBatch software ($R^2 < 0.8$, p-value > 0.05) and graphically plotted in the R software using the ggplot2 package. Data points represent fold changes in mRNA transcripts (n = 4, N = 1 per repeat).

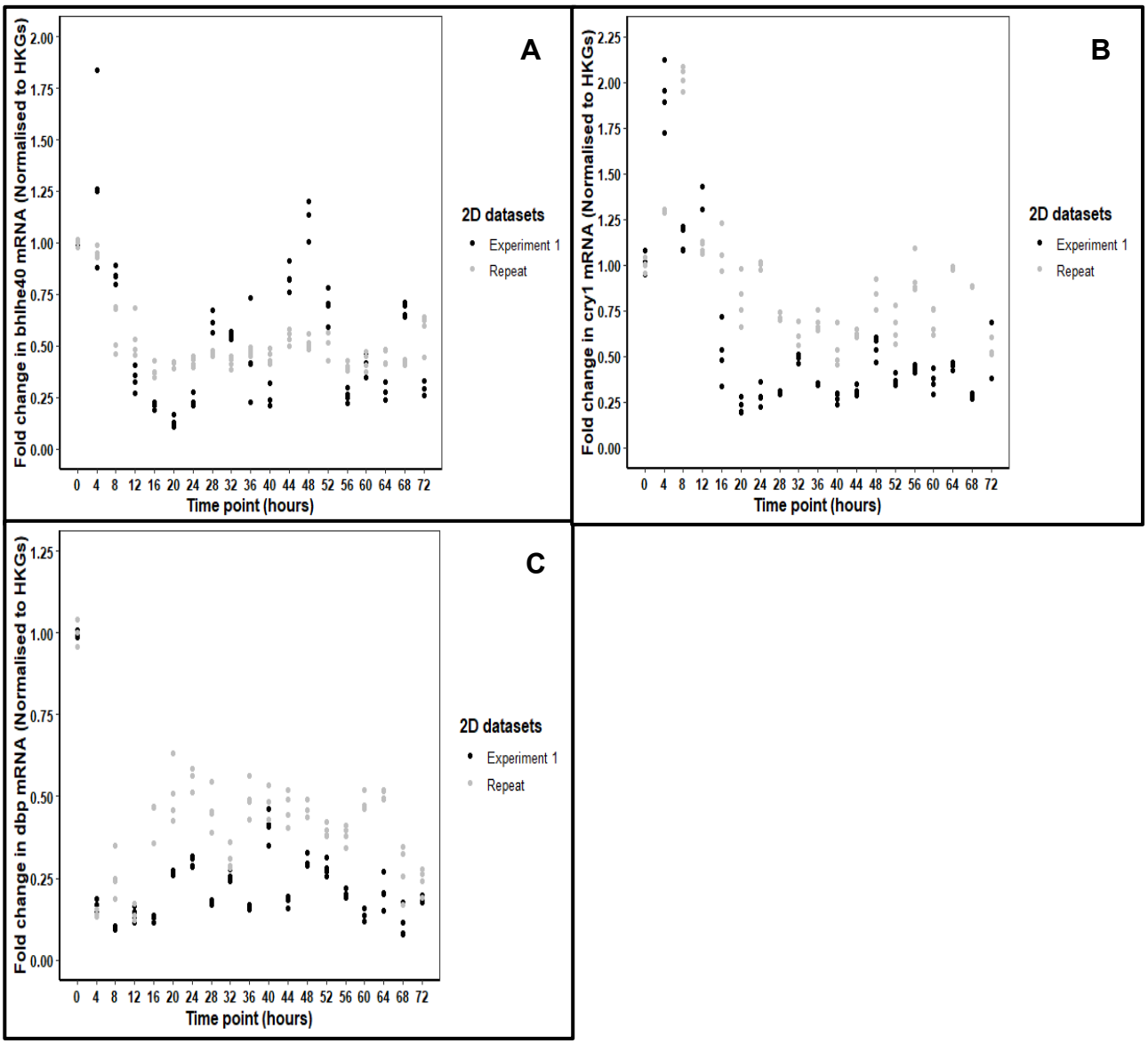

## Appendix 12

**Reproducible 2D cultures' baseline arrhythmic expression of *acan, col2a1 and sox9* transcription in two independent repeat experiments.** Fold changes in mRNA transcripts (normalised to *18s* and *hprt*) plotted against time of collection (4-hour interval) of control 2D chondrocyte cultures before qPCR quantification of the following cartilage matrix anabolism and chondrogenic gene markers within a 72-hour period: **A**) *acan*, **B**) *col2a1* and **C**) *sox9*. The absence of a cosinusoidal wave in a plot indicates arrhythmic expression patterns for a specific gene determined by the CircWaveBatch software ($R^2 < 0.8$, $p > 0.05$). Black dots; experiment 1 datasets, Grey dots; repeat experimental datasets. Data represent fold changes in mRNA transcripts (n = 4, N = 1 per repeat).

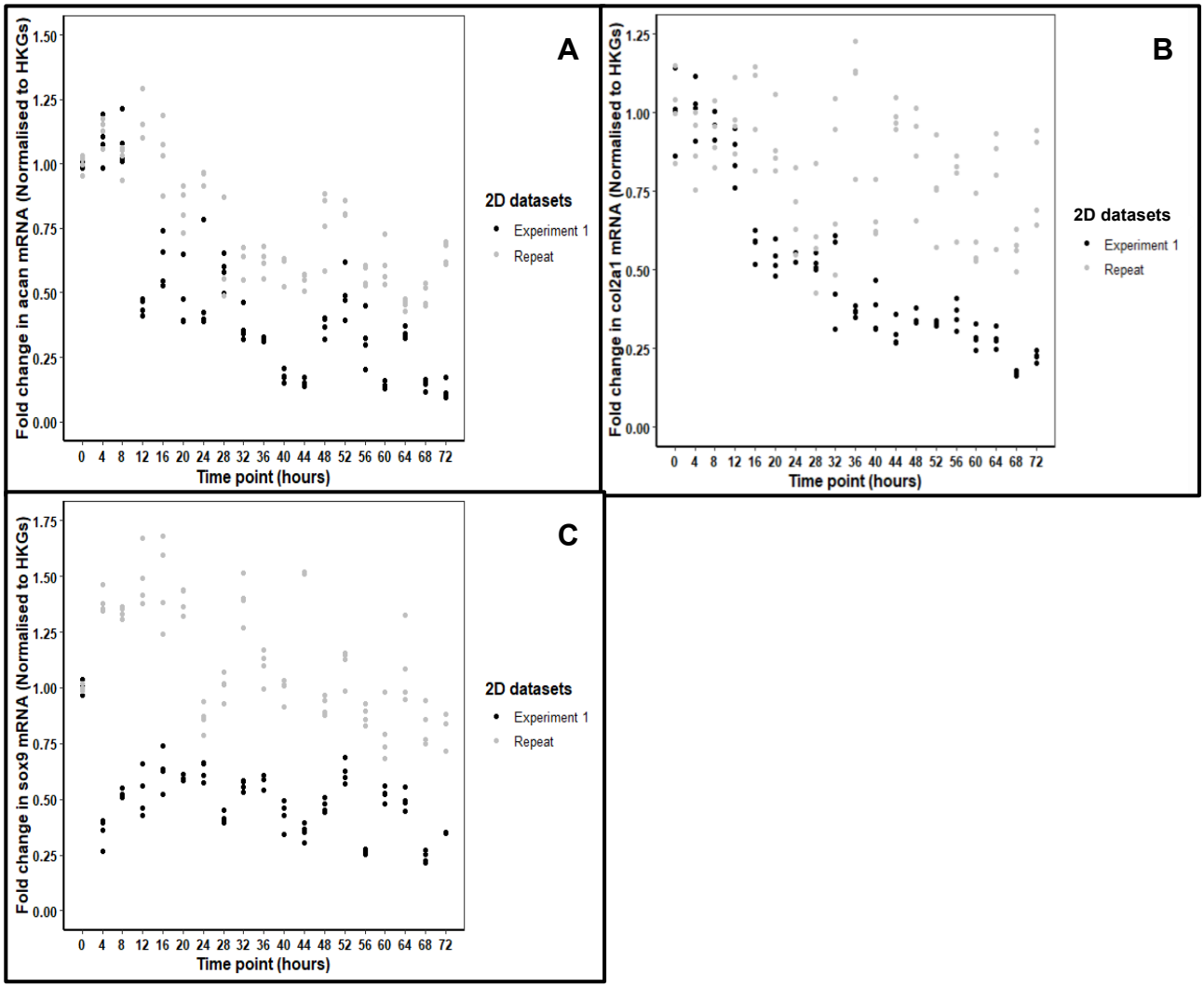

## Appendix 13

**Housekeeping gene stability rankings in control 3D chondrocyte cultures determined by the refFinder software which employs four different computational programs**. The graphs illustrate gene stability scores plotted against individual reference genes arranged in order from the most stable to the least stable gene by the following computer programs: A) BestKeeper, B) comparative Delta CT, C) Genorm, D) normFinder as well as E) the comprehensive gene stability ranking revealed by the refFinder software. Four-hour interval time series data within a 72-hour period for 8 reference genes (*18s*, *β-actin*, *gapdh*, *hprt*, *ppia*, *rpl4*, *sdha* and *ywhaz*) measured in control 3D pellet cultures were exported into the refFinder software for analysis and ranking of gene stability scores (n = 4, N = 1).

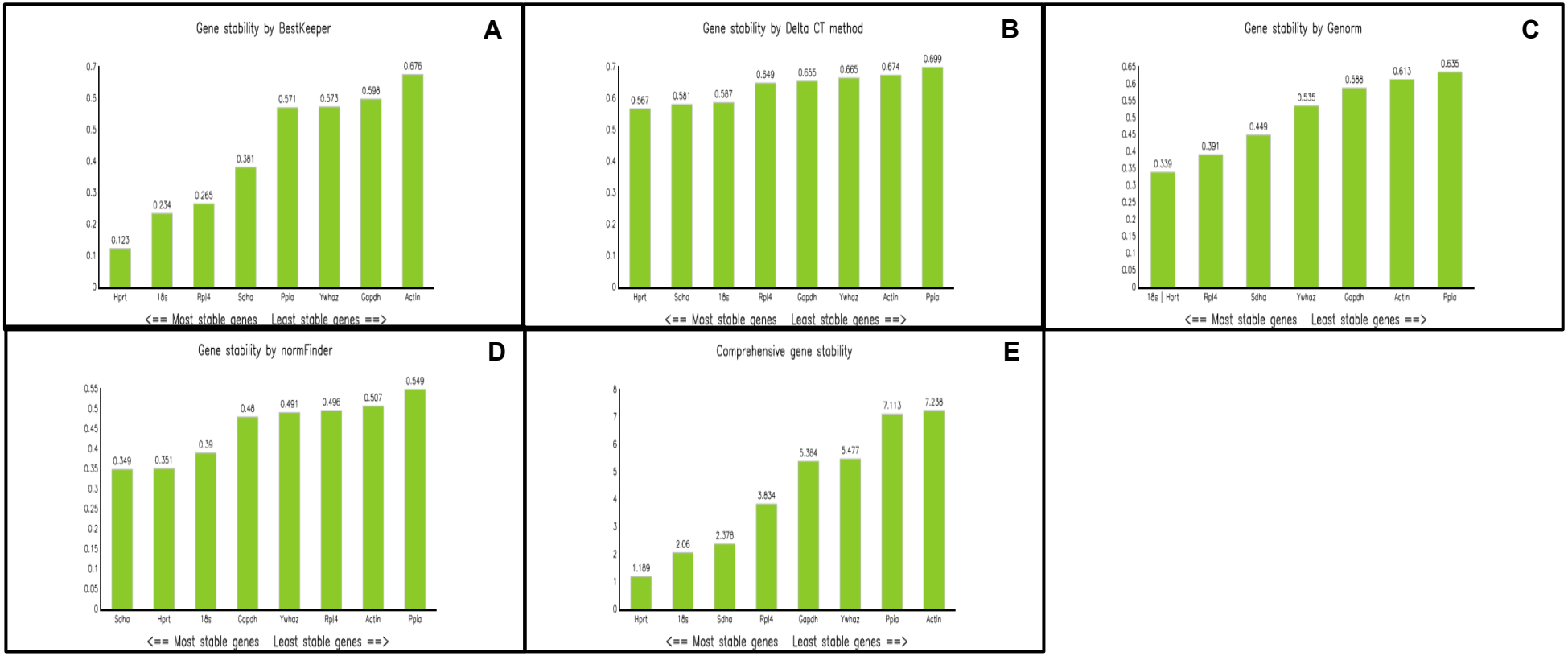

## Appendix 14

**Effect of 5ng/ml IL-1α in combination with 10ng/ml OSM on housekeeping gene stability in 3D chondrocyte pellets with no PCM determined by the refFinder software which employs four different computational programs**. The graphs illustrate gene stability scores plotted against individual reference genes arranged in order from the most stable to the least stable gene by the following computer programmes: A) BestKeeper, B) comparative Delta CT, C) Genorm, D) normFinder as well as E) the comprehensive gene stability ranking revealed by the refFinder software. 4-hour interval time series data within a 72-hour period for 8 reference genes (*18s*, *β-actin*, *gapdh*, *hprt*, *ppia*, *rpl4*, *sdha* and *ywhaz*) measured in cytokine-stimulated 3D chondrocyte pellet cultures (and their respective controls) were exported into the refFinder software for analysis and ranking of gene stability scores (n = 4, N = 1).

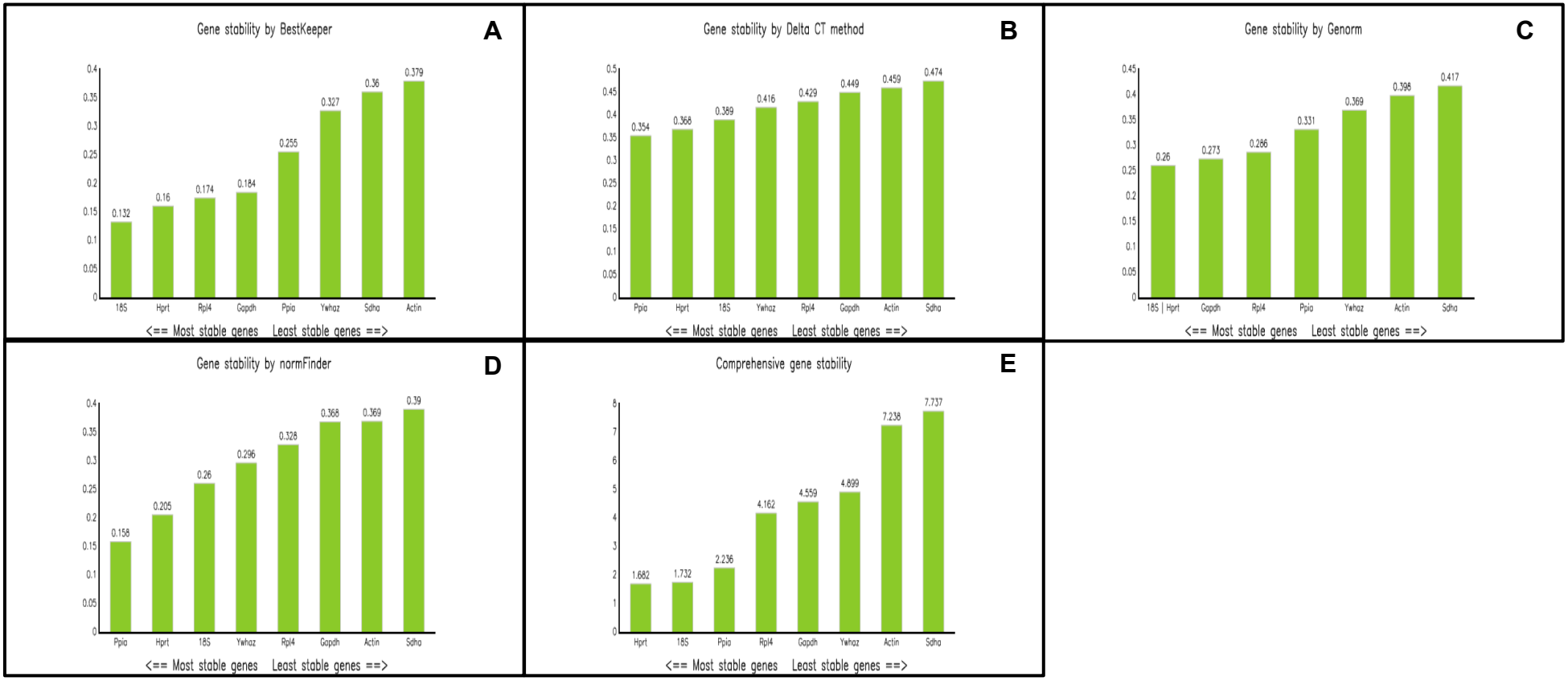

## Appendix 15

**Effect of applying Dex and once daily 770xg force on reference gene stability in inflammatory OA 3D pellets with no PCM**. Gene stability scores plotted against individual reference genes arranged in order from the most stable to the least stable gene by the following computer programs: **A)** BestKeeper, **B)** comparative Delta CT, **C)** Genorm, **D)** normFinder as well as **E)** the comprehensive gene stability ranking revealed by the refFinder software. Four-hour interval time series data measured in cytokine-stimulated (5 ng/ml IL1β plus 10 ng/ml OSM) 3D cultures prior to their exposure to continual Dex or once daily 770xg force (60 minutes) for 3-days were exported into the refFinder software (n = 4, N = 1). Only four genes were selected (*18s*, *hprt*, *rpl4* and *sdha*) based on their recurring stability demonstration following various stimuli due to financial constraints.

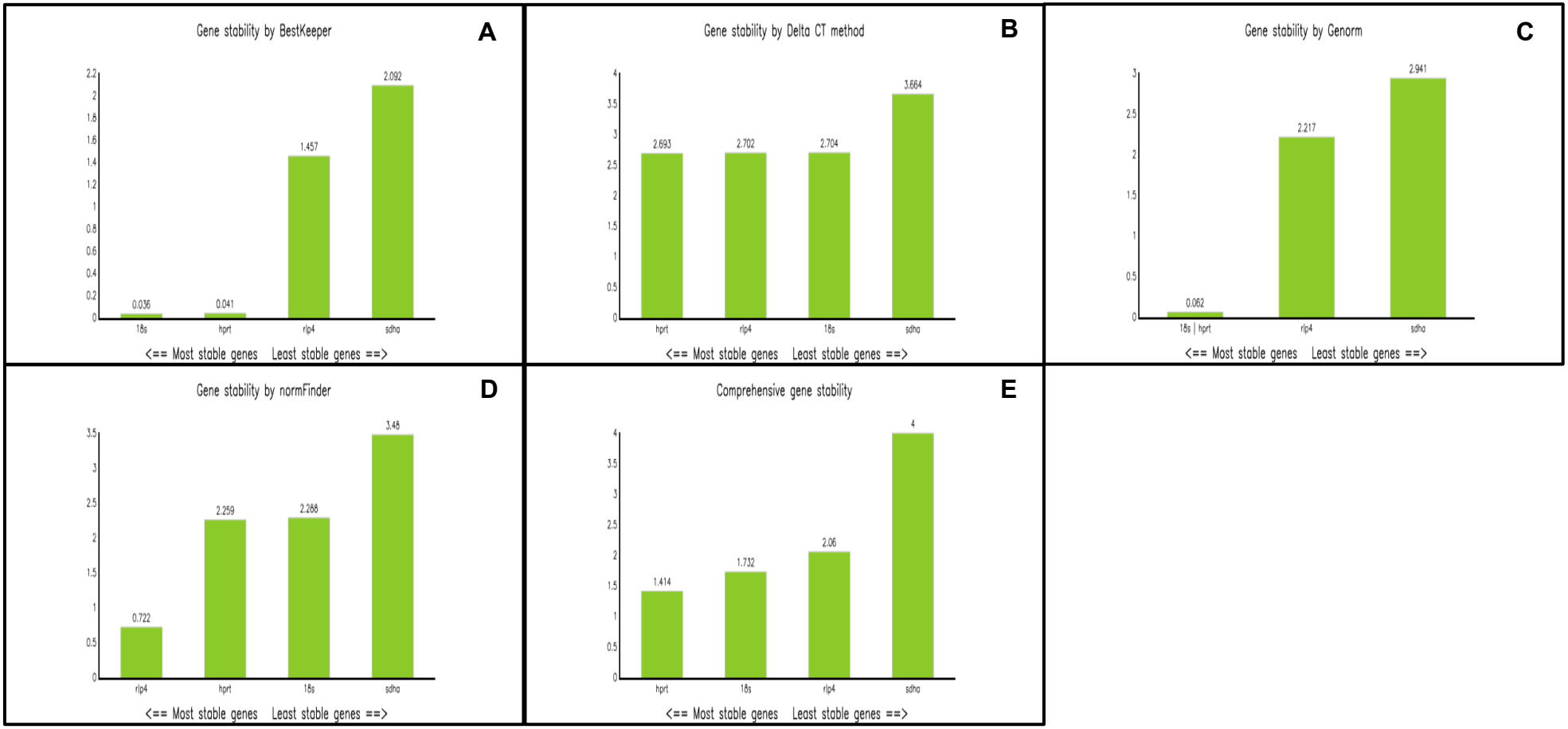

# Thank you!!!!!!